The effect of homocysteine on the oxidative folding pathway in the ER

Alice Appleby

2015

A thesis submitted for the degree of Doctor of Philosophy

School of Biological and Biomedical Sciences

University of Durham

Abstract

Upon translation into the endoplasmic reticulum (ER), ER resident proteins, and those destined for the secretory pathway, must be correctly folded into their native structure to be functional. During folding, many proteins must form disulphide bonds, a process facilitated by protein disulphide isomerase (PDI). Endoplasmic reticulum oxidoreductase 1 (Ero1) catalyses the formation of disulphides, using molecular oxygen as a terminal electron acceptor to drive the reoxidation of PDI. Ero1 must be tightly regulated to maintain the redox balance of the ER. One way in which this is achieved is by switching between an active or inactive state. Homocysteine, a precursor in the metabolism of cysteine and methionine, has been shown by the laboratory to induce the active form of Ero1α (OX1) in oesophageal cells. This finding was further investigated in this thesis using conformation-specific and anti-tag antibodies. Homocysteine is shown to induce an OX1 form in both transfected Ero1α and Ero1β. Ero1 OX1 was seen in multiple cell lines and in liver, but not pancreas tissue. This highlights the possibility that oxidative protein folding may be subjected to different regulation between tissues, depending on the redox poise. The site of homocysteine action, was investigated using Ero1α cysteine-to-alanine and Ero1β structural mutants. The data suggest that Ero1α is indirectly post-translationally modified by homocysteine at an antibody epitope site and not the CxxC redox-active cysteine residues.

The consequences of manipulating the oxidative folding environment were also examined by analysing a client protein, namely the MHC class II complex. These proteins are essential for the presentation of externally derived antigens to helper T cells. The disulphide containing

MHC II molecules are folded in the ER, and the laboratory have previously shown that there are differences between the 3 isotypes (HLA-DR, DP and DQ) in their requirements to form stable dimers. Work in this thesis shows that the thermal stability of DP$\alpha\beta$ heterodimers is greater than that of DR$\alpha\beta$ heterodimers. However, homocysteine does not influence the ability of MHC class II molecules to form stable dimers.

The studies presented in this thesis have implications for diseases such as cancer, where ER and oxidative stress may involve dysregulation of the oxidative folding machinery. High expression of Ero1α has recently been associated with cancers of the oesophagus and stomach, and low expression of Ero1 has been associated with poor prognosis of cancers such as osteosarcoma. Thus manipulating the ER redox poise through small molecules such as homocysteine may be worthy of further exploration to limit Ero1α activation during pathogenesis.

Table of contents

List of Figures

Table of abbreviations

AA	Ascorbic acid
AD	Activation domain
ADAM3	Disintegrin and metalloprotease domain 3
AHA1	ATPase homolog 1
APC	Antigen presenting cell
APS	Ammonium persulfate
ATF6	Activating transcription factor 6
BiFC	Bimolecular fluorescence complementation
BiP	Binding immunoglobulin protein
BSA	Bovine Serum Albumin
Btk	Bruton's tyrosine kinase
BZ	Bortezomib
CFTR	Cystic fibrosis transmembrane conductance regulator
CHOP	C/EBP homologous protein
CLIP	Class II associated invariant chain peptide
COPI	Coat protein I
Cy	Cystathionine
DBD	DNA-binding domain
DC	Dendritic cell
DLBCL	Diffuse large B-cell lymphoma
DTT	Dithiothreitol
DUB	De-ubiquitinating enzymes
E3	Ubiquitin ligase
EDEM	ER degradation-enhancing α-mannosidase-like protein
EGF	Epidermal growth factor
eIF2	Eukaryotic initiation factor 2
EndoH	Endoglycosidase H
ER	Endoplasmic Reticulum

ERAD	ER-associated degradation
ERAD-C	Cytosol ERAD
ERAD-L	Lumen ERAD
ERAD-M	Membrane ERAD
ERdj5	ER DNA J domain-containing protein 5
Ero1	Endoplasmic reticulum oxidoreductin 1
ERp	ER protein
FAD	Flavin adenine dinucleotide
FV	Factor V
FVIII	Factor VIII
GABARAP	Gamma-aminobutyric acid receptor-associated protein
GI	Gastrointestinal
GILT	Gamma-interferon-inducible lysosomal thiol reductase
GnRHR	Gonadotropin-releasing hormone receptor
GP	Glycoprotein
GPx	Glutathione peroxidase
GRP	Glucose regulated protein
GSH	Glutathione
GSSG	Glutathione disulphide
GT	UDP-glucose: glycoprotein glucotransferase
HC	Homocysteine
HERP	Homocysteine-induced ER protein
HIV	Human immunodeficiency virus
HLA	Human leukocyte antigens
HMGCR	3-hydroxy-3-methyl-glutaryl-CoA reductase
Hrd1	HMG-coA reductase degradation
HSP	Heat shock protein
IFN-β	Interferon-β
Ig	Immunoglobulin
Ii	Invariant chain
IL-1	Interleukin 1
IP	Immunoprecipitation

IP_3R1	Inositol 1,4,5-triphosphate receptor type 1
IRE1	Inositol-requiring kinase 1
IRF3	Interferon regulatory factor 3
JNK	C-Jun N-terminal kinase
LC3	Microtubule-associated proteins 1A/1B light chain 3A
LDLR	Low-density lipoprotein receptors
LPS	Lipopolysaccharide
M	Mock
mAB	Monoclonal antibody
MAMS	Mitochondrial associated ER membranes
methylTHF	N-5-methyltetrahydrofolate
MHC	Major histocompatibility complex
MIIC	MHC class II compartment
mV	Millivolt
MyD88	Myeloid differentiation primary response gene 88
NEM	N-ethylmaleimide
NMR	Nuclear magnetic resonance
NR	Non-reducing
OX1	Oxidised Ero1
OX2	Compact Ero1
P97	Valosin containing protein
pAB	Polyclonal antibody
PAMP	Pathogen associated molecular patterns
PDI	Protein disulphide isomerase
PERK	Pancreatic ER elF2a kinase
PLC	Peptide loading complex
PMA	Phorbol myristate acetate
Poly(I:C)	Polyinosinic:polycytidylic acid
PP1	Protein phosphatase 1
PPIase	Prolyl peptidyl *cis-trans* isomerase
Prx	Peroxiredoxin
R	Reducing

RAP	LDL receptor-associated protein
Red	Reduced Ero1
rER	Rough Endoplasmic Reticulum
ROS	Reactive oxygen species
S1P	Sphingosine-1-phosphate
S2P	Sphingosine-2-phosphate
SAH	S-adenosylhomocysteine
SAM	S-adenosylmethionine
SDS	Sodium dodecyl sulfate
SEL1L	Suppressor of Lin-12-like protein
sER	Smooth Endoplasmic Reticulum
SERCA	Sarco ER calcium ATPase
SNP	Signal recognition particle
SR	SRP-receptor
TBS	Tris buffered saline
TBST	Tris buffered saline with Tween
TEMED	N,N,N',N'-Tetramethylethylenediamine
TGPx	GPx-like peroxidase
TIRAP	TIR domain-containing adaptor protein
TLR	Toll like receptor
TNF	Tumour necrosis factor
TRAF2	TNF receptor-associated factor 2
TRAM	TRIF related adaptor molecule
TRIP	TRAF interacting protein
Trx	Thioredoxin
UBXD8	UBV domain containing protein
UPOM	Unfolded protein O-mannosylation
UPR	Unfolded protein response
WT	Wild type
XBP1	X-box binding protein 1
XBP1s	Spliced X-box binding protein 1
XBP1u	Unspliced X-box binding protein 1

µg	Microgram
µl	Microlitre

Acknowledgements

Thank you to my supervisor Adam Benham for your advice, guidance and help.

Thank you mum, dad and all of my friends for your continual support.

Most importantly,

thank you Ben, for everything.

1. General Introduction

1. General Introduction

1.1 Protein folding

The ability of denatured proteins, which have lost their native three-dimensional structure, to refold into a structure in which their original biological function is restored led to the idea that a proteins amino acid sequence holds all the necessary information for its correct folding (Anfinsen, 1973). In order to fold correctly, many proteins must form a compact structure where hydrophobic regions are buried within the structure and hydrophilic regions are accessible to solvents. When the secondary and tertiary structures have formed, and the protein has undergone any necessary processing and is able to function, it is said to be in its native state. According to Levinthal's paradox, it is not possible to acquire a native protein structure, to be compatible with biological constraints, by randomly or systematically testing all of the theoretical conformations (Levinthal, 1968). As the native structures of proteins tend to be the most thermodynamically favoured, the native interactions between amino acids in an unfolded or incompletely folded protein will be more stable, and so more persistent, meaning that not all conformations need to be sampled by the protein as it folds (Wolynes et al., 1995). The route to the native state is further directed by temporal, spatial and physical constraints, such as pH, temperature and protein concentration. However, even when these constraints are accounted for, *in vitro* it takes denatured bovine pancreatic ribonuclease 10 times longer to regain its native structure than it takes for the synthesis of this structure *in vivo.* Furthermore, the time taken to regain its native structure was increased and the misfolded protein load was increased when the concentration of denatured bovine pancreatic ribonuclease was folded *in vitro* at physiological concentrations (Goldberger, 1963). Thus, a number of strategies exist to optimise protein folding by preventing protein aggregation,

removing misfolded proteins and facilitating correct folding interactions. In the cell, these activities are governed by various folding factors, such as molecular chaperones, that start acting as soon as proteins are translated and continue until the protein has reached its intracellular or extracellular destination in a functional form.

1.2 Protein folding in the ER

There are two types of endoplasmic reticulum (ER). In the absence of bound ribosomes the ER is defined as smooth ER (sER), and is termed rough ER (rER) in their presence. sER is generally less common but can be found in abundance in certain specialised cells, especially those involved in lipid metabolism. In hepatocytes, for example, the sER contains the Cytochrome P450 family which are involved in metabolism and generally can detoxify a wide array of endogenous and exogenous compounds. Drug and cholesterol are examples of substances broken down by cytochrome P450s oxidative, peroxidative and reductive activities. The rER houses more translocation, folding and modification proteins (to be discussed further in sections *1.4, 1.5, 1.6* and *1.9*) (Gilchrist et al., 2006).

The rER is responsible for the folding and assembly of the majority of extraceullular, surface-expressed, secretory and endosomal eukaryotic proteins. As a separate compartment in the cell, it is able to provide an environment that differs significantly from the rest of the cell. The compartment has high molecular crowding with 300-400gL^{-1} protein, which is 3-6x more than that of the cytosol (Braakman, 2013; Gidalevitz et al., 2013). The redox potential of the ER is up to 200x more oxidising than the cytosol, which facilitates disulphide bond formation and supports a specialised chaperone and protein modification machinery (discussed in sections *1.4*, *1.5, 1.6* and *1.9*).

The distinct environment formed by the ER favours certain types of structural protein folds, thus influencing the folds that predominate in secreted and cell surface proteins. There are several such folds which are much more frequent in secretory pathway proteins, like the immunoglobulin (Ig) fold which consists of a pair of β-sheets linked by a disulphide bond and hydrophobic interactions (Berg et al., 2002). The Ig fold is frequently used by proteins of the immune system and can be found in antibody molecules, the major histocompatibility complex (MHC) proteins, integrins and interleukin receptors, (Geierhass, 2004). Other domains which require disulphide bonds are seen much more frequently in ER folded proteins, for example epidermal growth factor (EGF)-like domains, which are not found in cytosolic proteins, contain three disulphides which stabilise its β-sheet and flexible loop (Campbell, 1993). The EGF-like domain can be subdivided into the "human" hEGF-like domain and the cEGF-like domain (named after its discovery in the complement serine protease C1r). EGF-like domains often occur as tandem repeats and the two subtypes are probably descended from an ancestral 4 disulphide-containing domain (Wouters et al., 2005).

Folding in the ER is not perfect with many proteins never reaching their native conformation. An example of this is coagulation factor VIII (FVIII) which is secreted 10-fold less than the homologous factor V (FV) (Marquette et al., 1995; Pittman et al., 1994). This is due to FVIII forming high molecular weight aggregates retained in the ER by the chaperones Binding immunoglobulin protein (BiP), calnexin and celreticulin (discussed in *1.4*) (Swaroop et al., 1997; Tagliavacca et al., 2000). In addition to folding proteins destined for secretion, the ER will also fold viral gene products in virus-infected cells that are required for fusion of the viral envelope with host cell membranes. In contrast to the inefficient folding of FVIII, this process can be remarkably efficient; for example nearly 100% of influenza haemagglutinin is folded in influenza-infected cells (Braakman et al., 1991; Sanders and Myers, 2004).

1.3 Protein entry into the ER

To allow for proteins folded in the ER to reach their native state, they must first enter the ER lumen without prior folding elsewhere in the cell. A signal sequence of ~20 amino acids at the N terminus was first discovered when it was noticed that *in vitro*, the Ig light chain translational product was larger than that of the mature protein expressed *in vivo* (Blobel and Dobberstein, 1975). As this sequence emerges from the ribosome, it is bound by a signal recognition particle (SNP), made up of 6 polypeptides, which slows down translation and delivers the complex to the ER membrane by docking to the SRP-receptor (SR)(Wild et al., 2004).

Here the ribosome interacts with Sec61, through which the nascent protein enters the ER lumen. Sec61, the translocon, is a heterotrimeric integral membrane protein complex which forms a channel in which the traversing chain is protected from non-productive interactions (Brundage, 1990). In this channel folding is partially inhibited, likely due to the crowded conditions caused in part by the presence of many accessory proteins, but also by the channels diameter, which is not wide enough to allow efficient folding (Chen and Helenius, 2000). The channel was claimed to be 40-60 Å at its widest (Hamman et al., 1997). However a structure of the evolutionarily conserved archaea SecY, solved by X-ray diffraction of the *M.jannaschii* protein, is not consistent with this and shows a diameter of 20-25 Å at the open cytoplasmic entrance of its hourglass shape (Van den Berg et al., 2004). Although the channel is not large enough to permit folding, its diameter is still relatively large so a gating mechanism is present to maintain the permeability barrier across the ER membrane and maintain critical ion gradients.

The gate on the cytoplasmic side of the translocon is guarded by 2 transmembrane helices (TM2b and TM7) of Sec61. TM2b and TM7, the conformation of which is controlled by binding of the signal sequences, facilitate the opening of the plug domain, another Sec61 helical domain which seals the pore (Reithinger et al., 2014; Van den Berg et al., 2004).

On the luminal side of the translocon, BiP is the only soluble protein necessary and sufficient to seal the pore. BiP seals the pore in its ADP-bound conformation and requires conformational change, induced by ATP binding, to open the channel. BiP mutagenesis studies suggest that BiP binds to a membrane-bound J domain protein via its substrate binding domain to facilitate sealing of translocon pores (Alder et al., 2005). When a translocating protein reaches a threshold length of ~70 amino acids, it triggers the opening of the BiP mediated seal (Hamman, 1998).

The signal sequence of an ER targeted protein is usually 20-25 amino acids in length and is cleaved co-translationally after the synthesis of ~140 amino acids; however, examples of post-translational cleavage are known, such as the human immunodeficiency virus (HIV)-1 envelope glycoprotein (Land, 2003). Cleavage of the HIV-1 envelope glycoprotein occurs only after the formation of a set of unknown disulphide bonds and following slow folding (Land, 2003). In general, failure to cleave the signal sequence of a translocated protein can result in ER retention and misfolding (Shaw et al., 1988). The cleavage of signal peptides is controlled by a signal peptidase, although the sequence of the cleavage site varies significantly between proteins, it generally consists of a positively charged n-region, uncharged c-region and hydrophobic h region (Von Heijne, 1985). The nature of the signal sequence also determines the efficiency of protein targeting to the ER. Inefficient targeting can result in accumulation of proteins in the cytoplasm. Some of these proteins may be able to carry out their function here, whilst most others will be degraded (Karamyshev et al., 2014; Levine et al., 2005; Rane et al.,

2010; Shaffer et al., 2005). For example, the inefficient translocation of the ER chaperone calreticulin means that it can become available for functional interaction with the glucocorticoid receptor and facilitate gene activation (Shaffer et al., 2005). Although cytosolic calreticulin can drive the expression of luciferase from a glucocorticoid receptor reporter gene, the full biological significance of the dual targeting of calreticulin remains to be established.

1.4 ER Chaperones

The process of folding in the ER begins as a protein is translated into the lumen. This places certain constraints on the protein precursors. The tethering of the termini of the nascent chain to the ribosome limits its diffusion into the ER, preventing aggregation and non-native interactions of unfolded proteins (Frydman et al., 1994). This also allows local folding to occur first as the amount of conformational space that the chain is able to sample is greatly reduced (Alexandrov, 1993). The ER is likely to be organised to position proteins which assist in early folding near the ER membrane to associate with translating and newly formed polypeptide chains, whereas those which assist with near-native structures are found deeper in the ER lumen (Jansens et al., 2002; Snapp et al., 2006).

Molecular chaperones are proteins which aid other proteins in acquiring their native active conformation but are not part of the final protein structure (Ellis and van der Vies, 1991). They selectively interact with certain sequence and structural elements, such as hydrophobic regions, to prevent aggregation and facilitate folding by providing a protected environment. Within the ER, a classical heat shock protein (Hsp)70 chaperone (BiP), binds directly to the polypeptide chain (Haas and Wabl, 1983), and a carbohydrate-binding chaperone system (calnexin and calreticulin) interacts with hydrophilic glycan modifications (Slominska-

Wojewodzka, 2015). These chaperone systems ensure that despite the large array of proteins, they are all chaperoned as they are modified and mature as they move through the ER (Braakman, 2013).

1.4.1 Classical chaperones

The classical chaperones found in the ER belong to the Hsp70 and Hsp90 molecular chaperone families, both regulated by adenine-nucleotide binding. They identify unfolded proteins by detecting exposed hydrophobic segments, which will be buried in the core of native proteins, thus protecting client proteins from aggregation. The Hsp70 family couples the binding and release of substrate proteins to ATP hydrolysis. The peptide binding cleft of the chaperone is opened by a conformational change prompted by the binding of ATP at the Hsp70 N-terminal ATPase domain. Following hydrolysis of ATP, the binding cleft closes leaving ADP bound Hsp70 tightly interacting with the substrate (McCarty et al., 1995; Szabo et al., 1994). Hsp40 acts as a co-factor, retaining and targeting substrates to Hsp70. The Hsp40 family proteins are able to bind a diverse set of clients due to structural diversification, and the conservation of a J-domain means they are still able to bind Hsp70. Hsp40 passes the substrate to Hsp70 with help from a nucleotide exchange factor which facilitates ATP hydrolysis, increasing the substrate affinity of Hsp70 which can now outcompete Hsp40 (Summers et al., 2009).

The classical Hsp70 protein BiP binds to most proteins travelling through the ER at some point (Flynn et al., 1991) and, on average a protein is expected to contain a hydrophobic BiP binding region every 35 residues (Rudiger et al., 1997). BiP has been described as the master regulator of the ER, owing to its diverse set of roles involving assembly, transport and ultimately secretion of native proteins (Hendershot, 2004). During protein assembly, BiP is involved in facilitating insertion of precursor polypeptides into the translocon by gating the channel from

closed to open (Dierks, 1996). BiP acts as a molecular ratchet by binding the protein and preventing its movement back through the channel (Tyedmers et al., 2003). Another of BiPs many roles is at the end of a proteins life, where the solubility of misfolded protein aggregates is maintained by BiP to facilitate their disposal by the ER degradation machinery (Kabani et al., 2003).

The Hsp90 family has a varied set of functions with roles in cell cycle control as well as cell survival and cellular stress, Hsp90s also act as a hub for a complex chaperone machinery to interact with hundreds of substrate proteins, assisted by many co-chaperones such as CDC37 and activator of 90 kDa heat shock protein ATPase homolog 1 (AHA1) that determine the rate of chaperone cycling and client recruitment (Zhang and Burrows, 2004). Hsp90 is a dimer. Both subunits consist of a N-terminal ATP-binding domain, a middle domain, and a C-terminal dimerization domain. Hsp90 exists in an open formation, in which its lid segment is repositioned upon binding to ATP and a Hsp70/Hsp40/substrate protein complex. Following another conformational change resulting in a closed structure, ATP is hydrolysed, the original open formation is regained, and the folded client released. A number of other proteins can inhibit or post-translationally modify Hsp90, for example by phosphorylation, acetylation, oxidation and ubiquitination (reviewed by (Li et al., 2012; Lorenz et al., 2014)).

Glucose regulated protein (GRP) 94 belongs to the classical Hsp90 family and is one of the most abundant proteins in the ER; however, its client proteins are more restricted than those of other chaperones of a similar abundance. GRP94 appears to interact with substrates following their release from BiP and has a role in protein maturation (Melnick et al., 1994). The role of BiP and GRP94 is not limited to protein maturation. Both chaperones have been proposed to have diverse biological roles, with GRP94 able to induce T-cell immunity by

binding and delivering antigens to initiate an MHC class I-restricted T cell response (Li and Srivastava, 1993).

1.4.2 Carbohydrate-binding chaperones

Carbohydrate-binding chaperones, or lectin chaperones, are those that form hydrophilic interactions with N-linked glycans, rather than bind to the peptide backbone. Most proteins that pass through the secretory pathway are modified with the addition on N-linked glycans (to be discussed further in section *1.5*), which are subsequently trimmed, allowing the binding of chaperones to N-linked glycans at trimming intervals (Helenius and Aebi, 2004).

Calnexin and calreticulin are abundant lectin chaperones, binding monoglucosylated glycans (Kapoor et al., 2003). While calnexin binds to membrane proximal domain glycans, calreticulin interacts with those of ER luminal secretory proteins (Hebert, 1997). These chaperones perform largely the same function, giving the protein additional time and stability to fold into its native state, acting to prevent aggregation and recruiting protein disulphide isomerases like ER protein (ERp) 57 to promote disulphide bond formation and isomerisation. Following release from calnexin or calreticulin, substrate proteins are inhibited from rebinding to these chaperones, as the final glucose is removed by glucosidase II (Hammond, 1994). If a non-native conformation persists, the monoglucosylated state can be regenerated by the UDP-glucose: glycoprotein glucotransferase (GT). The level of misfolding determines whether reglycosylation occurs (Pearse et al., 2008), with GT detecting localised, disordered conformations and exposed hydrophobic patches of proteins with a nearly native conformation (Ritter and Helenius, 2000). Those proteins that can continue folding without the assistance of calnexin and calreticulin will be ignored by GT, as will those displaying major folding defects which instead attract BiP and are targeted for proteasome-mediated degradation (Hebert and

Molinari, 2007). Although primarily involved in carbohydrate binding, calnexin and calreticulin have been seen to bind and promote the folding of non-glycosylated proteins as well as preventing aggregation of non-glycosylated proteins (Danilczyk and Williams, 2001). Citrate synthase and malate hydrogenase are two non-glycosylated proteins which, when unfolded, interact with these lectin chaperones. Their folding is encouraged by retaining them in a conformation favourable for folding (Ihara et al., 1999; Saito, 1999). Examination of the binding specificity of calreticulin to non-glycosylated proteins shows a preference for hydrophobic peptides lacking acidic residues, and a minimum length of 10 residues (Jorgensen et al., 2000).

A recently discovered ER chaperone called malectin was proposed to be the first chaperone able to interact with glycans following removal of the first glucose, whilst it is in the diglucosylated state. Malectin is expressed under several ER stress conditions where it modulates the secretion of misfolded proteins (Galli et al., 2011). However, it has been proposed that malectin interacts with misfolded glycoproteins in a complex with ribophorin 1 (Qin et al., 2012). Malectin may therefore provide an initial round of quality control prior to the engagement of the calnexin/calreticulin cycle (Tannous et al., 2015).

1.4.3 Protein specific chaperones

Certain proteins containing unique structures and those which are present in extremely high concentrations require substrate specific chaperones. Low-density lipoprotein receptors (LDLR) is an example of this, where the LDL receptor-associated protein (RAP) provides additional support to allow its proper folding and prevent aggregation by preventing premature ligand binding. RAP binds to LDLR early in the secretory pathway, and the two proteins dissociate when they encounter the low pH of the Golgi (Li et al., 2002). Collagen, the most abundant

mammalian protein, interacts with many general chaperones, BiP and calnexin for example, but it also requires additional support from Hsp47 (Nagata, 1996). Hsp47 binds to procollagen upon formation of the collagen triple helix and facilitates further triple helix formation. Hsp47 is indispensable and its mutation can cause osteogenesis imperfecta and other collagen-related genetic diseases (Ishida and Nagata, 2011).

1.5 N-linked glycosylation

Upon entry to the ER most proteins undergo asparagine(N)-linked glycosylation at the acceptor site, Asn-X-Ser/Thr, with sequential processing of the N-glycan throughout the secretory pathway. A lipid anchor in the ER membrane provides an assembly point for the oligosaccharide substrate for N-glycosylation. Assembly of Man_5-$GlcNAc_2$ begins on the cytoplasmic side of the ER and is catalysed by glycosyltransferases using nucleotide activated monosaccharides. This oligosaccharide is translocated into the ER lumen and further glycosyltransferases add Glc_3Man_4 to the structure (Figure 1.1). The glycan can then be passed onto an asparagine residue by oligosaccharidetransferase (Schwarz and Aebi, 2011). N-linked glycans are frequently transferred co-translationally at ~13 amino acids into the ER lumen (Nilsson and Vonheijne, 1993).

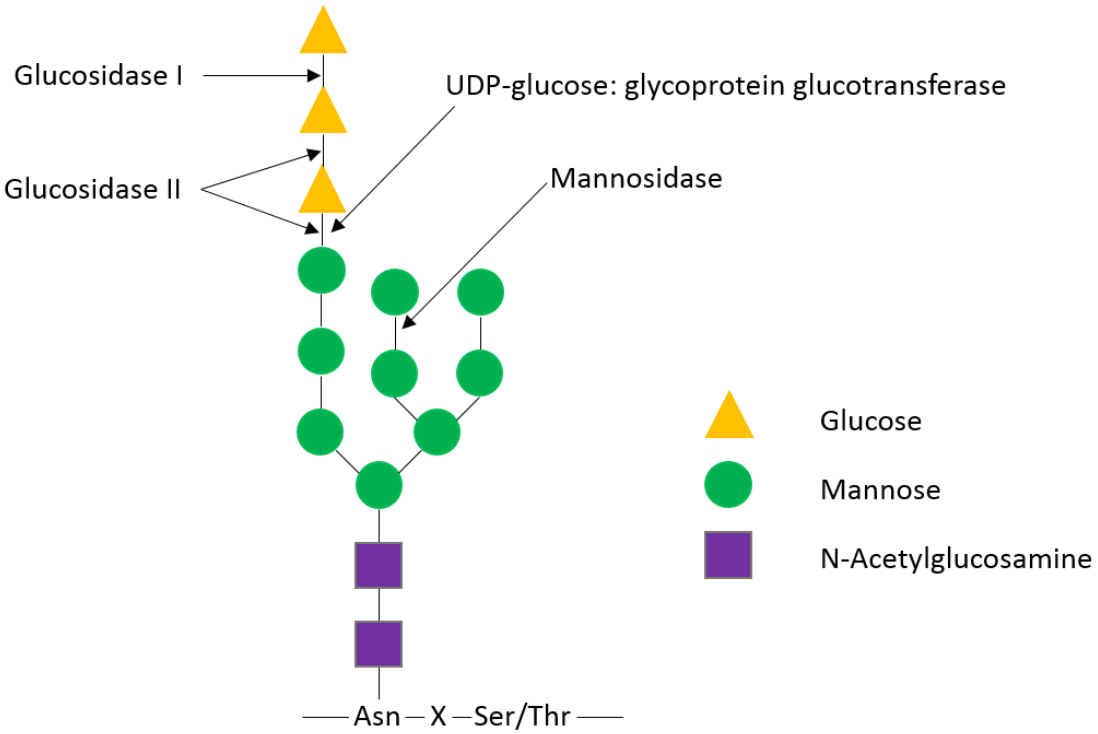

Figure 1.1. N-linked oligosaccharide structure

The N-linked glycan is composed of two N-acetylglucosamines, nine mannoses and three glucoses. The terminal glucose is removed by glucosidase I following which the remaining two glucoses can be removed by glucosidase II. A glucose can be replaced by UDP-glucose: glycoprotein glucotransferase. Mannosidase removes a terminal mannose.

Following the addition of N-linked glycans to ER proteins, they are subsequently trimmed. The intermediate sugars guide protein secretion and assembly in different ways; initially they assist in proper protein folding and quality control, following this and further trimming they act as signals in intracellular transport and finally, after the final trimming, they form part of the final protein structure. Glucosidase I removes the outermost glucose residue. The remaining two glucose residues can then be removed by glucosidase II (Figure 1.1). Once removed, glucose residues can be replaced by GT taking the glucose from UDP-glucose that has been transported from the cytosol into the ER lumen. The efficiency of glucosidase II and GT is dependent on the number of mannose resides in the glycan; they become less efficient as the mannose residues are removed, which is catalysed by mannosidase enzymes (Grinna and Robbins, 1980) (reviewed by (Aebi, 2013)). GT will only interact with improperly folded glycoproteins displaying high-mannose glycans. Those glycoproteins with small folding defects and exposed hydrophobic residues tend to have the most efficient interactions (Ritter and Helenius, 2000). The glucose cycle allows proteins that remain unfolded following their release from calnexin and calreticulin to reattach to these chaperones for another attempt at folding.

Glycoproteins that fail to fold are targeted for ER-associated degradation (ERAD) (discussed in section *1.7*). The length of time a protein spends folding in the ER provides an indicator as to whether proteins are misfolded and subunits are unassembled or whether the proteins are present as folding intermediates. Glycoproteins are given reasonable opportunity to fold, with a lag period dependent on the protein and their number and location of glycans. The average lag time is 30-90 minutes, after which they are degraded, as shown in labelling studies with ER retention mutants (Mancini, 2003). The status of the N-linked glycan provides an indication of how long the protein has been folding for, with mannosidase slowly removing mannose residues, thus acting as a timer. If unfolded proteins do not interact with calnexin or

calreticulin during the lag period they are immediately targeted for ERAD. Those proteins that do interact with these chaperones are protected during this period, but upon mannose trimming the ERAD targeting ER degradation-enhancing α-mannosidase-like protein (EDEM) starts to compete with them (Molinari et al., 2003). EDEM becomes more likely to interact with the proteins as the mannose residues are trimmed and GT and glucosidase II become less efficient (Grinna and Robbins, 1980). EDEM also has the ability to act as a mannosidase and, independently of substrate demannosylation, act as a chaperone inhibiting aggregation of misfolded proteins upon release of the calnexin/calreticulin cycle. The concentration of EDEM is strictly regulated, increasing during ER stress (reviewed by (Slominska-Wojewodzka, 2015)).

Not only does the addition of glycans recruit chaperones, but the folding, stability and maturation efficiency is increased by the altered physical properties of the protein, caused for example by the masking of hydrophobic stretches and proteolytic cleavage sites. These properties, along with the chaperones, help the protein reach its native state (Hanson et al., 2009; Kundra and Kornfeld, 1999). The addition and modification of N-linked glycans to some proteins do not have an appreciable effect on their folding properties. These glycans can be modified by the cell to allow self-recognition and provide information on stages of differentiation and transformation (Lowe and Marth, 2003).

About 90% of proteins that traverse the ER are modified with N-linked glycans (Apweiler et al., 1999) and whilst some of them are necessary for function, others only facilitate folding and maturation. When the N-linked glycan sites of MHC class I are mutated, the resulting nonglycosylated MHC class I is functional but their cell surface expression is diminished (Miyazaki et al., 1986). Other N-linked glycans are completely dispensable; for example, elimination of glycans in influenza hemagglutinin affects only the folding rate, either speeding it up or slowing it down, and not the functional outcome of folding (Hebert, 1997).

1.6 Other folding mechanisms

Prolyl peptidyl cis-trans isomerases (PPIases) are important in protein folding.Proline residues are inserted into the ER in the ER trans conformation, PPIases can isomerise the conversion of these into the cis conformation, and back again depending on the requirements of the proteins native structure. Often the nature of the proline residue is changed multiple times before the portein is fully folded. The enzymatic activity of PPIases is a slow process and therefore rate-limiting for folding in the ER (Reviewed in (Braakman, 2013)).

For oligomeric proteins, protein folding can involve the assembly of subunits before they are able to leave the ER. In these cases, folding of the multiple subunits must be orchestrated to ensure they are able to assemble. Igs are an example of this; made up of 4 subunits composed of 2 Ig heavy chains and 2 light chains, the free heavy chains are stably bound by BiP which recognises the conformation of the substrate and retains it in the ER (Marcinowski et al., 2013). Light chains are required to remove BiP from the heavy chain, allowing it to fold and proceed with subunit assembly (Lee et al., 1999). Many other chaperones are involved in regulating levels of assembly of subunits, but no general mechanism has been described as to how free subunits are distinguished from those which are assembled. Other oligomer subunits contain ER retention signals, such as the C-terminal KDEL or the dibasic (KKXX) motif, which upon subunit assembly are hidden. This allows progression of the oligomer out of the ER. In the case in the G protein-coupled $GABA_B$ receptor, competition between 14-3-3 proteins and the coat protein I (COPI) retrieval machinery has been proposed to control ER retention and hence cell surface expression of this receptor (Brock, 2005). Subunits which fail to assemble will not proceed out of the ER and will aggregate or become targeted for degradation.

Unfolded protein O-mannosylation (UPOM), a much less studied protein modification, parallels N-linked glycosylation, with both structural and quality control roles. Like N-linked glycosylation, the mannosylated substrate is produced on the cytosolic side of the ER membrane and flipped into the ER lumen to where a single mannosyl group is transferred from the dolichol phosphate β-D-mannose donor (Haselbeck, 1983). UPOM was originally thought to occur only co-translationally, but more recently has been shown to occur co- and post-translationally, to serine/threonine residues, with no sequence consensus yet known for this (Larriba et al., 1976; Loibl et al., 2014). As well as being structurally important UPOM has a broad role in protein quality control, with unfolded ER proteins becoming O-mannosylated. UPOM is not required for ERAD, and not related to the mannosylation that acts as a quality control marker for ERAD, but it enhances substrate solubility which is a prerequisite for ERAD (Harty et al., 2001; Nishikawa et al., 2001). Whilst mannosylation is required for degradation in some proteins it not always a signal for degradation, thus it operates as an independent quality control pathway for some proteins. Certain proteins require UPOM for ERAD, as has been demonstrated using KHN (a fusion construct of yeast hemagglutinin neuraminidase). Without UPOM, HMG-coA reductase degradation (Hrd1), one of the main ubiquitin ligases that function in ERAD does not target KHN, leaving KHN to accumulate in the ER. The O-mannosylation of other substrates like the yeast Deg1-Sec62 model fusion protein does not affect their susceptibility to Hrd1 (Rubenstein, 2012; Vashist et al., 2001).

1.7 ERAD

Recognition of nonglycosylated proteins for ERAD occurs when ER chaperones detect unfolded regions. BiP, and its regulation by DnaJ family proteins are mainly responsible for this, however calnexin and celreticulin are able to bind some nonglycosylated proteins implicating them in

the early stages of the ERAD pathway. It is believed that ERAD cofactors, such as EDEM, are recruited upon prolonged retention of proteins by BiP and lead to the their retrotranslocation from the ER and subsequent ubquitination (Otero et al., 2010). Once ubiquitinated in the cytosol, misfolded proteins are directed to the proteasome or to ubiquitin ligases for degradation via homocysteine-induced ER protein (Herp) which acts as a bridge for partially or fully translocated proteins (Okuda-Shimizu, 2007). ERAD must recognise folding inaccuracies in ER folded proteins, including cytoplasmic, membrane and lumen regions. As this constitutes a wide range of ERAD substrates, a range of accessory factors exist to assist in recognition. The two central ubiquitin ligases, Hrd1 and glycoprotein (gp) 78, are able to bind to these accessory factors, as well as others involved in substrate dislocation, allowing the coupling of substrate recognition and dislocation (Christianson et al., 2012).

EDEM is best known for its role in glycoprotein degradation however, glycosylation and glycan trimming is not necessarily required for EDEM-mediated targeting of substrate proteins for degradation. EDEM has been found to bind, in a highly substrate dependant manner, to non-native structures irrespective of their glycosylation status. EDEMs mannosidase-like domain, originally expected to be solely for substrate recognition, can bind to suppressor of Lin-12-like protein (SEL1L), a downstream ERAD machinery target containing 5 N-glycosylation sites. This suggests that it is not just the glycan status of substrates that is important, but also that of the ERAD machinery (Cormier et al., 2009). Three mammalian EDEM proteins have been characterised. Initially it was believed only EDEM3 possessed mannosidase activity, but further study showed that this activity could be induced by overexpression of EDEM1. This was determined by looking at mannose trimming of the ERAD substrate NHK in cells transfected with EDEM1, which showed an increase in N-glycans lacking terminal mannoses. No such increase in seen in transfected cells when EDEM1 was mutated at the proposed mannosidase

active site, or with EDEM 2 (Hosokawa et al., 2010). This work highlights that there are different EDEM functions which make up different ERAD pathways (Mast et al., 2005).

The short-lived EDEM protein is localised in double-membrane buds outside ER exit sites where, at steady state, they are degraded. This allows for EDEM to become rapidly available to the ER, without the delay involved in transcriptional responses (Bernasconi and Molinari, 2011). EDEM is stabilised by binding the oxidoreductase ER DNA J domain-containing protein 5 (ERdj5). This is the largest member of the PDI family at 90 kDa, and found at its highest concentrations in secretory tissues. It allows progression of misfolded proteins through ERAD by reducing disulphides in substrates. After disulphide bond reduction, the protein can now bind to BiP and dissociate from ERdj5, allowing BiP to target the protein for retrograde translocation (reviewed by (Okumura et al., 2015)). ERdj5 also aids retrograde translocation by preventing covalent interactions and aggregation which would make the substrate too large for the retrotranslocon channel (Ushioda, 2008). As well as this, ERdj5 can act as a chaperone by promoting productive folding following its reductase activity (Oka et al., 2013).

Following recognition by ERAD, misfolded substrates are taken back across the ER membrane into the cytoplasm. Those proteins which are ER luminal proteins must be fully retrotranslocated, whereas certain domains of membrane proteins can diffuse through the membrane exposing them to the cystosol. Ubiquitination is coupled to retrotranslocation of membrane proteins but occurs late on in luminal protein retrotranslocation and allows ATP dependent extraction from the membrane and targeting to the proteasome. Valosin containing protein (P97) moves the substrates from the membrane to the cytosol. This ATPase is recruited by UBV domain containing protein (UBXD8), an ER membrane-embedded ERAD factor that has also been linked to the control of triacylglycerol synthesis and the turnover of RNA-protein complexes in the cytosol. P97 also binds other ubiquitin modifying enzymes such

as the de-ubiquitinating enzymes (DUB), which have been shown to be necessary for retrotranslocation. The need for DUBs suggests that cycles of ubiquitination and de-ubiquitination exist. In support of this idea, substrates that are retrotranslocated but not ubiquitinated could indicate that factors other than the substrate are ubiquitinated (Bernardi et al., 2013; Ruggiano et al., 2014; Zhang, 2013). The ubiquitination is coordinated by a membrane associated ubiquitin ligase (E3 ligase) complex. The E3 ligase cofactors are likely needed to determine the specificity of the ligase (reviewed by (Ruggiano et al., 2014)), while others assist with the transfer of ubiquitin which must first be activated (E1) and conjugated (E2). Ubiquitin, a small 76 amino acid protein, is recognised by and degraded by the proteasome.

There is no definitive consensus as to the channel through which retrotranslocation occurs. Sec61 was first proposed as a retrotranslocon, backed up by findings that it interacted with ERAD substrates (Wiertz et al., 1996). These interactions were later found to be with proteins stuck on their way into the ER (Rubenstein, 2012). In addition, the pore diameter of Sec61 is unlikely to accommodate larger partially folded substrates. Subsequently, members of the Derlin family of membrane proteins, which have 4 membrane spanning domains, have been suggested to function as retrotranslocation channels, with their overexpression speeding up the degradation of ERAD substrates (Oda et al., 2006). However, the crystal structure of rhomboid protease GlpG, a similar protein of the same family, lacked any membrane channels suitable for retrotranslocation. Instead, it is more likely that the derlins organise ERAD components and bind substrates as they enter the cytosol (Greenblatt, 2011). Following release into the cytosol, substrates for degradation are kept soluble and transferred to the proteasome by cystolic proteins, like Rad23, or shuttle factors chaperones such as the BAG6 complex (Ruggiano et al., 2014; Xu, 2012).

Three ERAD sub-pathways have been described in *S. cerevisiae* based on the location of their degradation signal. These are ERAD-L (lumen), ERAD-M (membrane) and ERAD- C (cytosol) with each having its own E3 protein complex (Finley et al., 2012). Whether distinct subpathways exist in mammalian cells is unclear. Suggestions have been made that mammalian equivalents for the ERAD-L pathway exist. The mammalian Hrd1 E3 ligase is one of the most explored of the 6 described, and has been suggested to mediate the ERAD-L pathway (Ballar et al., 2011; Bernasconi et al., 2010). Overall, the data support the idea that distinct retrotranslocation pathways are present in the mammalian ER but these may not be as well defined as that in yeast (Okuda-Shimizu, 2007).

Occasionally ERAD targets proteins in their native state. This is a highly regulated event only occurring in certain proteins and often working as a feedback inhibition system for specific purposes, such as maintaining sterol homeostasis and preventing accumulation of toxic intermediate sterol metabolites. Three-hydroxy-3-methyl-glutaryl-CoA reductase (HMGCR), an enzyme in cholesterol synthesis, is one such protein. It is selectively targeted for ubiquitination to limit the rate of cholesterol production (Foresti, 2013; Song et al., 2005). Other proteins which, given the right circumstances, for example sufficient time, would fold properly can also be degraded. One of the best-known examples of this is the cystic fibrosis transmembrane conductance regulator (CFTR). CFTRs lengthy, inefficient, folding pathway leads to up to 80% being subjected to ERAD before it is able to fold (Cui et al., 2007; Lukacs et al., 1994; Lukacs and Verkman, 2012).

Macromolecules with structural restraints such as aggregates and large proteins cannot traverse the retrotranslocation channel, thus another pathway must exist to remove them from the ER. One alternative route for these proteins is autophagy. Autophagy enables the degradation of cell compartments by packing the substrates for degradation into a double-

membrane autophagosome and sending this to the lysosome, which is able to degrade large amounts of cellular material. The underlying mechanisms for this are largely unexplained, but one proposed method is that ER resident FAM134 reticulon protein family members facilitate autophagy by binding to autophagy modifiers microtubule-associated proteins 1A/1B light chain 3A (LC3) and gamma-aminobutyric acid receptor-associated protein (GABARAP). Subsequently, the ER becomes highly fragmented and degraded by the lysosome, as shown in experiments when the members of the FAM134 family are overexpressed (Khaminets et al., 2015). Specifically, autophagy is used to clear the ER of accumulated partially folded human gonadotropin-releasing hormone receptor (GnRHR) (Houck et al., 2014). Other protein aggregates can escape recognition by molecular chaperones which detect hydrophobic sequences hidden upon aggregation (Kopito, 2000). Proteins could potentially be targeted for autophagy by a buildup of polyubiquitinated proteins however this could be a consequence of aggregation. There is crosstalk between proteasomal and autophagic degradation pathways, with proteins involved in both pathways and in activating them. One such pathway is activated by the proteasome inhibitor bortezomib (BZ). BZ induces, and requires, the stabilisation of ATF4, a member of the PERK (See section *1.8.2*) pathway which is involved in proteasomal regulation, to bring about autophagy (Kawaguchi et al., 2011).

1.8 Unfolded protein response

A build-up of unfolded proteins can occur in many situations, including insufficient folding or degradation, paucity of chaperones when protein translation is increased, and changes in temperature or other stress conditions, which lead to unstable protein structures. Under these circumstances the unfolded protein response (UPR) is induced to adapt the ER to these conditions. Fluctuations in Ca^{2+}, oxidative stress, hypoxia and energy depletion, to name a few, disrupt ER homeostasis and thus optimal folding conditions. Here, the UPR acts to tightly

regulate ER conditions. If the level of unfolded/misfolded proteins is too high and cannot be resolved, cell-death signalling pathways are activated (reviewed by (Cao, 2012)). Otherwise specific protein folding and ERAD genes are transcriptionally activated, whilst global protein translation is diminished to moderate the newly synthesised protein load which requires folding.

The mammalian ER contains 3 transmembrane sensors to detect the folding capacity of the ER: inositol-requiring kinase 1 (IRE1), pancreatic ER elF2a kinase (PERK), and activating transcription factor 6 (ATF6). Each of these are at the start of a distinct UPR pathway (Figure 1.2).

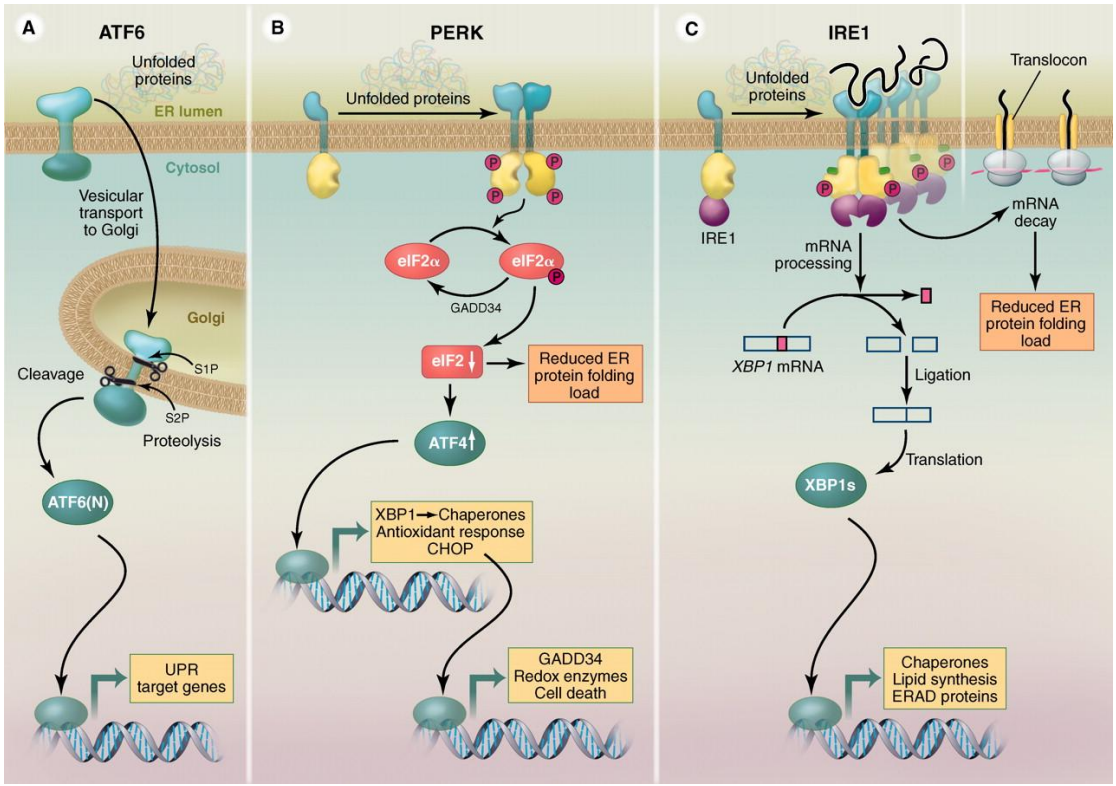

Figure 1.2. The unfolded protein response pathways

The three pathways detect a build up of unfolded ER proteins and activate transcriptional regulators. **A.** ATF6 travels to the golgi where it is cleaved by S1P and S2P to release its cytoplasmic transcription factor domain. **B.** PERK homodimerises and autophosphorylates allowing the phosphorylation of eIF2α which can prevent general protein translation, but increase the translation of the ATF4 transcription factor. **C.** IRE1 oligermerises and autophosphorylates causing the splicing of XBP1 mRNA, which allows the transcription regulator to be translated. Adapted from (Walter and Ron, 2011).

1.*8.1 IRE1*

IRE1 is the most evolutionarily conserved branch of the UPR, and the only one that exists in yeast (Cox, 1993). Two mammalian homologs exist, IRE1α which is expressed ubiquitously (Tirasophon et al., 1998), and IRE1β found mostly in the intestinal epithelium (Bertolotti et al., 2001). Under ER stress IRE1 dissociates from its partner, BiP, and homodimerises/oligermerises causing autophosphorylation. The phosphorylation induces the splicing of X-box binding protein 1 (XBP1) mRNA allowing translation of the DNA-binding domain (DBD) and transcriptional activation domain (AD) (Yoshida et al., 2001). The spliced XBP1 (XBP1s) protein travels to the nucleus where it upregulates the transcription of its target genes. Unspliced XBP1 (XBP1u) is constitutively translated. It was initially thought to be inactive and rapidly sent to the proteasome for degradation, however since then it has been shown to have a negative feedback regulatory function. XBP1u builds up in the recovery phase of ER stress and forms a complex with XBP1s which is rapidly degraded due to a degradation motif in the XBP1u version (Lee et al., 2003; Yoshida et al., 2006). How IRE1 detects ER stress has been questioned, although IRE1 could compete with unfolded ER luminal proteins for BiP binding. When BiP is in short supply, IRE1 would lose its bound BiP allowing its autophosphorylation (Kimata et al., 2007). Alternatively, ER stress could be sensed by binding of unfolded proteins directly to IRE1α. Initially this was thought to be via a deep groove, ideal for ligand binding, formed when IRE1 dimerises (Creddle, 2005). A fuller structural picture of the luminal and cytosolic domains of IRE1 is being developed on the back of more recent crystal structures (Lee et al., 2008).

An additional mechanism of IRE1 has been described in the UPR, with it promoting the degradation of other mRNAs, in addition to the splicing of XBP1, in order to reduce the ER protein folding load. IRE1 targets mRNAs, such as cCD59, with a CUGCAG consensus sequence

within its cleavage site making them substrates for exonucleolytic decay by the cytosolic exosome (Oikawa et al., 2010).

IRE1 and XBP1 are not limited to the role described above, but also partake in other pathways influencing protein expression and cell fate. This is exemplified by the cross talk between inflammatory pathways and IRE1. Upon activation, IRE1 binds TNF receptor-associated factor 2 (TRAF2) initiating the downstream NF-kB mediated proinflammatory cytokine production (Zha, 2015). IRE1 has also been shown to have a crucial role in glucose and lipid metabolism, with prolonged IRE1 mediated c-Jun N-terminal kinase (JNK) activation contributing to insulin resistance, more so than lipid accumulation (Sun et al., 2015). Under extreme ER stress IRE1 can bind the E3 ligase TRAF2 causing apoptotic signalling (Urano, 2000). These are just two examples of the wide range of IRE1 substrate interactions.

1.8.2 PERK

The stress-sensing mechanism of PERK is very similar to that of IRE1 due to structural homology between their ER luminal domains. Again, activation of PERK occurs upon dissociation from BIP, followed by homodimerisation, autophosphorylation, activation and subsequent phosphorylation of eukaryotic initiation factor 2 (eIF2). eIF2α associates with the 40S ribosomal subunit along with GTP, which is hydrolysed to GDP upon the addition of the large ribosomal subunit of the complex. The phosphorylation of eIF2α diminishes the conversion of GDP to GTP. Without the GTP eIF2 complex translocation cannot occur, alleviating the burden of additional protein synthesis (Ma et al., 2002). In general, phosphorylation of PERK and eIF2α reduce protein translation yet exceptions do exist in the form of the transcription factors ATF4 and ATF5, whose translation is facilitated. Transcription of genes concerned with amino acid metabolism and combating oxidative stress is increased

e.g. ATF4 (Harding et al., 2003) and TXNIP, which activates IL-1β and mediates ER stress-mediated β cell death by ATF5 (Oslowski et al., 2012). In addition to its general role in the UPR, the PERK pathway is thought to be especially vital for pancreatic β cell function, as its absence leads to β cell loss and hyperglycemia (reviewed by (Lee, 2014)). Translational attenuation caused by PERK signalling is transient owing to the dephosphorylation of eIF2α by protein phosphatase 1 (PP1). This is important to allow for the production of mRNA associated with protein folding functions.

1.8.3 ATF6

ATF6 is the principle sensor of the third UPR pathway and varies slightly from the other two. Like IRE1, its ER luminal domain senses ER stress by dissociating from BIP, which under normal conditions retains ATF6 in the ER. Without BIP bound, ATF6 travels to the golgi where it is cleaved by sphingosine-1-phosphate (S1P) and sphingosine-2-phosphate (S2P) releasing the cytoplasmic domain which forms a transcription factor. The cytosolic portion of ATF6 travels to the nucleus and induces transcription of its target genes. The transcriptional response overlaps with the response to XBP1 (reviewed in (Lee, 2014)).

When the ER stress is chronic or severe, the UPR results in apoptosis, and the PERK pathway is the main driver of the apoptotic response. C/EBP homologous protein (CHOP) is one of the proteins upregulated by PERK. It is a proapoptotic factor but can also induce the dephosphorylation of eIF2α, which increases protein synthesis. If this occurs when protein folding is compromised, the increased unfolded protein load will cause further pro-apoptotic signalling; however, if the protein folding machinery has been largely restored, this allows the diversion from a cell death to a cell survival pathway (Marciniak, 2004; Zinszner et al., 1998). Under severe stress, IRE1 will also induce cell death by indiscriminately degrading ER-localised

mRNA, the signalling mechanism for which has not been described (Hollien et al., 2009). Recent evidence suggests that the cell determines whether it should initiate cell survival or apoptosis by the relative timing of IRE1 and PERK signalling (Walter et al., 2015).

1.9 Disulphide bond formation in the ER

The formation of disulphide bonds is highly favoured in the ER, due to its redox conditions. The ER is highly oxidising compared to the cytosol, reflecting the status of the extracellular space in which the surface and secretory proteins produced will be exposed to following departure from the ER, when they have reached their native state. Surface and secretory proteins often possess multiple cysteines, most of which must form structural and stabilising intra- and inter chain disulphide bonds before they can leave the ER. Disulphide bonds are covalent bonds generally formed by the coupling and oxidation of two thiol (-SH) groups. Despite the oxidising conditions of the ER, in most cases this is a reversible, enzymatically catalysed dithiol-disulphide exchange with an electron acceptor with a disulphide bond that is subsequently reduced. In the ER there is a relay of disulphide exchange reactions, beginning with molecular oxygen and ending with the substrate protein. Although many disulphide oxidoreductases are known, the most central and best characterised is protein disulphide isomerase (PDI), which works together with endoplasmic reticulum oxidoreductin 1 (Ero1). A reduced substrate protein passes electrons to PDI, leaving the substrate protein oxidised and with a disulphide. PDI is now reduced. PDI is reoxidised by Ero1, which transfers the electrons received from PDI onto molecular oxygen producing hydrogen peroxide (H_2O_2) (Figure 1.3).

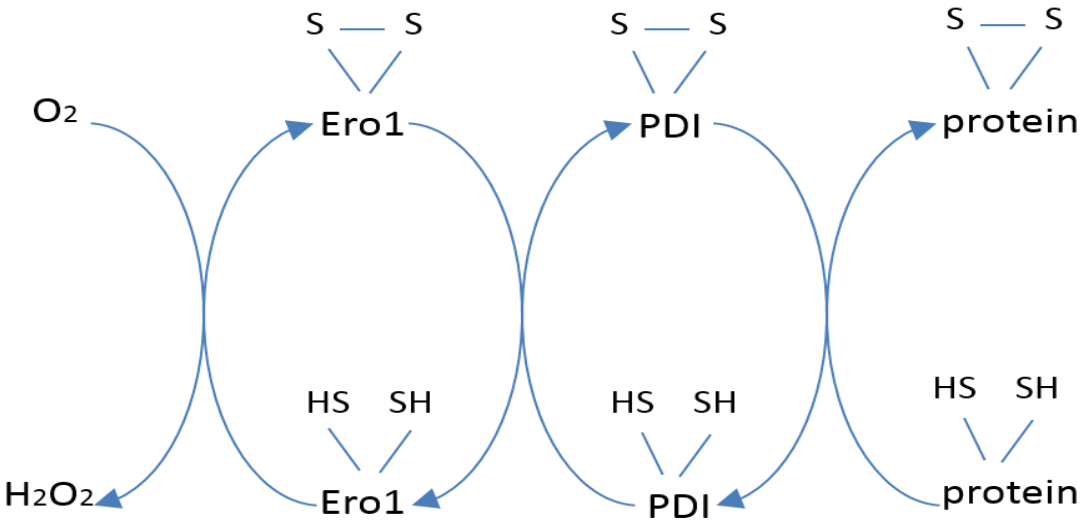

Figure 1.3. Thiol-Disulphide relay between Ero1 and target protein

In the ER, molecular oxygen is a terminal electron acceptor. The subsequent disulphide formed in Ero1 is passed to PDI and on to the folding substrate protein.

1.*9.1 Ero1*

The Ero1 family is a highly conserved ER disulphide generating catalyst, found in in almost all eukaryotes. In mammals two paralogs exist, Ero1α (Benham et al., 2000; Cabibbo, 2000) and Ero1β (Pagani et al., 2000). Some differences exist between the 2 mammalian Ero1 isoforms; both are upregulated by ER stress but only Ero1α by hypoxia (Gess et al., 2003; Pagani et al., 2000). The expression pattern of Ero1α and Ero1β also differs. Ero1α is universally expressed, with cell specific expression of Ero1β in the pancreas and stomach (Dias-Gunaseka, 2005). These differences suggest that the two isoforms may interact with specific PDI partners, and act in different ways. The enzymatic activity of Ero1β is about twice as fast as Ero1α, and regulation of Ero1β is much looser than in Ero1α, which is consistent with its location in secretory tissues, to give it more oxidative activity (Wang et al., 2011).

The yeast Ero1p crystal structure (Figure 1.4) shows 10 α helices make up a single domain formed from the entire chain. Two extended loops after helix α1 are separated by a three-stranded β sheet. This forms a flexible region, which holds a pair of cysteines called the shuttle cysteines. The following α helices form the core structure of the protein. The space in between α2 and α3 holds a Flavin adenine dinucleotide (FAD) cofactor. This buries the FAD isoalloxazine ring within the protein, positioning it next to the active-site cysteines (Cys351-Cys355) (Figure 1.5). No clear channel is seen in this crystal structure for oxygen to reach this ring. It was suggested that, due to the lack of a visible O_2 channel, a gating system may exist (Gross et al., 2004). Two cysteine pairs are involved in thiol-disulphide exchange with PDI, both of which are conserved in the mammalian Ero1α and Ero1β proteins (Bertoli et al., 2004). The Ero1α Cys94-Cys99 pair is found on the flexible loop, the interaction of the loop with PDI allows a conformational change which brings Cys94-Cys99 into contact with the Cys394-Cys397 pair, thus they are known as the shuttle cysteines (Figure 1.5). The Cys394-Cys397 disulphide forms

an active-site near the FAD isoalloxazine ring (Inaba, 2010). Another disulphide is formed between the cysteine pair Cys85-Cys391. This has a structural role, and its absence by mutation leads to a destabilised Ero1α structure which has an abnormal gel migration (Benham et al., 2000).

The human Ero1α protein has also been crystallised to 2.35Å (Inaba, 2010) and has overall similarities to the yeast protein. The shuttle loop of Ero1α, which accepts electrons from PDI, is composed of a co-factor binding, four-helix bundle core region found next to the Cys-X-X-Cys active site. The binding of PDI allows a conformational change, which brings this loop into contact with the other functional region.

For each disulphide produced by Ero1α, one molecule of H_2O_2 is created. This potential reactive oxygen species can generally be dealt with by the cells antioxidant systems and in some cases is utilised or acts as a messenger in other pathways (Veal, 2007). H_2O_2 becomes a potential problem when its amount exceeds the cells ability to deal with it and leads to harmful ER oxidative stress. Due to increased capacity for disulphide production, the overexpression of Ero1p in yeast shows amplified H_2O_2 production.

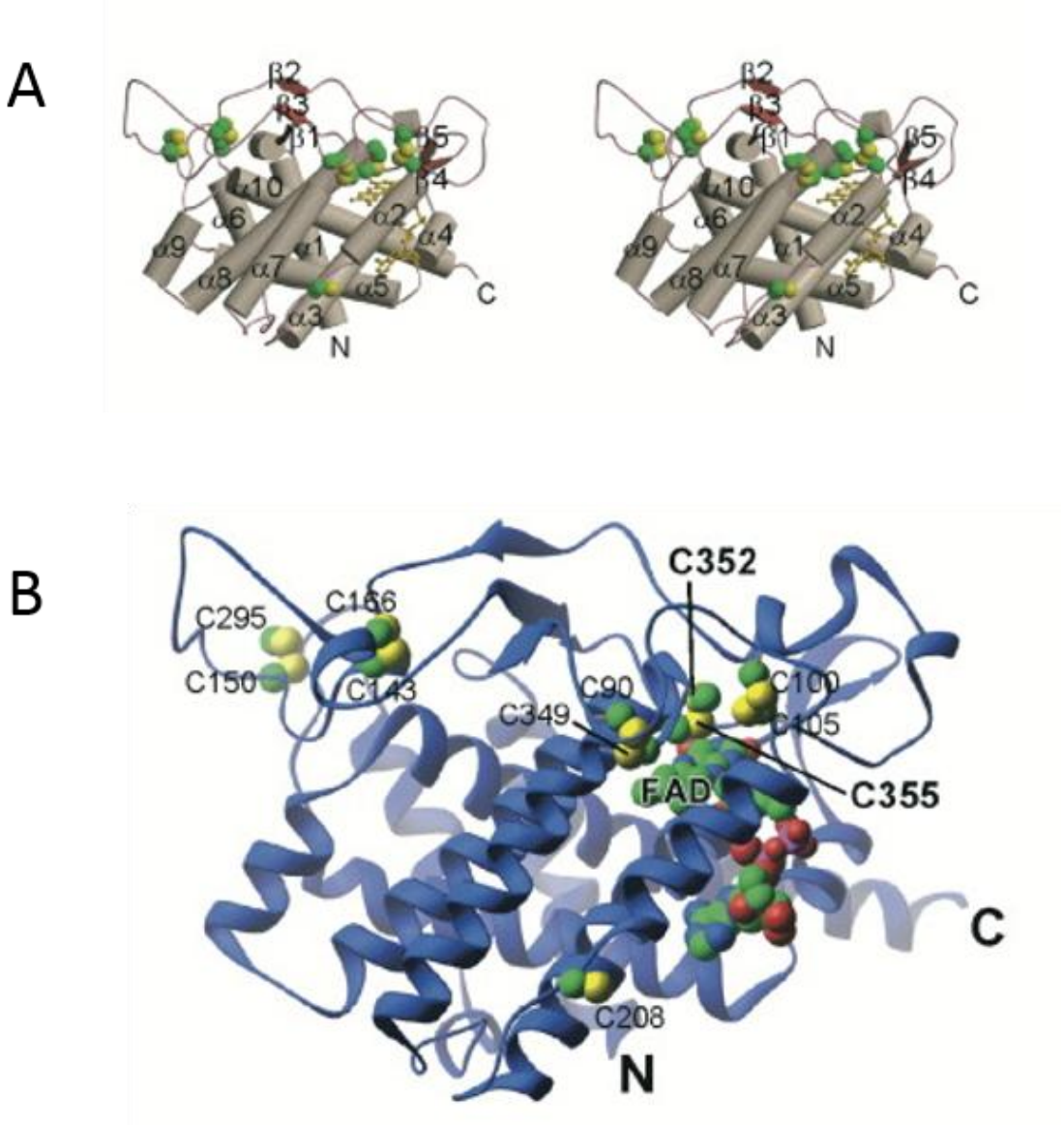

Figure 1.4. Structure of Ero1p

A. Ero1p α helices and β strands, represented by cylinders and arrows respectively, numbered from N to C terminus. The FAD cofactor is represented by gold ball-and-stick and cysteine residues by green and yellow balls. **B**. Ero1p α helices and β strands are represented by ribbons and arrows respectively. The cysteine residues are labelled, numbered and represented by green and gold balls. FAD is labelled and represented by green, red, blue and purple balls. Adapted from (Gross et al., 2004)

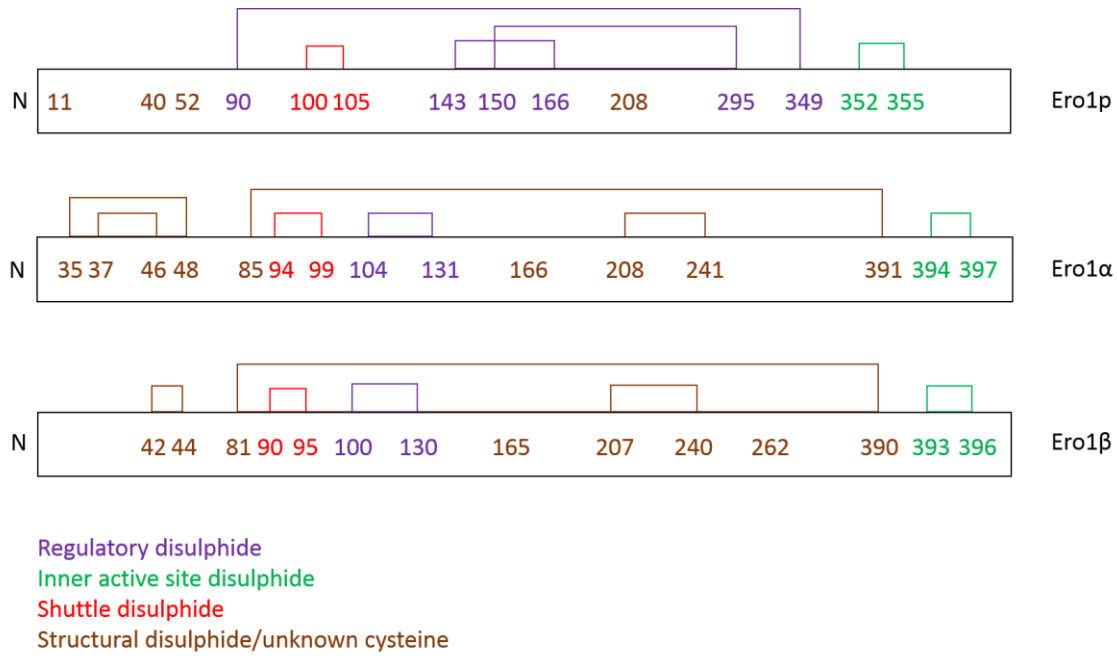

Figure 1.5. Comparison of the disulphide bond arrangements in Ero1p, Ero1α and Ero1β

Cysteine residues are labelled according to amino acid position. Those forming regulatory disulphide bonds are coloured in purple, the inner active sites are in green, the shuttle cysteines are in red and the structural cysteines or those with unknown roles are in brown.

Disulphide bond production must be controlled by the ER environment to prevent hyperoxidation and the oxidative stress associated with excess H_2O_2. Although the oxidising capacity of the ER can be controlled by modifying gene expression levels of Ero1, this is a relatively slow process. A much more rapid system exists at the level of protein modulation. This is in the form of a feedback mechanism within the Ero1 protein, which senses the ER redox status and modifies Ero1 activity appropriately, preventing futile cycles and hyper oxidation. A change in the positioning of an Ero1 disulphide acts as a switch, allowing it to exist in an active or inactive state. This was first found in Ero1p, which was proposed to have two catalytic (Cys352-Cys355 and Cys100-Cys105) and two regulatory (Cys150-Cys295 and Cys90-Cys349) cysteine pairs. When the ER environment is overly oxidising, a disulphide bond is formed between the regulatory cysteines which reduces the activity of the catalytic cysteines. The opposite occurs in relatively reducing ER conditions, with the regulatory cysteines reduced and the catalytic ones active (Sevier, 2007). In the yeast system, PDI1p is the main regulator of activation of Ero1p. It reduces Ero1p regulatory bonds thus causing Ero1p activation (Kim et al., 2012).

The existence of regulated Ero1α forms in mammals was implied from observations of monomeric Ero1α, which appeared as three bands on a non-reducing gel: a reduced form (Red), an oxidised form (OX1) and a compact form (OX2), with the Red form migrating the slowest, and the OX2 form the fastest. The faster migrating OX2 form was favoured under oxidising conditions, and the Red form was apparent when Ero1α was fully reduced (Anelli et al., 2002; Benham et al., 2000). An Ero1α/PDI complex was also seen by SDS-PAGE when transfected cell lysates were subjected to alkylation along with other high molecular weight complexes. The switch mechanism in Ero1α was later identified as a regulatory disulphide formed between Cys94 and Cys131, which blocks the catalytic Cys94-Cys99 disulphide (Appenzeller-Herzog et al., 2008; Chambers et al., 2010). The Cys131 residue competes with

PDI for the interaction with Cys94. A high presence of PDI in reducing conditions would outcompete the Cys131 residue, allowing the activity of Ero1α to be re-established (OX1). In oxidising conditions, Cys131 would not have as much competition and so interacts with Cys94, inactivating Ero1α (OX2) (Appenzeller-Herzog et al., 2008) (Figure 1.6). The regulatory disulphides can be reoxidised by molecular oxygen, however this is a relatively slow compared to catalysis by oxidised PDI (Sheperd, 2014).

The interaction of Ero1α and PDI was initially thought not to be solely dependent on inter-molecular disulphide bonds, since PDI devoid of all of its active site cysteines is still able to induce the OX1-OX2 conversion of Ero1. An additional noncovalent interaction between the two proteins has been suggested, with PDIs redox dependent conformation exploited to optimise delivery of oxidative equivalents (Otsu et al., 2006). More recent studies have shown that a single catalytic domain of PDI, or an octapeptide containing the PDI active site, is sufficient to regulate the activity of Ero1. This regulation is abolished by an active site modifying PDI inhibitor (Zhang, 2014). Zhang also noted that the conformational flexibility of the loop between the regulatory cysteines increases following their reduction, which would allow hydrophobic interactions with PDI.

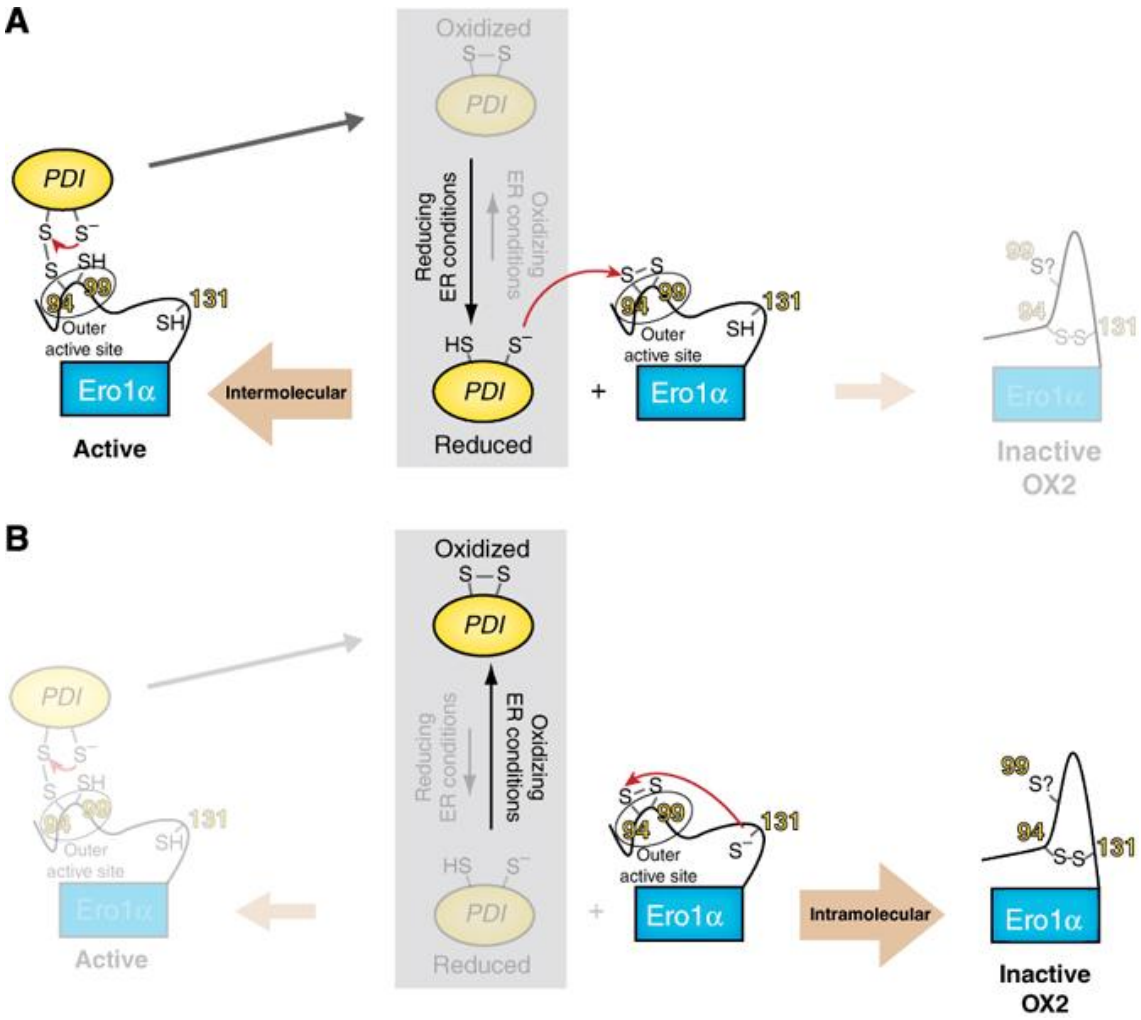

Figure 1.6. ER redox conditions regulate Ero1α outer active site/shuttle cysteines

A. Under reducing ER conditions PDI exists in the reduced form and interacts with the Ero1α cys94, preventing the interaction between the Ero1α active site and regulatory cysteines. The intermolecular disulphide is exchanged, leaving PDI oxidised. **B.** Under oxidising ER conditions PDI exists in the oxidised form and does not compete for the Ero1α outer active site disulphide bond; therefore the Ero1α active site cysteines preferentially interact and form a disulphide bond with the regulatory cysteines. Adapted from (Appenzeller-Herzog et al., 2008).

The regulatory disulphides are conserved between Ero1α and Ero1β. However, Ero1β does contain an extra cysteine, Cys262, which was proposed to engage with Cys100 to form a regulatory bond (Wang et al., 2011). However, molecular modelling of the Ero1β structure showed the Cys262 side chain to be completely buried. Furthermore, mutation of Cys100 or Cys130 hyperoxidises both ERp57 and ER-localised glutathione (GSH) sensors, implicating them as regulatory disulphide bond forming cysteines. As the Ero1α and Ero1β regulatory disulphides are likely to be shared, it can not explain the loose regulation of Ero1β compared to Ero1α. Instead, this has been explained by the inner active site sequence of Ero1β, Cys-Asp-Lys-Cys, which when mutated into Ero1α in place of its active site Cys-Phe-Lys-Cys substantially increases the oxidase activity of Ero1α (Hansen, 2014).

Another level of control has been described in the reoxidation of yeast Ero1p by molecular oxygen, suggesting that this reaction is conditional on the levels of free FAD. Ero1p tightly bound to FAD can undergo numerous rounds of reduction and oxidation. Despite this, high levels of free FAD stimulate the oxidation of Ero1p whilst low levels hinder it. Free FAD is unlikely to act as a terminal electron acceptor; instead a low affinity Ero1p binding site could bind FAD and act as a sensor, modulating the strongly bound FAD, which couples reoxidation of Ero1p to the reduction of oxygen (Tu, 2002). The ER FAD concentration is determined by the cytosol, with an FAD equilibrium existing between the two compartments. Such a dependence on free FAD could link disulphide production to the metabolic or nutritional status of the cell. No such level of control has been seen in mammalian Ero1α, the reason for which is unclear (Sheperd, 2014).

Ero1p maintains its ER localisation via a 127-amino acid terminal extension whilst the plant Ero1 found in the developing endosperm of rice has a rER membrane targeting signal at the N-terminal region (Onda et al., 2009). No such targeting signal exists in Ero1α or Ero1β. Instead the interaction with PDI is required for the ER retention of mammalian Ero1 proteins. Other protein-protein interactions also facilitate the secretory pathway localisation of mammalian Ero1, for example interactions with the PDI homolog ERp44. It is the C-terminal RDEL motif of ERp44 that helps to prevent Ero1 secretion (Anelli et al., 2003; Otsu et al., 2006). Although ERp44 and ERp57 appear to form complexes with Ero1, much evidence has been provided to suggest that PDI is its main interactor: the amount of PDI that co-immunoprecipitates with Ero1 is higher than any other protein, and on western blots PDI is the predominant complex formed with Ero1. As well as this, unlike other ER interacting proteins, PDI is required for ER reoxidation after Dithiothreitol (DTT) treatment and its depletion and over-expression regulate the activity status of Ero1α (Appenzeller-Herzog et al., 2010), although this was later disputed when individual over expression of PDIp, P5, ERp46 or ERp57 was shown to accelerate the inactivation of Ero1α *in vitro.* This means that Ero1α is controlled by the redox balance of an ensemble of PDIs, which is especially important as it indicates that many PDIs with differential expression in particular cell types can also control Ero1α (Zhang, 2014). Regulation is also vital in preventing a build-up of misfolded and misoxidised proteins. An uncontrolled system would result in hyper oxidising conditions with PDI unavailable to perform its role in isomerisation and reduction of misoxidised proteins.

1.9.2 PDI structure

There are over 20 members of the PDI family, most having between one and three redox active sites and all with at least one thioredoxin (trx) domain (Kozlov et al., 2010). Thioredoxins are small reductases made up of five central β-sheets surrounded by four α helices with a

conserved –CGPC- active site motif at the N-terminal of α2 (Eklund et al., 1991). The founding member of the family, PDI, is composed of four trx domains, **a-b-b'-a'**, with an interdomain of 19 residues (x-linker) between the **b'** and **a'** domain (Figure 1.7).

The **b'** domain forms a hydrophobic pocket where the specificity for oxidation by Ero1α lies (Denisov et al., 2009; Inaba, 2010). Some PDIs, such as ERp57, differ in their **b'** domains, where they have different protein surface and electrostatic potentials. These differences result in ERp57 having an intrinsically low reactivity for Ero1α which can be greatly increased by the substitution of its **b'** domain with that of PDI. Consistently, the replacement of the **b'** domain of PDI with that of ERp57 resulted in extremely slow oxidation of Ero1α. The **b'** domain is PDIs main binding site for substrate proteins, however the other domains are also involved in binding larger proteins. This hydrophobic pocket accommodates the protruding β-hairpin of Ero1α and upon removal of the β -hairpin by mutation the interaction between PDI and Ero1α is substantially impaired (Inaba, 2010). Upon formation and cleavage of redox active disulphides within PDI, there is a change of conformation which results in at least a 10 fold lower affinity for Ero1α. This allows PDI to be efficiently cycled as an oxidised PDI will dissociate and not readily bind to ERO1α (Masui, 2011).

As well as binding to Ero1, PDI must also bind effectively to a variety of substrate proteins and release them upon oxidation. The large size of the binding pocket allows this by having a low degree of specificity for hydrophobic ligands, facilitating release upon acquisition of the native structures with fewer hydrophobic residues exposed (Denisov et al., 2009).

Figure 1.7. Schematic of PDI domain structure

PDI is made up of two a domains, **a** and **a'**, and two b domains, **b** and **b'**. **a'** and **b'** are connected by an X linked, and a KDEL ER retention motif is found at the C terminal end.

Initial nuclear magnetic resonance (NMR) studies of individual PDI domains demonstrated that the **b** and **b'** domains show little identity in structure to the **a** and **a'** domains; despite this, the trx fold is preserved whilst the active site it lost along with the cis-proline residue located near the active sites which forms an active site stabilising cis peptide bond (Kemmink et al., 1999).

The redox potential of purified PDI was originally calculated to be E_0' = -175 +/- 15 mV, using a defined GSH redox buffer, and is thus a good oxidant of protein thiols (Lundstrom and Holmgren, Biochemistry 1993). The **a** and **a'** domain hold active sites and individually have similar redox potentials, however the active site in **a'** is preferentially oxidised than that in the **a** domain. When the positions of these 2 domains are switched, it is the **a** domain that is more active, therefore the differences in oxidation can be attributed to the active site next to the C-terminal of **b'** being favourably oxidized by Ero1α (Wang et al., 2009).

In its reduced state, the interface between **a'** and **b'** created by extensive packing shields parts of the substrate binding sites, with the hydrophobic residues found here being characteristic of ligand binding. Upon oxidation of the **a'** active site, its compact conformation is loosened to expose the substrate binding sites. This provides a model helping to explain the activity of PDI. It is believed that Trp-396, which is adjacent to the **a'** active site and interacts with the **b'** domain when PDI is reduced, senses the redox change and has an important role in triggering a conformational change, upon which Trp-396 is exposed (Wang et al., 2012).

The ability of PDI to undergo redox-regulated conformational changes is dependent on the presence of the x linker proceeding an active trx-like domain. When mapped out biochemically, **b'xa**' is the minimal structure required for the conformational change caused when PDI is

oxidised by Ero1α. Although PDI has 4 separate trx-like domains, crystal structures show that they tightly pack to form one compact structural entity integrated by the x linker (Wang et al., 2012).

1.9.3 PDI functions

Oxidative folding is not perfect and errors are often made. A common mistake made by the ER machinery is to create a disulphide too early in the folding of a protein. These are often non-native and cause further misfolding, as cysteines that form bonds in the native structure are forced out of range. Unless such mistakes are corrected, the misfolded proteins are either degraded or aggregate. Oxidoreductases help prevent this from happening as they have the capacity to reduce or isomerise non-native disulphides (Kojer and Riemer, 2014).

Other than its oxidoreductase role, PDI also acts as a chaperone and targets misfolded proteins for ERAD. The catalytic cysteines of PDIs active sites are not involved in the chaperone activity, and so PDI can assist in the folding of model proteins lacking disulphides like GAPDH, citrate synthase and alcohol dehydrogenase (Cai et al., 1994; Primm et al., 1996; Quan et al., 1995).

PDI also engages in other functional protein interactions. For example, PDI acts as a subunit to prolyl-4-hydroxylase (involved in collagen modification and quality control) and triglyceride transferase, stabilising these complexes and localising them to the ER (Bottomley et al., 2001; Pihlajaniemi et al., 1987; Wetterau et al., 1990). PDI also forms aggregates with other chaperones allowing networks to be created before they bind unfolded proteins, rather than assembling on these proteins (Meunier et al., 2002). Chaperone complexes containing PDI are

also found in the ER lumen and at the cystolic face of Sec61 where proteins being translated acquire the correct topology (Stockton et al., 2003).

PDI has been implicated in certain neurodegenerative and protein misfolding diseases. In Parkinson's and Alzheimer's disease, a nitric oxide group is added to both the PDI **a** and **a'** domain active site cysteines, although only a small fraction is modified, it affects their function, and disables the protection PDI provides against the accumulation of protein aggregates. This results in a sustained and non-resolving UPR (Uehara et al., 2006).

Although PDI is found mainly in the ER, where is can reach milimolar concentrations (Hillson et al., 1984; Lyles and Gilbert, 1991), PDI is occasionally found in other compartments such as the cell surface, cytosol and at mitochondrial associated ER membranes (MAMS), where it accumulates in neurons when mutant misfolded huntingtin proteins are expressed. In these circumstances, PDI could trigger apoptotic cell death via mitochondrial outer-membrane permeabilisation. In contrast, inhibiting PDI in rodent brain cells alleviated the toxicity of mutant huntingtin, suggesting that PDI could be therapeutically targeted in neurological diseases like Huntington's chorea (Hoffstrom et al., 2010). On the cell surface, PDI modulates free thiols on activated platelets influencing platelet aggregation (Burgess, 2000). Although there is a growing body of literature to support the recruitment of PDI to plasma membranes, the mechanism by which this is achieved and controlled has remained elusive.

The diversity of the PDI family (21 members in humans) allows them to perform a wide array of specific functions owing to different arrangements of their Trx-like domains (Benham, 2012). ERp44 possess an **a** domain endowed with a CRFS motif, followed by the inactive **b** and **b**' domains and a carboxy-terminal ER retrieval signal. The CRFS motif reduces its efficiency as an

oxidoreductase, but means that disulphides are longer lived due to the absence of the second cysteine, making it especially efficient at its role in quality control and protein transport in the secretory pathway (Anelli et al., 2003). ERp44 possesses another role as a redox sensitive modulator of inositol 1,4,5-triphosphate receptor type 1 (IP_3R1) channel proteins that mediate Ca^{2+} release from the ER. ERp44 binds IP_3R1, inhibiting its channel activity and modifying the generation of Ca^{2+} signals from the ER (Higo, 2005).

ERp57 is a close homologue of PDI, with 33% amino acid sequence identity. It differs at the substrate binding **b'** domain, where it has diverged to preferentially interact with calnexin and calreticulin allowing the promotion of oxidative folding of newly synthesised glycoproteins (Araki and Nagata, 2011; Frickel et al., 2004). ERp57 also forms part the core of the MHC class I peptide loading complex along with tapasin with which it forms a covalent interaction accounting for the stability of the complex (Dick et al., 2002). ERp57 is required for proper functioning of tapasin whose function involves peptide loading and editing functions (Dong et al., 2009). As with ERp44, another of ERp57s roles is in maintaining ER calcium levels. The Ca^{2+} pump sarco ER calcium ATPase (SERCA), is involved with the reuptake of Ca^{2+} into the ER. ERp57 binds and oxidises SERCA when the ER Ca^{2+} stores are full; the resulting disulphide bond inhibits the activity of the pump. When Ca^{2+} stores are low ERp57 dissociates, leaving behind the reduced, more active, SERCA (Li and Camacho, 2004).

PDIp is one of the few PDI family members with specific tissue distribution. Originally throught to be only found in the pancreas and involved in proenzyme folding, it was later found in other tissues, mainly in digestive enzyme-secreting cells, suggesting its expression and function is limited (Desilva, 1997). However, PDIp has a broader role than originally thought, and is especially involved in folding secretory digestive enzymes with high expression levels in gastric chief cells as well as pancreatic acinar cells (Fu et al., 2009).

PDILT is another PDI member with specific localisation (Van Lith et al., 2007). Found in the post-meiotic germ cells of the testis, it interacts with the testis-specific calreticulin-like chaperone, calsperin, and with the calnexin homolog calmegin, to mediate the quality control of disintegrin and metalloprotease domain 3 (ADAM3), required for sperm migration and zona pellucida binding. With only one cysteine in the two **a** domain active sites, PDILT is not involved in disulphide bond oxidation or reduction, but is likely to have a chaperone or scaffolding function (Tokuhiro, 2012).

1.9.4 Reactive oxygen species

One molecule of H_2O_2 is generated for every disulphide produced and molecular oxygen consumed by Ero1α. If kept at sufficiently low concentrations (submillimolar), H_2O_2 has been shown to refold model proteins, meaning two disulphides could be produced from molecular oxygen without harmful by products. This refolding could occur directly by the peroxide, or via PDI (Nguyen et al., 2011). Despite this potential for recycling H_2O_2, and although other mechanisms exist to offset this H_2O_2 production, if disulphide production is not regulated, excess H_2O_2 produced is detrimental to the cell. However, such regulation also has to maintain the ER redox conditions and optimise oxidative folding of native disulphide bonds, so the regulation of the Ero1α cycle is not necessarily solely designed to minimise H_2O_2 production. There is some evidence to suggest that disulphide bond formation, and the resulting reactive oxygen species (ROS), does not induce oxidative stress *per se;* rather it is misfolded proteins, in conjunction with resulting ROS, which is responsible for oxidative stress (Malhotra et al., 2008). This means that effective systems to offset the production of H_2O_2 must be present. There are three peroxidases within the mammalian ER that may do this, namely peroxiredoxin IV (PrxIV), GSH peroxidase 7 (GPx7) and GSH peroxidase 8 (GPx8). There are 8 members of the human

GPx family, and despite their name suggesting they are catalysts in a reaction between peroxide and reduced GSH, the 2 ER resident GPx members (GPx7 and GPx8) lack the GSH recognising residues and GPx catalytic residues found in the other GPx family members. They instead are members of the GPx-like peroxidase (TGPx) family with PDI peroxidase activity. Their expression increases the activity of 4 out of 5 PDI family members tested *in vitro*. ERp57, whose activity was not increased by GPxs, differs in its substrate specificity and **b'** binding site. This may provide an explanation as to why GPx7 and GPx8 does not increase the activity of ERp57 (Nguyen et al., 2011). GPx7 (and probably GPx8) is able to offset the production of H_2O_2 by H_2O_2 oxidising Cys57 to a sulfenic acid, leaving H_2O to be released. Cys86 then attacks Cys57 or the PDI **a** active site cysteine forming an inter- or intra-molecular disulphide; again this releases an H_2O molecule. The disulphide is now transferred to the PDI active site to leave PDI oxidised and GPx7 reduced (Figure 1.8). *In vitro*, GPx7 interacts with the **a** domain of PDI whilst Ero1α does so with the **a'** domain in a sequential manner. Consequently, it has been suggested that GPx7 may also be transiently close to PDI during the oxidative folding cycle (Wang, 2014).

There is some evidence from bimolecular fluorescence complementation (BiFC) to suggest that GPx7 and GPx8 can physically and functionally interact with Ero1α. GPx8 (and presumably GPx7) associates with an Ero1α molecule, stabilising the 32 amino acid loop region between Cys208 and Cys241. Mutation of this region in Ero1α led to a decreased BiFC signal. This position puts GPx8 in close proximity to the site of peroxide exit from Ero1α allowing the peroxide to be utilized immediately (Nguyen et al., 2011; Ramming et al., 2015). Gpx8 is predicted to be a type 1 transmembrane protein, with its catalytic domain in the ER and a short N-terminal cytoplasmic region.

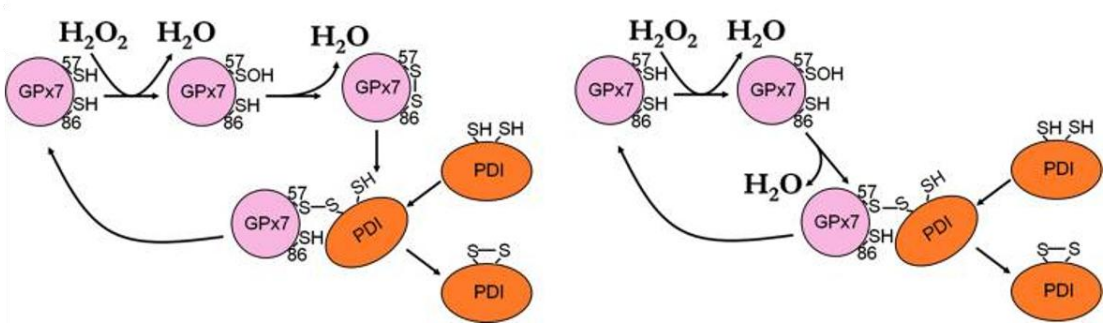

Figure 1.8. Catalysis of disulphide bond formation by GPx7 and PDI from H_2O_2

H_2O_2 oxidises GPx7, with Cys57 forming a sulfenic acid and releasing H_2O. Another H_2O is released upon forming a disulphide between GPx7 Cys57-Cys86, which is passed onto Cys57-PDI through thiol-disulphide exchange (shown on left). Alternatively, upon release of the second H_2O, a disulphide is formed directly between Cys57-PDI (shown on the right). Finally the intermolecular disulphide bond is passed onto PDI to form an oxidised PDI active site. Adapted from (Wang, 2014).

Knockdown of GPx8 causes an elevation of the UPR and antioxidant response markers as well as increasing oxidation of the cytosol. Knockdown of PrxIV does not induce the same response, suggesting that there is some functional separation between the two proteins, with PrxIV targeting H_2O_2 of an unknown origin and only reacting with H_2O_2 produced by Ero1α when it is at high concentrations. It is likely that the interaction between Ero1α and Gpx8 prevents PrxIV from gaining access to Ero1α derived H_2O_2 (Ramming et al., 2014). Further to this, GPx8 is potentially stabilised by its interaction with Ero1α. Such a reliance may provide further evidence for a functional separation (Ramming et al., 2015).

Another method of disulphide generation is via the VKOR enzyme. VKOR is a transmembrane protein with two conserved cysteine pairs, which catalyse the reduction of vitamin K epoxide to vitamin K hydroquinone, an activity that is crucial for the function of blood clotting factors. Homologues of the human VKOR enzyme have been described as an alternative oxidiser of PDI in humans and is present in numerous other organisms, such as bacteria, including cyanobacteria, and mammals (Schulman, 2010; Singh et al., 2008). Oxidised VKOR is able to exchange its disulphide with trx-like oxidoreductases. When VKOR or Ero1 is knocked down alone in HepG2 cells, the effects are minimal, but when both genes are ablated in combination, disulphide bond formation in the model protein albumin is delayed (Rutkevich and Williams, 2012).

The presence of multiple oxidative folding pathways, which are independent of Ero1 is implied by mice with complete loss of function of Ero1. Although these mice have an enhanced load of unfolded protein intermediates and are subjected to the UPR, along with other abnormalities,

they are still viable (Zito et al., 2010). The same loss of function is fatal in *C. elegans,* suggesting that the presence of extra oxidative pathways is exclusive to mammals.

1.9.5 ER oxidising equivalents

The oxidising conditions in the ER must be maintained for optimal disulphide bond formation. GSH plays a huge part in ensuring redox homeostasis by acting as a redox buffer. GSH is a low molecular weight thiol synthesised in the cytosol, where it is maintained in its reduced form by GSH reductase. This maintains the reducing conditions in the cytosol, meaning disulphides are rarely formed here (Hwang et al., 1992). GSH is delivered into the ER where it serves as a reducing equivalent and balances oxidation by Ero1. Once in the ER, part of the GSH pool becomes oxidised and this GSH disulphide (GSSG) can no longer diffuse out of the ER (Banhegyi et al., 1999). Under reducing conditions, GSSG can oxidise reduced PDI, which in turn regulates Ero1 activity. Although disulphide formation can occur in the absence GSH and GSSG, it is thought that they still play an important role in the ER, with low GSH levels accelerating non-native disulphide formation (Chakravarthi and Bulleid, 2004). Furthermore, GSH levels rise during oxidative stress and help eliminate ROS, indicating that GSH has both protective and disulphide bond forming roles (Chakravarthi et al., 2006). However, a more recent study shows that depletion of GSH does not have measurable effects on ER disulphide bond formation and thus is not needed to maintain thiol redox or folding homeostasis (Tsunoda et al., 2014). This questions the importance of GSH in ER redox and suggests that other small molecule thiols exist with the same function.

1.10 The MHC

Oxidative protein folding in the ER introduces disulphide bonds into client or substrate proteins, and the main client to be considered in this thesis is the Major Histocompatibility Complex (MHC). The MHC is a family of genes that play a significant role in the immune system by presenting peptide antigens to T cell receptors. The MHC proteins are synthesised in the ER and therefore a knowledge of their disulphide bond formation and ER quality control is important for understanding susceptibility to infection, autoimmunity and immune disease. In humans the genes for the MHC, called human leukocyte antigens (HLA), encompasses about 3.6 megabase pairs and is found on the short arm of chromosome 6 at 6p21.3 (Fernando et al., 2008). The HLA gene cluster is divided into three regions, encoding class I, II and III genes. Class I and II are classical HLA genes, the proteins they code for bind peptides intracellularly and present them at the cell surface to provide a means of self-identification for subsequent immune recognition.

1.10.2 MHC class I

MHC class I molecules are found on nearly all nucleated cells (Ploegh et al. 1981). These transmembrane heterodimers and are composed of a highly polymorphic heavy (α) chain composed of three domains, α1, α2 and α3. Domains α1 and α2 make up the antigen binding site, and α3 associates with the light chain β2 microglobulin (Figure 1.9). The MHC class I molecule binds intracellular peptides (e.g. those derived from viruses) that have been transported from the cytosol into the endoplasmic reticulum. The process of MHC class I assembly and binding to high affinity peptides requires the assistance of a set of the ER chaperones including calnexin, calreticulin and ERp57 (previously discussed in sections *1.4*) which make up the peptide loading complex (PLC). This is responsible for recognising and

loading of peptides onto the MHC class I- β2 microglobulin heterodimer. The PLC begins to form following the synthesis of the heavy chain, which interacts with BiP and calnexin. The light chain attaches to this complex prompting calreticulin to replace calnexin and stimulating the recruitment of the other PLC components, namely tapasin, ERp57 and TAP (the peptide antigen transporter). Upon completion of peptide loading, the removal of a last glucose residue allows MHC class I trafficking and progression through the secretory pathway. Quality control mechanisms prevent MHC class I molecules which are unstably bound to peptide from exiting the ER; these molecules are re-glycosylated and given another opportunity to bind high affinity peptides (reviewed in (Hulpke and Tampe, 2013)). Recently Ero1α has also been described to have a role in the correct formation of the PLC. MHC class I has two disulphide bonds in the α2 and α3 domains which must be created before interaction with the MHC class I light chain. Whilst the heavy chain is complexed with calnexin, it has been proposed that Ero1α associates with the heavy chain through calnexin and, via PDI, mediates heavy chain oxidation (Kukita et al., 2015).

The MHC class I molecule traffics to the cell surface once a high affinity peptide has been bound. Here CD8+ T cell receptors recognise antigen derived peptides in the context of MHC class I, causing them to proliferate and induce the destruction of the cell that is presenting a "foreign" peptide (Madden, 1995).

1.10.1 MHC class II

MHC class II molecules present peptides from extracellular material to T-cells to initiate an immune response. They present the peptide in such a way that they can be bound by specific T cell receptors on the surface of $CD4^+$ T cells. This activates further downstream effects, such as T-cell proliferation, antibody production and effector T-cell function, which help form an

immune response to eliminate the pathogen (Berger and Roche, 2009). These transmembrane glycoproteins are able to bind a vast array of peptides due to their highly variable peptide-binding site. This is formed by the interaction of the two chains of the MHC class II molecule. This heterodimer consists of a 33-35 KDa α chain and a 26-28D Kd β chain, both of which have a transmembrane region, a cytoplasmic unit and two extracellular domains (named α1/α2 in the α chain, and β1/β2 in the β chain). The peptide binding site is formed by β-pleated strands and α helical formations made by the α1 and β1 domains (Marsh, 2000)(Figure 1.9).

In humans, three different loci encode class II MHC molecules: HLA-DP, DR and DQ. Although these isotypes are about 70% similar to each other the proteins have different stabilities and requirements for their intracellular assembly (discussed in *1.10.4*). Variation in the repertoire of peptides able to bind to MHC class II molecules is not only created by the different isotypes, but also by the great level of polymorphism seen within them, most of which is concentrated in, or around, the peptide-binding site. MHC class II molecules are co-dominantly expressed, which increases the range of presented peptides that CD4+ T cells are able to respond to.

MHC class II molecules are found in professional antigen presenting cells (APC) (Hitbold, 2002). Professional APCs include dendritic cells, macrophages and B-lymphocytes. These are cells whose specialized function is to acquire, process and express exogenous antigens at the cell surface in the context of MHC class II. In general, CD4+ cells, which are only able to recognise peptides presented by MHC class II molecules, are either activated or induced to become regulatory cells according to the affinity of the presented peptide and the nature of the local cytokine environment. The ligation of co-receptors provides co-stimulatory signals for activation, with T cell receptors such as CD28 interacting with CD80 or CD86 in APCs. Their expression of MHC class II may differ as they develop and their role changes, for example,

dendritic cells show a rapid increase in MHC class II transcription following maturation (Landmann et al., 2001).

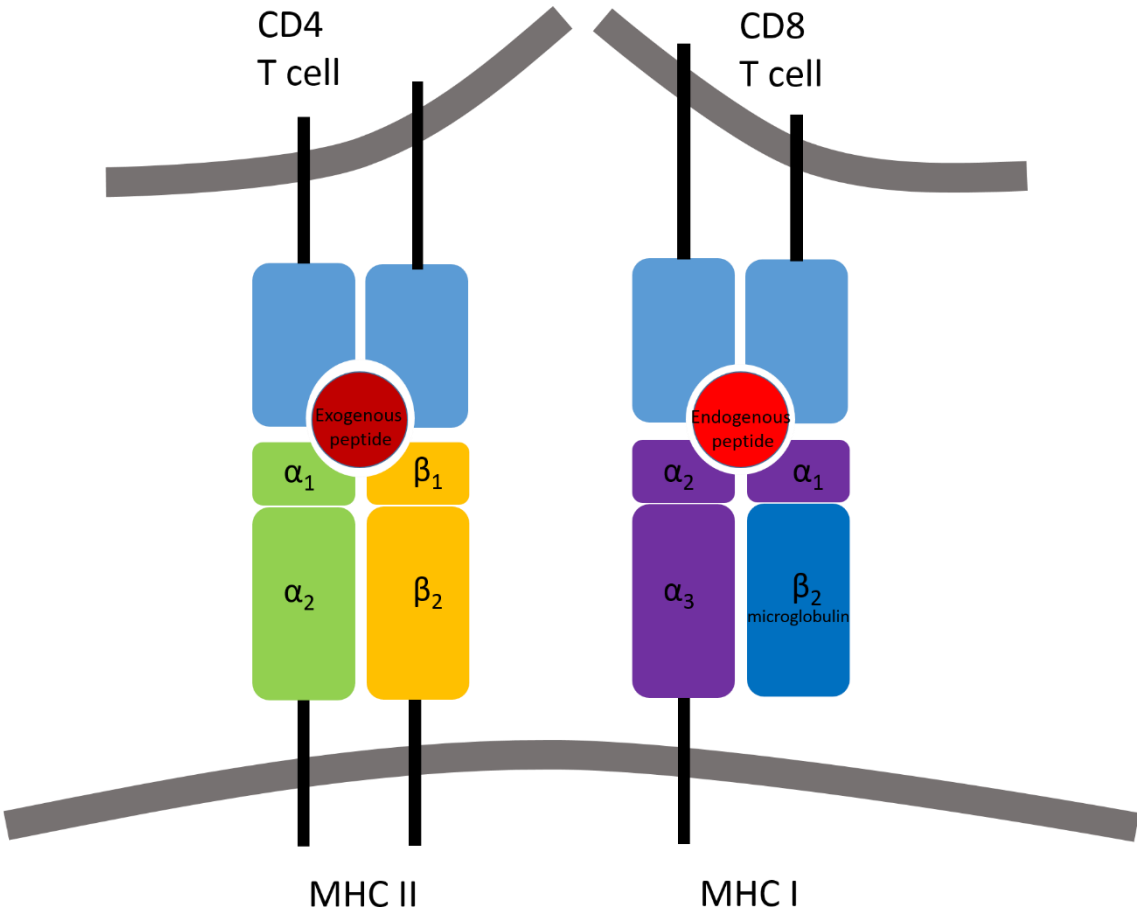

Figure 1.9. Comparison of MHC class I and II molecules

MHC class II mollecules are composed of an α chain (composed of α_1 and α_2) and a β chain (composed of β_1 and β_2). α_1 and β_1 make up the peptide binding site which binds exogenous peptides and presents them to CD4 T cells. MHC class I molecules are composed of three α domains, α_1, α_2, and α_3, of which α_1 and α_2 make up the peptide binding site, and α_3 associates with β_2 microglobulin. They bind endogenous peptides which are presented to CD8 T cells.

1.10.3 MHC class II assembly

The trafficking of MHC class II molecules is slightly more complicated than MHC class I as they must be prevented from binding cytosolically derived peptides following biosynthesis in the ER, where the α and β chain join to form a heterodimer. To prevent the loading of ER localised peptides into the MHC class II peptide binding site, the invariant chain (Ii) associates with this groove. By preventing premature peptide binding, Ii allows the MHC class II molecules to continue assembling and folding correctly.

The mechanism by which the MHC class II subunits assemble with Ii is still open to question. MHC class II α and β chains are able to efficiently form dimers however these tend to be misfolded, resulting in lost epitopes and inefficient transport through the secretory pathway, as found from experiments using conformation specific antibodies (Anderson and Miller, 1992). Ii acts as a chaperone, promoting effective association and folding of the α and β chain. Four forms of Ii exist, all synthesised from the same precursor mRNA by alternate splicing (Strubin et al., 1986). The two short versions, p41 and p43 have low expression levels and a protease inhibitory domain, whereas the 2 most predominant ones, p33 and p35, have a ER retention sequence in an extended N-terminal cytoplasmic domain (reviewed in (Cresswell and Roche, 2014)). p33 and p35 can form mixed trimers via the Ii trimerisation domain, that acts as a scaffold for the attachment of 3 MHC class II αβ pairs. The trimer is retained in the ER by a retention signal in p35; the ability to leave the ER may be attained by a change in conformation in the cytoplasmic tail, or by the masking of the retention signal by the α and β chains (Lamb, 1992). This model has been questioned recently by the idea that Ii matches the αβ pairings by binding only one α chain in the scaffold which it then matches to a β chain (Koch, 2007, 2011). Although $\alpha\beta$Ii nonamers have been demonstrated for HLA-DR1, it is not clear whether HLA-DP

or HLA-DQ class II molecules are assembled by the same route, or whether all HLA-DR allelic variants require nonamer formation for their onward transport.

A leucine-isoleucine motif found in the cytoplasmic tail of Ii targets the Iiαβ trimer to a late endosomal compartment known as the MHC class II compartment (MIIC), thus Ii also acts as a trafficking protein (Pieters J, 1993). In order to reach the MIIC, MHC class II travels through the endosomal-lysosomal pathway. Here the compartments become increasingly acidic, activating various cathepsin proteases which start to break down Ii into a small fragment, Class-II-associated invariant chain peptide (CLIP), found in the peptide binding groove of the MHC class II αβ heterodimer. CLIP is exchanged for antigenic peptides in a process mediated by the MHC class II chaperone HLA-DM (Figure 1.10).

Unlike the classical HLA molecules, such as HLA-DP, DR and DQ, DM is not expressed on the cell surface but assists in antigen presentation. HLA-DM binds directly to the αβCLIP complex in the MIIC, releasing CLIP from the peptide-binding site, and allowing peptide exchange. There is a vast array of peptides in this compartment originating from internalized exogenous molecules. These travel through the endocytic membrane transport pathway where they encounter resident proteases and are broken down into short peptides, to which MHC class II molecules are able to bind. The exchange of these peptides is catalysed until a stable αβpeptide complex is formed by an incorporated, generally high affinity, antigenic peptide (Busch et al., 2005). Peptide loaded MHC class II molecules are presented at the cell surface after the membrane fusion of complexes from endosome derived vesicles (Hitbold, 2002).

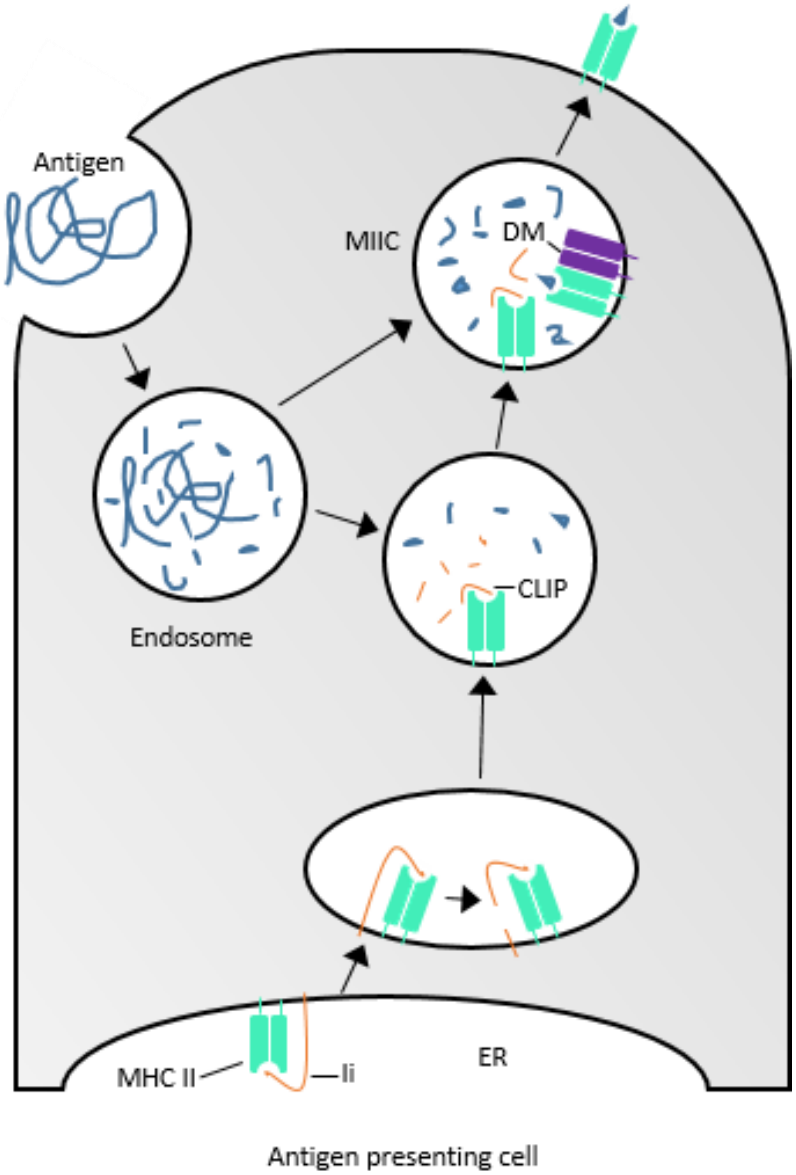

Figure 1.10. MHC class II trafficking

MHC class II heterodimers assemble in the ER. The binding of Ii at the peptide binding site prevents premature binding to antigenic peptides, stabilises the dimer, and targets it for the endosomal pathway. Caspases in the early endosome cleave Ii into CLIP, which is removed with the assistance of HLA-DM allowing MHC class II to bind protein antigens, which have been internalised and broken down. The peptide-MHC class II complex is then trafficked to the plasma membrane.

1.10.4 MHC class II haplotypes

Although the three haplotypes, HLA-DP, DR and DQ, perform the same general function of presenting peptides to $CD4^+$ T lymphocytes, the properties of individual allelic variants and the peptides they are able to present differ. DR and DQ have been studied more extensively than DP and, in comparison, much more is known about these two isotypes. The differences between the three isotypes infer differences in their selectivity in binding peptides. DR molecules are most likely to shelter aromatic and hydrophobic residues in the conserved peptide binding pockets whilst DQ prefers relatively short side chains (Raddrizzani et al., 1997). These differences allow a large repertoire of peptides to be bound and presented by HLA molecules. However, DP molecules are only able to bind a much more limited set of peptides in comparison with DR and DQ (Sidney et al., 2010).

Cell surface expression of DP molecules is significantly less than that of DR and DQ (Diedrichs and Schendel, 1989). This has implications for the level or nature of immune responses they are able to initiate, with the possibility that alterations in expression level could lead to associations with disease. Unusually high expression of certain DP alleles, such as DPB1*01:01, may provide a functional basis for increased susceptibility to chronic hepatitis B virus (Thomas et al., 2012).

As well as there being variability in the binding of peptides between the three classical MHC class II molecules, there are also differences in their assembly and stability requirements. Although all three isoforms require Ii for their targeting to endosomal compartments, a portion of DP molecules can form a stable dimer in its absence (van Lith, 2010). The three MHC class II molecule types also differ in their requirement for HLA- DM. DP and DQ can form stable dimers without DM, however the amount of dimer always increases when DM is introduced.

The ability of DP to form stable dimers without Ii and DM may indicate that other, unknown, accessory factors may help stabilise DP dimers. It is not known whether these dimers are stabilised by ER derived peptides or whether DP$\alpha\beta$ complexes are intrinsically more stable than their DR or DQ counterparts.

Although MHC class II molecules are highly specialised and their function closely regulated, they are often linked to immune diseases. Different HLA- DP alleles are often protective against, or make an individual more susceptible to, immune dysfunction and autoimmune diseases. The potential of there being different accessory factors involved with DP could provide an explanation as to why certain diseases, like chronic hepatitis B, are linked to DP (Kamatani et al., 2009). Often it is unknown why certain MHC class II molecules are associated with disease, but sometimes this can be explained by inefficient interactions with peptides or accessory proteins. Examples of this include the possibility that different alleles are less susceptible to cathepsins which reduce Ii to CLIP (Hsing and Rudensky, 2005), that different alleles have lower or higher affinities for CLIP (Busch et al., 2005), or that different class II-peptide complexes have different susceptibilities to the action of HLA-DM. Often the “classical” HLA molecules are associated with protection against diseases, and in some of these cases the expression of certain genes is linked with an increase in the levels of HLA-DM. This results in increased stability of MHC class II molecules, leading to an elevated immune response. An example of this is in acute myeloid leukemia where a good clinical outcome is associated with a chromosomal abnormality, bringing the ETV6 and AML1 genes together. This rearrangement increases the expression of HLA-DR and HLA-DM (Jastaniah et al., 2006).

Certain HLA-DR or DQ molecules associated with autoimmune diseases may bind inefficiently to Ii, for example in rheumatoid arthritis (Patil et al., 2001). Whether this kind of inefficient binding in relation to DP molecules would also initiate an autoimmune response is

questionable due to its ability to form stable dimers without Ii. Although less is known as to how DP contributes to immune dysfunction, it is known that DP is associated with hepatitis B (Kamatani et al., 2009), and beryllium disease. In beryllium disease, DP molecules with a glutamic acid at position 69 have been linked with susceptibility (Richeldi et al., 1993). This glutamic acid may change the conformation of a pocket within the peptide binding groove, making it larger and allowing access to beryllium. Additionally, a solvent-exposed pocket amino acid may also favour beryllium binding. It is the increased affinity for and subsequent binding of beryllium that triggers an adverse immune response to the heavy metal in the environment (Silveira et al., 2012). Further investigation into DP folding and quality control could prove valuable in helping to explain such relationships.

1.11 Thesis aims

Both Ero1a and Ero1b are tightly regulated in the ER. This allows the introduction and isomeration of native disulphide bonds by PDI whilst also maintaining the ER redox balance. This thesis aims to investigate Ero1 and its putative substrate MHC class II by:

Gaining a better understanding of how Ero1 activity is controlled, and how Ero1 structures are affected and contribute to the impact of homocysteine treatment.

Investigating the difference between the control of Ero1α and Ero1β and whether this changes in different cell types.

How changes in Ero1 activity affect the ER folded MHC class II, as well as factors influencing the stability of MHC class II.

2. Materials and Methods

2. Materials and Methods

2.1 Cell culture

The human melanoma MelJuso cell line and the human fibrosarcoma HT1080 cell line were maintained in Dulbecco's modified Eagle's medium (DMEM, Gibco, ThermoFisher Scientific), and the human cervical carcinoma HeLa cells in Minimum essential medium (MEM, Gibco, ThermoFisher Scientific). The media was supplemented with 2mM glutamax (Gibco, ThermoFisher Scientific), 8% foetal calf serum (Sigma), 100 Units ml^{-1} penicillin and 100 micrograms ml^{-1} streptomycin (Sigma). The human monocytic leukemia THP-1 cell line and the human lower esophageal adenocarcinoma OE33 cell line were maintained in RMPI 1640 (Gibco, ThermoFisher Scientific) supplemented with 2mM glutamax, 100 Units ml^{-1} penicillin, 100 micrograms ml^{-1} streptomycin, and 10% foetal calf serum. All of these cultures, except THP-1 cells, were passaged every 48-72 hours, when at about 90% confluent. To passage the adherent cells, they were washed twice with phosphate buffered saline (PBS) (Sigma) and trypsinised using 0.05% trypsin (Gibco, ThermoFisher Scientific) for 5 minutes at 37°C until the cells lost their attachments to the dish. The cells were resuspended in fresh media, and diluted 1:10 into fresh media for reseeding onto 10cm dishes or flasks. The THP-1 cell line was passaged by spinning down at 218 g for 4 mins, washing with PBS and resuspending. The media was refreshed once a week. All cells were free from mycoplasma and maintained at 5% CO_2 and 37 ^{o}C in a humidified incubator (BINDER).

2.2 Tissue samples

Tissue samples were obtained from FVB or C57BL/6 mice by dissection after schedule 1 killing. Liver and pancreas tissue samples were either cut into small pieces and snap frozen placed in liquid nitrogen, or placed into a vessel containing PBS on ice for immediate usage. Single cell suspensions were made by passing tissue through a 40 μm cell strainer (BD biosciences) in PBS. The suspended cells were pelleted at 400g for 5 min and resuspended in complete media. HT1080 cells were trypsinised, washed in PBS, and resuspended in complete media to make single cell suspensions.

2.3 Antibodies

The polyclonal rabbit antisera against PDI was generated by immunising rabbits with a purified rat PDI protein preparation, as described (Benham et al., 2000). The polyclonal D5 antiserum against Ero1α was raised in rabbits against a purified MBP-Ero1α fusion protein (Mezghrani et al., 2001). The monoclonal antibody 2G4 was raised against recombinant Ero1α and was a kind gift from Prof. Roberto Sitia. The polyclonal antibody against Ero1β (4131) was raised against a unique internal peptide YTGNAEEDADTKTLL and generated for the laboratory by Sigma Genosys (Dias-Gunasekara, 2005).

The mouse monoclonal antibody raised against βactin (Abcam, ab8224), the mouse monoclonal antibody raised against myc (antigen EQKLISEEDL, Cell Signalling, 9B11), the mouse monoclonal antibody raised against HA (antigen YPYDVPDYA, Cell Signalling, 262K), the mouse monoclonal antibody raised against V5 (antigen GKPIPNPLLGLDST, Invitrogen, 46-0705),

and the mouse monoclonal antibody raised against TLR3 (Imgenex, 40C1285.6) were commercially available.

The mouse monoclonal antisera HC10, raised against free MHC class I B and C allele heavy chains (Stam et al 1986), the mouse monoclonal 1B5, which was raised against the C-terminus of the MHC class II DRα heavy chain, the rabbit polyclonal antisera raised against the MHC class II DP, which recognises the DPβ and weakly recognises the DPα when DPαβ are co-expressed, and the rabbit polyclonal antisera raised against the MHC class II DRβ and DP, which primarily recognises the DPβ chain, but also faintly detects DPα chain, were kind gifts from Prof. J. Neefjes, Netherlands Cancer Institute, The Netherlands. The concentrations or dilutions of the antibodies used are shown in Table 1.

2.4 Chemicals

For leupeptin and NH_4Cl treatments, cells were incubated with complete media containing 15 nM leupeptin, 20 mM NH_4Cl or mock treated with complete media only for 1 hour. Cells were washed with PBS and analysed by immunofluorescence.

Homocysteine and cystathionine treatments were carried out by incubating cells with 0, 0.1, 1 or 10 mM homocysteine or cystathionine in complete media for 1 hour. Cells were then washed and lysed for protein analysis.

Table 1- Antibody concentrations and dilutions used for western blotting and immunofluorescence

Antibody	**Application**	**Dilution**
Anti-PDI (pAb)	WB	1:1000
D5 (pAb)	WB	1:1000
Anti-actin (mAb)	WB	1:1000
Anti-myc (mAb)	WB	1:1000
Anti-HA (mAb)	WB	1:2000
Anti-V5 (mAb)	WB	1:500
Anti-TLR3 (mAb)	WB	1:500
Anti-TLR3 (mAb)	IF	1:25
HC10 (mAb)	WB	1:200
Anti-DRβ (pAb)	WB	1:1000
Anti-DP (pAb)	WB	1:1000
Anti-DP (pAb)	IF	1:200
1B5 (mAb)	WB	1:1000
1B5 (mAb)	IF	1:200
4131 (pAb)	WB	1:200

Ascorbic acid treatments were carried out alongside 0, 1 or 10 mM homocysteine incubations, as described above. Zero, 10, 100 µM or 1 mM ascorbic acid was mixed with each concentration of homocysteine in complete media prior to application, and the cells were incubated with these reagents for one hour. After incubation, cells were lysed for protein analysis.

The single cell suspensions were treated with either 10 mM homocysteine or 10 mM DTT in complete media, or mock treated with complete media alone for 1 hour with agitation. Cells were lysed and the lysates taken for protein analysis, as previously described.

ER Tracker or Lyso Tracker (both Invitrogen) were applied to cells at a 1:2000 or 1:5000 dilution respectively, 10 mins prior to imaging cells.

The chemicals used were obtained from Sigma unless otherwise stated.

2.5 RNA extraction

To obtain nucleic acids from tissue culture cells, the cells were washed twice with PBS and lysed in 250µl TRI-reagent (Sigma). After the addition of 50µl chloroform, the lysates were vortexed and centrifuged for 15 mins at 4°C at 16,100 g in a bench-top centrifuge (Eppendorf). The top phase was removed, added to 125µl isopropanol, vortexed, left on ice for 10 mins and then centrifuged for 10 mins at 16,100 g. The supernatant was removed and the pellet was washed with 400 µl 75% ethanol, vortexed and spun at 7,600 g for 5 mins. The supernatant was removed, pellets air dried and resuspended in 10 µl nuclease free water.

2.6 RT-PCR

Spectrophotometry was used to determine the concentration of extracted RNA using a spectrophotometer (ND-1000 LabTech international). Samples were diluted to 50 ng/µl for RT-PCR. An AccessQuick RT-PCR kit (Promega) was used to subject 50 µg RNA to RT-PCR. The cycling protocol used for RT-PCR was 45 °C for 1 hr, 94 °C for 2 mins, (94 °C for 30 secs, 60 °C for 1 min, 72 °C for 1 min) 30 times, then 72 °C for 5 mins with the PCR being held at 4°C upon completion of the cycle. Resulting cDNA was run on 1% agarose gel (1% agarose w/v made up in 120 ml of TE buffer and 5.5 µl ethidium bromide (Fisher Scientific), to stain the gel) at 100 mV for about 40 mins. The DNA was visualised by exposure of the agarose gel to UV light and the gel photographed on a Uvidoc system. The primers designed and used in this study are shown in Table 2.

2.7 Cell lysis for protein analysis

Cells in tissue culture were washed twice with PBS and lysed for subsequent protein analysis at 4°C in MNT lysis buffer (1% Triton-X100, 20 mM MES, 30 mM Tris-HCl, 100 mM NaCl, pH 7.4 and the protease inhibitors cystatin, leupeptin, antipain and pepstatin A at 1 microgram/ml). Unless stated, lysis buffer was supplemented with 20mM N-ethylmaleimide (NEM) to prevent disulphide bond rearrangement. Lysates were centrifuged at 16,100 g for 10 minutes at 4°C to remove nuclei. The post nuclear supernatants were either snap frozen in liquid nitrogen or taken forward for further analysis by sodium dodecyl sulfate (SDS) -PAGE.

Table 2- RT-PCR primers

mRNA Target	**Product size**	**Direction**	**Primer**
β-actin	823	Forward	CCACACCTTCTACAATGAGC
β-actin		Reverse	ACTCCTGCTTGCTGATCCAC
TLR3	749	Forward	CACGCAAACCCTGGTGGTCCC
TLR3		Reverse	ACACCCGCCTCAAAGTCCCT

2.8 Determination of protein concentration

Protein concentration of cell lysates was carried out using the Biorad DC Protein Asssay kit, an assay based upon the colour change of a Coomassie Brilliant Blue G-250 dye in response to different protein concentrations. Twenty µl of each protein sample was mixed with 100 µl of the dye reagent, vortexed and incubated at room temperature for 5 mins. Absorbance was measured at 595 nm using an Eppendorf Biophotometer. A blank was made with lysis buffer. Protein standards from 0.2-0.9 mg/ml were made with Bovine Serum Albumin (BSA) and used as samples to make a standard curve.

2.9 SDS-PAGE

Prior to analysis, lysates were prepared by the addition of 2x Laemmli loading buffer (4% SDS, 20% glycerol, 120 mM Tris-HLC pH 6.8, 0.02% bromophenol blue) and where stated, 50mM DTT was added to the samples to reduce disulphide bonds. Samples were boiled for 5 mins at 95°C unless otherwise stated, and spun down for 1 min at 16,100 g. Samples were run on 12% SDS-PAGE gels (Running gel: 24% ProSieve 50 acrylamide solution (Lonza), 600 mM Tris pH 8.8, 0.1% SDS, 0.1% ammonium persulfate (APS) and 0.04% N,N,N',N'-Tetramethylethylenediamine (TEMED, Sigma). (Stacking gel: 5% ProSieve 50 acrylamide solution, 130 mM Tris pH 6.8, 0.1% SDS, 0.1% APS and 0.075% TEMED). The running gel was cast and left to polymerise for ~40 mins topped with 500 µl of water. The water layer was removed, the stacking gel was cast on top of the running gel, a 10 or 15 well comb was placed in the stacking gel and the stack was left to polymerise for ~20 mins. Once the gel had polymerised, cell lysates in Laemmli sample buffer were loaded alongside a protein marker (Fermentas or Biorad) and the gel was run in Tris-Glycine-SDS running buffer (Biorad) for ~1 hour at 50mA. After SDS-PAGE, the gels were either stained using Coomassie blue or taken for western blotting.

2.10 Comassie staining

Following electrophoresis, the gel was fixed for 30 minutes in fixing solution (Sigma). The fixing solution was removed and the gel was covered in working solution (4 parts Brilliant blue G-colloidal concentrate (Sigma), 1 part methanol (Fisher Scientific)) and stained overnight with constant agitation. The gel was then destained with 10% acetic acid (Fisher Scientific) in 25% methanol for 60 seconds, washed with 25% methanol, and destained in 25% methanol for up for 24 hours with constant agitation. The gel was then dried on a SICE-PLAS gel drier.

2.11 Western blotting

Following electrophoresis, the proteins on the gels were transferred to polyvinylidene difluoride (PVDF) membranes which had been primed in methanol for 20 seconds. Transfer took place in transfer buffer at 4 ^{o}C (25 mM Tris, 1.5 M Glycine and 20% methanol), either for 2 hr at 150 mA or overnight at 30 V. Membranes were blocked overnight in 4% w/v milk powder dissolved in Tris buffered saline (TBS) (10 mM Tris pH 8, 150 mM NaCl) with 0.1% Tween (TBST). Membranes were incubated with primary antibody diluted to the appropriate concentration (see Table 2) in 1% milk in TBST for between 40 mins and 1 hr, then washed four times for 5 mins with TBST. Following this, membranes were incubated with the corresponding secondary antibody, either goat anti-mouse HRP or swine anti-rabbit HRP (both DAKO) diluted to 1:3000 in 1% w/v milk powder in TBST for 40 mins, and again washed four times for 5 mins in TBST. The membranes were visualised by the application of 500 µl ECL (GE Healthcare) which was prepared from mixing equal parts of luminol solution and peroxide solution. The ECL mix was applied to the membrane for 1 min under Saran wrap, to ensure even distribution of the fluid. Following this step, excess ELC was removed, and the membranes wrapped in fresh Saran

wrap. The membrane was exposed to photographic film (Kodak,) which was developed using an X-ray developer machine (XOMAT).

2.12 Immunofluorescence

Cells in tissue culture were grown on cover slips distributed into 6 cm dishes or 6 well plates. The cover slips were treated with 10% poly-l-lysine for 10 mins and washed with sterile PBS. After cell adherence and growth in tissue culture medium, the cells were washed twice with PBS fixed with 4% paraformaldehyde for 15 mins and washed in PBS++ (PBS with 1 mM $CaCl_2$ and 0.5 mM $MgCl_2$). Free aldehyde groups were quenched with PBS++ containing 50 mM NH_4Cl_2, and cells were again washed three times in PBS++. Cells were permeabilised with 0.1% Triton x 100 in PBS++. Following a wash in PBS++, and two washes in PBS++ with 0.2% BSA, coverslips were incubated in 20 µl primary antibody diluted to the appropriate concentration (see Table 2) in PBS++ with 0.2% BSA for 20-40 mins in a dark moist chamber. Primary antibody was washed off with three washes of PBS++ with 0.2% BSA, and coverslips were incubated with the corresponding fluorescent conjugated secondary antibody, either goat anti-mouse Alexa Fluor 488 (green), donkey anti-rabbit Alexa Fluor 488 (green), and donkey anti-rabbit Alexa Fluo594 (red) (all from Molecular Probes), diluted to a concentration of 1:1000. Coverslips were washed twice with PBS++ with 0.2% BSA, twice with PBS++, once with PBS++ containing 1x DAPI (Invitrogen) to counter stain the nuclei, and once with water to remove excess PBS. The coverslips were mounted onto slides by inverting them onto a drop of mountant containing ant-fade (Vectashield) and secured with nail varnish. The coverslips were imaged using either an inverted UV microscope (Zeiss) or a laser scanning confocal SP5 microscope (Leica).

2.13 Live cell imaging

Live cell imaging was used to investigate the ER of tissue culture cells. Cells were grown on 35 mM glass-bottomed μ-dishes (Ibidi). Ten minutes prior to treatment, cells were incubated with ER tracker (Invitrogen ThermoFisher). Cells were treated with 10 mM homocysteine in complete media, 10 mM DTT in complete media, or mock treated, and immediately imaged. Images were taken every 10 minutes for an hour using an Andor Revolution XD spinning disk confocal microscope with Olympus 60x UPlanApo lens. The collected images were converted to a movie format using ImageJ software.

2.14 Immunoprecipitation

Cell lysates were incubated with antibody (see Table 2 for dilutions used) immobilised on Protein A sepharose beads in 1.5 ml eppendorf tubes. The primary antibodies were mixed with 50μl of a 20% suspension of beads in lysis buffer (without NEM or CLAP) and rotated in a fridge for 2 hours at 4°C. Beads bound with antigen-antibody complexes were washed 3 times in lysis buffer (without NEM or CLAP); they were collected in between washes by centrifugation for 1 min at 8,000g at 4^{o}C. After washing, the beads were resuspended in Laemmli sample buffer, boiled for 5 mins in the presence or absence of 50 mM DTT, centrifuged for 2-3 mins at 16,100 g at room temperature and subjected to SDS-PAGE analysis.

2.15 Transformation and Transfection

Plasmid cDNAs (shown in Table 3) were used to transform DH5α *E.coli* bacteria. One µg purified plasmid DNA was preincubated at 42°C for 1 minute, followed by addition of 50 µl competent bacteria which were heat shocked by a further incubation at 42°C for 1 minute. Nine hundred µl LB media was added to the bacteria and the mixture was incubated at 37°C for 45 min. The bacteria were pelleted by centrifugation at 218 g for 1 min. The pellets were resuspended in 100 µl LB media, spread on to LB-agar plates supplemented with 0.1 mg/ml ampicillin and incubated overnight in a 37 ^{o}C incubator. After overnight growth, individual colonies were picked and were resuspended in 5 ml LB media supplemented with 0.1 mg/ml ampicillin and incubated overnight. Plasmid DNA was purified from the cultures using QIAprep Spin Miniprep Kit (according to manufacturers instructions). The overnight culture was pelleted, resuspended and lysed for 5 mins after which a neutralisation buffer was added and centrifuged for 10 mins at 16,100 g. The supernatant was applied to the QIAprep spin column where a silica membrane absorbs the DNA. The column was centrifuged at 16,100 g for 30 secs, and washed twice with wash buffer to remove impurities. The DNA was eluted by the addition of elution buffer, incubating for 1 min, and centrifuged for 1 min at 16,100g.

Table 3- Plasmid cDNA

Plasmid	Full plasmid name	Source
Ero1α WT	pcDNA3.1 Ero1a-myc	Sitia laboratory
Ero1α C104A/C131A	pcDNA5 Ero1a C104A/C131A-V5-His	Bulleid laboratory
Ero1α C391A	pcDNA3.1 Ero1a C391A-myc	Benham laboratory
Ero1α C394A/C397A	pcDNA3.1 Ero1a C394A/C397A-myc	Benham laboratory
Ero1α C391A/C394A/C397A	pcDNA3.1 Ero1a C391A/C394A/C397A-myc	Benham laboratory
Ero1β WT	pcDNA3.1Ero1b-myc	Sitia laboratory
Ero1β H254Y	pcDNA3.1 Ero1bH254Y-myc	Benham laboratory
Ero1β G252S	pcDNA3.1 Ero1bG252S-myc	Benham laboratory
HLA-DRα	pcDNA3.1 DRA*0101	Neefjes laboratory
HLA-DRβ	pcDNA3.1 DRB*010101	Neefjes laboratory
HLA-DMα	pcDNA3.1 DMA-HA	Benham laboratory
HLA-DMβ	pcDNA3.1 DMB-myc	Benham laboratory
Invariant chain (CD74)	pcDNA3.1 Ii	Neefjes laboratory

For transfection, cells were grown to ~80% confluency in 6 cm dishes. Transfections were either with Superfect transfection reagent (QIAGEN) or Lipofectamine 3000 (Invitrogen ThermoFisher). For transfections with Superfect, 1 µg DNA and 5µl Superfect were added to 400 µl serum free media, vortexed and incubated at room temperature for 5-10 minutes. This mixture was added to washed cells, along with 1.5 ml supplemented media (as described in the cell culture section). The cells were incubated for 2-3 hours, washed and the spent media was replaced with fresh media. Lipofectamine was used according to manufacturers instructions for 6-well use. Unless stated, where 7.5 µL volumes was used, 3.75 µL Lipofectamine 3000 reagent was diluted in 125µL Opti-MEM media. One µg DNA was added to 125 µL Opti-MEM media and 5 µL P300 reagent. The diluted DNA was added to the diluted Lipofectamine and incubated at room temperature for 5 mins, after which it was added to the cells, along with 1.75 mL complete media.

2.16 Differentiation and activation of macrophages

THP-1 cells in 25^2 cm flasks were treated with 50 nM phorbol myristate acetate (PMA) in complete media to differentiate them into adherent cells with a macrophage-like phenotype. When differentiated, as determined by adherence, cells were mock treated or treated with 10 µg/ml lipopolysaccharide (LPS) in complete media for 4 hours. Cells were washed with PBS twice and lysed for protein analysis (by SDS-PAGE) or RNA analysis (by RT-PCR). For activation by polyinosinic:polycytidylic acid (Poly(I:C)), cells were washed with PBS and incubated with complete media containing 10 or 50 µg/ml Poly(I:C) for 6 hours, washed in PBS twice and RNA extracted for analysis by RT-PCR.

2.17 Temperature treatments of cell lysates

As described in the SDS-PAGE section, 2x Laemmli loading buffer was added to post-nuclear supernatants from cell lysates. These mixtures were then heated in a heating block to 60°C, 90°C or left at room temperature (20°C) for 5 minutes. The samples were spun down at 16,100 g for 5 min at room temperature and run on a 12% SDS-PAGE gel. Western blotting was used to determine the amount of stable MHC class II heterodimers (see western blotting section).

2.18 Endo H treatments

Lysates were denatured with 10x glycoprotein denaturing buffer at 100°C for 10 minutes. The lysates were either mock treated or digested with 5% endoglycosidase H (EndoH) enzyme (New England Biolabs) and 1x G5 Reaction Buffer (0.5 M Sodium Citrate, pH 5.5) at 37°C for 1-2 hours. Post digestion, the lysates were mixed with reducing 2x Laemmli sample buffer, boiled for 5 min, centrifuged for 1 min at 16,100g at room temperature, and subjected to analysis by SDS-PAGE.

3. Induction of Ero1α OX1 by homocysteine

3. Induction of Ero1α OX1 by homocysteine

3.1 Introduction

3.1.1 Homocysteine

Homocysteine is a sulphur containing amino acid precursor and although non-protein forming, it is an intermediate in the remethylation and transsulphuration metabolic pathways (Figure 3.1) with respective end products methionine and cysteine (Selhub, 1999). Remethylation involves the transfer of a methyl group to homocysteine. N-5-methyltetrahydrofolate is the main donor with the reaction being vitamin B12 dependant. This process is reversible, with some of the methionine being converted by ATP activation into S-adenosylmethionine, a methyl donor. Homocysteine is regenerated when S-adenosylhomocysteine (SAH), the by-product of these methylation reactions, is hydrolysed. The hydrolysis is reversible and favours SAH.

The alternative pathway for homocysteine is transsulphuration. Cystathionine β-synthase catalyses the irreversible condensation of homocysteine with serine to form cystathionine, which is hydrolysed by γ-cystathionase to form cysteine and α-ketobutyrate. Excess cysteine can be excreted in the urine or can be oxidized to taurine or inorganic sulphates, thus excess homocysteine can be removed via transsulphuration. When one of these pathways is disrupted there is a build-up of homocysteine which is transferred into the blood, although this removes the potential of toxicity from the cell, this risk is passed onto vascular tissue.

The pathway that is taken in humans is thought to be nutritionally regulated with an increase in dietary methionine resulting in an increased use of the transsulphuration pathway and less remethylation cycling. SAM is thought to play a part in this regulation as an activator of cystathionine β-synthase.

Excess intracellular homocysteine can be toxic, so along with its catabolism, a cellular export mechanism assists its removal from the cell. This export results in a small amount of homocysteine in the plasma. When a disruption in homocysteine metabolism occurs, the resulting built-up homocysteine is deposited by the export mechanism into the blood. Hyperhomocysteinemia generally results from a deficiency in the vitamins involved in homocysteine metabolism or defects in the enzymes involved in homocysteine metabolism. Severe hyperhomocysteinemia, an elevation in total plasma homocysteine, can result in plasma homocysteine concentrations of up to 400 μM, but even an increase to 5 μM increases the risk of coronary heart disease by 60-80%.

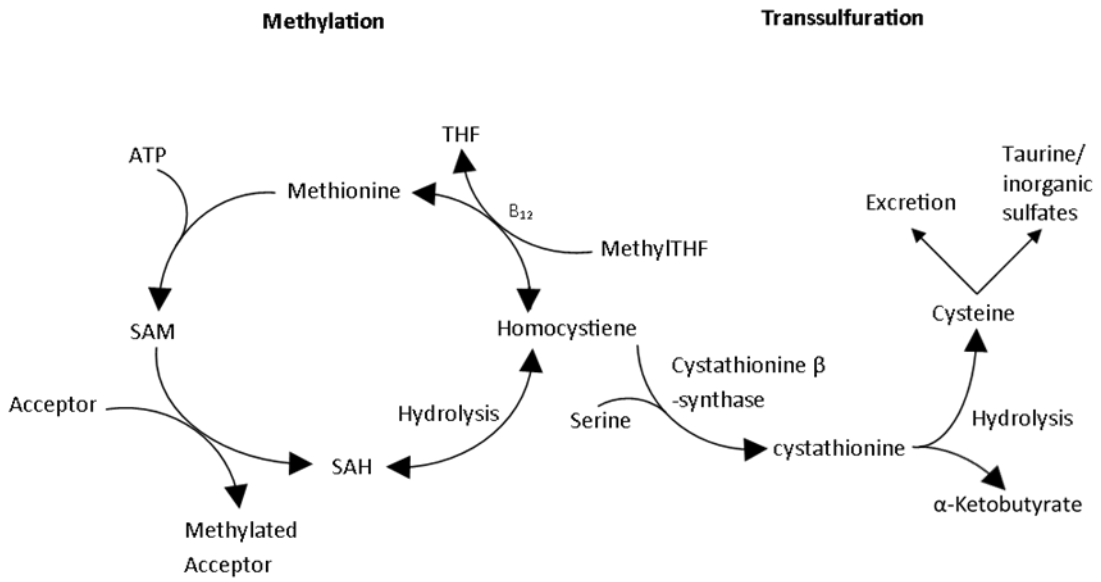

Figure 3.1. The methylation and transsulphuration pathways of homocysteine metabolism

In the Methylation pathway the vitamin B12 dependant transfer of a methyl group to homocysteine forms Methionine, which is subsequently activated by ATP to form the methyl donor SAM. SAM transforms to SAH by donating its methyl group to a methylation substrate. Homocysteine is regenerated upon hydrolysis of SAH.

In the Transsulphuration pathway homocysteine is condensed with serine to form cystathionine through the action of Cystathionine β-synthase. Cystathionine is hydrolysed to Cysteine which is excreted or oxidized to taurine or inorganic sulphates.

Hyperhomocysteinemia is associated with an increased risk of vascular disease, stroke, infarction and potentially a number of other disorders implicated by the development of these conditions, such as Alzheimer's disease (Boushey et al., 1995; Seshadri et al., 2002). Homocysteine damages the endothelium (McCully, 1969), in particular causing structural and functional disruption of cerebral blood vessels through oxidative stress. Homocysteine has been shown to increase lipid peroxidation and oxidation of proteins, explained by increases in ROS generated by homocysteine autoxidation (Derouiche et al., 2014). However, the underlying pathophysiological mechanisms of homocysteine-mediated vascular damage are not well understood (Akalin et al., 2008; Faraci and Lentz, 2004).

The production of NO within the endothelium acts as a relaxing factor to vessel walls. Hyperhomocysteinemia impairs endothelium dependant relaxation and in addition to this, it also elevates the levels of peroxynitrite, reactive nitrogen species and potent oxidants in the vessel wall. This happens upon the reaction of NO with superoxide and has numerous detrimental effects (as does superoxide) at the vessel wall, as well as being an activator of poly (ADP-ribose) polymerase, a mediator of vascular dysfunction (Soriano et al., 2001). It may also divert the formation of NO in favour of superoxide (Faraci and Lentz, 2004).

3.1.2 What is already know about Ero1α and homocysteine?

Battle et al (2013) have previously looked into the relationship between Ero1α and homocysteine in OE33 oesophageal cells, which in the gastrointestinal epithelia would be exposed to homocysteine in the diet. Ero1α, which was strongly expressed and mainly in the OX2 state, could be post translationally regulated, with homocysteine causing a 25 fold increase of Ero1α in the OX1 state (Battle et al., 2013) (Figure 3.2, compare lanes 3 and 4).

This effect of homocysteine was reversible as upon removal of homocysteine, and when normal conditions were restored, the OX1/OX2 balance returned to that of before treatment within 60 minutes. Titration experiments showed that 1 mM homocysteine induced OX1 strongly, whereas 100 µM homocysteine also induced OX1 but to a lesser extent. Homocysteine was not acting as an indiscriminate reductant as there was no change to other proteins sensitive to ER redox conditions upon treatment with homocysteine. Other antioxidants and redox active metabolites such as N-acetylcysteine and riboflavin did not have the same effect; riboflavin, like homocysteine, is found in the diet, and so also potentially influences the GI epithelia. As it seemed Ero1α appeared to be detecting the presence of homocysteine, amino acids downstream of homocysteine, (methionine and cysteine) which are also sulphur containing, were also applied to OE33 cells in culture (Battle et al., 2013). Treatment of cells with excess methionine and cysteine did not initiate any change in Ero1α Ox1 levels, suggesting that Ero1α sensing might be restricted to a control point or points in the synthesis of sulphur containing amino acids.

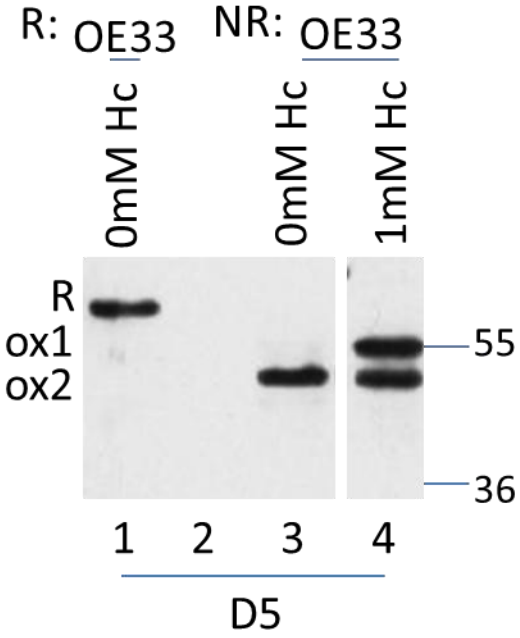

Figure 3.2. Homocysteine induces Ero1α OX1

Ero1α exists in three states, active (OX1), inactive (OX2) and reduced (R). When analysed by SDS-PAGE and immunoblot with the αEro1α antibody D5, the three states can be seen. OX1 is induced upon treatment with homocysteine (HC), and R is seen under reducing SDS-PAGE. Adapted from (Battle et al., 2013).

3.1.3 Ero1α mutants

The mutation of regulatory and structural Ero1α cysteines is a useful tool for investigating its function. The Ero1α C104A/C131A mutant is unable to form the regulatory bond Cys94-Cys131 which keeps Ero1α in its inactive OX2 form, thus this is a constitutively active mutant, with oxygen consumption assays confirming that it is more active than the WT, leading to hyper oxidation of PDI (Araki and Nagata, 2011; Baker et al., 2008). When transfected with this mutant, cells undergo transcriptional changes to 159 genes, most of which are related to the UPR resulting in UPR target protein levels similar to that when treated with inducers of UPR. This apparent UPR response may be due to proteins misfolded by sulph(i/o)nylation which is mediated by H_2O_2 (Hansen, 2012).

Whilst the Ero1α WT migrates entirely in the OX2 form on a western blot, the C104A mutant migrated mostly as OX2 with a tiny amount of OX1, unable to form Cys99-Cys104, Cys94-Cys131 is believed to be destabilised and lost. When Cys104-Cys131 is lost in C131 mutants there would not be a noticeable shift in the OX1 band if Cys99-Cys104 is also lost. It is therefore unclear whether Cys99-Cys104 is also lost.

The Ero1α C85/C391 double mutant migrates as 2 bands, one at a molecular weight between that of OX1 and OX2; this is thought to contain the Cys94-Cys131 disulphide bond. The other band migrates at a weight the same as that of when Ero1α is fully reduced, R. In this form Cys94-Cys131 has been destabilised. Again, it is unclear whether Cys99-Cys104 is also destabilised (Hansen, 2012).

Ero1α is normally retained in the ER, but is in part secreted when over expressed, possibly due to the localization mechanism being saturated (Anelli and van Anken, 2013). When misfolded, Ero1α forms high molecular weight aggregates which do not pass ER quality control and so are not secreted. The lack of any such aggregates suggests that these mutants are still able to fold into the correct formation, further evidence of this is provided by the presence of the OX1 and OX2 forms in various mutants. These mutants are still able to interact with PDI, with only slight variations in molecular weight due to changes in the molecular weight of Ero1α.

3.1.4 Ascorbic acid

Ascorbate, or vitamin C, is an abundant anti-oxidant and cofactor for enzymatic reactions, like collagen crosslinking, which underlies the pathogenesis of scurvy. Despite this, its function is not restricted to collagen crosslinking, and deficiency also leads to ER stress and an unfolded protein response. An ascorbic acid deficiency can be due to a lack or ascorbate in the diet or its cellular consumption in excess. Excess consumption can occur if a free cysteine is not converted quickly enough to a disulphide. In this case the free cysteine interacts with and mops up ROS with H_2O_2, being oxidised to sulphenic acid. Sulphenic acid can go down one of two pathways: it can be reduced to a disulphide, creating a disulphide relay, or it can be reduced and return to a free thiol with the conversion of ascorbic acid to the chemically unstable dehydroascorbate. If this occurs in excess the consumption of ascorbic acid leads to its deficiency. Such consumption is unlikely when PDI is present in the reduced form as the PDI quickly converts free cysteines into disulphides (Zito et al., 2012).

Any altered kinetics of disulphide bond formation may affect ER function as it provides a delay sufficient to expose free thiols. Such a disturbance can be seen in In Ero1α knockout mice where the lack of Ero1α results in a 5 fold lower procollagen 4 hydroxyproline content, whose

formation is ascorbate dependant, depleting collagen maturation. No other severe abnormalities are seen as disulphide bond formation can continue at the expense of ascorbate (Zito et al., 2012). However, dehydroascorbate has also been argued to be an electron acceptor for reduced PDI, and has been shown to result in a decreased protein thiol concentration when given to human liver microsomal vesicles. The rate of thiol oxidation was 30% less than that when ascorbate was used instead, with much reduced thiol consumption upon the inhibition of ascorbate oxidation. All the tested means to curtail ascorbate oxidation resulted in a decrease in thiol oxidation. This is due to the need for ascorbate to be oxidised to dehydroascorbate before it can act as an electron acceptor (Csala et al., 1999). Ascorbate oxidation occurs in the cytoplasm, as only ascorbate in its oxidised form can be transported into the ER (Banhegyi et al., 1998). This could mean that in the absence of Ero1α, PDI is oxidised by dehydroascorbate with H_2O_2 produced by ascorbate oxidase enzymes (Szarka and Lorincz, 2014).

3.1.5 N-Ethylmaleimide

Protein thiols are extremely sensitive to their redox environment and any changes in this environment are reflected in their oxidation state. The redox status of thiols and disulphides can be trapped chemically to prevent changes during cell lysis and analysis. This procedure must be quick to prevent changes in equilibria and to prevent the action of redox active enzymes that can rearrange disulphides. It must also be irreversible to further prevent rearrangement. NEM achieves this quenching by thiol alkylation (Hansen and Winther, 2009). It reacts with sulfhydryls to form stable thioether bonds. NEM can only react with available thiols, thus those buried in the three-dimensional structure will not be quenched. If the three-dimensional structure is lost, these free thiols will be exposed and subject to potential rearrangement.

3.2 Results

3.2.1 Detecting Ero1α in cells treated with homocysteine

Previous observations show changes in the Ero1α oxidation state upon treatment with homocysteine (Battle et al., 2013). As the regulation of disulphide bond formation and the oxidative status of Ero1α at steady state differs between cell types (Benham et al., 2013), here it is first investigated whether such changes could be replicated in cell lines other than the oesophageal cancer cell line OE33 which was originally used. To compare with the OE33 cells, which have high levels of Ero1α expression, the human cervical carcinoma cell line, HeLa, and the immortalised fibrosarcoma cell line, HT1080, were used.

Previous experiments have shown that the oxidation status of Ero1α can be regulated by the addition of as little as 100 µM homocysteine, but more noticeably, 1 mM homocysteine to the cell. Using the same method of treatment, the conditions used in Battle et al (2013) were replicated, but rather than using the D5 polyclonal antiserum to detect Ero1α, the 2G4 monoclonal antibody was used. HT1080 and HeLa cell lysates were analysed by non-reducing SDS-PAGE and a western blot was probed with the 2G4 antibody (Figure 3.3A and C, lanes 1,3 and 5). The result shows that Ero1α exists in a fast-migrating and likely inactive (OX2) form at steady state, consistent with previous data (Benham et al., 2013). By using non-reducing conditions, disulphide bonds were preserved, allowing disulphide-dependent conformations to be observed. Upon addition of DTT to the cell lysates the Ero1α band shifts up to a higher molecular weight, meaning it is fully reduced (Figure 3.3A and C, compare lanes 1 and 2; 3 and

4; 5 and 6). Although OX2 is present, the change to Ero1α OX1 upon homocysteine treatment could not be seen. Unlike D5, the polyclonal antibody previously used in Figure 3.2 (Battle et al., 2013), the monoclonal antibody 2G4 did not appear to detect the OX1 form of Ero1α, which is expected to start appearing upon treatment with 1 mM homocysteine (Figure 3.3A and C, lane 5) and to form a clear band with 10 mM homocysteine (Figure 3.3A and C, lane 7). The complete disappearance of an Ero1α signal (Figure 3.3A, lane 7) suggests either that Ero1α is not present in this sample or that Ero1α exists in a form that is unrecognisable to the 2G4 antibody. Under reducing conditions OX2 Ero1α should be completely reduced as seen with all other homocysteine concentrations in this experiment. However, there was no reduced Ero1α signal upon treatment with 10 mM homocysteine (Figure 3.3 A, lane 8). The HC10 antibody, which recognises free MHC class I heavy chains, was used to reprobe the membranes for MHC 1 (Figure 3.3 B and C). The reprobe with HC10 showed equal loading between the lanes and that there was protein present in lanes 7 and 8, where there was an absence of signal for Ero1α. The apparent molecular weight of the MHC class I heavy chain changed between NR and R lanes (1 and 2, 3 and 4, 5 and 6, 7 and 8) as the disulphides were broken, providing further evidence that the change in Ero1α molecular weight is due to the reducing conditions.

The homocysteine treatments were performed on both the HT1080 and HeLa cell line to see whether the disappearance of Ero1α at 10 mM homocysteine in the HT1080 fibrosarcoma cells was cell specific. Ero1α could not be detected in either cell line after 10 mM homocysteine treatment (Figure 3.3A and C, lanes 7 and 8), further suggesting that OX1 was not detected by the 2G4 antibody. Using the MHC 1 antibody HC10 as a positive control (Figure 3.3 B and C, lanes 7 and 8), it was confirmed that 10 mM homocysteine resulted in a loss of detection of Ero1α by the 2G4 antibody in both cell lines (Figure 3.3C lanes 7 and 8).

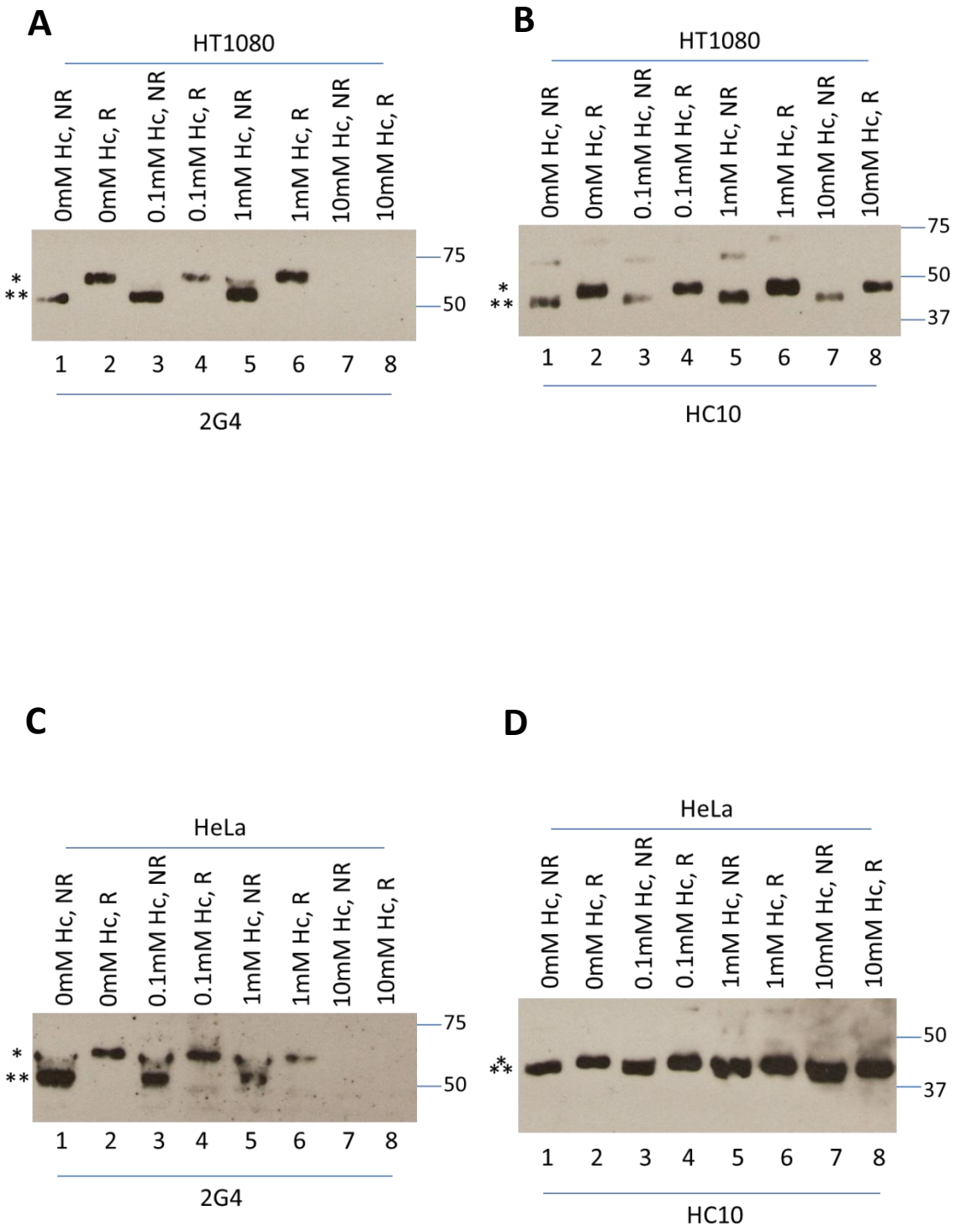

Figure 3.3. Homocysteine prevents the detection of Ero1α by the 2G4 monoclonal antibody

HT1080 (**A**,**B**) and HeLa (**C**,**D**) cells were treated with 0, 0.1, 1 and 10 mM homocysteine for 1 hour then lysed in MNT buffer. Cell lysates were then subjected to reducing (R) or non-reducing (NR) SDS-PAGE and subsequent western blotting with the monoclonal antibodies 2G4 (**A**,**C**) and HC10 (**B**,**D**). Reduced (*) and non-reduced (**) forms of Ero1α and MHC class I are visible.

3.2.2 Induction of Ero1α OX1 by homocysteine in cells transfected with WT Ero1α

In order to determine whether the lack of Ero1α signal in the previous experiments (Figure 3.3) was due to homocysteine causing the removal of Ero1α from the cell or due to the antibody not detecting Ero1α, the homocysteine treatments were repeated on HT1080 cells transfected with myc tagged wild type (WT) Ero1α. These lysates, alongside mock transfected cell lysates treated with 0, 1 or 10 mM homocysteine, were analysed by SDS-PAGE and western blotting. Again, only 1 oxidation state (OX2) was present and there was no signal upon 10 mM homocysteine treatment when using the 2G4 antibody (Figure 3.4A), meaning that the homocysteine treatments had the same effect on transfected cells. In this figure, 2G4 detected the endogenous Ero1α, which is present in all samples, as shown by its presence in mock (M) transfected cells (Figure 3.4A lane 1). When the lysates were probed for PDI, each lane had an equal amount of PDI showing that all samples contained protein (Figure 3.4B).

The transfected lysates were probed with the D5 antibody (Figure 3.4D) used by Battle et al (Battle et al., 2013). The results show that it was possible to see the change in Ero1α OX state from OX2 to OX1 upon the addition of homocysteine (compare lanes 2 3 4), first reported by Battle (Battle et al., 2013).

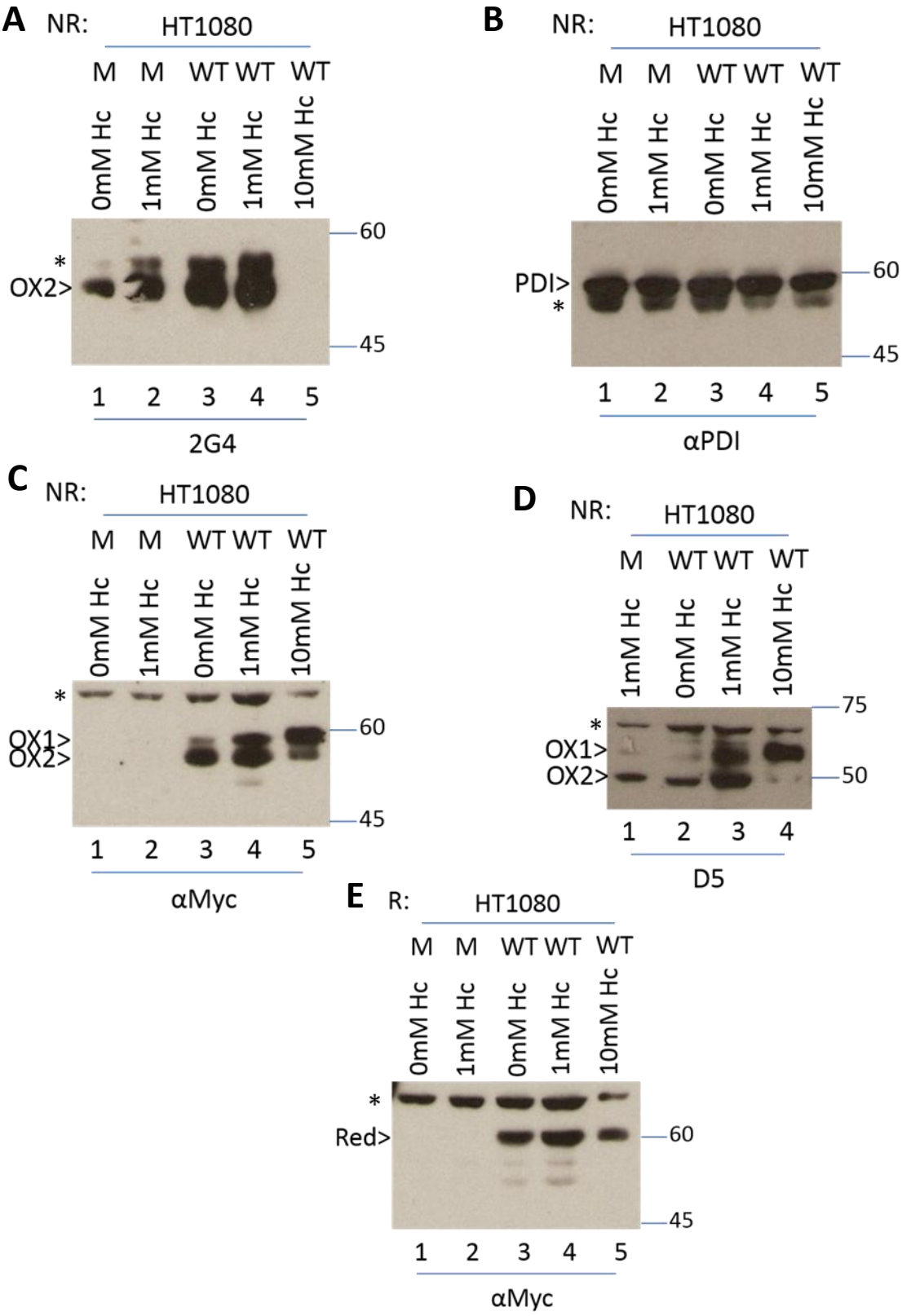

Figure 3.4. Induction of OX1 by homocysteine in cells transfected with WT Ero1
Following transfection with wild type (WT) Ero1α or mock transfection (M), HT1080 cells treated with 0, 0.1, 1 and 10 mM homocysteine for 1 hour were lysed in MNT buffer. Cell lysates were then subjected to non-reducing (NR) or reducing (R) SDS-PAGE and subsequent western blotting with the antibodies αMyc (**C** and **E**), αPDI (**B**), 2G4 (**A**) or D5 (**D**). Ero1α monomer oxidation states are labelled OX1, OX2 or reduced (Red). The upper band in C and E is a non-specific protein reacting with the anti-myc antibody that acts as a loading control. Background bands are indicated (*****).

When the lysates were probed with αMyc (Figure 3.4C), there was no signal in mock transfected cells as there was no myc tagged protein present (Figure 3.4C, lanes 1 and 2). As there was no signal in the mock sample and there was a signal in the transfected samples (Figure 3.4C, lanes 3, 4 and 5), it can be concluded that the signal was the myc tagged Ero1α. The addition of the myc tag on Ero1α increases its apparent molecular weight, explaining the difference in size when comparing the transfected Ero1α detected by αMyc (Figure 3.4C), and the endogenous Ero1α detected by 2G4 (Figure 3.4A). The transfected Ero1α was not detected by 2G4 in this experiment, as shown by the absence of a heavier molecular weight Ero1α in Figure 3.4A. Myc tagged Ero1α was present in the OX2 form (Figure 3.4C lanes 3, 4, and 5), confirming the findings that Ero1α OX2 is present in cell samples when probed with the anti-myc antibody. When treated with 10 mm homocysteine (Figure 3.4C lane 5) most of the OX2 changed to OX1; when the equivalent sample was probed with the D5 antibody (Figure 3.4D lane 4) all of the OX2 signal was lost in favour of OX1. This change from OX2 to OX1 could be an explanation for the loss of Ero1α signal seen with 2G4. If 2G4 was not able to detect Ero1α in the OX1 form, no Ero1α would be detected in Figure 3.4A lane 5, as at this level of homocysteine only the OX1 exists. However, this explanation should also account for the disappearance of the fully reduced Ero1α after 10 mM homocysteine treatment (Figure 3.3A lane 8). Analysing the transfected lysates under reducing conditions, resulted in a single reduced Ero1α band, showing that the shift in the molecular weight of myc-tagged Ero1α under non-reducing conditions was a result of disulphide bond formation, not degradation. The addition of DTT eliminated the OX1 form (which 2G4 does not appear to detect) and reduces Ero1α-myc into the same reduced state as seen with lower concentrations of homocysteine treatments (Figure 3.4E). Taken together, the results in Figures 3.3 and 3.4 suggest that the loss of Ero1α signal when probing with 2G4 could be due to covalent modification of Ero1α by high concentrations of homocysteine, which renders it unavailable to detection by 2G4.

By transfecting cells with tagged WT Ero1α, and probing for the tag, it was possible to see all forms of Ero1α, unlike probing with 2G4. The αMyc analysis showed a change in Ero1α oxidation state, with the ratio of OX1:OX2 moving from OX2 being favoured at low concentrations of homocysteine to OX1 being favoured at higher concentrations. This was a trend seen over many repeats, and although the OX2:OX1 ratio varied slightly between experiments, there was a clear trend towards Ero1α becoming more, what appears to be, "active" upon treatment of homocysteine with increasing concentrations. The average OX2:OX1 ratio over 6 experiments was 27.6:1 at 0 mM, 4.7:1 at 1 mM and 0.2:1 at 10 mM homocysteine. These results reinforce those done previously, showing that the control of Ero1α activation status by homocysteine can be replicated in multiple cell lines. Figure 3.4 also highlights the inability of 2G4 to effectively detect the Ero1α OX1 state. Interestingly the results show that 2G4, a monoclonal antibody, is able to detect a modification of Ero1α by loss of binding.

To further investigate the effects on the oxidative folding machinery induced by homocysteine, the homocysteine treatments were repeated on HT1080 cells. Following cell lysis, the lysates were analysed by SDS-PAGE and western blot with the 2G4 (Figure 3.5A, lanes 1, 2, 3 and 4) and αPDI (Figure 3.5B) antibodies, or used in an immunoprecipitation with an αPDI antibody and then analysed by western blotting (Figure 3.5A, lanes 5, 6, 7 and 8). Figure 3.5A shows that Ero1α co-immunoprecipitated with PDI at the same quantity when treated with 0, 0.1 or 1 mM homocysteine. As there was no immunoprecipitated Ero1α signal at 10 mM homocysteine, Ero1α was either not immunoprecipitating with PDI or if they are co-immunoprecipitating, the interaction did not protect Ero1α from the homocysteine induced modification which is prevented 2G4 from detecting Ero1α. The signal of the antibody used in the immunoprecipitation (Figure 3.5 A, lanes 5, 6, 7 and 8) acts as a loading control. Reprobing the membrane with the αPDI antibody (Figure 3.5B) shows that there was a similar level of PDI protein in all samples.

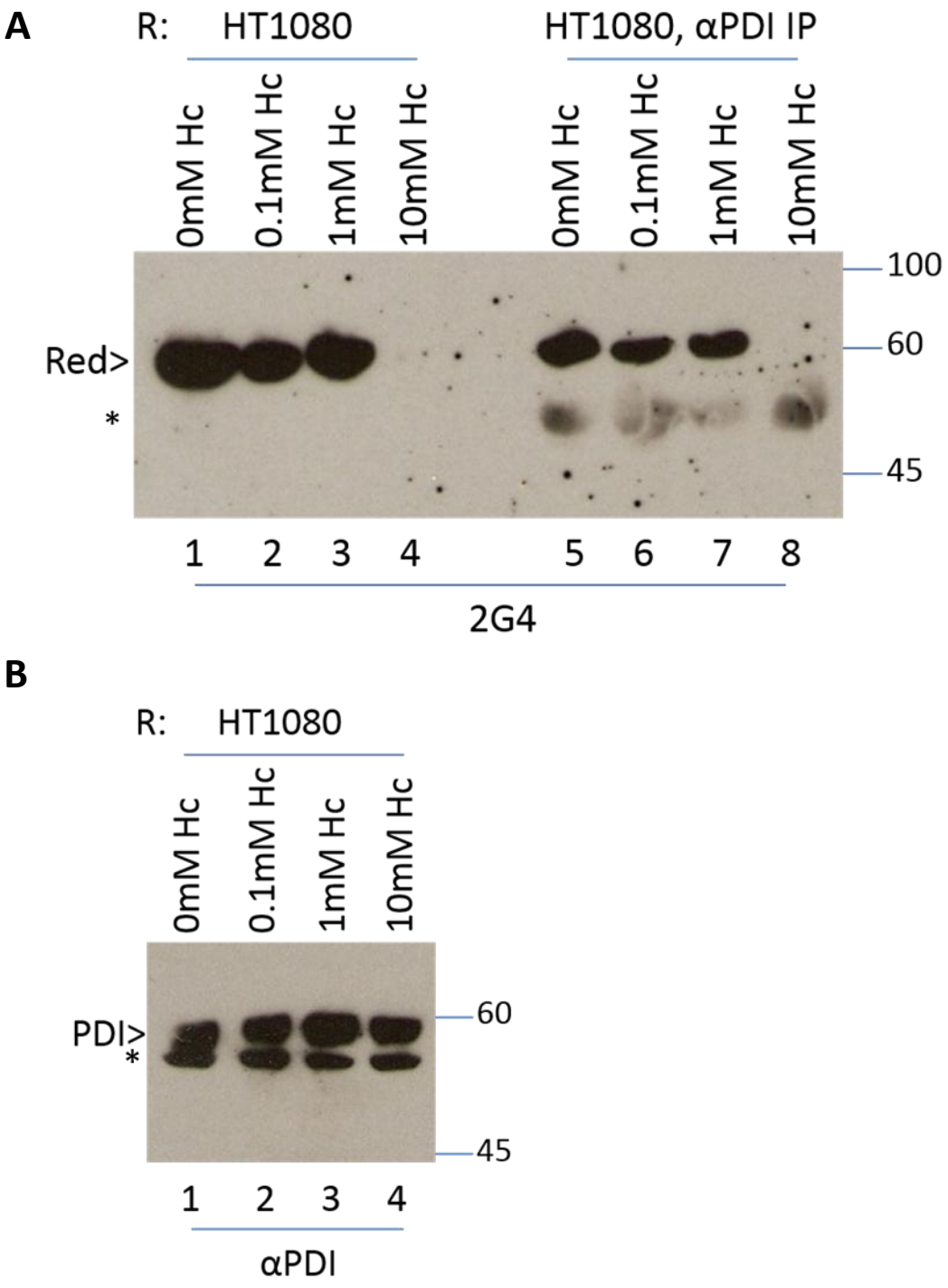

Figure 3.5. Detection of Ero1α PDI complexes in homocysteine treated cells
HT1080 cells treated with 0, 0.1, 1 and 10 mM homocysteine (HC) for 1 hour were then lysed in MNT buffer. Cell lysates were immunoprecipitated with αPDI and subjected to reducing (R) SDS-PAGE and subsequent western blotting with the antibody 2G4 (**A**). Cell lysates were subjected to reducing (R) SDS-PAGE and subsequent Western blotting with the αPDI antibody (**B**). The reduced Ero1α monomer is labelled Red. Background bands are indicated (*****).

3.2.3 The effect of homocysteine on Ero1α in cells transfected with the mutant Ero1α C104A/C131A

The oxidation state of Ero1α is dependent on the formation of a disulphide bond between Cys94-Cys99, the outer active site, which can be transferred to PDI and makes it oxidised (OX1) (Figure 3.6A and B). The formation of Cys94-Cys131 blocks Cys94 making it unavailable for interaction with Cys99, and forming the inactive (OX2) Ero1α. Homocysteine appears to push Ero1α into the OX1 form. It is unknown whether this effects the regulatory control mechanism depicted in Figure 3.6A and B. To investigate how homocysteine mediates its effects, HT1080 cells were transfected with a constitutively active mutant Ero1α to see if homocysteine directly regulates Ero1α through partial reduction.

The Ero1α C104A/C131A mutant is constitutively active as the regulatory disulphide Cys94-Cys131, which blocks the catalytically essential shuttle Cys94, is absent (shown schematically in Figure 3.6 C). This leaves the Cys94 to form a disulphide with Cys99, and interact with PDI under all conditions; this form is Ero1α in OX1.

HT1080 cells transfected with a V5 tagged C104A/C131A Ero1α mutant were lysed and the lysates were probed with αV5 antibody (Figure 3.7A). The transfectants expressed Ero1α only in a state which appear to be OX1, regardless of treatment, or non-treatment, with homocysteine. The addition of DTT to samples in Figure 3.7B caused a shift in molecular weight of these bands to the fully reduced form and shows that the Ero1α in Figure 3.7A was in the oxidised state. The addition of homocysteine to the transfected cells did not affect the migration of tagged C104A/C131A Ero1α, as OX1 was evident and OX2 absent at all concentrations. Homocysteine appears to push WT Ero1α into the OX1 form, however

C104A/C131A Ero1α exists in this form under all conditions, and no change was observed in this experiment.

As with the detection of the myc tag (used in Figures 3.4B and C), the antibody against the V5 tag used in Figure 3.7A and B detected Ero1α OX1 at a higher molecular weight than expected for non-tagged Ero1α. This was due to the tag increasing the molecular weight of the protein. This result can be compared with Figure 3.7C, where the OX2 form of Ero1α recognized by 2G4 was considerably lighter than the OX1 recognized by anti-V5 (Compare Figure 3.7A and C). OX2 Ero1α was present in the samples as it is the endogenous pool which was not constitutively active, and not V5 tagged. The disappearance of this OX2 Ero1α upon treatment with 10 mM homocysteine acts as a positive control, confirming that the homocysteine treatment had worked. Probing the samples again with αPDI showed equal levels of endogenous protein between samples, and that there was protein loaded in the 10 mM homocysteine treated sample (Figure 3.7D).

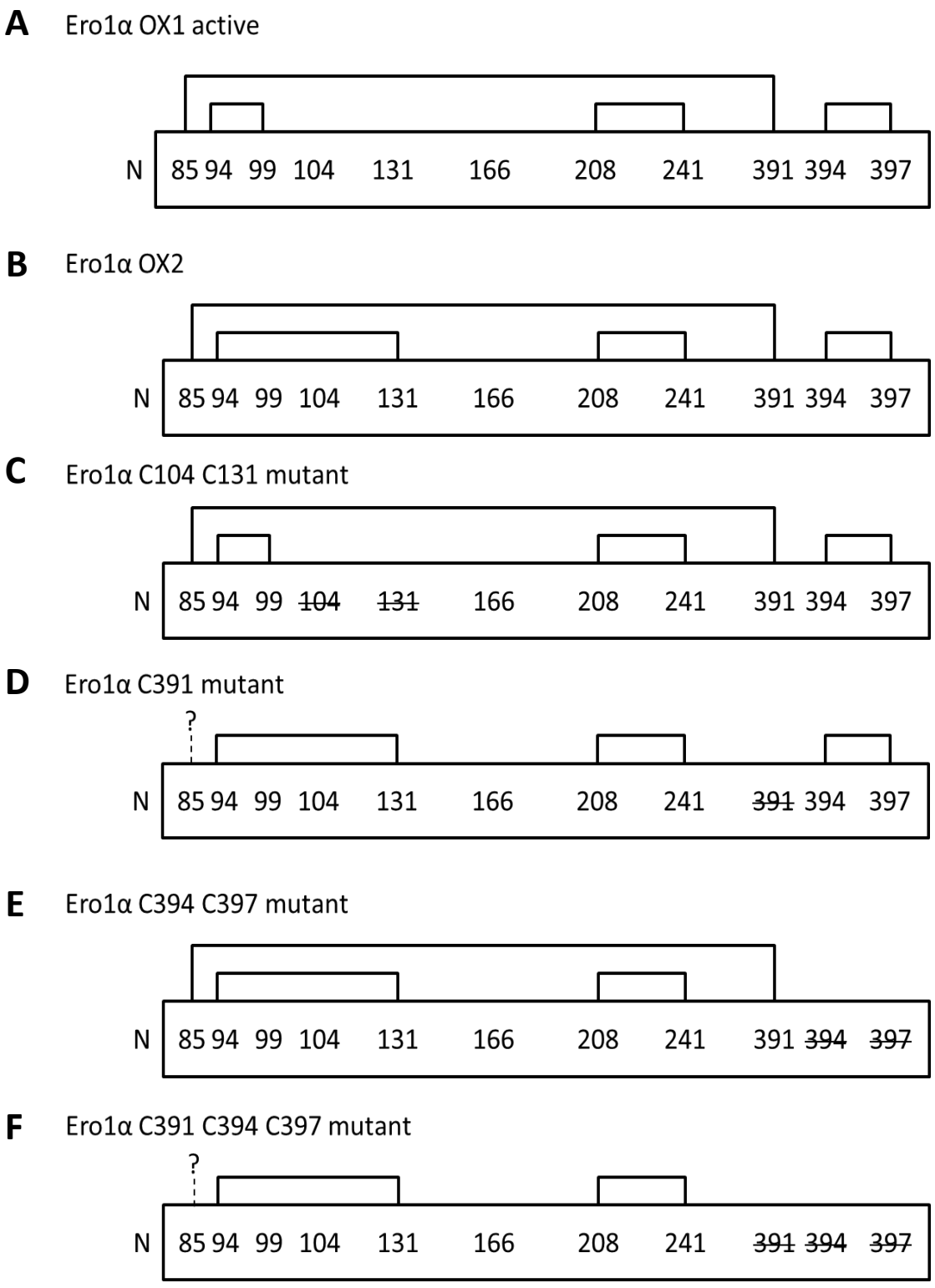

Figure 3.6. Schematic representation of Ero1α regulation
Schematic representation of cysteines and their disulphide links in OX1 (**A**) OX2 (**B**) and the OX2 Ero1α mutants C104A C131A (**C**), C391A (**D**), C394A C397A (**E**), C391A C394A C397A (**F**) Ero1α.

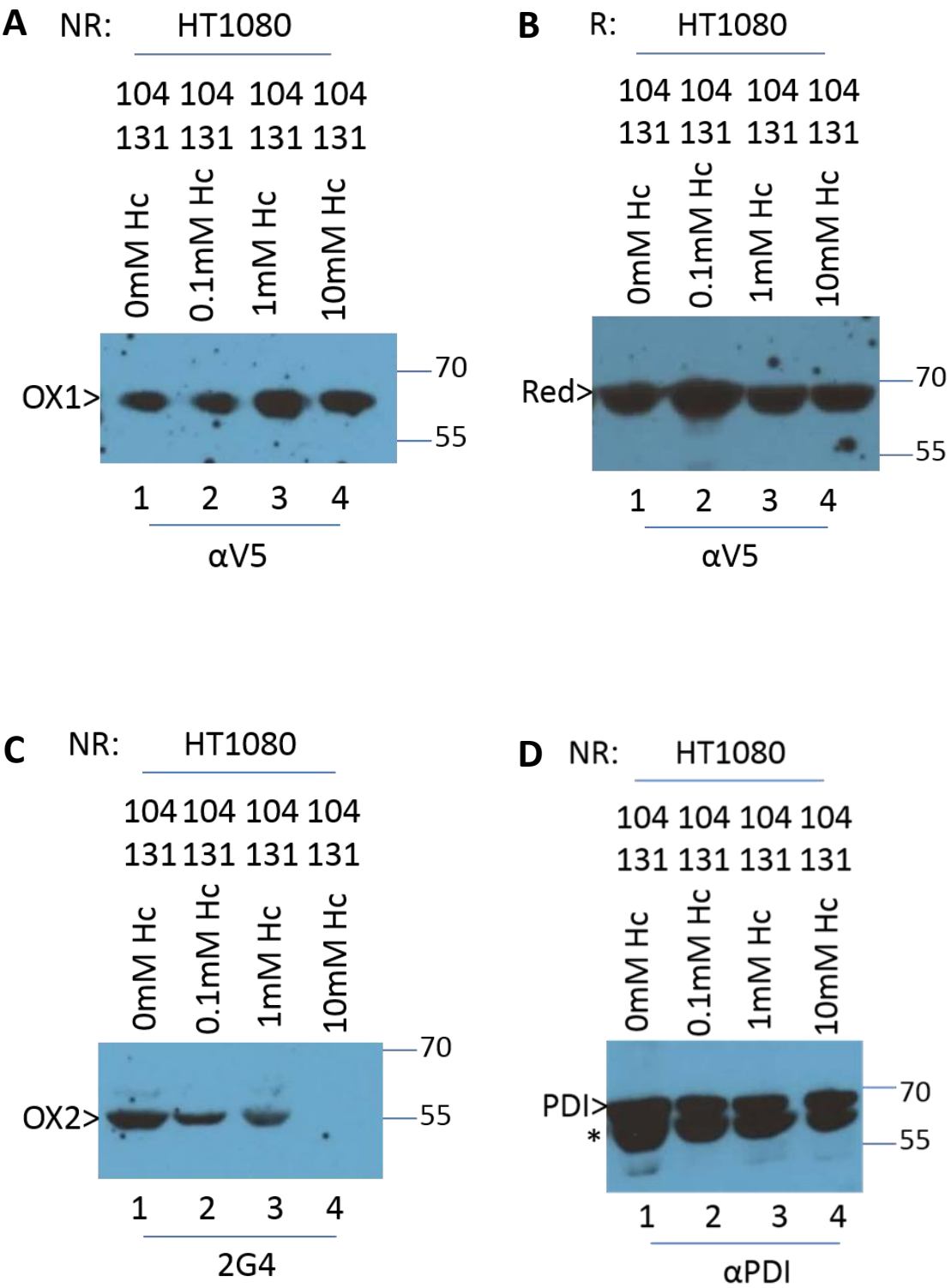

Figure 3.7. Induction of OX1 by homocysteine in cells transfected with C104A/C131A Ero1α

Following transfection with Ero1α V5 tagged C104A/C131A, HT1080 cells were treated with 0, 0.1, 1 and 10 mM homocysteine for 1 hour then lysed in MNT buffer. Cell lysates were then subjected to non-reducing (NR) or reducing (R) SDS-PAGE and subsequent Western blotting with the antibodiess αV5 (**A**,**B**), αPDI (**D**) or 2G4 (**C**). Ero1α monomer oxidation states are labelled OX1, OX2 or reduced (Red). Background bands are indicated (*****).

3.2.4 The effect of homocysteine on Ero1α in cells transfected with the mutant Ero1α C391A

A structural disulphide bond connecting Cys85 and Cys391 is thought to bring together the two active sites of Ero1α, thus facilitating electron transfer between them. On SDS-PAGE, the C391A mutant Ero1α runs at a molecular weight intermediate to the OX1 and R form, as without the long range disulphide its structure is a lot more similar to that of the completely reduced form (Benham et al., 2000). It is not known if the Cys85 is able to form a bond with another free Cys in the absence of Cys 391 (shown schematically in Figure 3.6D).

Figure 3.8A shows that in HT1080 cells transfected with the myc tagged C391A mutant, Ero1α existed as 2 partially oxidised forms. The lower mobility form migrated the same as the reduced form seen in Figure 3.8B, making it likely that the bands seen in Figure 3.8A were OX1-like and reduced-like forms of Ero1α. Despite the shift in molecular weight, due to the loss of the long range disulphide, there was still the same pattern of change with the addition of homocysteine. From this we can conclude that the homocysteine induced change in the structure of Ero1α was not due to a change in the regulatory bond between Cys85 and Cys391. Ero1α is still able to function as an oxidoreductase in this form, however the lack of the regulatory bond means that oxidative folding via Ero1α is less efficient (Mezghrani et al., 2001).

The 2G4 antibody was used again to ensure that the change in compactness of the C391A mutant was due to homocysteine treatment. The absence of signal upon 10 mM homocysteine treatment showed that the homocysteine treatment had led to the disappearance of the 2G4 epitope (Figure 3.8C). Probing for PDI showed the presence of endogenous protein in all samples (Figure 3.8D).

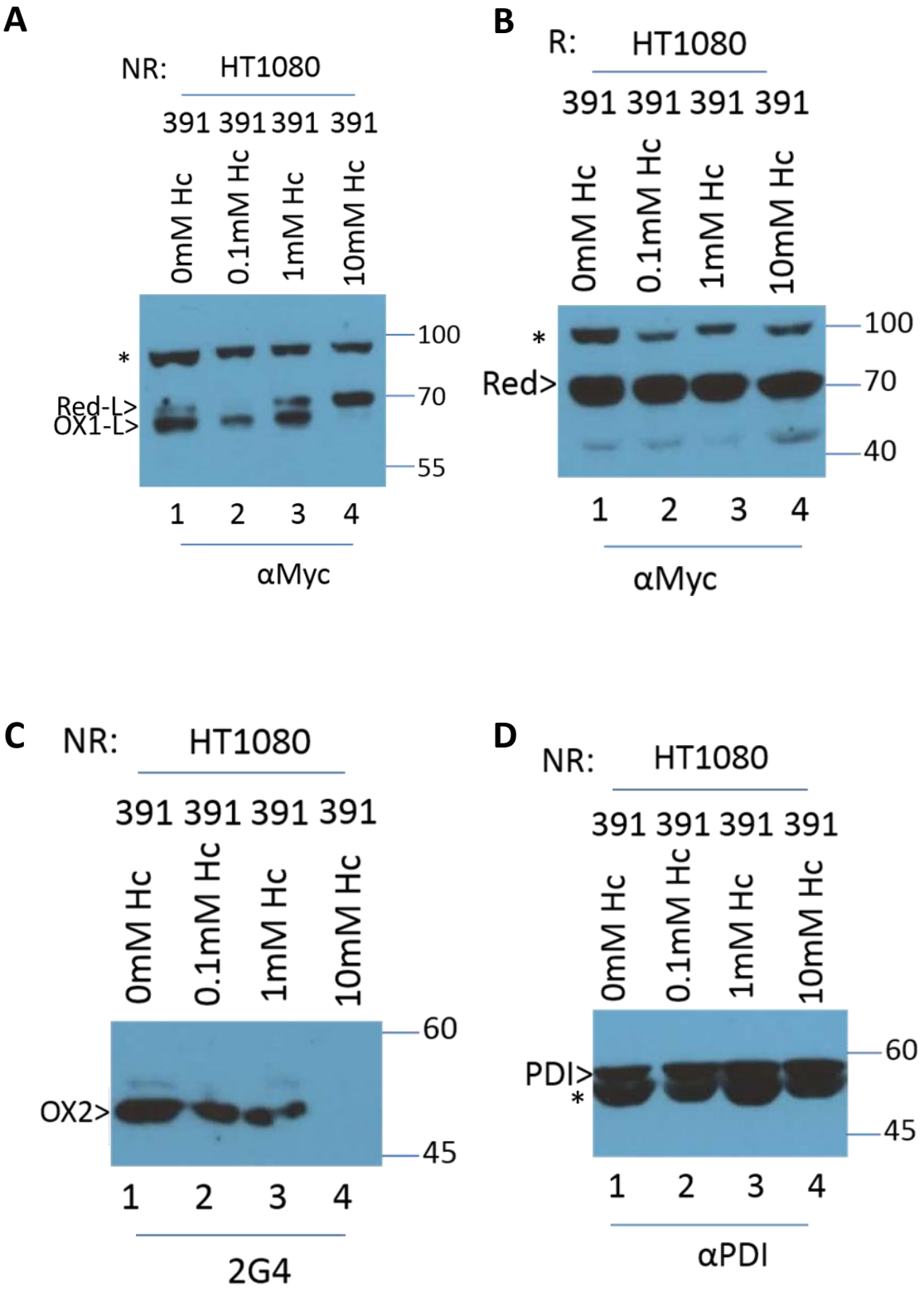

Figure 3.8. Induction of OX1 by homocysteine in cells transfected with C391A Ero1α
Following transfection with myc-tagged Ero1α-C391A, HT1080 cells were treated with 0, 0.1, 1 and 10 mM homocysteine for 1 hour then lysed in MNT buffer. Cell lysates were then subjected to non-reducing (NR) or reducing (R) SDS-PAGE and subsequent western blotting with the antibodies αMyc (**A**,**B**), 2G4 (**C**) or αPDI (**D**). Ero1α monomer oxidation states are labelled OX2, OX1-Like (OX1-L), reduced-like (Red-L) or reduced (Red). Background bands are indicated (*).

3.2.5 The effect of homocysteine on Ero1α in cells transfected with the "active site" mutants Ero1α C394A/C397A and C391A/C394A/C397A

Cys394-Cys397 make up the inner active site of Ero1α. Mutation of Cys394 or Cys397 inhibits oxidative folding (Mezghrani 2001), as the inner active site cannot form and regenerate disulphides to pass on to the outer active site (shown schematically in Figure 3.6E). This leaves the outer active site without a source of disulphide bonds, making it redundant.

HT1080 cells transfected with myc tagged C394A/C397A Ero1α showed an increase in OX1-like levels of Ero1α that lacked the inner active site (Figure 3.9A). This is consistent with other studies where mutation of Cys394 or Cys397 causes an increase in OX1-like compared to OX2 Ero1α (Appenzeller-Herzog et al., 2008). In Figure 3.9A upon the addition of homocysteine, Ero1α was further converted into an apparent OX1 state, as was previously seen with WT Ero1α. This would suggest that the homocysteine effect is independent of the inner active site Cys394-Cys397. This result does not rule out the possibility that homocysteine is taking its affect via the outer active sites Cys94-Cys99, and inducing OX1 regardless of whether Ero1α is able to take part in oxidative folding.

To analyse whether the absence of both the long range disulphide and the 'inner' active site influenced the response of Ero1α to homocysteine, a myc-tagged triple mutant was used (C391A/C394A/C397A). When HT1080 cells were transfected with this mutant, two bands, likely OX1-like and reduced-like Ero1α, existed in similar amounts prior to treatment with 10 mM homocysteine (Figure 3.9C). Unlike the Ero1α WT and the individual C391A and C394A/C397A mutants, the amount of the upper band, here reduced-like, did not increase when cells were treated with homocysteine, however the lower band was still lost at 10 mM homocysteine. This result can be attributed to the combination of mutating the active site and

the long range disulphide, as the constant upper band size was not seen with C394A/C397A Ero1α. Figures 3.9B and D show these samples having been probed with PDI as a loading control. Probing the lysates used in this experiment with the 2G4 antibody proved inconclusive, meaning it was not possible to tell if the triple mutant had lost the 2G4 epitope.

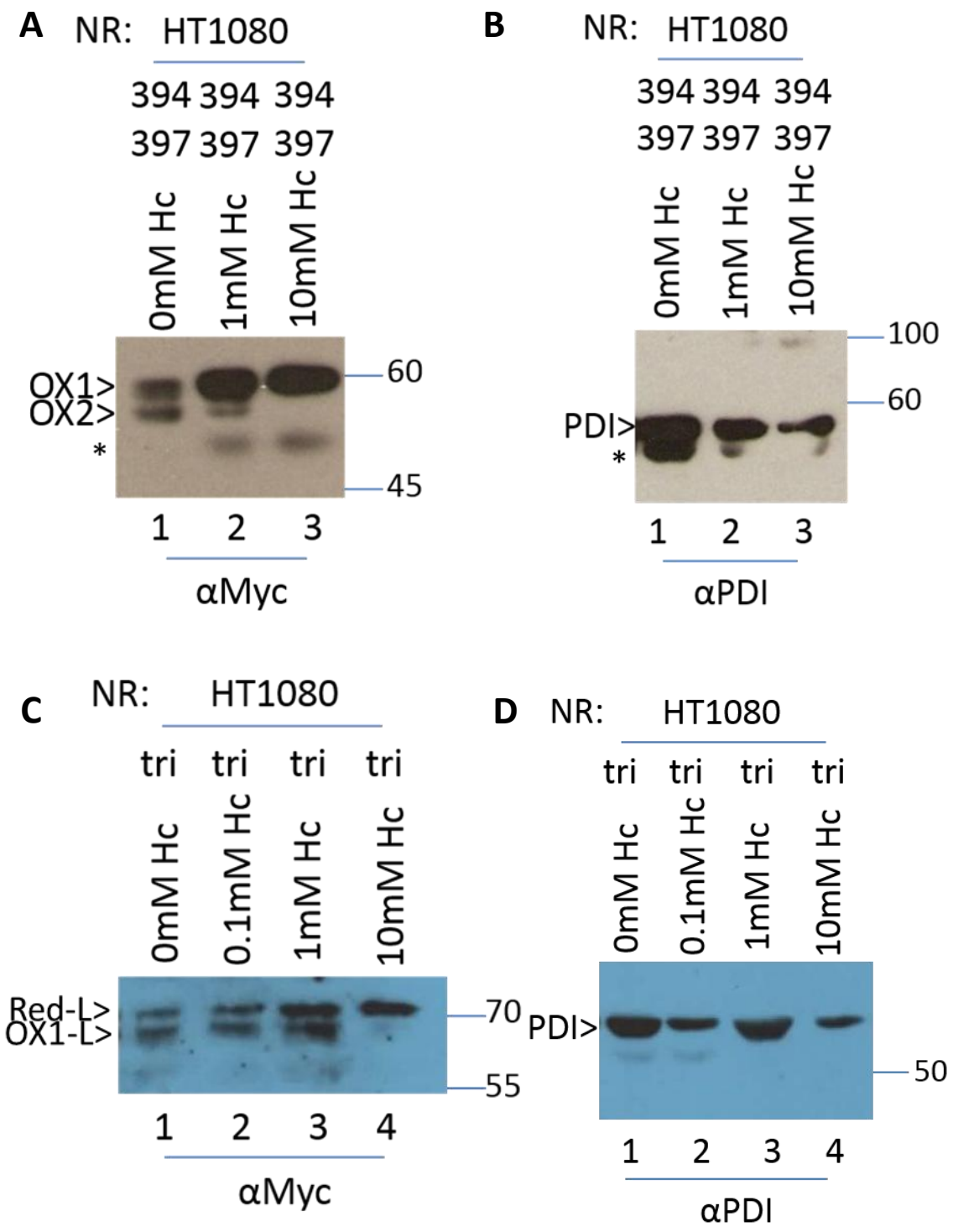

Figure 3.9. Induction of OX1 by homocysteine in cells transfected with C394A/C397A or C391A/C394A/C397A Ero1α

Following transfection with C394A/C397A (**A**,**B**) or C391A/C394A/C397A (tri) (**C**,**D**), HT1080 cells were treated with 0, 0.1, 1 and 10 mM homocysteine for 1 hour then lysed in MNT buffer. Cell lysates were then subjected to non-reducing (NR) SDS-PAGE and subsequent Western blotting with the antibodies αMyc (**A**,**C**) or αPDI (**B**,**D**). Ero1α monomer oxidation states are labelled OX1 or OX2, OX1-Like (OX1-L) or reduced-like (Red-L). Background bands are indicated (*).

3.2.6 Homocysteine and the interaction between Ero1α and PDI

Ero1α and PDI interact which, when visualised via western blot, gives a complex of about 120 kDa (Benham 2000). Whilst investigating the impact of homocysteine on the oxidation state of Ero1α, changes in the Ero1α/PDI complex were observed. In Figure 3.5, for example, the co-immunoprecipitation of Ero1α and PDI could no longer be seen after cells were treated with 10 mM homocysteine. To investigate the interaction between Ero1α and PDI more closely, a further series of experiments were performed. When analysed under non-reducing conditions, HT1080 cell lysates appeared to show no change in their Ero1α/PDI complex when treated with 0, 0.1 or 1 mM homocysteine and probed with the 2G4 antibody (Figure 3.10A, lanes 1-3). Upon the addition of 10 mM homocysteine, as previously seen (Figure 3.1) Ero1α monomers disappeared (Figure 3.10A, lane 4). Here, the Ero1α/PDI complex also disappeared, which is probably a result of it not being recognised by 2G4 (Figure 3.10A, lane 4).

When these samples were probed with αPDI under non-reducing conditions (Figure 3.10B) the Ero1α/PDI complex appeared at the same molecular weight as that seen upon probing with 2G4, but only upon treatment with 0 or 0.1 mM homocysteine. The PDI/Ero complex disappeared with the addition of 1 or 10 mM homocysteine. Note that the anti-PDI antibody recognised another double band at a higher molecular weight. This doublet was relatively resistant to the effects of homocysteine, and may represent an interaction between PDI and a client protein.

With the transfection of cells with myc tagged WT Ero1α it was possible to investigate the behaviour of the PDI/Ero1α complex by identifying it using an αmyc antibody (Figure 3.10C and D). The band representing the Ero1α/PDI complex in Figure 3.10C became much narrower with 10 mM homocysteine. As there was a bigger pool of OX1-like Ero1α at high concentrations of

homocysteine it might be expected that this would provide a larger available pool to interact with PDI; this, however, does not appear to be the case. The loss of the 120 kDa complex was observed over many repeats of this experiment, as well as other experiments where cells were transfected with WT or mutant Ero1α. The loss of the 120 kDa complex was seen for both endogenous and tagged/transfected Ero1α. In general when western blotted lysates were probed with αPDI, the Ero1α/PDI complex completely disappeared at 10 mM homocysteine, but often started to disappear at 1 mM homocysteine.

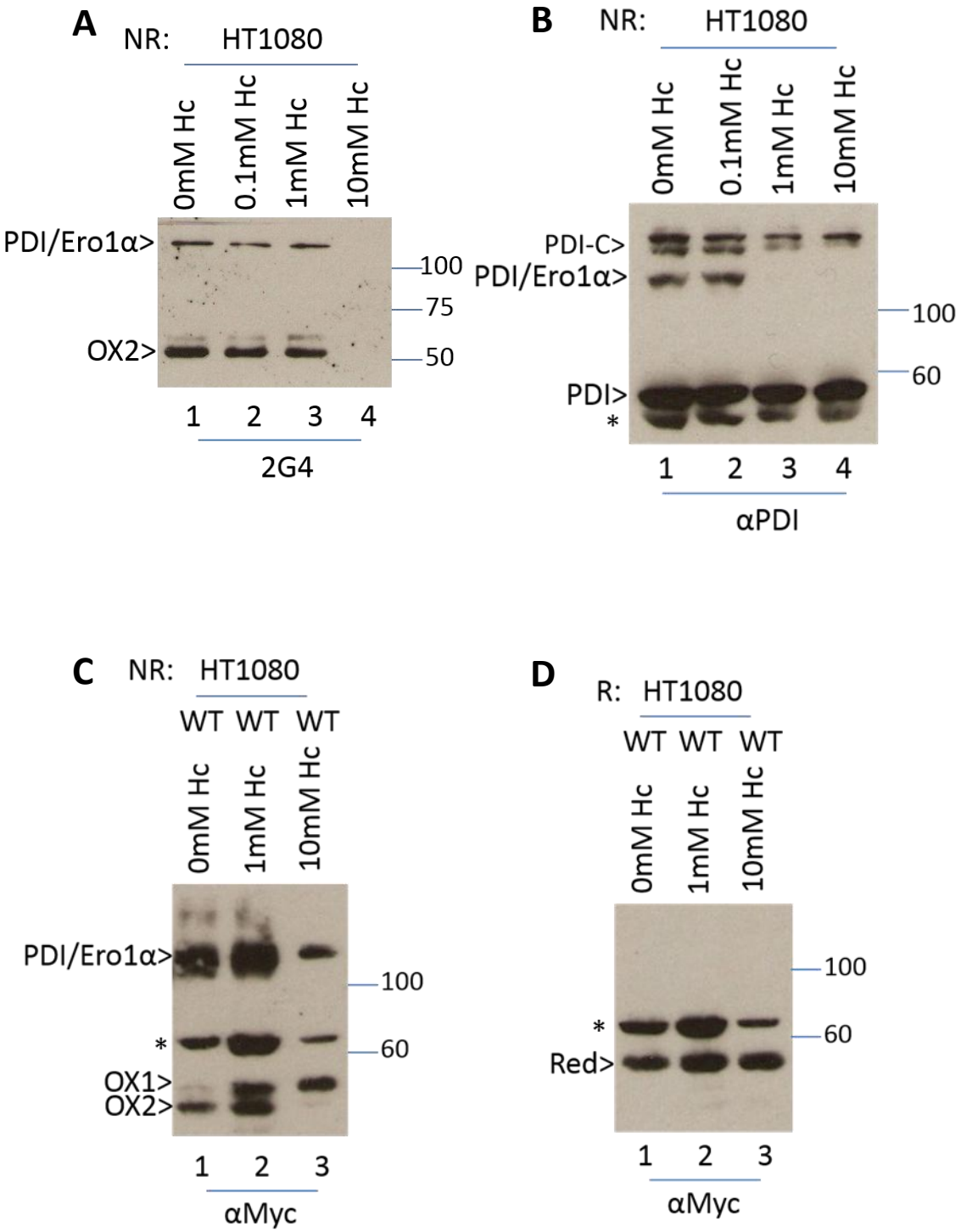

Figure 3.10. The effect of homocysteine on PDI/Ero1α complexes
Following transfection with Ero1α WT (**C** and **D**) HT1080 cells, as well as untransfected HT1080 cells (**A** and **B**) were treated with 0,1 and 10 mM homocysteine for 1 hour then lysed in MNT buffer. Cell lystaes were then subjected to non-reducing (NR) or reducing (R) SDS-PAGE and subsequent Western blotting with the antibodies 2G4 (**A**), αPDI (**B**) or αMyc (**C** and **D**). Ero1α monomer oxidation states are labelled OX1, OX2 or reduced (Red). PDI-Ero1α complexes (PDI/Ero1 α) and PDI-client complexes (PDI-C) are labelled . Background bands are indicated (*****).

3.2.7 Homocysteine and the interaction between PDI and the mutant Ero1α C104A/C131A, C391A, C397A/C397A and C391A/C394A/C397A

It has been demonstrated that PDI-complexes are diminished upon the addition of 10 mM homocysteine (Figure 3.10). To investigate whether the diminishing complexes are due to the change in Ero1α activity status or due to the method by which homocysteine has its effect, the previously used Ero1α mutants (3.2.2.3-3.2.2.5) were looked at further.

Cells transfected with the Ero1α mutants C104A/C131A, C391A, C394A/C397A or C391A/C394A/C397A were subjected to non-reducing SDS-PAGE and subsequent western blotting with αtag antibodies. No PDI complex could be detected between V5-tagged Ero1α C104A/C131A and PDI under non-reducing conditions (data not shown).

The Ero1α C391A mutant, (Figure 3.11A, a repeat of Figure 3.8A showing the PDI/Ero1α complex) had the same pattern of change in what appears to be Ero1α OX1 and OX2, as seen in the wild type (Figure 3.10). There was also a similar pattern of PDI/Ero1α complex loss, with most of the complex lost with 10mM homocysteine treatment. The bands representing the Ero1α complex in Figure 3.11A spanned a greater range of molecular weights than that seen in the wild type. The loss of the regulatory disulphide Cys391-Cys85 and subsequent loss of structure may cause complexes of different sizes to be formed, or free cysteine residues resulting from the mutation may interact with PDI or other proteins to form complexes of different weights.

This pattern seen in Ero1α C391A was also seen in the Ero1α C394A/397A mutant in Figure 3.11B, which showed a larger range of molecular weights than seen in Figure 3.9A. The

PDI/Ero1α complex spanned a greater range of molecular weights than the wild type, and the lower molecular weight bands diminish at 10 mM homocysteine, with the band resolving into 2 separate bands. The change in molecular weight of these bands could suggest that the complexes are pushed into different conformations upon homocysteine treatment.

A faint band or bands were formed at about 120 kDa in Ero1α triple mutant (C391A/C394A/C397A) in the absence of homocysteine treatment. These disulphide-dependent complexes became slightly fainter when cells expressing Ero1α were treated with homocysteine, however it is not clear which bands represent the Ero1α/PDI complex (Figure 3.11C). The PDI/Ero1α complex may only exist in small quantities in cells expressing this mutant.

The PDI/Ero1α complex diminished upon 10mM homocysteine treatment in cells transfected with wildtype Ero1α, but also when cells were transfected with mutant Ero1α which showed the same pattern of Ero1α OX1-like/OX2 change as the wild type.

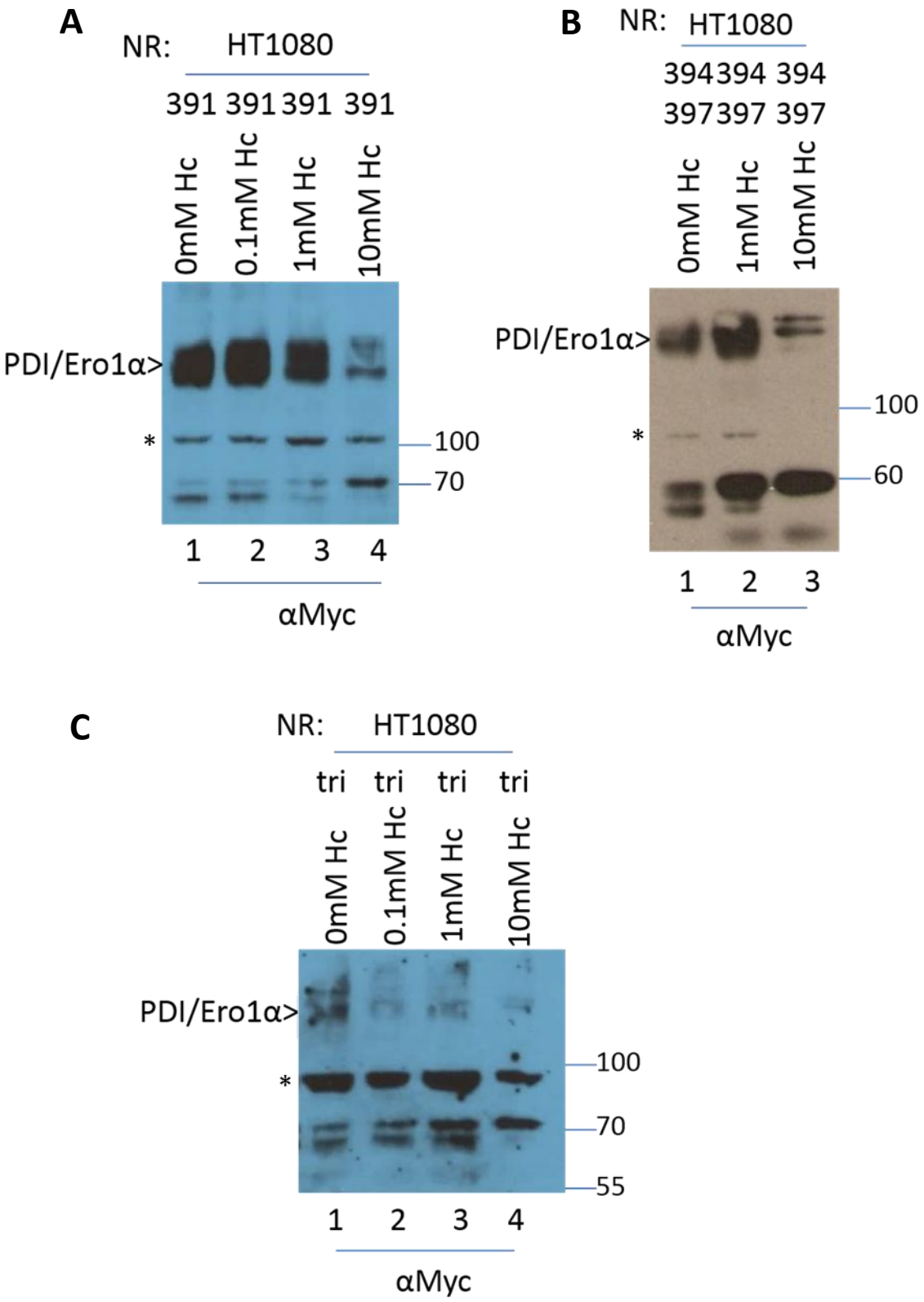

Figure 3.11. The effect of homocysteine on PDI/mutant Ero1α complexes
Following transfection with Ero1α mutants C391A (**A**), C394A/C397A and (**B**), C391A/C394A/C397A (**C**) HT1080 cells were treated with 0, 0.1, 1 and 10 mM homocysteine for 1 hour then lysed in MNT buffer. Cell lysates were then subjected to non-reducing (NR) SDS-PAGE and subsequent Western blotting with the αMyc antibody. Background bands are indicated (*****).

3.2.8 NEM and Ero1α disulphides

We have seen that homocysteine alters the activation state of Ero1α and the PDI/Ero1α complex, both of which are controlled by disulphide bonds. Homocysteine also affects Ero1α mutants which have altered disulphides. To investigate whether homocysteine exerts its effect by altering the availability of free –SH groups, cells were lysed with or without the thiol-alkylating agent NEM. All of the experiments carried out so far have used lysis buffer containing NEM which is often used to prevent disulphide rearrangement by blocking the –SH groups, and is particularly effective as it is very quick to permeate cell membranes.

Under reducing or non-reducing conditions, lysates were subjected to SDS-PAGE and western blot with 2G4 (Figure 3.12). In the absence of homocysteine, Ero1α from HT1080 cells existed in the OX2 form both in the presence and absence of NEM under non-reducing conditions (Figure 3.12A lanes 1 and 2). With the addition of 1 mM homocysteine Ero1α existed in the OX2 form. The shadow band (*) previously observed (Figure 3.4A) can also be seen, however in the presence of homocysteine, there was another band with a slightly higher molecular weight (**) than the shadow band which was not observed when NEM was present. This suggests that the addition of homocysteine reduces an –SH group that becomes available for disulphide rearrangement after lysis or that Ero1α favours rearrangement to an already existing –SH group in the presence of homocysteine. When the homocysteine concentration was increased to 10 mM, Ero1α OX2 disappeared; however the additional band in the absence of NEM, as seen in lane 3, remained. When the samples were analysed under reducing conditions, all Ero1α existed in the reduced form. Like the previous treatments with 10 mM homocysteine, the Ero1α signal completely disappeared, but without the addition of NEM (Figure 3.12A, lane 11) the reduced Ero1α remained. This signal could be the same as the reduced form of the band recognised in lane 5.

When the same lysates were probed with an αPDI antibody under non-reducing conditions, the PDI/Ero1α complex was not detected in either the NEM or non-NEM lysed cell lines with 10 mM homocysteine. This would suggest that the less compact Ero1α protein found in Figure 3.12A lane 5 was not able to bind PDI. The PDI/Ero complex could be seen with all other combinations of homocysteine and NEM tested (Figure 3.12B lanes 1, 2, 3 and 4). A higher molecular weight complex ~160kDa could also be seen, which increased in intensity with the addition of homocysteine in the presence of NEM.

When the same experiment was carried out in the OE33 cell line using 2G4 to detect Ero1α in cell lysates +/- NEM (Figure 3.12C), the same results were seen, with a slower migrating, partly reduced higher molecular weight Ero1α band appearing in the presence of homocysteine and in the absence of NEM. This suggests that homocysteine partially reduces Ero1α and that as the Ero1α protein becomes partially reduced, it exposes a sulhydryl group that is accessible to alkylation by NEM, resulting in loss of the 2G4 epitope. What is seen in HT1080 is not cell specific, but also can be applied to other cell lines.

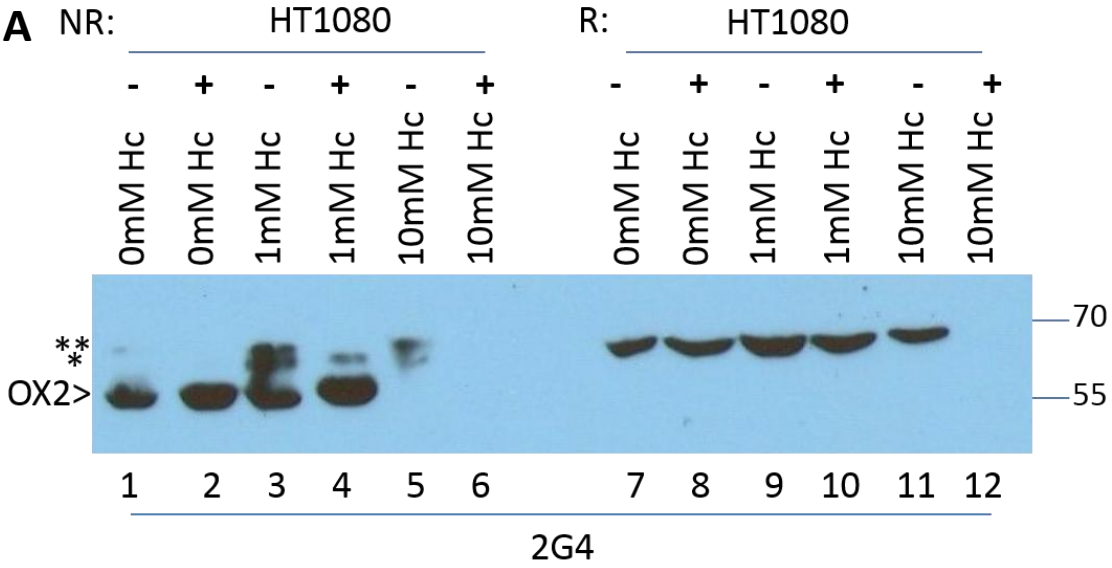
A
NR:
HT1080
R:
HT1080
- + - + - +
0mM Hc
0mM Hc
1mM Hc
1mM Hc
10mM Hc
10mM Hc
- + - + - +
0mM Hc
0mM Hc
1mM Hc
1mM Hc
10mM Hc
10mM Hc
**
*
OX2>
70
55
1 2 3 4 5 6 7 8 9 10 11 12
2G4

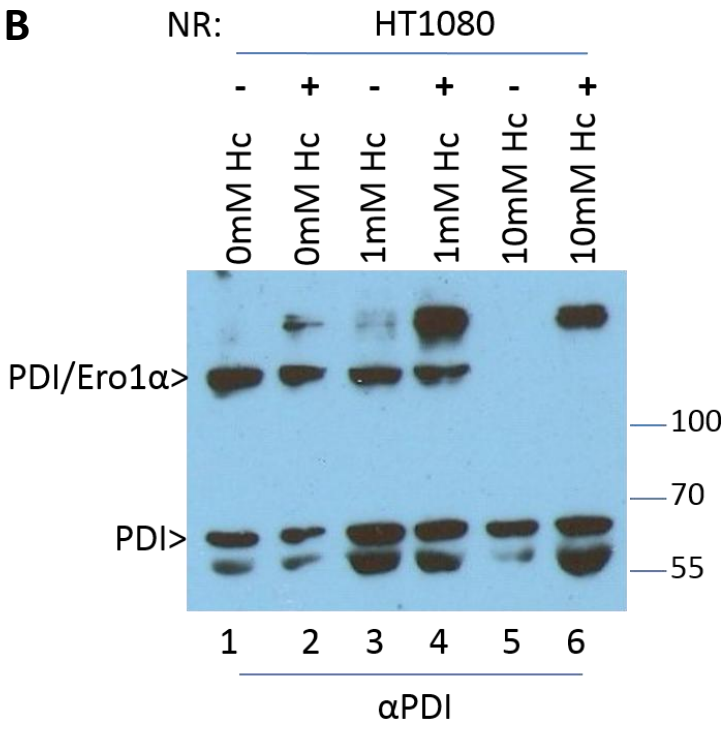
B
NR:
HT1080
- + - + - +
0mM Hc
0mM Hc
1mM Hc
1mM Hc
10mM Hc
10mM Hc
PDI/Ero1α>
PDI>
100
70
55
1 2 3 4 5 6
αPDI

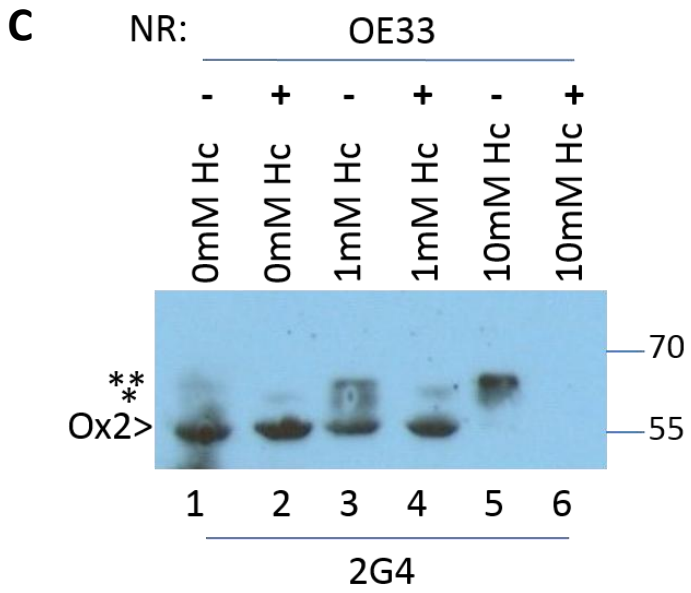

Figure 3.12. NEM effect on disulphide bonds in homocysteine treated cells
HT1080 (**A** and **B**) and OE33 (**C**) cells were treated with 0, 1 and 10 mM homocysteine for 1 hour then lysed in MNT buffer in the presence (+) or absence (-) of 50 mM NEM. Cell lysates were then subjected to non-reducing (NR) or reducing (R) SDS-PAGE and subsequent Western blotting with the antibodies 2G4 (**A** and **C**) or αPDI (**B**). Background bands are indicated (*)(**).

3.2.9 Cystathionine does not impact the oxidation state of Ero1α

To further investigate how homocysteine mediates its effect on Ero1α, cells in culture were treated with an intermediate in the homocysteine metabolism pathway, cystathionine. Battle et al (Battle et al., 2013) observed that the control of Ero1α by homocysteine did not extend to the amino acids cysteine and methionine in OE33 cells. By using cystathionine, the product of the first step in the metabolism of homocysteine to cysteine, it is possible to deduct whether homocysteine directly effects Ero1α or if it is working through cystathionine in this pathway.

The conditions of the cystathionine treatments were the same as that for homocysteine, using concentrations up to 10 mM since all Ero1α existed as OX1 at this concentration of homocysteine. Neither HT1080 nor OE33 cells showed a change in oxidation state upon treatment with cystathionine (Figure 3.13A and B respectively). There also appeared to be no change in the migration or level of the PDI/Ero1α complexes (Figure 3.13A), disregarding a small decrease in the band intensity for the PDI/Ero1α complex in 1 mM cystathionine treated HT1080 cells (Figure 3.13 A lane 4), which was most likely due to sample loading variation. The experiments suggest that it is not the cystathionine intermediate in the homocysteine metabolic pathway which mediates the homocysteine effect.

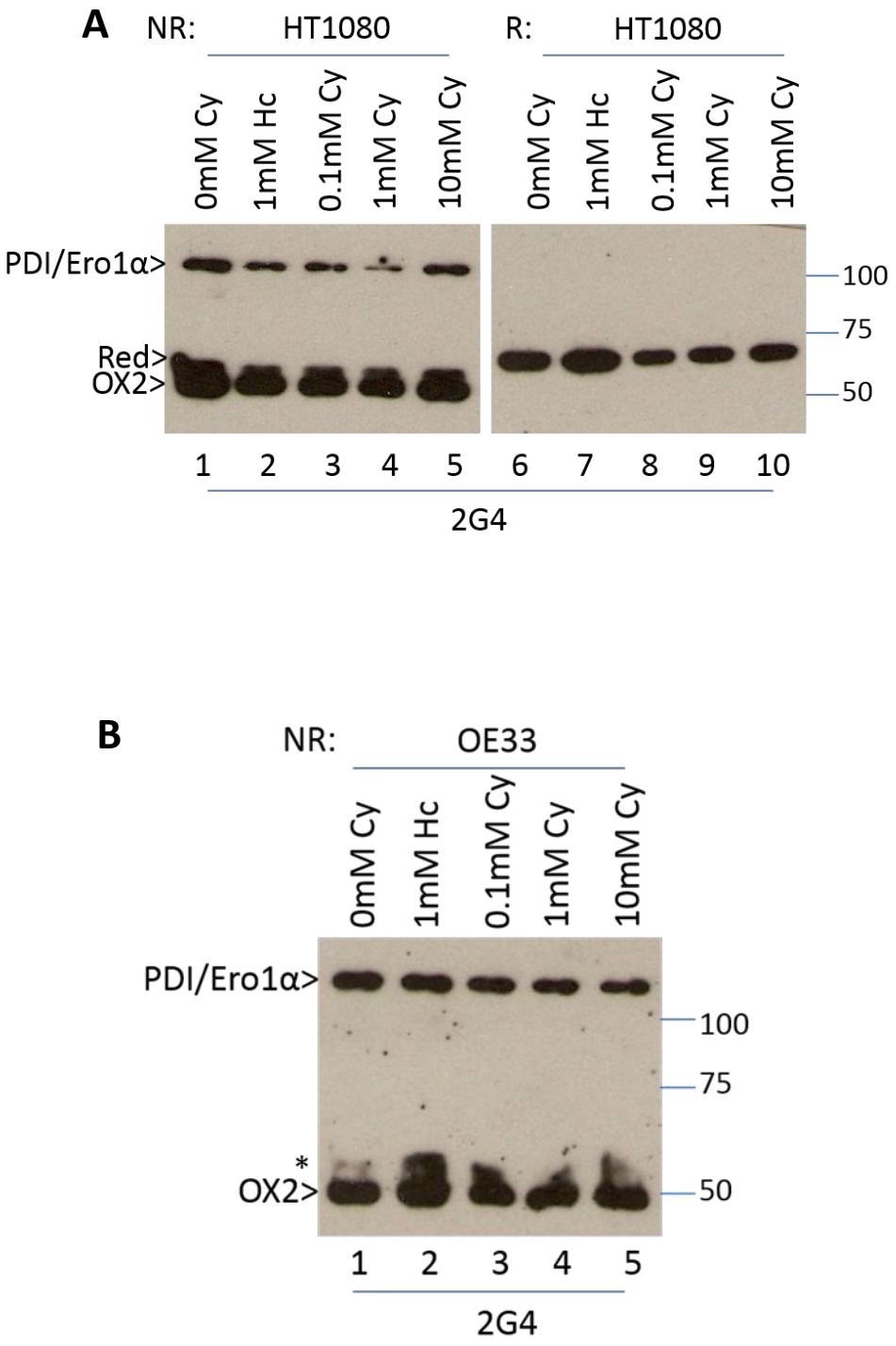

Figure 3.13. Cystathionine does not change the recognition of Ero1α by the 2G4 antibody or increase Ero1α OX1
HT1080 (**A**) and OE33 (**B**) cells were treated with 0, 0.1, 1 and 10 mM cystathionine for 1 hour then lysed in MNT buffer. Cell lysates were then subjected to reducing (R) or non-reducing (NR) SDS-PAGE and subsequent Western blotting with the monoclonal antibody 2G4. Ero1α monomer oxidation states are labelled OX2 or reduced (Red). Background bands are indicated (*****).

3.2.10 Ascorbic acid does not impact the oxidation state of Ero1α or its recognition by 2G4

Despite the Ero1α in cell lines existing predominantly in the OX2 state, different cell types vary in their OX1:OX2 ratios under normal conditions. This is likely due to differences in their secretory load, and thus the amount of protein they are responsible for folding. However in culture, cell lines thrive and thus are maintained in different media compositions, including differing amounts of ascorbic acid. Ascorbic acid may contribute to the redox poise of the cell, particularly when the normal Ero1-PDI pathway or ER redox conditions are perturbed. Whether ascorbic acid, or the lack of it, has an effect on the Ero1-PDI axis and homocysteine control was therefore investigated.

OE33 and HT1080 cells were treated with increasing concentrations of ascorbic acid (AA; 0 µM, 10 µM, 100 µM and 1 mM; an appropriate range to induce cellular changes (Blaschke et al., 2013; Minor et al., 2013)) with or without either 1 or 10 mM homocysteine. No change was seen in the ability of 2G4 to detect Ero1α in any of the treatment combinations. When treated with ascorbic acid alone (Figure 3.14 A, B, D and E, lanes 3, 5 and 7) there was no change in Ero1α OX2. As this band also did not appear to change upon the addition of 1 mM homocysteine, the homocysteine effect was not enhanced by ascorbic acid. If such an effect did exist there would be a potential shift towards the Ero1α OX1 state, as seen with 10 mM homocysteine, at higher ascorbic acid concentrations. Consistent with previous results, the Ero1α band disappeared with 10 mM homocysteine in both HT1080 and OE33 cells (Figure 3.12B and E). There was no recovery of signal when homocysteine-treated cells were co-incubated with ascorbic acid. This suggests that ascorbic acid neither enhances nor diminishes the effects of homocysteine on Ero1α.

Despite there being no change to Ero1α monomers, in OE33 cells treated with ascorbic acid, a change was seen in the bands seen above the PDI/Ero1α complexes at about 140 kDa, which increased with the addition of ascorbic acid (Figure 3.14F). The addition of 1mM homocysteine prevented this increase. A similar pattern is seen in HT1080 cells, with the exception of lane 5, where an air bubble may have blocked the signal (Figure 3.14C).

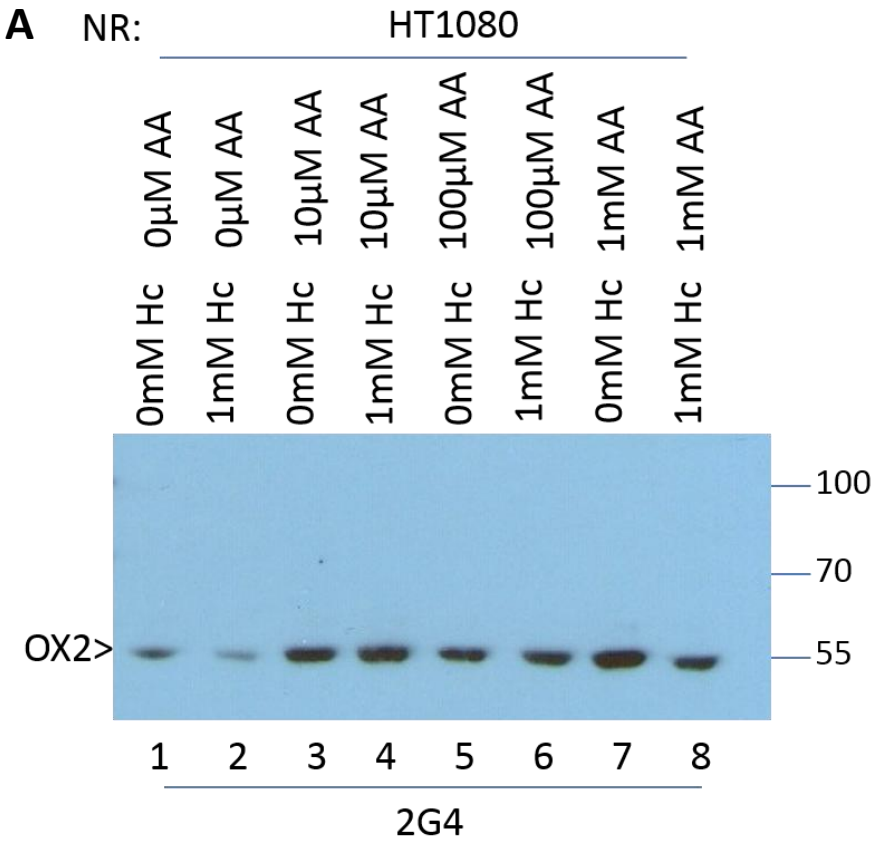
A
NR:
HT1080
0μM AA
0μM AA
10μM AA
10μM AA
100μM AA
100μM AA
1mM AA
1mM AA
0mM Hc
1mM Hc
0mM Hc
1mM Hc
0mM Hc
1mM Hc
0mM Hc
1mM Hc
100
70
55
OX2>
1 2 3 4 5 6 7 8
2G4

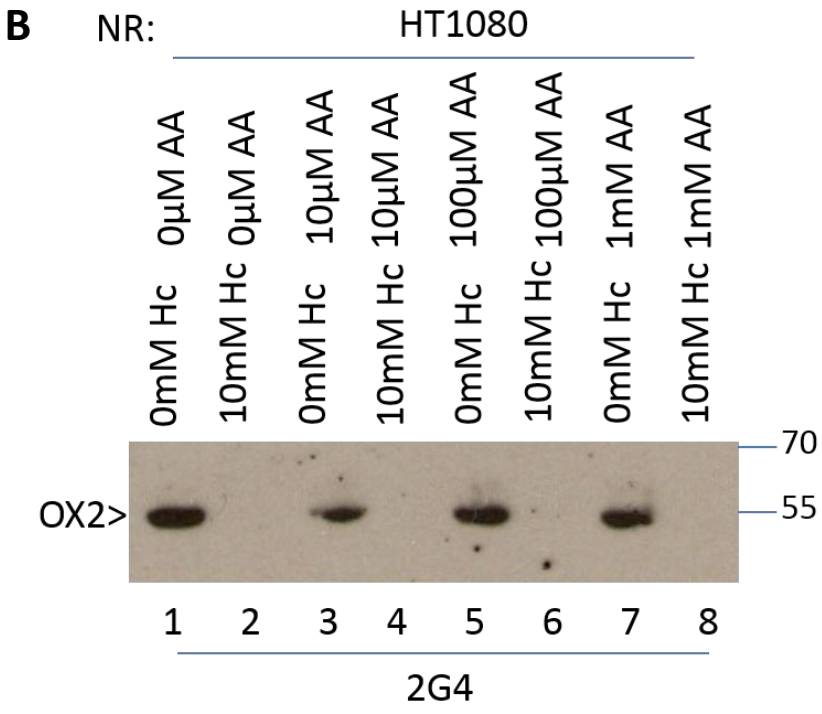
B
NR:
HT1080
0μM AA
0μM AA
10μM AA
10μM AA
100μM AA
100μM AA
1mM AA
1mM AA
0mM Hc
10mM Hc
0mM Hc
10mM Hc
0mM Hc
10mM Hc
0mM Hc
10mM Hc
70
55
OX2>
1 2 3 4 5 6 7 8
2G4

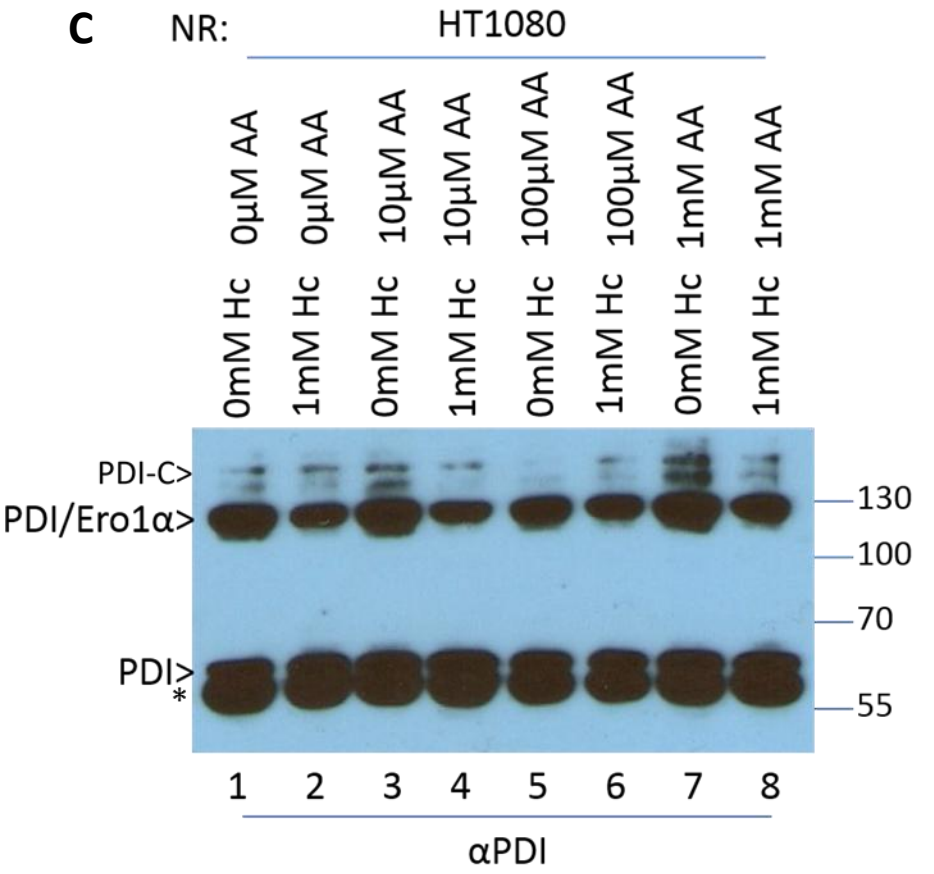
C
NR:
HT1080
0µM AA
0µM AA
10µM AA
10µM AA
100µM AA
100µM AA
1mM AA
1mM AA
0mM Hc
1mM Hc
0mM Hc
1mM Hc
0mM Hc
1mM Hc
0mM Hc
1mM Hc
PDI-C>
PDI/Ero1α>
PDI>
*
130
100
70
55
1 2 3 4 5 6 7 8
αPDI

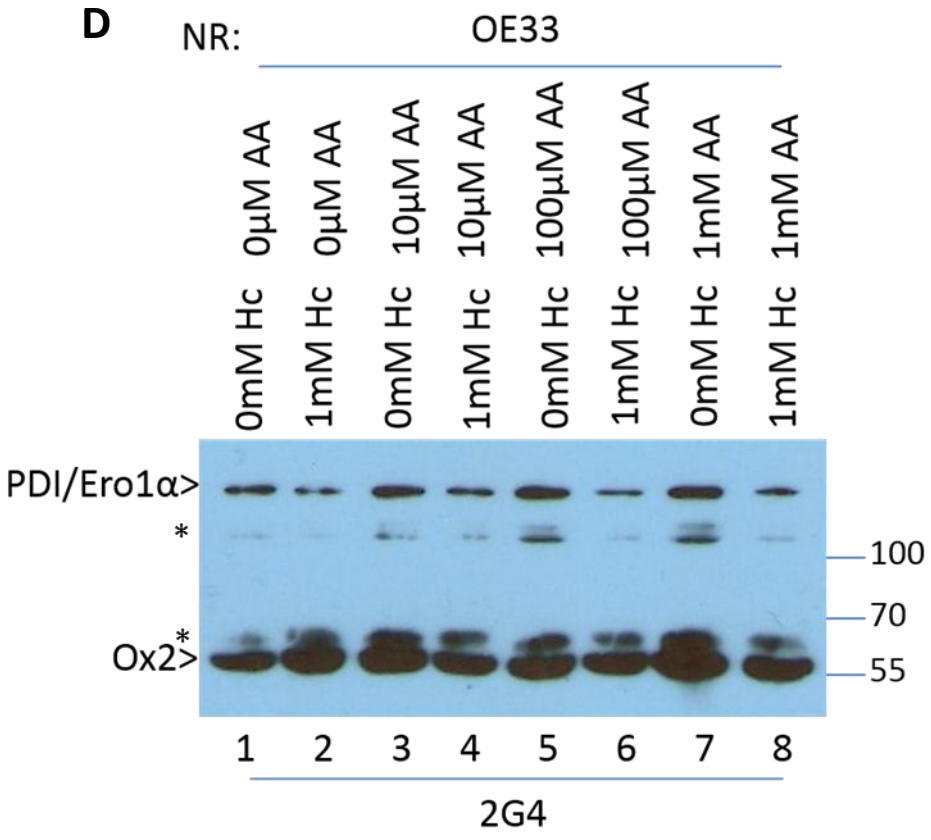
D
NR:
OE33
0µM AA
0µM AA
10µM AA
10µM AA
100µM AA
100µM AA
1mM AA
1mM AA
0mM Hc
1mM Hc
0mM Hc
1mM Hc
0mM Hc
1mM Hc
0mM Hc
1mM Hc
PDI/Ero1α>
*
Ox2*>
100
70
55
1 2 3 4 5 6 7 8
2G4

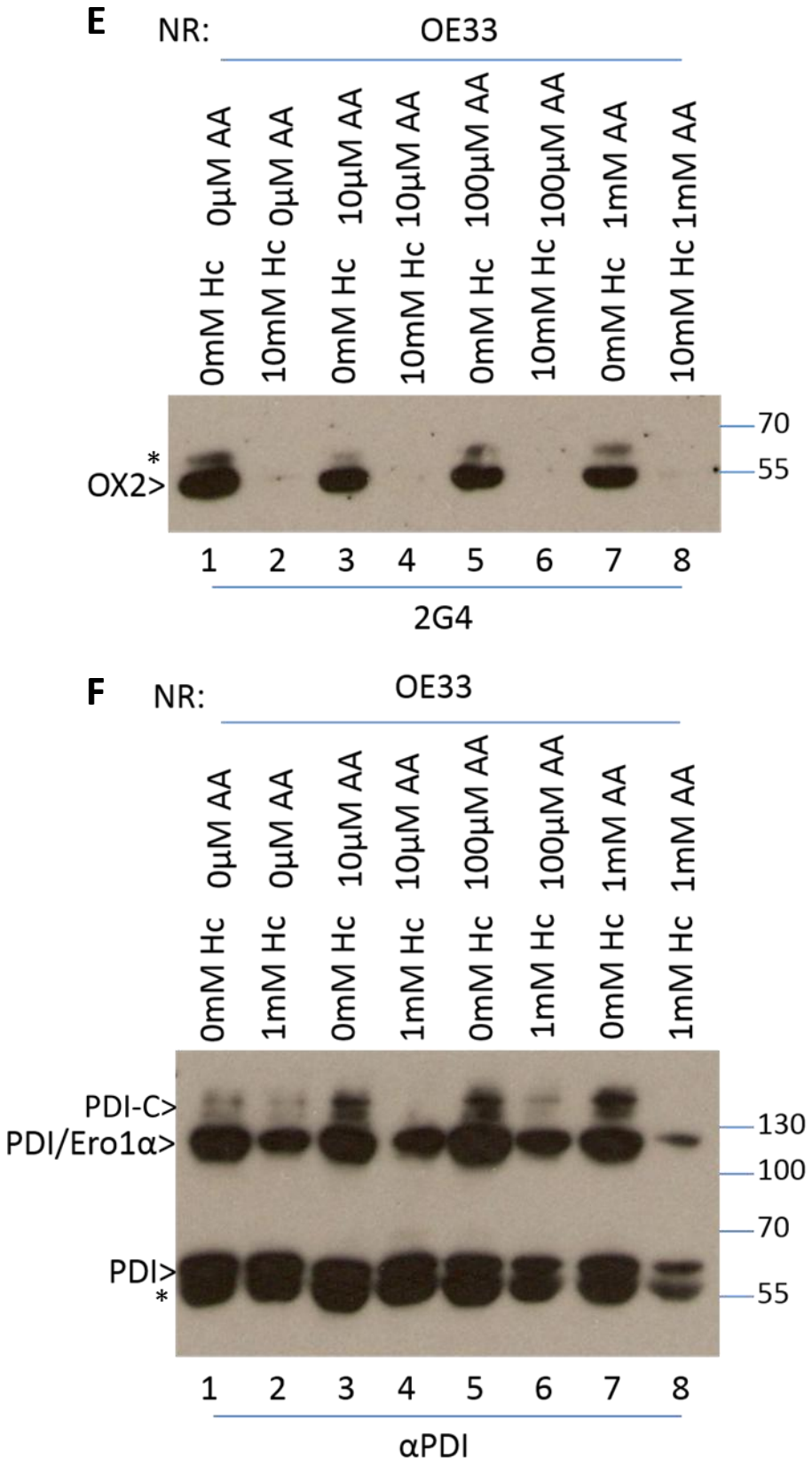

Figure 3.14. Ascorbic acid does not affect the recognition of Ero1α by 2G4
HT1080 (**A**, **B** and **C**) and OE33 (**D**, **E** and **F**) cells were treated with 0, 1 and 10 mM homocysteine in combination with 0, 10 100 µM and 1 mm ascorbic acid (AA) for 1 hour then lysed in MNT buffer. Cell lysates were then subjected to non-reducing (NR) SDS-PAGE and subsequent Western blotting with the monoclonal antibody 2G4 (**A**, **B**, **D**, **E**) or αPDI (**C** and **F**). Ero1α monomer oxidation state labelled OX2. PDI-Ero1α complexes (PDI/Ero1 α) and PDI-client complexes (PDI-C) are labelled . Background bands are indicated (*****).

3.2.11 Homocysteine does not cause gross changes in ER morphology

To further characterise how homocysteine influences Ero1α, and the general effects of this molecule on the ER, HT1080 cells were mock treated or treated with homocysteine or DTT and subjected to live cell imaging at 10 minute intervals (Figures 3.15, 3.16 and 3.17). A blue/white ER tracker was used to visualise the ER. The morphology of the ER did not change over the course of 50 minutes in the untreated cells (Figure 3.15). The ER had a characteristic perinuclear appearance. Although the signal from the ER tracker became progressively brighter with time, the morphology remained consistent. HT1080 cells treated with homocysteine presented a very similar picture, with a perinuclear staining of similar size and density (Figure 3.16). In contrast, when cells were treated with DTT, changes to the ER occured very quickly, in the time between cell treatment and the first image being taken (Figure 3.17). The perinuclear staining was different to that seen in Figure 3.15 and 3.16, with gross changes occurring and smaller vesicles becoming visible. The addition of DTT to the ER makes it much more reducing thus preventing proper protein folding, inducing oxidative stress and eventually causing cells to detach and die.

Taken together these experiments suggest that, unlike DTT, homocysteine does not have a general reducing effect on the ER and lay the groundwork for live cell imaging of ER proteins involved in oxidative protein folding.

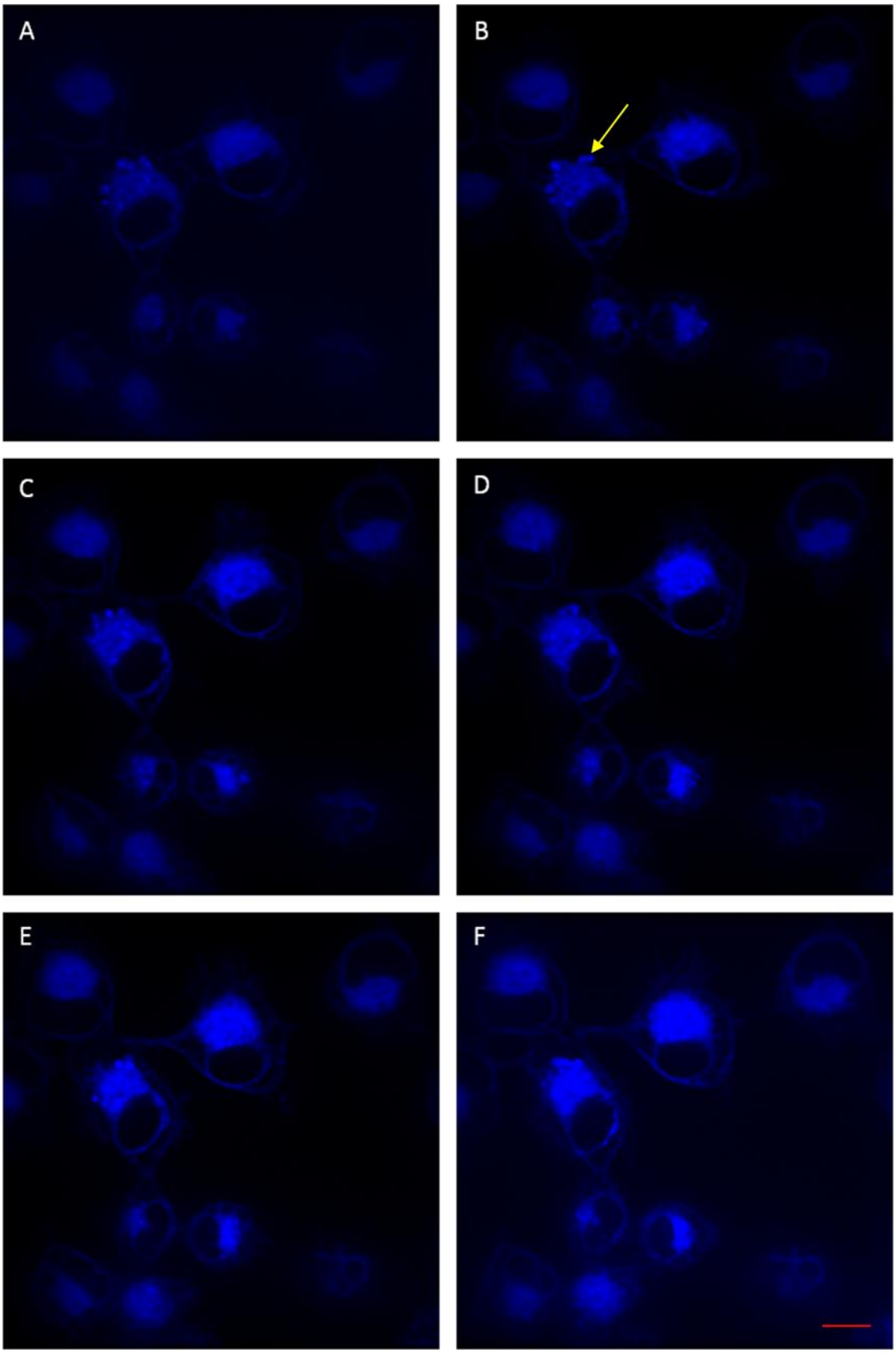

Figure 3.15. ER morphology in untreated HT1080 cells
HT1080 cells were incubated with ER tracker for 10 minutes. Following this cells were imaged, and imaged again every 10 minutes. 0 minutes (**A**), 10 minutes (**B**), 20 minutes (**C**), 30 minutes (**D**), 40 minutes (**E**), 50 minutes (**F**). Red scale bar=10 microns. Yellow arrow indicates an example of ER perinuclear staining.

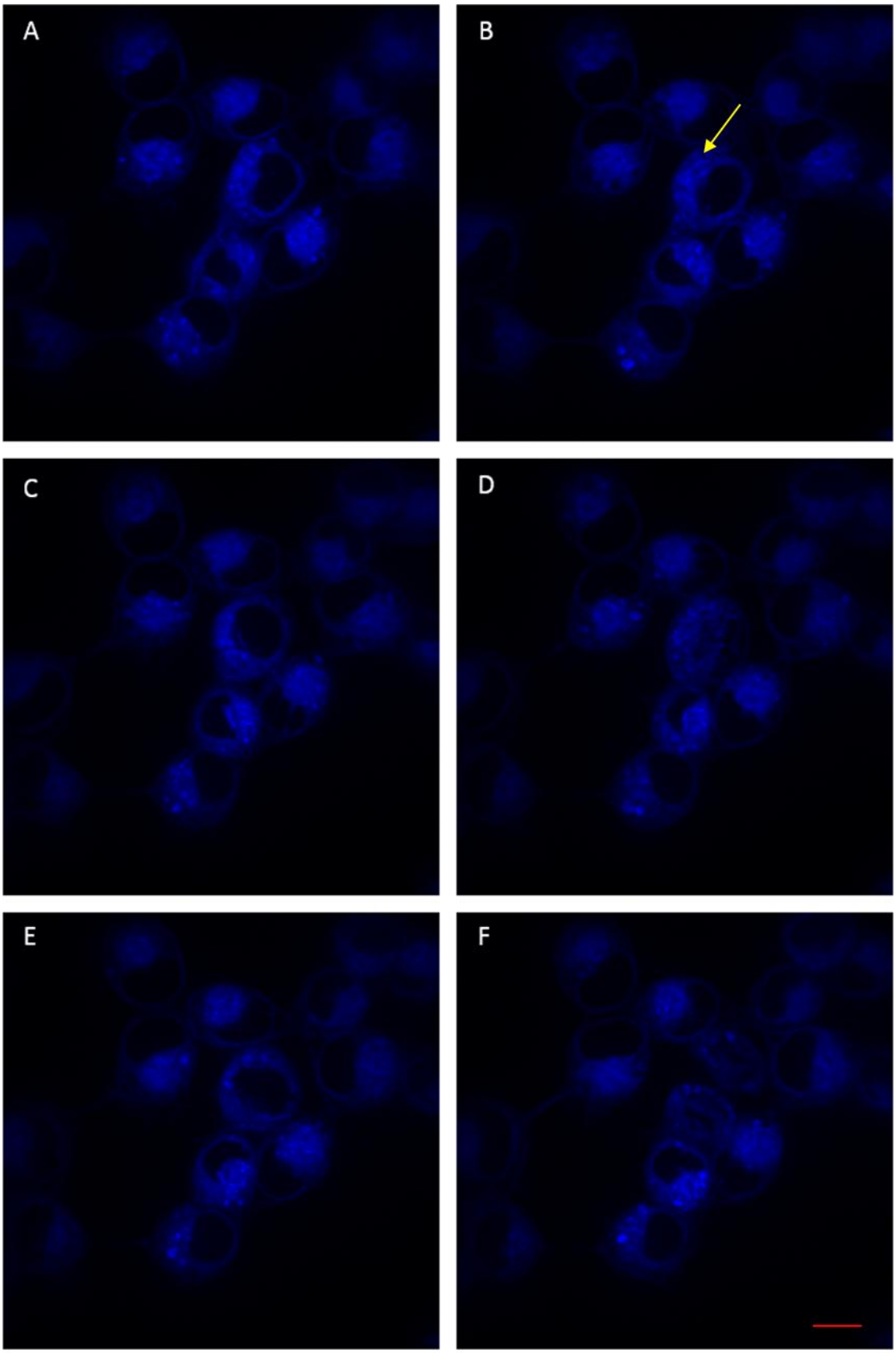

Figure 3.16. ER morphology in homocysteine treated cells
HT1080 cells were incubated with ER tracker for 10 minutes. Following this, cells were treated with 10 mM homocysteine and imaged, and imaged again every 10 minutes after this. 0minutes (**A**), 10 minutes (**B**), 20 minutes (**C**), 30 minutes (**D**), 40 minutes (**E**), 50 minutes (**F**). Red scale bar=10 microns. Yellow arrow indicates an example of ER perinuclear staining.

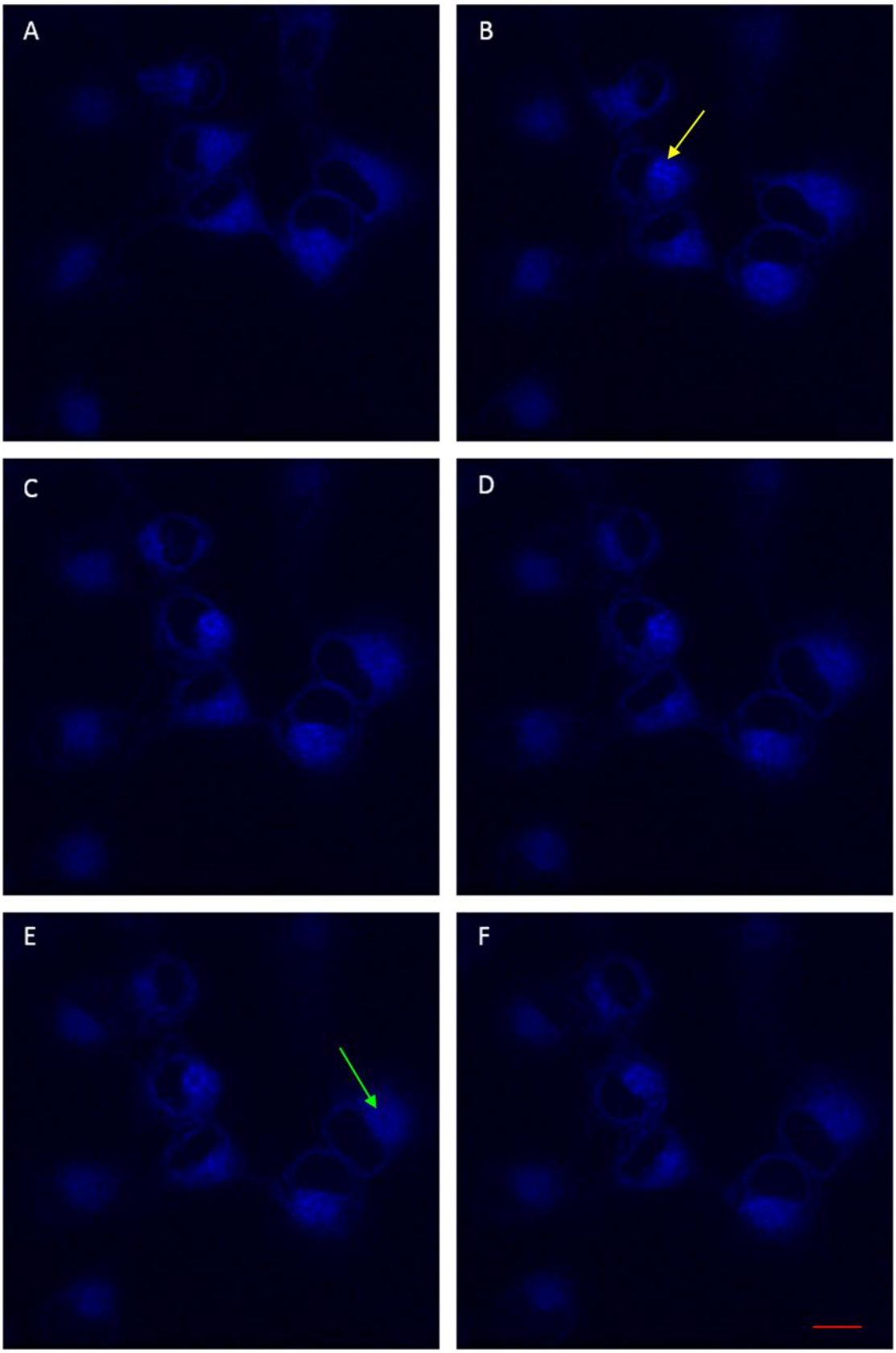

Figure 3.17. ER morphology in DTT treated cell
HT1080 cells were incubated with ER tracker for 10 minutes. Following this, cells were treated with 10 mM DTT and imaged, and imaged again every 10 minutes after this. 0 minutes (**A**), 10 minutes (**B**), 20 minutes (**C**), 30 minutes (**D**), 40 minutes (**E**), 50 minutes (**F**). Red scale bar=10 microns. Yellow arrow indicates an example of ER perinuclear staining, green arrow indicates an example of the small perinuclear vesicles formed.

3.3 Discussion

Ero1α has a complex system of control which is highly regulated and although a mechanism exists to explain this control, much remains to be known about its regulation. By looking at homocysteine, which has previously been shown to influence the oxidation state of Ero1α, it is possible to explore novel ways in which Ero1α is controlled. Investigating how, and at what point, homocysteine takes an effect would give insight into this.

As well as the change in oxidative state previously seen with homocysteine (Figure 3.2), here another change is seen in the disappearance of Ero1α signal when using the monoclonal antibody 2G4 (Figure 3.3A and C). There was no Ero1α OX1 signal seen in any cell type when lysates were probed with 2G4, so although the antibody could potentially not detect Ero1α in its OX1 form, the lack of signal upon reduction of Ero1α suggests that it is not the oxidative state of Ero1α *per se* that prevents it from being bound by 2G4. As a monoclonal antibody, 2G4 recognises a specific Ero1α epitope. The data in this chapter suggest that this site is no longer accessible to the 2G4 antibody when the protein is both non-reduced and reduced. There is a possibility that homocysteine induces some form of post translational modification which prevents 2G4 from binding to Ero1α. As the epitope of the 2G4 antibody has not yet been mapped, it is difficult to establish the nature of any potential modification. However, the experiments with Ero1α mutants in this chapter suggest that it is not the active site or regulatory disulphide that are important for 2G4 recognition of Ero1α. These experiments could be followed up with the analysis of Ero1α truncation mutants. Were such a post translational modification to be found, it could be a molecular switch for instigating the activation of Ero1α OX1, or eradicating the OX2 form. Although Ero1α may exist in the OX1 form when the protein is analysed by SDS-PAGE, it does not necessarily mean it is functional. Thus further experiments to determine whether homocysteine may perturb the function of

purified Ero1α may be warranted. This potential for regulation of Ero1α by homocysteine is shown by the decrease in Ero1α/PDI complexes (Figure 3.10). This loss of complex may correlate with a decrease in disulphide transfer to PDI, or to client proteins. However, certain Ero1α mutants with altered structural cysteines bind less PDI than the WT whilst retaining functional activity, showing that Ero1α can still retain some function, with lower levels of PDI binding.

By using cells transfected with tagged Ero1α it was possible to replicate the Ero1α OX2 to OX1 change seen upon the addition of homocysteine, using a different antibody to that originally used (D5). As well as this, the experiments presented in this chapter have shown that the homocysteine effect occurs in transfected Ero1α, and not only with endogenously expressed Ero1α, allowing the investigation of mutant Ero1α, via transfection, to proceed. The Ero1α mutants C104A/C131A, C391A, C394A/C397A and C391A/C394A/C397A exist at different oxidation states in the cell when untreated but, like the WT, these mutants all appear to be pushed into a more reduced state, with the complete disappearance of OX2 at 10 mM homocysteine. Some of these mutants, such as Ero1αC391A, lack compact structure, due to the loss of a structural cysteine. Others, such as the “active site” mutants, may not be able to complete a full cycle of electron transfer, due to loss of active site cysteine’s. This means the homocysteine effect is not reliant on complete electron transfer, nor on the compact Ero1α structure.

Differences in the Ero1α/PDI complex are observed between Ero1α mutants. The experiments in this chapter suggest that the complex formation between PDI and Ero1 is not affected by low concentrations of homocysteine, but can be manipulated by higher concentrations. The Ero1α C391A and C394A/C397A mutants form a disulphide-bonded complex with PDI and possibly other proteins which when represented in Figure 3.11A and B, appears to span a

range of molecular weights. This band is likely to be made up of a number of merged bands, which become more discrete upon homocysteine treatment. The narrowing in size of this band could be due to Ero1α losing the ability to bind PDI, or PDI losing its interactions with Ero1α in order to form another interaction. In an Ero1α C391A/C394A/C397A mutant, the Ero1α PDI complex diminished to a smear of much less abundance than seen in the other mutants (Figure 3.11C); even less of the complex is seen upon addition of homocysteine, where it almost disappears. It seems unlikely that this change in complex is due to the homocysteine, as such small concentrations of homocysteine have not been seen to have an effect in other experiments, however structural change caused by the C391A/C394A/C397A mutation could open up the structure and potentiate the effect of homocysteine.

Treatment of cells with cystathionine (Figure 3.13), and as previously shown methionine and cysteine, does not impact the oxidation state of Ero1α. Cystathionine, cysteine and methionine are downstream of homocysteine in the sulphur amino acid biosynthetic pathway (Battle et al., 2013). Thus it does not appear to be the case that Ero1α can detect high levels of sulphur through cystathionine, which could potentially act to alert the ER to oncoming elevated protein synthesis and trigger the activation of Ero1α as a precautionary measure for an increased folding load. In situations of high cysteine concentrations, methionine catabolism is reduced in a process called “methionine sparing”. This process also does not appear to affect the control of Ero1α directly.

The level of Ero1α expressed differs between cells (Battle et al., 2013). The reason for such variation is yet to be fully determined, however it may be a consequence of the function of the cell type. It would be expected that cells with a high secretory, and thus high folding capacity would have high levels of Ero1α. Previously, the effect of homocysteine has only been shown on a gastro-intestinal adenocarcinoma cell line, which may have elevated Ero1α due to factors

including dysregulation of gene expression and increased translation induced by hypoxia. Furthermore, this cell type would be expected to have greater exposure to homocysteine in the diet. By looking at other cell lines, this study has established that homocysteine influences the behaviour of Ero1α in disparate immortalised cancer cell types (fibrosarcoma and cervical cancer), which may not be exposed to homocysteine in the diet, but may have changed expression levels of oxidative protein folding factors to increase cell survival or facilitate metastasis.

4. The oxidation state of Ero1β in cells and tissues

4. The oxidation state of Ero1β in cells and tissues

4.1. Introduction

There are two different human Ero1 paralogs. Ero1α and Ero1β are regulated differently with both upregulated by ER stress, whereas only Ero1α is regulated by hypoxia (Gess et al., 2003; Pagani et al., 2000). They also have tissue specific expression where there are potentially differences in their roles. Whilst Ero1α is universally expressed, Ero1β is found in the stomach and pancreas (Dias-Gunasekara, 2005). As Ero1β is found in secretory cells, further studies of Ero1β could improve the understanding of how proteins secreted by these cells fold, and allow the manipulation of Ero1β to improve protein folding. This would be valuable for proteins such as Insulin. Insulin is secreted by beta-cells, which are the most common cell type in the pancreatic islets of Langerhans (Brange and Langkjoer, 1993). Whilst Ero1β promotes the folding of the disulphide linked chains of insulin, its expression is decreased in diabetic mice which have impaired insulin secretion, and increased ER stress upon overexpression (Awazawa et al., 2014).

4.1.1 Ero1β mutants

The FAD binding site is conserved between Ero1α, Ero1β and Ero1p. The α2 and α3 helices of a 4 α helix bundle hold the FAD cofactor between them, where is it positioned next to the CXXCXXC active site (Figure 4.1).

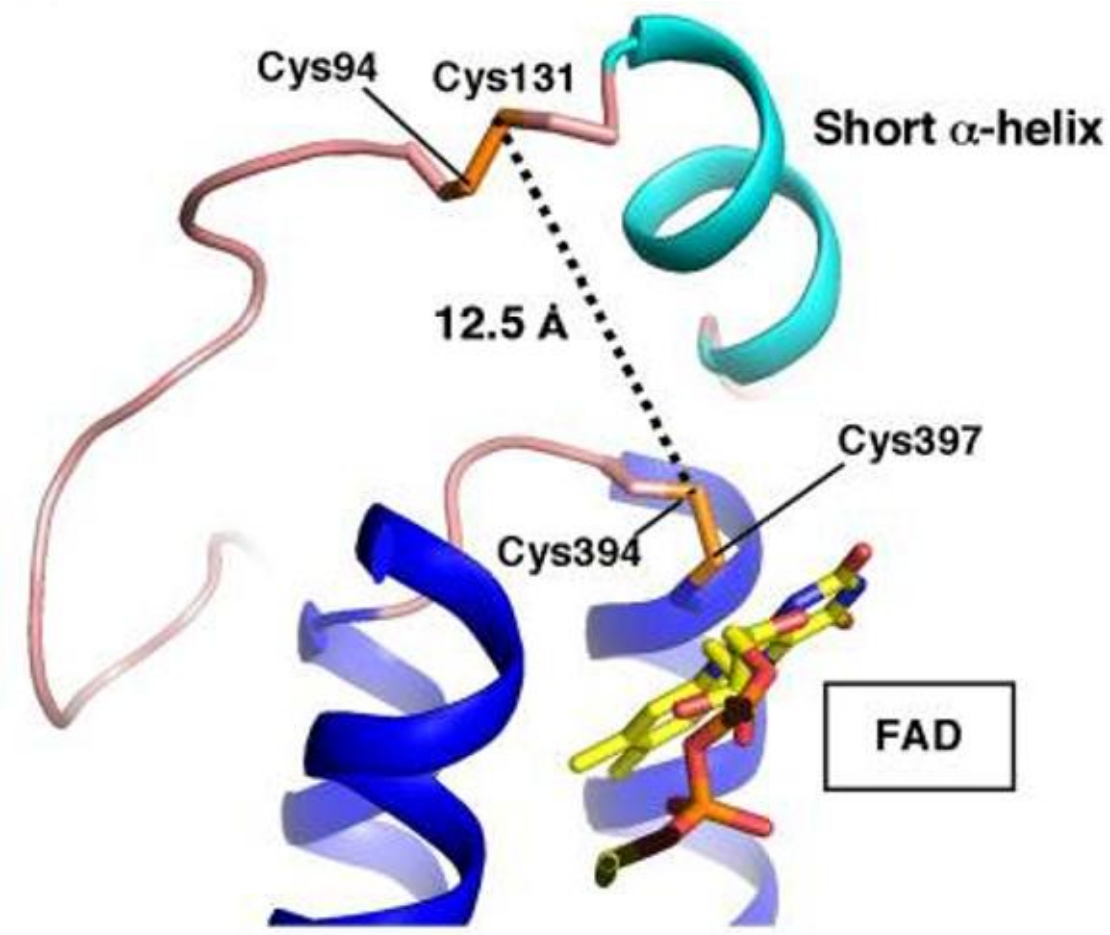

Figure 4.1. Ero1 active site

FAD is held between the α2 (left) and α3 (right) helices, shown as dark blue. Inner active site and regulatory cysteines are labelled. The Ero1α structure is adapted from (Inaba, 2010). The Ero1β structure has not yet been solved.

Two Ero1p mutations positioned near residues forming contacts with FAD impair the enzymes function (Frand and Kaiser, 1998; Pollard et al., 1998). The single amino acid substitution G229S results in a protein that has temperature sensitive maturation defects and ER retention of the disulphide containing secretory proteins carboxypeptidase Y and Gas1p, whereas the Ero1p-H231Y mutant yeast strain showed a slight UPR up regulation under normal conditions and was overly sensitive to DTT (Gross et al., 2004). By aligning the FAD binding regions of the Ero1 protein from *S. cerevisiae* and *H. sapiens*, it was possible to determine the equivalent Ero1β residues, G252 and H254, respectively (Dias-Gunasekara, 2006).

The Ero1β G252S and H254Y mutants do not undergo gross conformational changes and protein biosynthesis appears normal. They are also still able to form non-covalent interactions with PDI; however, covalent interactions with PDI (mediated by disulphide bridges) are disrupted in Ero1β G252S. The Benham laboratory has previously shown that unlike the Ero1β wild type protein, which is mostly reduced and loses most of its disulphide dependant interactions upon *in vivo* treatment with DTT, Ero1β-H254Y complexes are not easily reduced by DTT and the G252S mutant counter-intuitively forms a greater number of higher molecular weight complexes. Incubation of cells transfected with the Ero1β wild type at temperatures of 24^{o}C and 42^{o}C had no effect on Ero1β misfolding, whereas at 24^{o}C both Ero1β mutants lose their disulphide complexes and at 42^{o}C they are both misoxidised. Gunasekara et al (Dias-Gunasekara, 2006) suggested that disruption of contacts with FAD in these mutants may result in loss of FAD binding, or result in a loss of structural stabilisation that makes the protein prone to misoxidation during stress. As well as this, there may be disruption to the charge of the FAD binding fold, resulting in defects in electron transfer. Under such conditions normal disulphide dependant interactions cannot be maintained, and so it has been proposed that this more readily exposes thiols to form aberrant disulphide bridges (Dias-Gunasekara, 2006). Given the

laboratories background in the biology of Ero1β, it was decided to use Ero1β as a tool to further understand the effect of homocysteine on the oxidative protein folding machinery.

4.2 Results

4.2.1 Initial transfection analysis of Ero1β

To better understand the control of Ero1 proteins by homocysteine, Ero1β was investigated to determine whether mutations that had a known effect on protein conformation and function were also subject to homocysteine modulation. If there is a similar affect on Ero1α and β, the affect homocysteine has is likely to be a result of conserved sequences between the two proteins.

Ero1β is not expressed in immortalised cell lines. In the absence of a cell line with sufficiently high expression of Ero1β to be examined, Ero1β-HA was transfected to explore its behaviour. This meant that Ero1β was expressed in the same cell line(s) and thus subjected to the same conditions as for Ero1α, explored in the previous chapter. The transfected HT1080 cells were lysed and the cell lysates subjected to SDS-PAGE and immunoblotting using the anti-HA mAb and the polyclonal anti-Ero1β serum 4131 (Figure 4.2). Initially, the transfected cells did not express the wild type Ero1β-HA. The αHA antibody detected a large amount of non-specific binding, with no additional specific bands in the transfected cells when compared to the mock transfected cells (Figure 4.2A, compare lanes 1 and 2). When the samples were run next to a mouse pancreatic tissue lysate, which expresses Ero1β, and probed with pAb 4131, it was clear that Ero1β had not been transfected successfully (Figure 4.2B, lanes 1 and 3). The pancreatic lysate showed two bands, a lower one of the expected weight of Ero1β OX2, and a higher reduced band running at ~75 kD. To optimise the transfection, HT1080 cells were compared to HeLa cells, which are easier to transfect. As well as transfecting the cells using the original concentration of transfection reagent, the amount was doubled (see methods chapter).

Protein expression and complex formation was analysed by reducing and non-reducing SDS-PAGE followed by Western blotting (Figure 4.2C). When equal amounts of cell lysates from the transfectants were compared using the anti-HA antibody, the transfection of HeLa cells appeared to be more efficient, with a band representing Ero1β appearing at ~55 kDa at both transfection reagent concentrations (Figure 4.2C, lanes 5, 6, 11 and 12). In HT1080 cells, Ero1β was only weakly visible under reducing conditions at the higher concentration of transfection reagent (Figure 4.2 C, lane 9), with a possible background band appearing at the lower concentration under non-reducing conditions (Figure 4.2 C, lanes 2 and 3). The increase in molecular weight seen in Ero1β under reducing conditions (Figure 4.2 C, compare lanes 3 and 9, 5 and 11, 6 and 12), and the absence of signal in the mock transfections (Figure 4.2 C, lanes 1 and 7) provides evidence that the signal is specific to Ero1β. As the transfection efficiency of Ero1β was higher in HeLa cells, they were used to investigate the homocysteine effect on Ero1β.

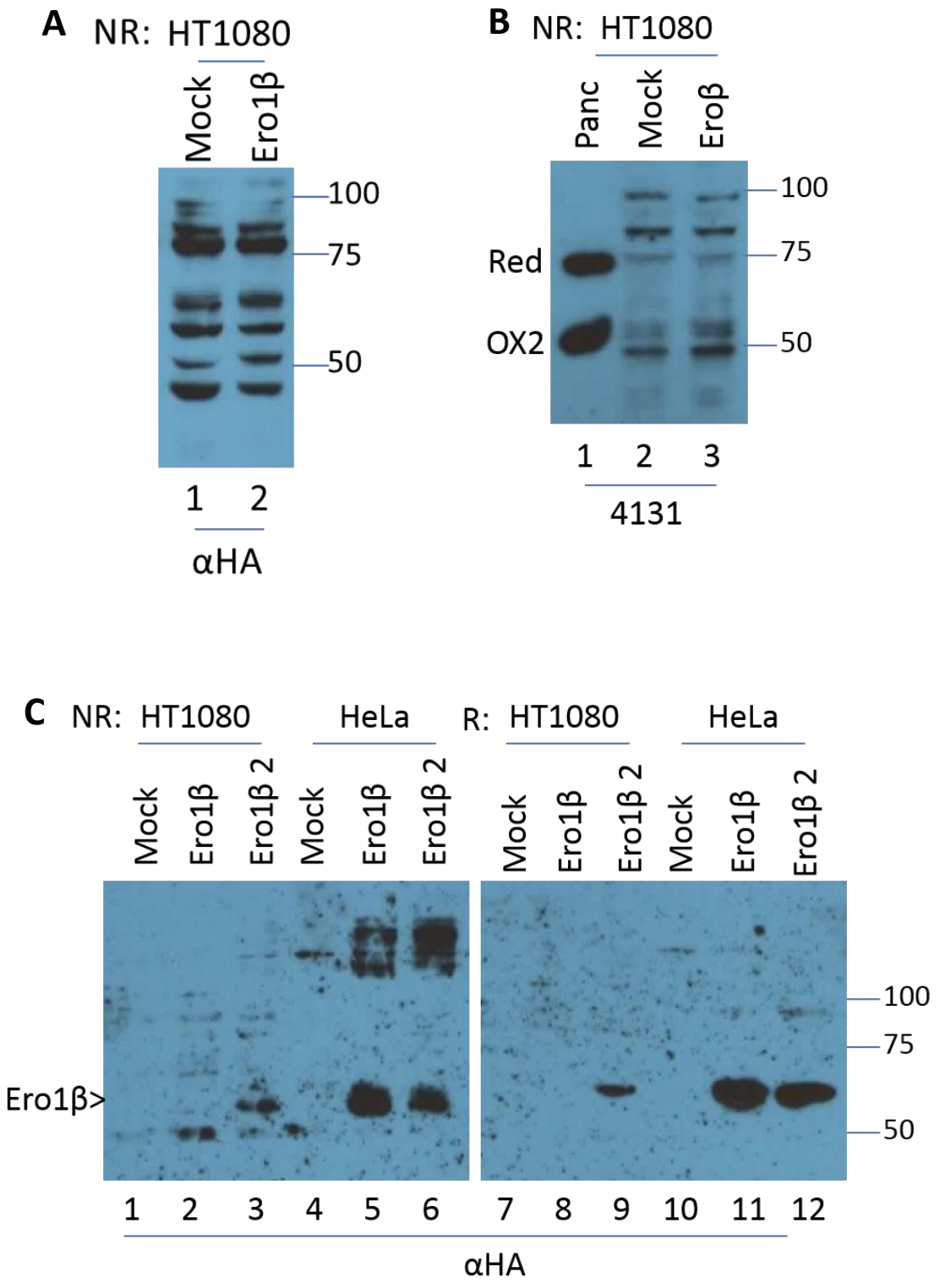

Figure 4.2. Detection of Ero1β in transfected cells

A. and **B.** Following transfection with Ero1β or mock transfection (M), HT1080 cells were lysed in MNT buffer and the resulting cell lysates, and pancreas tissue lysate (**B**), subjected to non-reducing (NR) SDS-PAGE and subsequent Western blotting with the αHA (**A**) or 4131 (αEro1β) (**B**) antibodies. **C.** HT1080 and HeLa cells were mock transfected or transfected with Ero1β using the initial amount, 3.75 µL, of transfection reaction (Ero1β) or double the original amount, 7.5µL (Ero1β 2). These cells were then lysed in MNT buffer and the resulting cell lysates subjected to non-reducing (NR) SDS-PAGE and subsequent Western blotting with the αHA antibody.

4.2.2 The effect of homocysteine on Ero1β in cells transfected with the WT and mutant Ero1β H254Y and G252S

The Ero1β G252S and H254Y mutants misoxidise at 42^{o}C and upon mild DTT stress (Dias-Gunasekara, 2006). Such responses are not seen in the wild type and do not occur with other stresses such as hydrogen peroxide challenge or glutathione deprivation. The misoxidation of Ero1β in these mutants affects its capacity to build disulphide bonds with PDI. As a loss of PDI interactions has been seen with Ero1α when cells are treated with homocysteine, there could be the same effect on wild type Ero1β, which may or may not be influenced by the G252S and H254Y mutants.

To investigate Ero1βs interaction with PDI, and whether homocysteine has the same capacity to reduce the Ero1β monomer, HeLa cells were transfected with wild type, G252S or H254Y HA tagged Ero1β. The transfected cells were subjected to homocysteine treatment. When the cell lysates were analysed by SDS-PAGE under non-reducing conditions, there was a shift in the monomer to a slightly higher molecular weight when cells were treated with 10 mM homocysteine (Figure 4.3A, compare lanes 3 and 4, 5 and 6, 7 and 8), suggesting that homocysteine had the same reducing effect on Ero1β monomers as it did on Ero1α. This shift could be seen in both the wild type and the mutants. The difference disappeared when the protein was analysed under reducing conditions (Figure 4.3B). This is because Ero1β was fully reduced by DTT in the sample buffer, thus proving that the change in molecular weight was due to changes in disulphide bonds.

Ero1β/PDI complexes are expected to appear at ~130 kDa. In the wild type transfectants, there were two high molecular bands, of which the ~130 kDa one is likely to be the Ero1β/PDI complex (Figure 4.3A, lane 3). Since Ero1β is known to form homodimers (Dias-Gunasekara, 2005), the lighter band of ~120 kDa could be an Ero1β/Ero1β disulphide linked complex. The wild type Ero1β protein showed disulphide dependant complexes, which were dispersed when the proteins were reduced by DTT in vitro (Figure 4.3A and C, lanes 3 and 4), and were reduced to a single complex present at a much lower intensity, upon addition of homocysteine to the living cells (Figure 4.3A, lane 4). Both the G252S and H254Y Ero1β mutants formed a ladder of complexes, as expected from previous work in the laboratory (Figure 4.3A, lanes 5, 6, 7 and 8). Both of the Ero1β FAD mutants lost the highest molecular band with the addition of homocysteine. Compared with Ero1β G252S, the Ero1β H254Y mutant lost more disulphide-dependent interactions after homocysteine treatment, reminiscent of the result obtained when cells transfected with these mutants were challenged with DTT (Dias-Gunasekara, 2006).

To distinguish the PDI complexes amongst the ladder of disulphide dependent Ero1β interactions, the lysates shown in Fig 4.3B were subjected to immunoblotting and probed with αPDI (Figure 4.3C). There was no reproducible change in PDI/Ero1β complexes upon the addition of homocysteine to the Ero1βG252S and H254Y transfectants or to the mock. In this experiment, there was a change in the wild type where there was a decrease in the PDI complex upon homocysteine treatment (Figure 4.3C, lane 4); however this change was not reproducible and is likely to be caused by an air bubble whilst transferring the SDS-PA gel onto the membrane for western blotting. It is likely that some PDI complexes detected here are those interactions with client proteins. Overall, this experiment suggests that homocysteine can partially reduce Ero1β and can alleviate oxidative misfolding of the H254Y and G252S mutants.

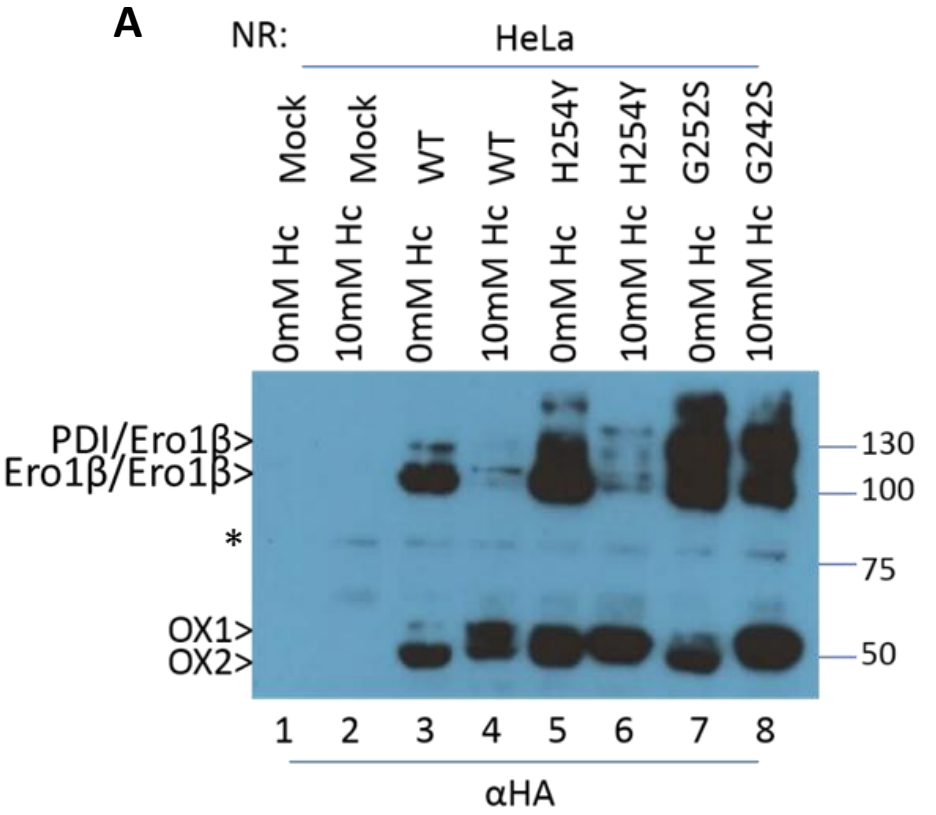
A
NR:
HeLa
Mock
Mock
WT
WT
H254Y
H254Y
G252S
G242S
0mM Hc
10mM Hc
0mM Hc
10mM Hc
0mM Hc
10mM Hc
0mM Hc
10mM Hc
PDI/Ero1β>
Ero1β/Ero1β>
*
OX1>
OX2>
130
100
75
50
1 2 3 4 5 6 7 8
αHA

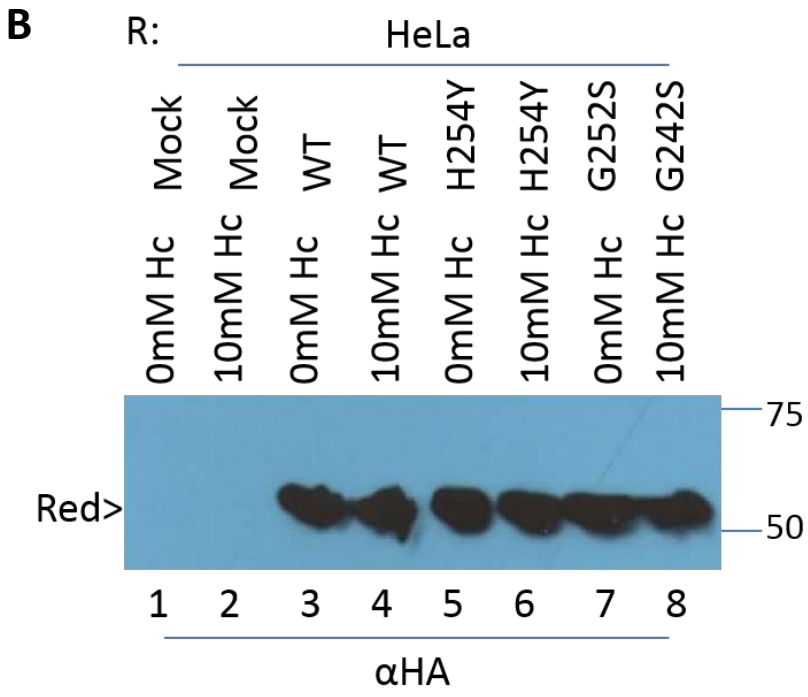
B
R:
HeLa
Mock
Mock
WT
WT
H254Y
H254Y
G252S
G242S
0mM Hc
10mM Hc
0mM Hc
10mM Hc
0mM Hc
10mM Hc
0mM Hc
10mM Hc
Red>
75
50
1 2 3 4 5 6 7 8
αHA

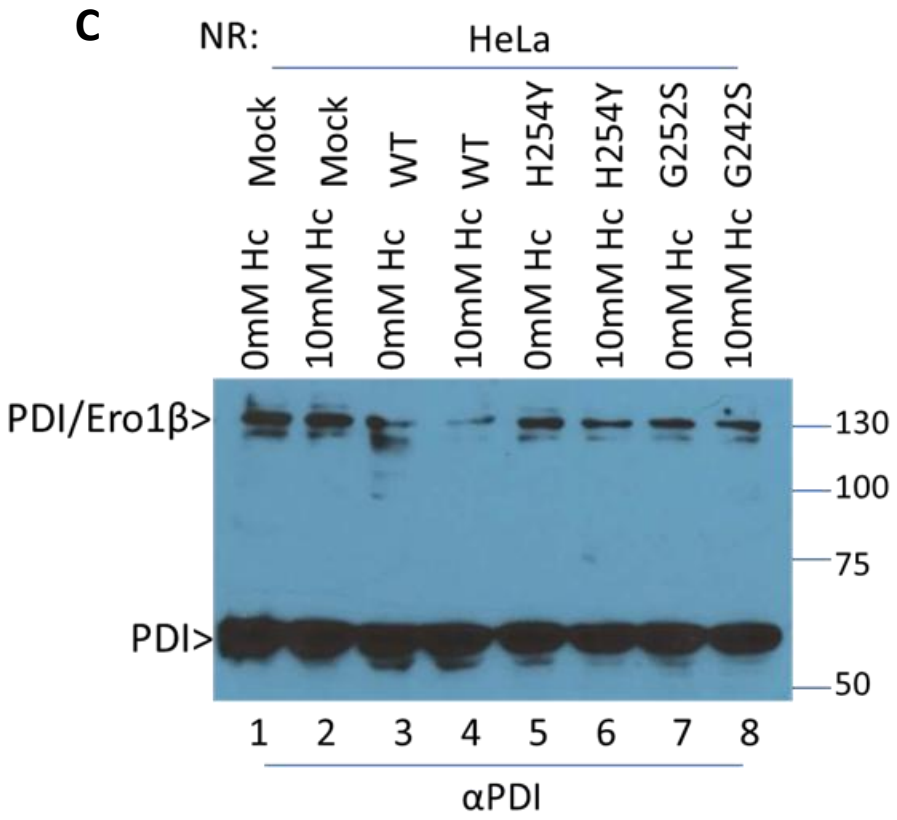

Figure 4.3. The effect of homocysteine on WT, H254Y and G252S Ero1β
Following mock transfection (M), or transfection with Ero1β WT, H254Y or G252S, HeLa cells were treated with 0 or 10 mM homocysteine (HC) for an hour. These cells were then lysed in MNT buffer and the resulting cell lysates were subjected to non-reducing (NR), or reducing (R) SDS-PAGE and subsequent Western blotting with the αHA (**A** and **B**) or αPDI (**C**) antibody. Ero1α monomer oxidation states are labelled OX1, OX2 or reduced (Red). PDI-Ero1β complexes (PDI/Ero1 β) and Ero1β-Ero1β complexes (Ero1β/ Ero1β) are labelled. Background bands are indicated (*****).

4.2.3 Further characterisation of the effect of homocysteine on Ero1β in cells transfected with mutant Ero1β G252S

To further investigate the shift in migration seen in Ero1β following homocysteine treatment, HeLa cells transfected with Ero1β G252S were treated with a wider range of homocysteine concentrations, as has been done with Ero1α. The change between oxidation state is not as clear as that seen in Ero1α, with a smooth change in molecular weight with the changing homocysteine concentrations (Figure 4.4A, lanes 2, 3, 4 and 5). A clear change in the amount of complexes was observed when transfectants were treated with a range of homocysteine concentrations, with the top band lost at 1 mM homocysteine (Figure 4.4 A, lane 4), and the next at 10 mM (Figure 4.4 A, lane 5). There appeared to be fewer complexes at 0 mM homocysteine compared to 0.1 mM homocysteine (Figure 4.4 A, lane 2), but this is likely due to unequal loading of protein, as the band representing the Ero1β monomer in lane 2 is also fainter. All higher molecular weight complexes were broken under reducing conditions when DTT was added to the samples (Figure 4.4 A, lanes 6-10), proving that the interactions disrupted by homocysteine were disulphide dependant.

The same cell lysates were subjected to western blotting and probed with an αPDI antibody to provide a blotting control (Figure 4.4B).

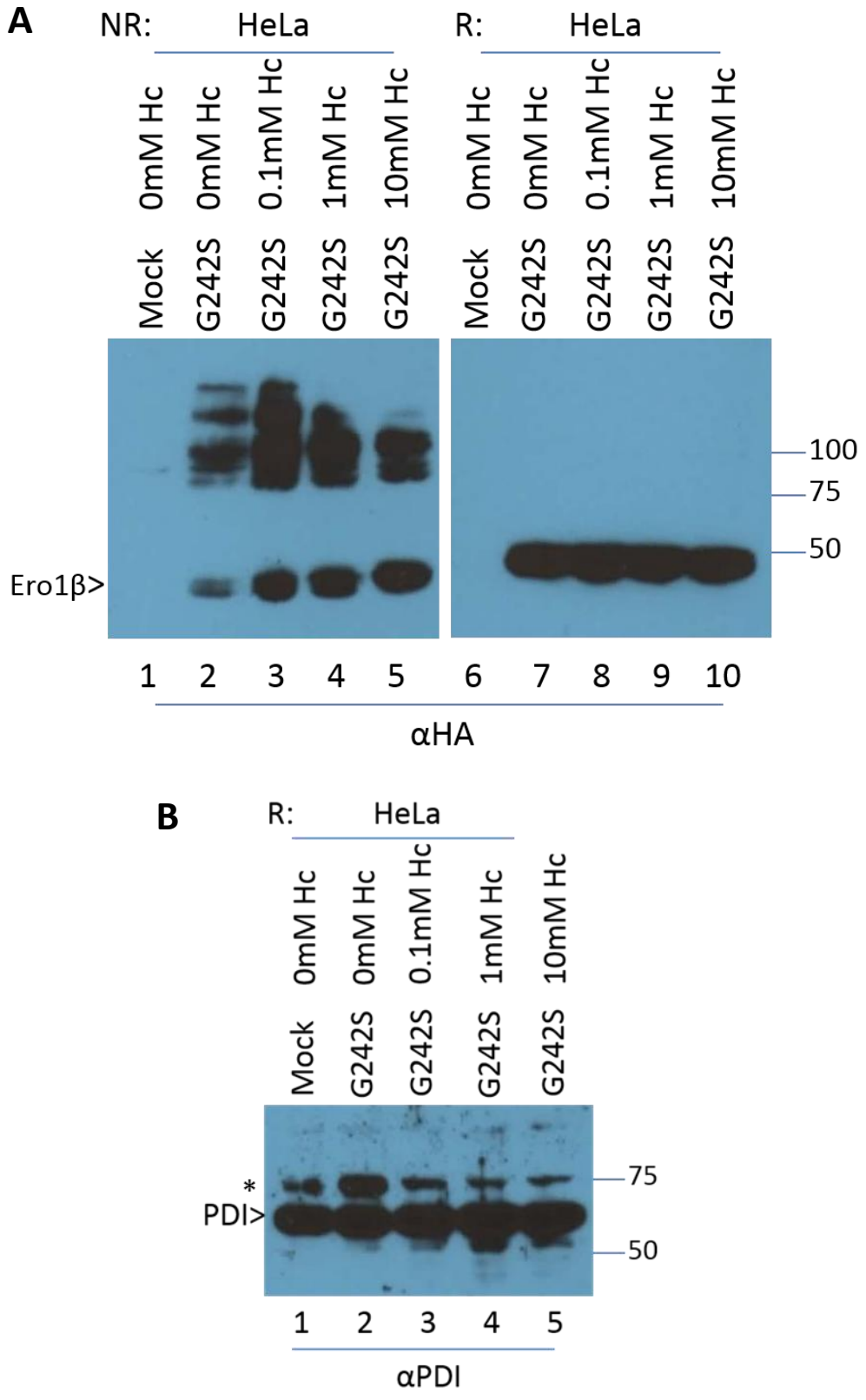

Figure 4.4. The effect of homocysteine on the G252S Ero1β mutant
Following mock transfection (M), or transfection with Ero1β G252S, HeLa cells were treated with 0, 0.1, 1 or 10 mM homocysteine (HC) followed by lysis in MNT buffer. The resulting cell lysates were subjected to non-reducing (NR), or reducing (R) SDS-PAGE and subsequent Western blotting with the αHA (**A**) or αPDI (**B**) antibody. Background bands are indicated (*).

4.2.4 The effect of homocysteine on Ero1β in HT1080 cells transfected with the mutant Ero1β H254Y and G252S

Despite their limited capacity to be transfected with Ero1β, it was possible to transfect HT1080 cells with the G252S and H254Y Ero1β HA tagged mutants and to detect expression in some experiments. This allowed the determination of whether the results seen in HeLa cells could be replicated in HT1080 cells, one of the cell lines used to investigate Ero1α in the previous chapter. The transfected HT1080 cells were treated plus or minus 10 mM homocysteine and the cell lysates were analysed by non-reducing SDS-PAGE and western blotting (Figure 4.5A and B). Although not as clear as the results seen in HeLa cells, there was a demonstrable change in migration of the monomeric Ero1β FAD mutants, which became more compact with homocysteine treatment (Figure 4.5A, lanes 6 and 8). This shift could be seen in both mutants (Figure 4.5A, compare lanes 5 and 6, 7 and 8) but not in the wild type, because transfection of the wild type was unsuccessful. Compared to the HeLa lysates shown in Figure 4.4, two distinct monomeric Ero1β bands could be seen more clearly in this experiment (Figure 4.5), with both an oxidized and partially reduced form apparent in the successfully transfected samples (lanes 5, 6, 7 and 8). The presence of multiple background bands act as loading controls, but make the interpretation of the effect of homocysteine on Ero1β mutant misoxidation difficult for HT1080 cells. When analysed under reducing conditions, Ero1β was reduced to a single band, showing that the change in molecular weight was due to changes in disulphide bonds (Figure 4.5B).

The HT1080 lysates were immunoblotted and probed with αPDI as a control (Figure 4.5C).

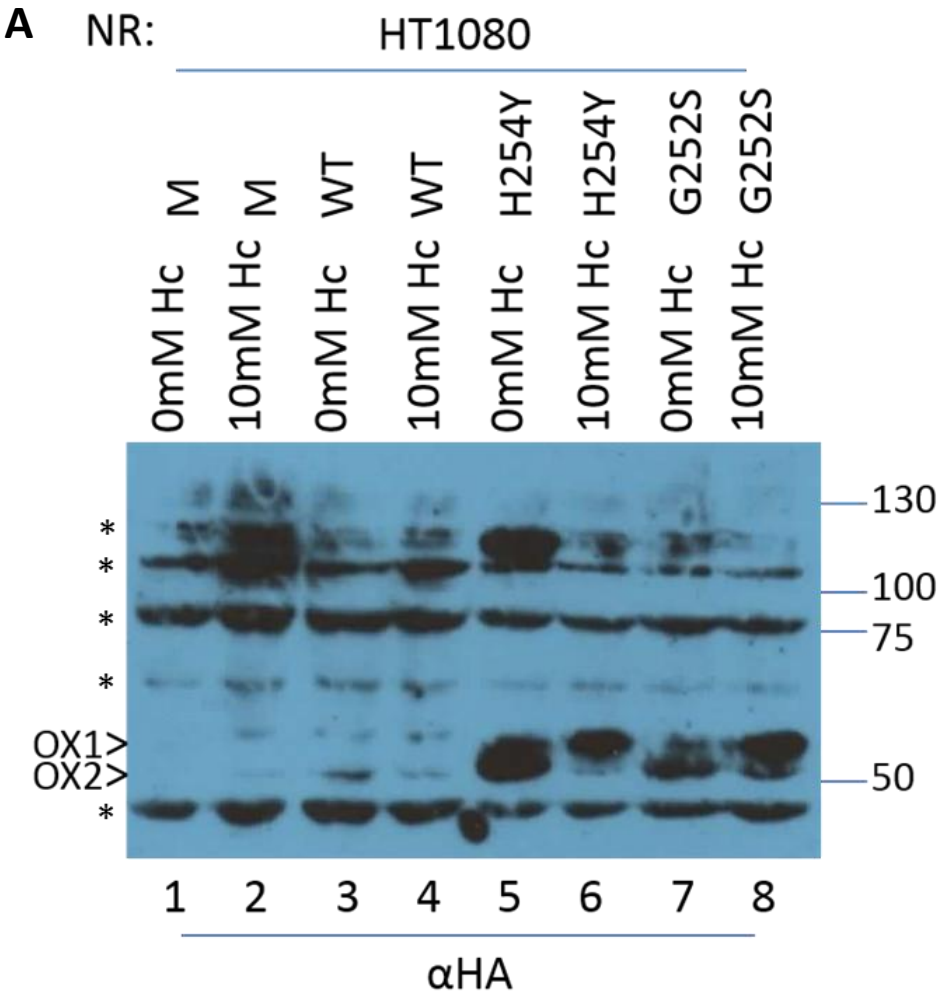
A
NR:
HT1080
M
M
WT
WT
H254Y
H254Y
G252S
G252S
0mM Hc
10mM Hc
0mM Hc
10mM Hc
0mM Hc
10mM Hc
0mM Hc
10mM Hc
130
100
75
50
*
*
*
*
*
OX1>
OX2>
1 2 3 4 5 6 7 8
αHA

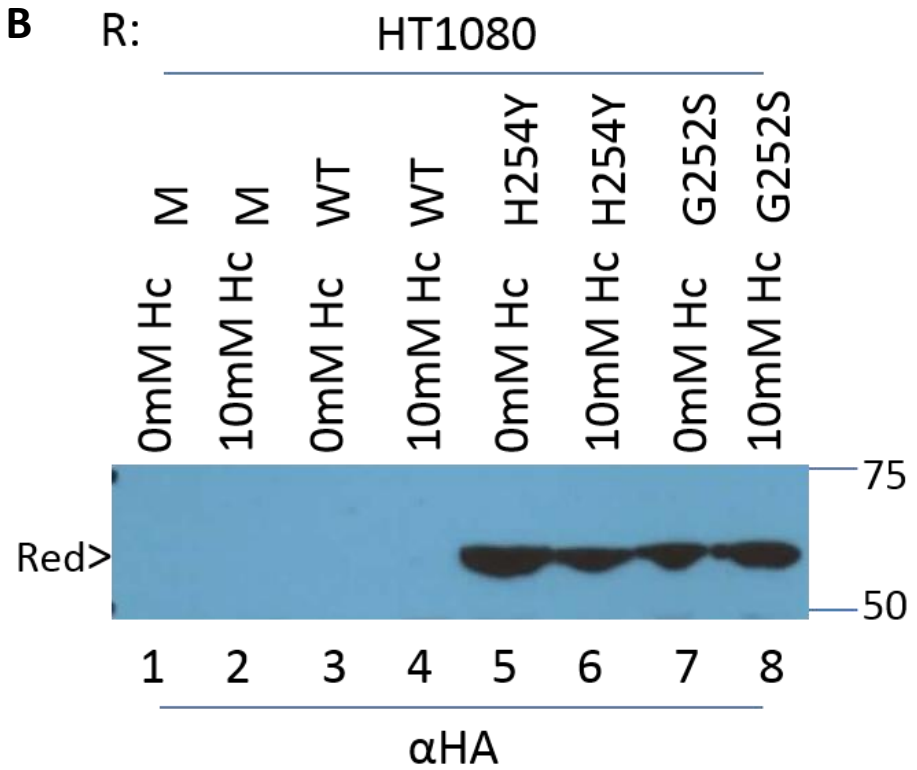
B
R:
HT1080
M
M
WT
WT
H254Y
H254Y
G252S
G252S
0mM Hc
10mM Hc
0mM Hc
10mM Hc
0mM Hc
10mM Hc
0mM Hc
10mM Hc
75
50
Red>
1 2 3 4 5 6 7 8
αHA

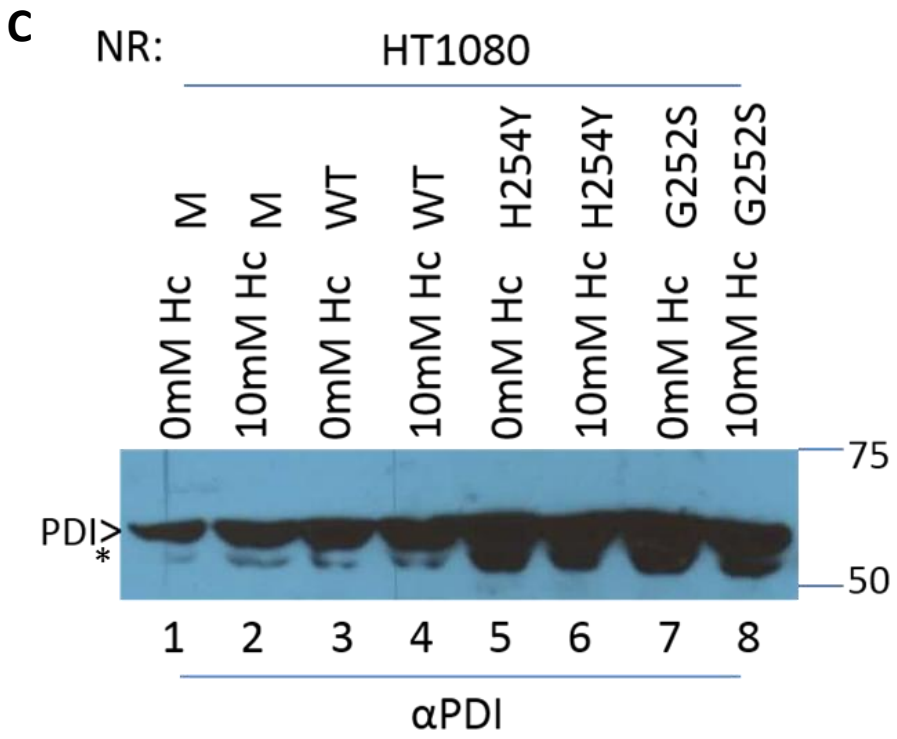

Figure 4.5. The effect of homocysteine on H254Y and G252S Ero1β mutants in HT1080 cells

Following mock transfection (M), or transfection with Ero1β WT, H254Y or G252S, HT1080 cells were treated with 0 or 10 mM homocysteine (HC) for 1 hour. They were then lysed in MNT buffer. The resulting cell lysates were subjected to non-reducing (NR), or reducing (R) SDS-PAGE and subsequent Western blotting with the αHA (**A** and **B**) or αPDI (**C**) antibody. Ero1β monomer oxidation states are labelled OX1 and OX2 or reduced (Red). Background bands are indicated (*****).

4.2.5 Initial treatment of tissue cells with homocysteine

The results shown in Chapter 3 and the Figures 4.2-5 above demonstrate that both Ero1α and Ero1β are pushed into less compact forms upon treatment with homocysteine in immortalized cell lines. However, to understand how these proteins behave *in vivo*, tissues can be used to see whether homocysteine acts in the same way on primary cell types.

Single cell suspensions were made from mouse liver and pancreatic tissue, chosen because these tissues have high expression of Ero1α and Ero1β, respectively. Liver and pancreas cells along with HT1080 cells also in suspension, were treated with homocysteine (Figure 4.6). HT1080 cells were used as the effect of homocysteine on these cells is known and will indicate whether the different treatment method used here (treatment of cells in suspension) has been successful. HT1080 and liver samples analysed by SDS-PAGE and western blotting were probed with the anti-Ero1α mAB 2G4. The pancreas sample was not probed with 2G4 as it expresses Ero1α at a much lower level. As found previously, HT1080 samples lost the 2G4 Ero1α signal at 10 mM homocysteine, when lysates were analysed under both non-reducing and reducing conditions (Figure 4.6A, lanes 2 and 6). Actin controls show that there was protein in these samples (Figure 4.6B). The liver sample contained a small amount of monomeric Ero1α, but it existed mainly as a complex (*) in untreated cells (Figure 4.6A, lane 3). Upon homocysteine treatment, no monomeric Ero1α was visible and other Ero1α complexes (**) were formed with a slightly lower molecular weight than that present in the untreated cells (Figure 4.6A, lane 4). Under reducing conditions, the fully reduced Ero1α could be visualised. Unlike in HT1080, the signal was not lost, meaning that the 2G4 mAB was still able to detect the fully reduced form. As no monomeric Ero1α signal was present under non-reducing conditions, 2G4 may not be able to detect the alkylated OX1 form of Ero1α. To

further investigate this, liver single cell suspensions were treated with DTT as well as homocysteine (Figure 4.6C). Again, Ero1α lost its monomer signal upon homocysteine treatment under non-reducing conditions, but not reducing conditions. When treated with DTT, Ero1α was partially reduced and the complexes were lost. A difference in molecular weight could be seen when comparing the Ero1α under non-reducing and reducing conditions. This confirmed that Ero1α was not completely reduced by the DTT treatment. In the liver cells, 2G4 could still detect the OX1 form of Ero1α, meaning that treatment with 10 mM homocysteine pushed all the Ero1α into complexes. As the complex seen in untreated liver cells (*) seemed to decrease with homocysteine, and a complex of a slightly lower molecular weight appeared (**), the treatment may be encouraging other interactions to occur at the expense of the monomer and the heavier complex (Figure 4.6C).

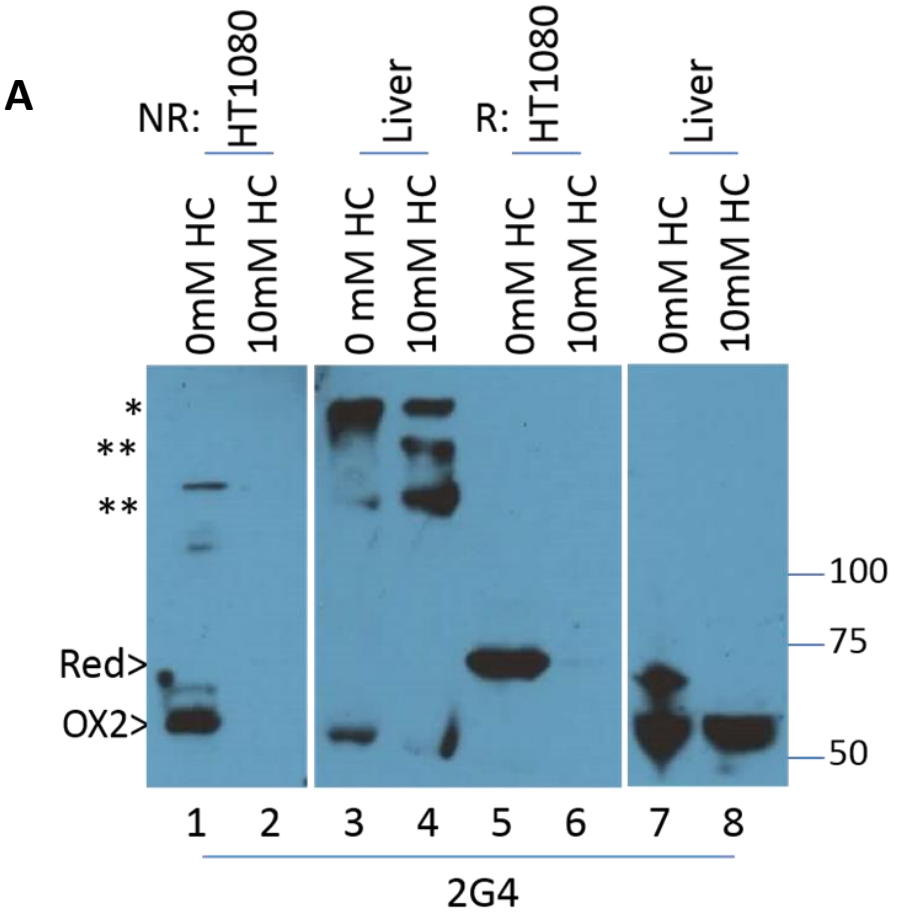
A
NR:
HT1080
Liver
R:
HT1080
Liver
0mM HC
10mM HC
0 mM HC
10mM HC
0mM HC
10mM HC
0mM HC
10mM HC
*
**
**
Red>
OX2>
100
75
50
1 2 3 4 5 6 7 8
2G4

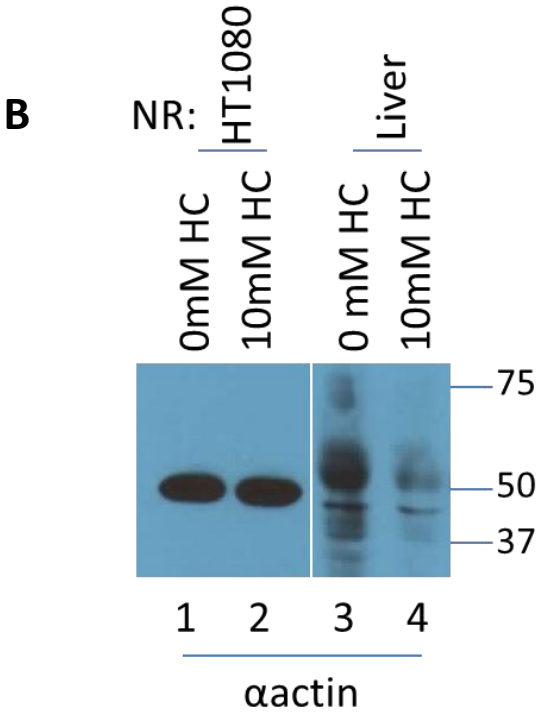
B
NR:
HT1080
Liver
0mM HC
10mM HC
0 mM HC
10mM HC
75
50
37
1 2 3 4
αactin

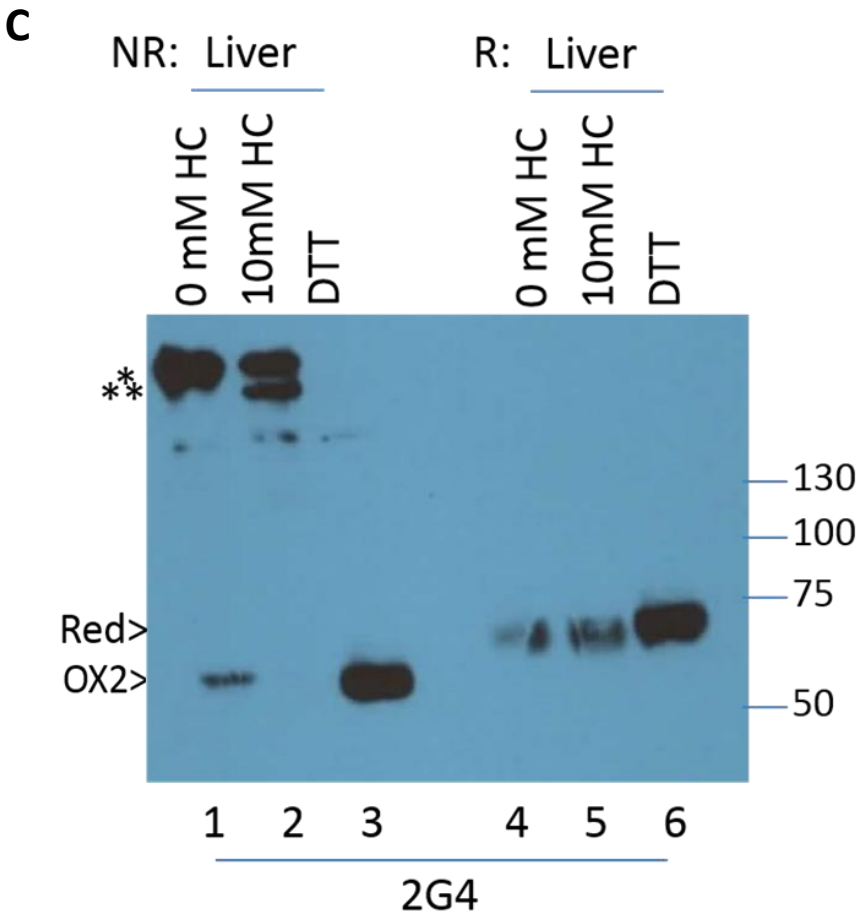

Figure 4.6. Homocysteine disperses Ero1α complexes in liver cell suspensions
Liver and HT1080 cells in single cell suspension were treated with 0 or 10 mM homocysteine (HC) or with 10 mM DTT. The cells were washed, lysed in MNT buffer and were subjected to non-reducing (NR), or reducing (R) SDS-PAGE and subsequent Western blotting with the 2G4 (**A** and **C**) or αactin (**B**) antibody.
Ero1α complexes in liver are labelled (*)(**).Ero1α monomer oxidation states are labelled OX2 or reduced (Red).

4.2.6 The effect of homocysteine on Ero1β in pancreatic cells

Ero1β is expressed in the pancreas, with high expression in the islets but lower expression in the surrounding enzyme secreting cells. PDI shows the opposite pattern, with lower expression in the islets compared to the surrounding cells. The expression of the pancreas specific PDIp is only found in the acinar cells. As Ero1β and PDI do not strictly co-localise, PDI may not be the primary electron donor for Ero1β in the pancreas (Desilva, 1997; Dias-Gunasekara, 2005). Thus the regulation of Ero1β may differ in the pancreas, depending on the relative competition for PDI and other electron donors.

When a pancreas cell suspension was lysed and probed for Ero1β using the 4131 antibody, two bands appeared with molecular weights of ~50 and ~70 kDa under non-reducing conditions (Figure 4.7A, lanes 1, 2, 3 and 4). The heavier band is likely to be the reduced form. Ero1β is predicted to be ~ 50kDa (without glycans); the lower band is likely to consist of a background band (*) and Ero1β OX2 which is highly expressed, giving it the appearance of being a single band. Under reducing conditions the Ero1β OX2 form was reduced, leaving only the background band at this molecular weight (lanes 3 and 4). The background band was also found in the liver lysates (Figure 4.7A, lanes 5, 6, 7 and 8). To further confirm that the heavier molecular weight band in the pancreas was Ero1β, cell lysates were treated with endoH to digest immature sugar residues (Figure 4.7 B, compare lanes 1 and 2, 3 and 4). There was a decrease in the molecular weight of Ero1β following endoH treatment, consistent with published reports that Ero1β is glycosylated.

The cells in this experiment were treated +/- 10 mM homocysteine. No change in apparent molecular weight (or signal intensity) of the Ero1β reduced or OX2 bands was observed upon

treatment of the pancreatic cells with homocysteine (Figure 4.7A, lanes 1 and 2). No high molecular weight complexes were observed. Although the effectiveness of the 4131 antisera at detecting Ero1β complexes remains open to question, this result suggests that Ero1β existed mainly as a monomer in the pancreas. In contrast to the pancreas, abundant PDI complexes were detected in the liver. These complexes did show a decrease when liver cells were incubated with homocysteine (Figure 4.7C, lanes 3 and 4). Taken together, these results suggest that the susceptibility of the Ero1-PDI oxidative folding pathway to homocysteine may vary between tissues.

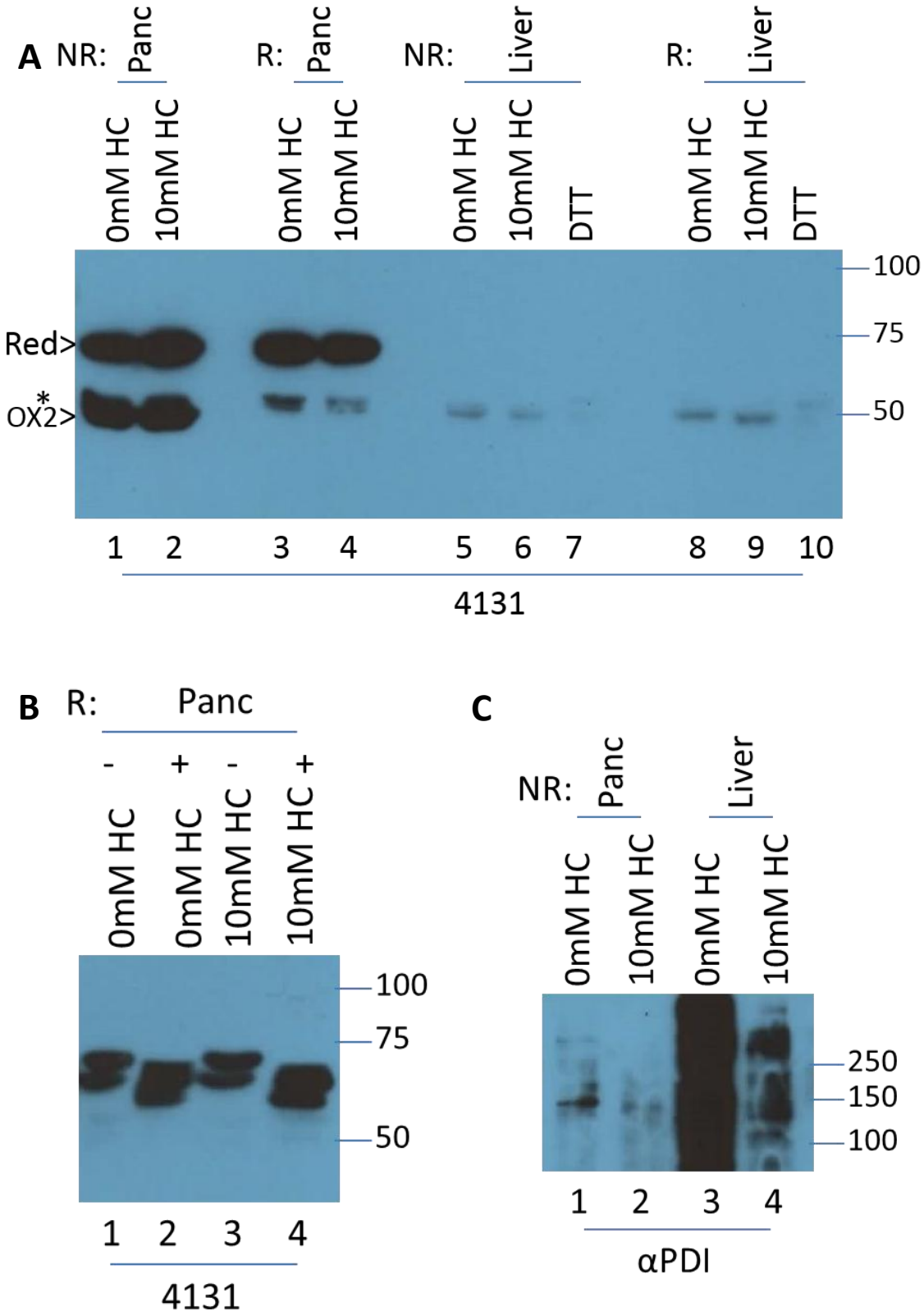

Figure 4.7. Homocysteine has no detectable effect on pancreatic Ero1β
Liver and pancreas cells in single cell suspension were treated with 0 or 10 mM homocysteine (HC). The cells were lysed in MNT buffer and were directly (**A** and **C**), or following endoH treatment (**B**), subjected to non-reducing (NR), or reducing (R) SDS-PAGE and subsequent Western blotting with the 4131 (**A** and **B**) or αPDI (**C**) antibody. The Ero1β monomer oxidation state is labelled OX2, the reduced form is labelled (Red), and the background band is labelled *.

4.3 Discussion

The results of this chapter show that homocysteine has a reducing effect on Ero1β as well as on Ero1α when Ero1β is expressed in cell lines (Figures 4.3 and 4.5). As the structural differences between Ero1α and Ero1β do not change the effect of homocysteine, it is unlikely that the method through which homocysteine takes its effects is through the sites of difference. Figure 4.8 shows the differences in cysteine residues between the two homologues, but also highlights that most are conserved between the two. It should also be noted that there is a difference in the number of N-glycosylation sites. Whilst Ero1α has two glycans, Ero1β has four, but there is no evidence to suggest that these affect protein function (Pagani et al., 2000).

The occurrence of Ero1β complexes decreased with homocysteine treatment (Figure 4.3 and 4.4). In both wild type and the Ero1β H254Y mutant, there was a dramatic loss in Ero1β/PDI complexes. A loss of homodimers was also observed (Figure 4.3 and 4.4), which could be a result of reduction by homocysteine or homocysteine preventing them from binding via post-translational modifications. It is also possible that Ero1β forms homodimers as a regulatory mechanism (Dias-Gunasekara, 2005); when Ero1β is in what appears to be its active state e.g. induced by homocysteine treatment, it may be unable to form homodimers.

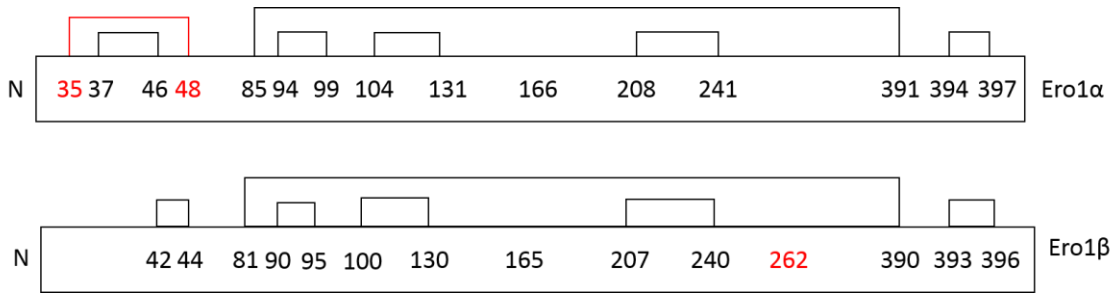

Figure 4.8. Comparison of the disulphide bond arrangements in Ero1α and Ero1β

Cysteine residues are labelled according to amino acid position. Cysteine residues and disulphide bonds conserved between Ero1α and Ero1β are black, whilst those which are not are coloured red.

A slightly different result was seen in Ero1β G252S with only a loss of the heaviest complex, which was not seen in the wild type (Figure 4.3). Homocysteine did not appear to affect the formation of homodimers, or the abundance of Ero1β/PDI complexes. These results are similar to those seen upon DTT treatment of the Ero1β G252S mutant, where an increase in higher molecular weight complexes was seen by Gunasekara et al (2006). Upon treatment with homocysteine, a redistribution of the complexes was seen. The results seen with the Ero1β H254Y mutant are also similar to when treated with DTT, with a decrease, but not complete loss of the complex signal (Figure 4.3). This would suggest that the treatment of homocysteine is similar to that of DTT in that it is having a reducing effect. The treatment with homocysteine may be taking Ero1β out of complexes, thus preventing misoxidation of the FAD mutants. This could potentially, in some circumstances, protect Ero1β against stress-induced oxidative misfolding.

It is unlikely that the G252S mutation has a direct effect on the Ero1β-PDI interaction, as this interaction occurs at a site unaffected by the mutation. However, as the mutation destabilises the binding of the electron acceptor FAD, it may prevent the reoxidation of Ero1β. PDI can act as a chaperone as well an electron donor for Ero1. Since the G252S mutation potentially confers structural instability to the protein this could require additional chaperone assistance from PDI.

During temperature stress both of the Ero1β FAD mutants are known to misoxidise and their disulphide-dependent interactions are disrupted. In the Ero1p equivalents of these mutants, such stress is lethal, but viability can be restored by oxidising agents like diamide (Frand and Kaiser, 1998). It would be interesting to see the effect of such agents in conjunction with homocysteine to further characterise homocysteines reducing function.

By using the known reducing effect of homocysteine on Ero1α, and the accompanying loss of signal from the antibody 2G4, it was possible to show that homocysteine also affected cells from tissues. The cell line HT1080 showed the same response when in single cell suspension as when grown and treated in a monolayer.

The transfection of Ero1β into a cell line represents an overexpressed system where molecular interactions can be influenced by non-physiological concentrations of proteins. However, it should be noted that the expression of Ero1α in the liver and Ero1β in the pancreas is at least as high as that achieved in transfected cells. The pool of Ero1α in liver cells was found to exist mostly in complex form (more so than in HT1080 cells). This could be a consequence of a high level of expression, or a high activity level, either of which are likely due to the protein secretory function of the tissue type. Upon homocysteine treatment, all detectable Ero1α was found in complex form, with additional complexes becoming visible. These additional complexes may be released from the heavier complexes following modification; alternatively homocysteine may cause Ero1α to misoxidise and form unusual intermolecular disulphides. Unlike HT1080 cells, liver cells did not completely lose the 2G4 antibody signal with 10 mM homocysteine. There was still a 2G4 signal arising from Ero1α associated non-reducing complexes. It is likely that the Ero1α monomers were either recruited into complexes upon treatment with homocysteine, or Ero1α was released from greater molecular weight aggregates into ~ 150kDa complexes (Figure 4.6). It is clear that homocysteine is having an effect on liver tissue, but the persistence of the 2G4 signal at 10 mM homocysteine, which has not been observed in the other cell lines tested, is likely to mean that any modification which prevented the detection of Ero1α by 2G4 is not effective here. This may be due to the modification not occurring in the liver or due to there being a system which buffers the modification by higher protein or metabolite concentrations.

Treatment of liver cells with DTT reduced all Ero1α complexes, however DTT did not induce a change in the molecular weight of the Ero1α monomer, suggesting that in normal conditions, Ero1α exists in an OX1 form (Figure 4.6). When compared to the Ero1α in the HT1080 cell line which becomes less mobile, potentially induced to the active state, with homocysteine, perhaps Ero1α in a PDI complex represents a more active form which is induced by homocysteine.

When Ero1β was observed in pancreas tissue, it was present in two forms under non reducing conditions, oxidised and reduced. The presence of the reduced form in non-reducing conditions may be due to high expression, the regulatory poise of the pancreas, or because the reduced form may have another function e.g as a chaperone. Alternately this could be the OX1 form of Ero1β running at a molecular weight very similar to that of reduced Ero1β at ~55kDa.

No change to Ero1β was seen upon homocysteine treatment of pancreas cells, despite having seen a change in Ero1β oxidation state in the HT1080 cell line transfected with Ero1β. As homocysteine only appears to have an effect on Ero1β in certain cell types there may be other factors regulating its behaviour in pancreatic cells.

5. Quality control of the ER folded MHC class II molecules

5. Quality control of the ER folded MHC class II molecules

5.1 Introduction

The previous chapters have focussed on the quality control machinery in the ER, characterising the function of Ero1α and Ero1β. This chapter will explore the quality control of the client protein MHC class II, which assembles in the ER. This involves further characterising the stability of the MHC class II dimer, and how its stability is affected by the homocysteine induced changes in Ero1α.

5.1.1 Toll-like receptors

Toll-like receptors (TLR) are type 1 transmembrane receptors possessing an extracellular leucine-rich repeat domain (Medzhitov et al., 1997), and an intracellular Toll/ Toll-interleukin 1 (IL-1) receptor domain (Rock et al., 1998). TLRs recognise specific structural patterns of microbial components known as pathogen associated molecular patterns (PAMP), and respond to these by activating a range of signal transduction pathways which are either specific to the activated TLR or shared by all TLRs (Medzhitov et al., 1997). Activation of these pathways recruits IL-1 receptor domain-containing adaptor proteins, with each TLR recruiting a different combination of the four versions, MyD88, TIRAP, TRIP and TRAM. In all pathways this activates the transcription factors NF-kB and AP-1, resulting in inflammatory cytokine and chemokine expression. Other TLR specific pathways are also activated, for example the transcription factor IRF3, which controls type 1 interferon production, is activated upon TLR3 stimulation (Barton and Medzhitov, 2003) (Figure 5.1). Such pathways are also involved in activating the

adaptive immune system via the upregulation of cell surface expression of co-stimulatory molecules (CD80 and CD86) and MHC class II molecules on antigen presenting cells (Medzhitov et al., 1997).

Along with their classical function, MHC class II molecules play a number of other roles in immune responses such as maintaining the full activation of the TLR triggered immune response. Full TLR activation of innate responses have been shown in the murine system to be reliant on MYD88 and TRIF dependant pathways, which are enhanced by interaction with the tyrosine kinase Btk (Figure 5.1). Intracellular MHC class II has been shown by immunoprecipitation to complex with CD40 which physically associates with and maintains the activity of Btk, allowing it to interact with MyD88 and TRIF and promote TLR signalling (Liu et al., 2011). When MHC class II is removed from macrophages and dendritic cells by use of knockout mice, there is a reduction in TLR prompted production of proinflammatory cytokines and type I interferon.

Both TLRs and MHC class II molecules are found mainly on APCs, allowing this non-classical relationship to exist. Previous studies have shown that the MHC class II isotypes have different requirements for the formation of SDS-stable dimers, with DP4, unlike DR and DQ, able to form SDS-stable dimers in the absence of Ii (van Lith, 2010). Given the differences in stability between MHC class II isotypes, and the relationship between MHC class II and TLR signalling, it is possible that interactions with the TLR signalling machinery could account for the unusual stability seen in DP.

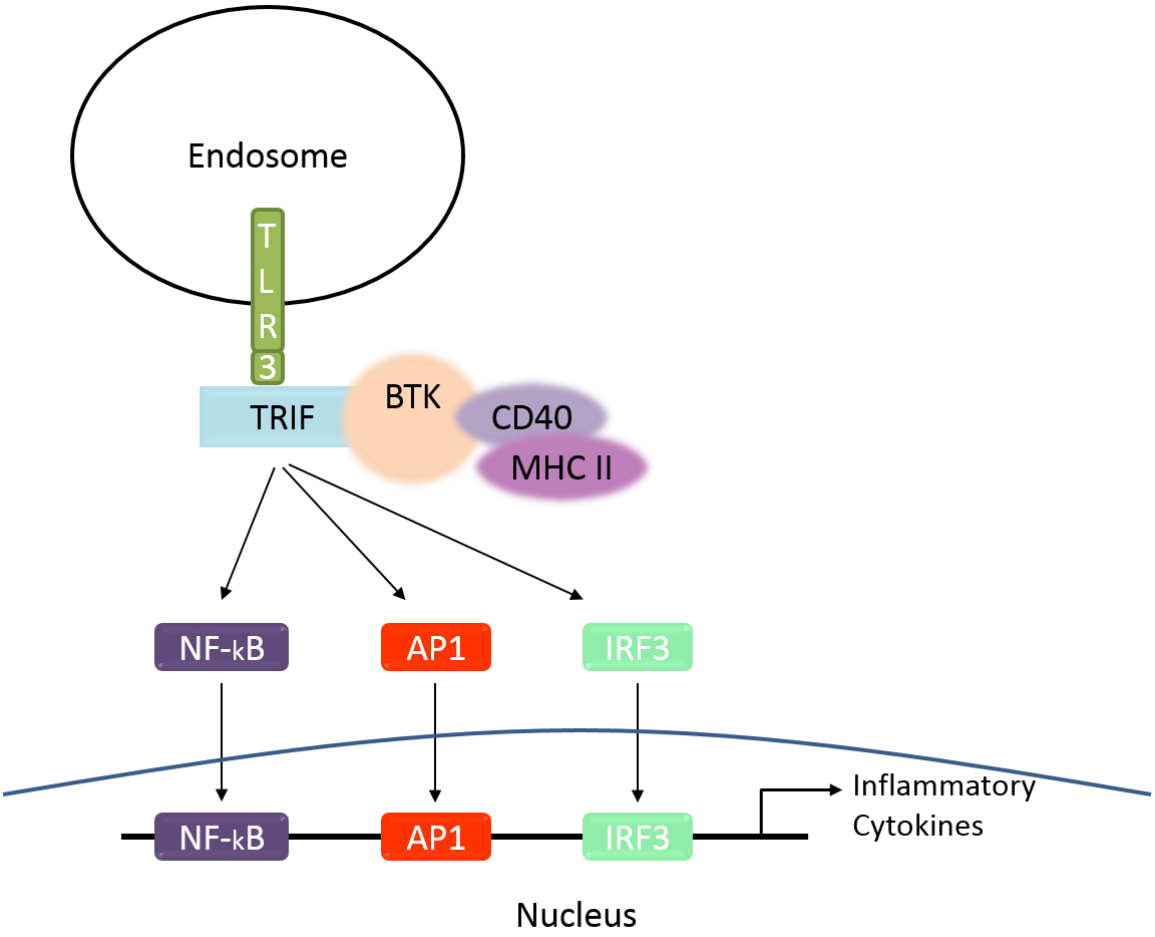

Figure 5.1. TLR3 Signalling pathway

Activation of TLR3 leads to the recruitment of the adaptor protein TRIF, which via a signal transduction pathway activates the transcription factors NF-kB, AP1 and IRF3 resulting in inflammatory cytokine expression. High activity of TRIF is maintained by an interaction with Btk. MHC class II (MHC II) has been proposed to interact with CD40, which binds to, and maintains activity of Btk.

5.1.2 Leupeptin/ammonium chloride

The MHC class II pathway of peptide presentation at the cell surface involves the endosome/lysosome, where breakdown of the Ii by cathepsin proteases allows processing and eventual displacement of the CLIP fragment by antigenic peptides. This pathway can be disrupted by leupeptin as well as ammonium chloride. Leupeptin is a cysteine/serine protease inhibitor, which prevents the complete degradation of Ii, whilst ammonium chloride neutralizes lysosomal pH also preventing endosomal cathepsins from functioning. Without this Ii degradation, MHC class class II molecules cannot bind to peptides and accumulate in the MIIC (endosomal/lysosomal) compartments (van Lith, 2010).

5.2 Results

5.2.1 MHC class II molecules have different levels of stability

MHC class II molecules are stabilised by antigenic peptides or high affinity self-peptides bound at the peptide binding site, however before this can happen MHC class II molecules must first fold into their native structure and then bind a peptide which will bind stably. The chaperones Ii and DM facilitate this process. Differences have been observed between the three classical MHC class II molecules, HLA-DR, DP and DQ, in their requirements for these chaperones to assist in the formation of SDS-stable MHC class II dimers. Unlike DR and DQ, DP4 is able to form SDS-stable dimers in the absence of Ii. This property can be assessed by a stability assay (Germain and Margulies, 1993; van Lith, 2010). When lysates from cells expressing DPα and β chains are incubated in an SDS-containing buffer at room temperature, a portion of the DP molecules remain as a dimer, but when boiled, noncovalent interactions between the heavy chains are disrupted, leaving α and β monomers.

To investigate whether, when Ii is present, the stability of DP differs from DR, lysates from the model antigen presenting cell line MelJuso, following lysis, were subjected to a range of temperatures in an SDS stability assay. These were analysed by SDS-PAGE and western blot and probed with conformation independent 1B5 (αDRα) and αDPβ antibodies. Figure 5.2 shows that DR dimers only resist denaturation at the lowest temperature tested, 20˚C, with no band representing DR dimers at 60 or 90˚C (Figure 5.2, compare lanes 1, 2 and 3). As expected, the DRα monomer was found at all temperatures tested. Like DR, DP monomers were found at all temperatures (Figure 5.2, compare lanes 4,5 and 6), however the amount did not remain

constant. This may be a result of the DP antibody being less efficient at detecting the monomer. Unlike DR, some DP dimers remained stable at 60˚C, despite there being less of them shown by the reduction in band size compared to the 20˚C band. The DP dimers were denatured at 90˚C (Figure 5.2, lane 4). A background band of about 50 kDa, slightly lighter than the DP dimer, was detected by the αDP antibody. When this band has previously been detected by the antibody, it has not influenced the recovery of stable DP dimers (van Lith, 2010).

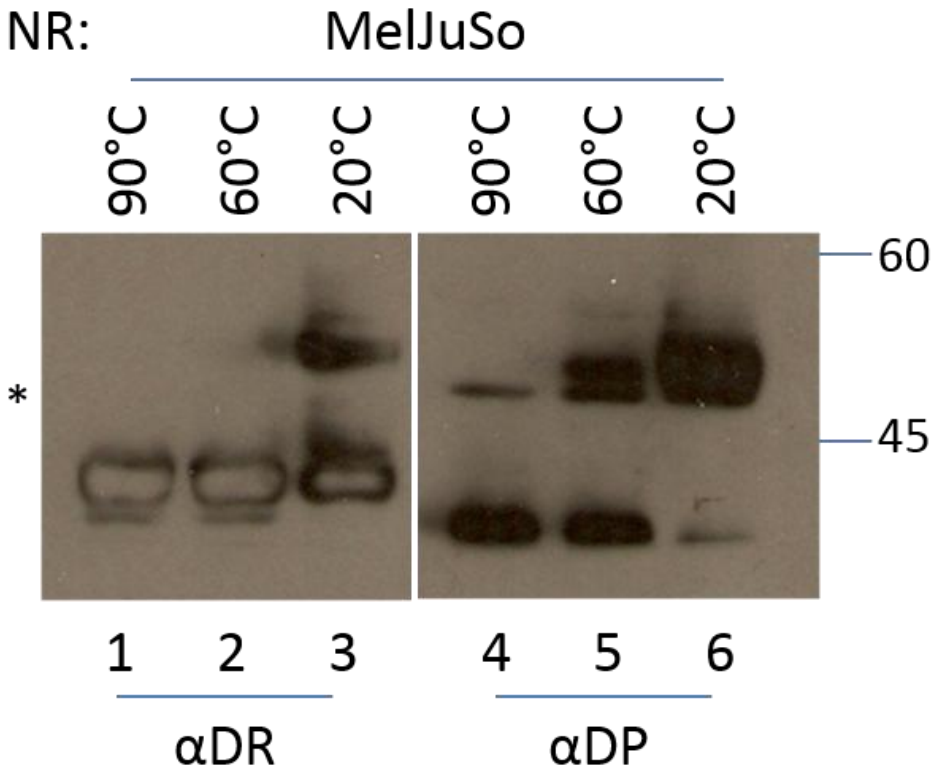

Figure 5.2. HLA –DR and DP have different levels of stability

MelJuSo cells were lysed in MNT buffer. Cell lysates in sample buffer were heated to 20°C, 60°C or 90°C for 5 minutes. Cell lysates were then subjected to non-reducing (NR) SDS-PAGE and subsequent Western blotting with the αDR (1B5) or αDP antibody. Background bands are indicated (*****).

5.2.2 DP and DR localisation

Differences in the stability of DR and DP in MelJuSo cells could be explained by differential localisation within the secretory pathway. Therefore, the cellular distribution of HLA-DP and –DR were determined using immuno-localisation in MelJuSo cells to determine whether DP and DR co-localise. Cells were treated +/- leupeptin and ammonium chloride, which prevent the trafficking of DP and DR through the endocytic pathway, to determine if DP has an alternative pathway or is found in compartments other than those where DR is located. Alternative DP trafficking and localisation could indicate that DP molecules gain access to an unconventional peptide pool or interact with as yet unknown accessory proteins that may influence heavy chain stability. Following treatment with leupeptin or ammonium chloride, cells were fixed, permeabilised and co-stained with DAPI, and stained with a DP or DR antibody. Analysis by fluorescence microscopy of mock treated cells showed characteristic ER and punctate staining, indicative of endosomal localisation for both DP and DR (Figure 5.3A and 5.4A). This localisation did not change after treatment with leupeptin for either DP (Figure 5.3C) or DR (Figure 5.4C). When treated with ammonium chloride, DR appeared mainly in the ER (Figure 5.4B), whilst DP localisation (Figure 5.3B) varied, with a mixture of ER only staining and ER and what appears to be endosomal staining in the cells. To assess the lysosmal compartments in the presence or absence of ammonium chloride and leupeptin, the experiment and analysis was carried out again and the cells incubated with lysosotracker. However, the signal from the lysosotracker was not distinct enough to determine whether the lysosomes were enlarged following the treatments (data not shown).

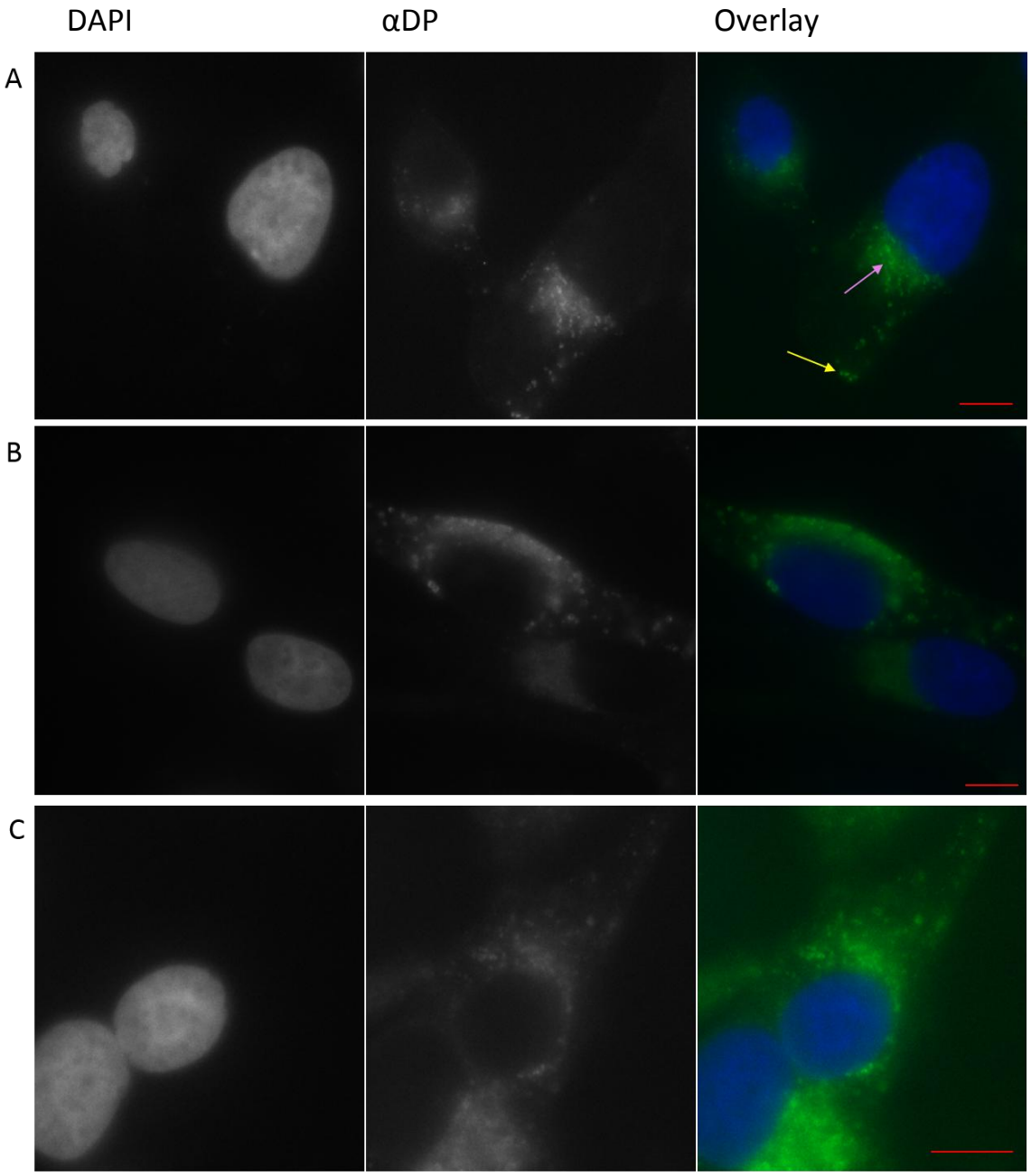

Figure 5.3. Localisation of HLA –DP in mock, NH_4Cl and leupeptin treated MelJuSo cells
MelJuSo cells were mock treated (A) or treated with NH_4Cl (B) or leupeptin (C) and stained with DAPI and αDP antibody. Yellow and pink arrows indicate examples of endosomal and ER staining, respectively. Red scale bar=10 microns.

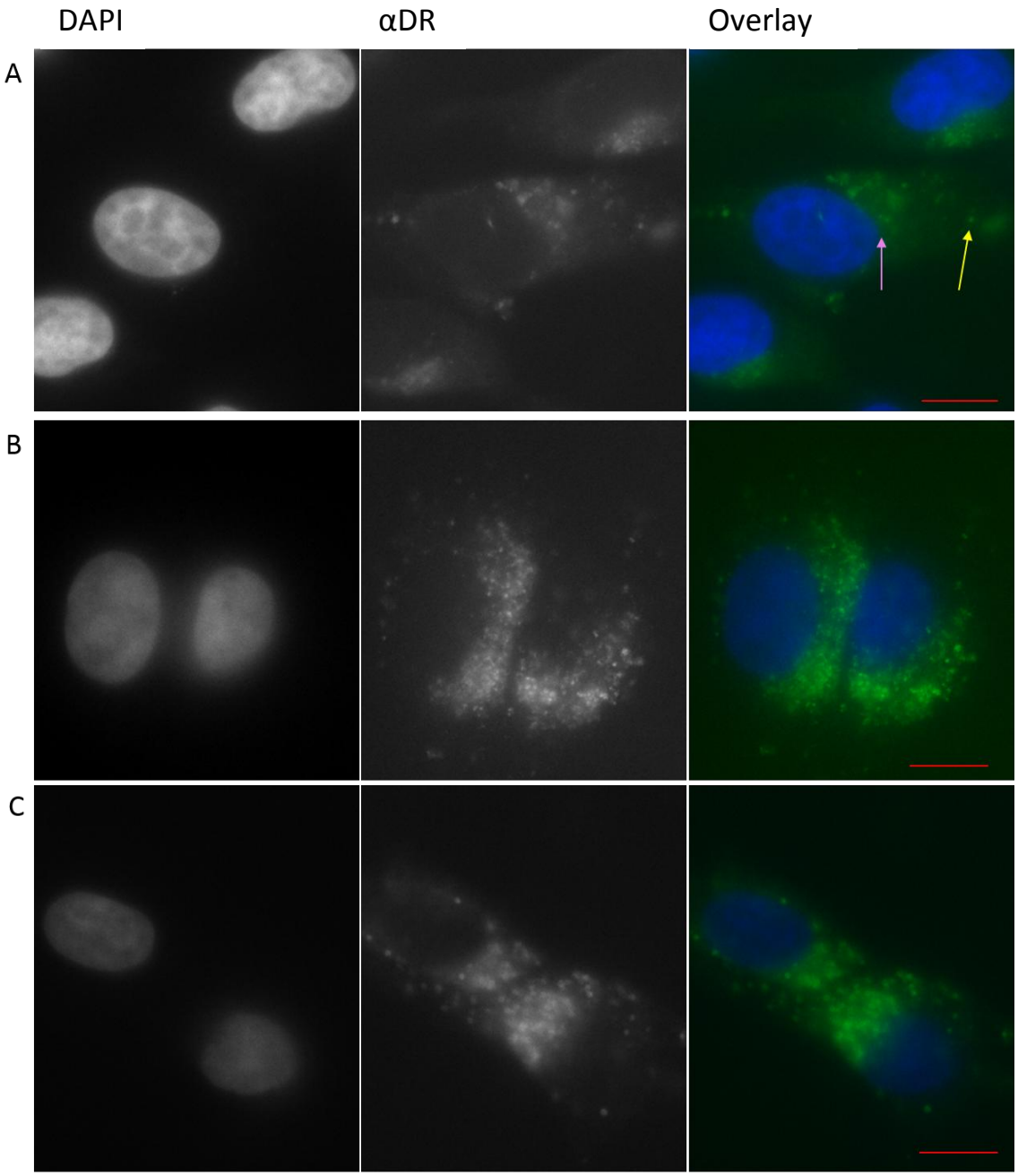

Figure 5.4. Localisation of HLA –DR in mock, NH_4Cl and leupeptin treated MelJuSo cells
MelJuSo cells were mock treated (A) or treated with NH_4Cl (B) or leupeptin (C) and stained with DAPI and αDR antibody. Yellow and pink arrows indicate examples of endosomal and ER staining, respectively. Red scale bar=10 microns.

5.2.3 Is TLR3 stabilising DP?

Full TLR3, 4 and 9 activation of innate responses is reliant on MYD88 and TRIF dependant pathways, which are enhanced by interaction with the tyrosine kinase Btk. Mouse models have shown that Intracellular MHC class II complexes with CD40 in endosomes to maintain the activity of Btk (Liu et al., 2011). If such an interaction is present in human cells, it may potentially account for the differing stabilities of the HLA isotypes, in particular the unusual stability of HLA-DP.

To investigate whether the TLR3 machinery could potentially interact with and stabilise MHC class II molecules, a cell line which endogenously expresses TLR3 in the presence or absence of MHC class II expression was required. Cells which do not naturally express MHC class II can be transfected with these molecules, meaning their assembly, trafficking, interactions and chaperone requirements (e.g. for HLA-DM and Ii) can be controlled.

Experimenting with a cell line which naturally expresses MHC class II would not be suitable. The transfection of MHC class II molecules would result in the overexpression of MHC class II, which in mice does not affect Btk activation, whereas restored expression of MHC class II in deficient mice activates Btk (Liu et al., 2011).

In accordance with its role in immune surveillance, TLR3 is highly expressed in tissues in contact with the external environment, for example epithelial cells in the lung (Zarember, 2002). However, there are conflicting views regarding the expression of TLR3, especially in leukocytes. There are several reports that it is only expressed in Dendritic cells (DC) (Muzio et

al., 2000), whilst others suggest it is expressed in a wider variety of cell types such as T or NK cells (Zarember, 2002).

Here, the human monocytic leukemia THP-1, the human melanoma MelJuSo and, the human fibrosarcoma HT1080 cell lines were investigated for their expression of TLR3. THP-1 cells are an immortalised monocyte-type suspension cell line that can be differentiated into adherent macrophages by treatment with mitogens e.g. PMA. RNA was extracted from these cell lines and subjected to RT-PCR using primers against TLR3 and β-actin to examine RNA levels. β-actin acts as an expression and amplification control and was strongly expressed in all 3 cell lines, confirming that the RT-PCR had been successful (Figure 5.5, lanes 1, 3, 5 and 7). HT1080 had the highest amount of TLR3 RNA (Figure 5.5, lane 8) whereas the MelJuSo cell line showed no detectable expression (Figure 5.5, lane 2). Despite published data claiming that TLR3 is not expressed in monocytes (Matsumoto and Seya 2008), small amounts were found in the THP-1 cell line as shown in Figure 5.5, lane 4, as well differentiated THP-1 macrophages as shown in Figure 5.5, lane 6.

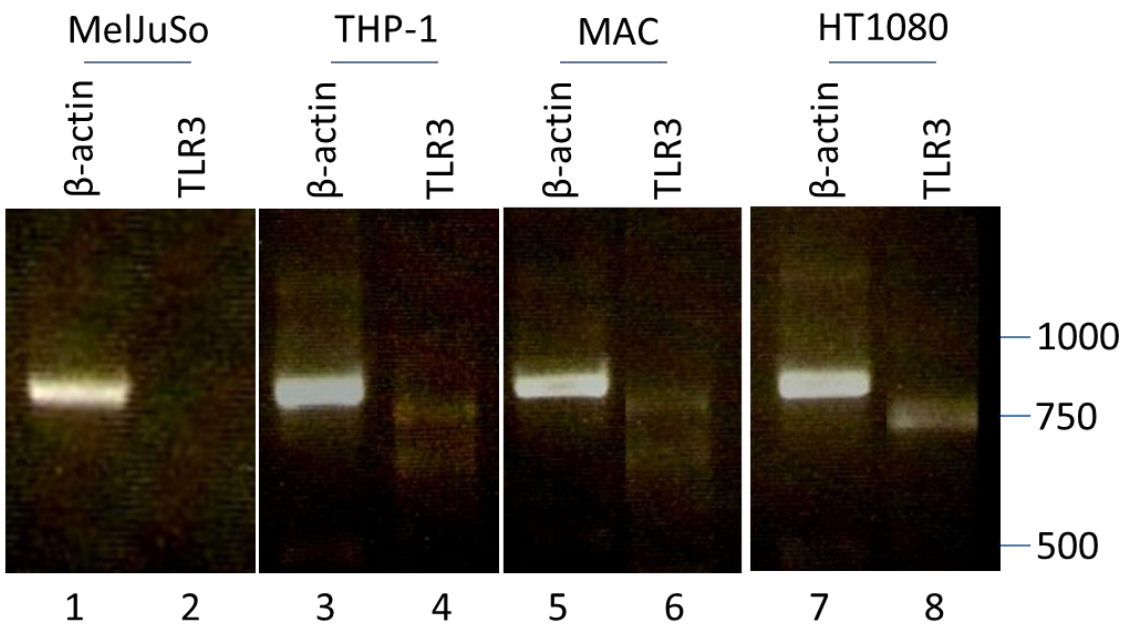

Figure 5.5. TLR3 expression in the MelJuSo, THP-1, HT1080, and macrophage cell lines

RNA extracted from MelJuSo, THP-1, HT1080 and THP-1 derived macrophage cells was converted to cDNA and used to test for the presence of actin and TLR3 expression.

Studies show that TLR3 expression is higher in resting macrophages than in monocytes and even higher in activated macrophages, so upon differentiation and maturation of the THP-1 cell line, TLR3 is expected to be upregulated (Heinz *et al.* 2003). The previous RT-PCR on RNA (cDNA) extracted from THP-1 cells showed no difference in TLR3 levels after differentiation (Figure 5.5, compare lanes 4 and 6). To verify this, western blotting was used. THP-1 cells were treated with PMA and LPS. The differentiated cells were lysed and examined with a TLR3 antibody following SDS-PAGE. A TLR3 signal appeared in HT1080 and undifferentiated THP1 cells in similar amounts (Figure 5.6A, lanes 1 and 2). A much fainter band could be seen (Figure 5.6A, lanes 3 and 4) when THP-1 cells were differentiated (+PMA; Figure 5.6A, lane 3) and differentiated and activated (+PMA and LPS; Figure 5.6A, lane 4). Probing these lysates with a PDI antibody shows equal loading of the samples (Figure 5.6B, lanes 1-4), demonstrating that the changes in the TLR3 signal were not due to differences in overall protein loading. This result is inconsistent with the literature; however, the molecular weight of the band supposedly representing TLR3 in Figure 5.6A is about 60kDa, and does not correspond to the predicted TLR3 molecular weight of 104 kDa. To assess whether the band seen in Figure 5.6A was likely to be a genuine TLR3 polypeptide, an endoH digestion experiment was performed. TLR3 is highly glycosylated, so upon endoH treatment the migration of this band should increase. Following such treatment of the HT1080 and THP1 lysates, no change in molecular weight was seen (compare Figure 5.6C, lanes 1 and 3, and lanes 2 and 4). In addition, a mouse intestinal lysate run alongside the cell lysates showed a band of about 100 kDa (and some higher molecular weight material) and is likely to be TLR3 (Figure 5.6C, lane 5). Probing the western blotted lysates with an Ero1α antibody showed that the endoH treatment was effective, with a decrease in the molecular weight of Ero1α in both HT1080 and THP-1 cells following deglycosylation (Figure 5.6D, compare lanes 1 and 3 and, 2 and 4).

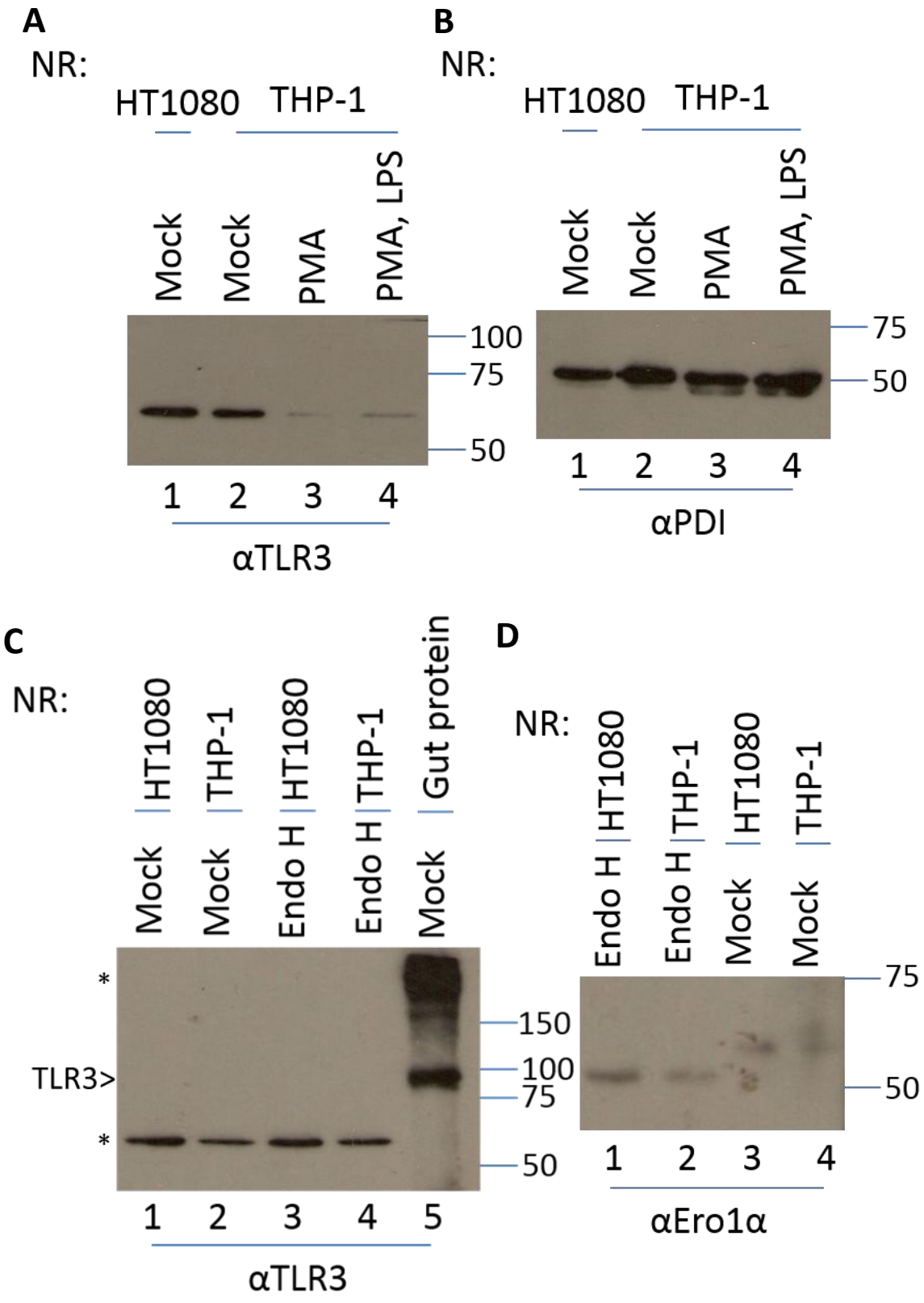

Figure 5.6. Increasing THP-1 TLR3 expression

THP-1 cells were treated with PMA, PMA and LPS or, mock treated, then, along with HT1080 cells, lysed in MNT buffer. Cell lysates were treated +/- endoH (**C** and **D**). Cell lysates, endoH treated cell lysates and gut lysates were subjected to non-reducing (NR) SDS-PAGE and subsequent Western blotting with the αTLR3 (**A** and **C**), αPDI (**B**) or αEro1α antibody (**D**). TLR3 and background bands are indicated (*****).

Taken together, these experiments suggest that the TLR3 antibody was able to detect TLR3 in tissue, but not in the immortalised cell lines, where a non-specific protein was bound.

The experiments shown in Figure 5.5 suggested that TLR3 expression in HT1080, MelJuSo and THP-1 cells was too low to allow a putative MHC class II-TLR3 interaction to be investigated. Another method of upregulating TLR3 is by ligand stimulation. Treatment of cells with the TLR3 ligand poly(I:C) should induce such a response (Ritter et al., 2005). Thus RNA was extracted from HT1080 cells treated with 50 or 100 μg/ml poly(I:C) and subjected to RT-PCR using primers to amplify TLR3. However, there appeared to be no change in the expression of TLR3 upon poly(I:C) stimulation of HT1080 cells (Figure 5.7, lanes 1, 2 and 3).

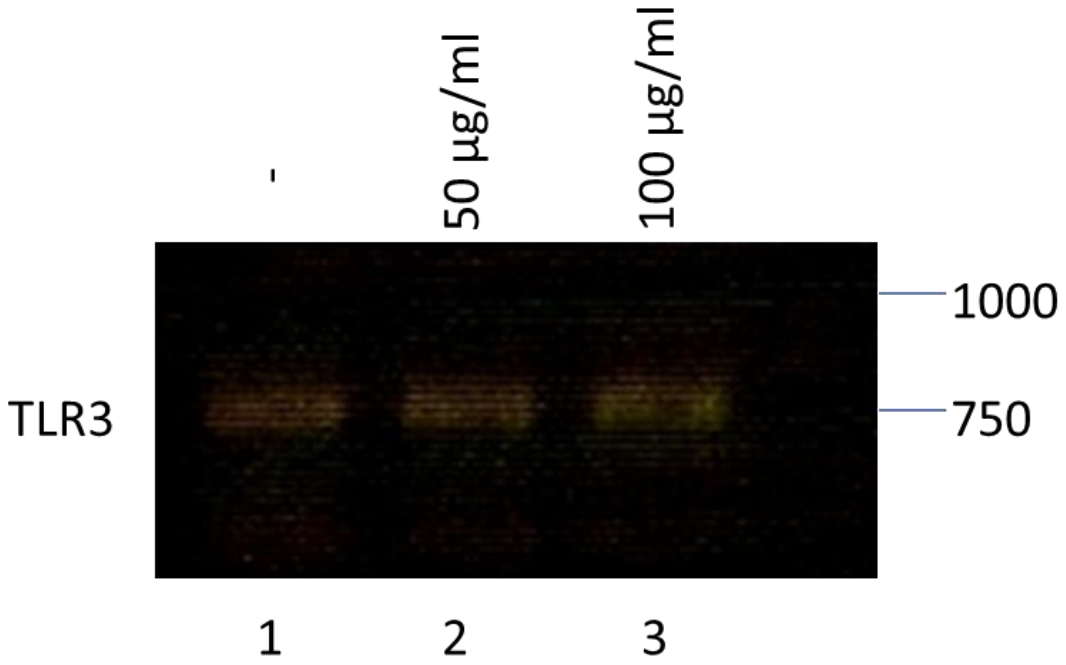

Figure 5.7. TLR3 expression in activated HT1080 cell lines

RNA extracted from HT1080 cells treated with 0 (-), 50 or 100 µg/ml poly(I:C) was reverse transcribed to cDNA and amplified by PCR for the presence of TLR3.

For an interaction between HLA-DP and TLR3 to occur they must co-localise. HLA-DP has been shown to reside in the ER and endocytic pathway (Ritter et al., 2005). TLR3 is generally thought to be found intracellularly, residing at the endosomal membrane, and binding to endosomal ligands (Johnsen et al., 2006). This reflects its role in detecting viral dsRNA. However, as with the conflicting opinions regarding TLR3 expression, there is debate as to its cellular location. These molecules have been found on the cell surface, which is characteristic of many other TLRs, in human fibroblast cells (Matsumoto *et al.* 2002). Such expression would be advantageous as it would give cells the ability to detect extracellular, most likely nonviral, dsRNA. Johnsen *et al.* (2006) provide further evidence of TLR3 localisation being dependant on cell type. As the HT1080 cell line has the highest TLR3 expression of the cell lines tested, its localisation was explored. Cells were fixed, permeabilised and stained with DAPI and a TLR3 antibody. Fluorescence microscopy was used to visualise the localisation of TLR3 in HT1080 cells (Figure 5.8). The DAPI stained shows clearly identifiable nuclei, however the pattern of staining for TLR3 is indistinct, with the localisation difficult to interpret. Taken together with the data in Figure 5.6, the experiments suggest that although TLR3 mRNA is synthesised to some extent in HT1080 cells, the level of protein expression is too low to analyse by western blotting and immunofluorescence.

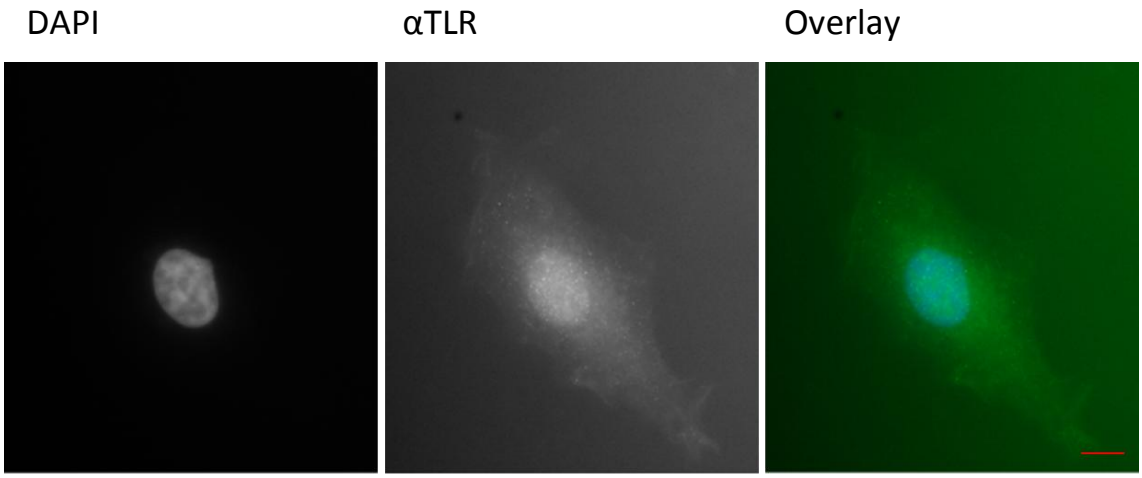

Figure 5.8. TLR3 expression in HT1080 cells

HT1080 cells were fixed and immunostained with the αTLR3 antibody. Nuclei were stained with DAPI. Red scale bar=10 microns.

By introducing the HLA isotypes DR and DP into a TLR 3 expressing cell line, their ability to complex with CD40, and enhance the activity of TLR3 activated Btk can be tested. This could be done by measuring the levels of TNF, IL-6 and IFN-β, the production of which increases upon TLR3 activation. Expression of both the MHC class II α and β chain are required for enhancement of Btk activity, meaning it is important that both the MHC class II α and β chain are expressed, together with the components needed for their assembly- DMα, DMβ and Ii. The plasmids for these components were transfected in different combinations to determine if a stable MHC class II dimer could be expressed. DRβ was transfected either alone, + DRα and Ii or +DRα and DMα (Figure 5.9A). The transfected cell lysates were analysed by western blot alongside mock transfected HT1080 cells, as well as HLA-DR expressing MelJuSo cell lysates. The PVDF membranes were probed using an anti DRβ antibody. The MelJuSo positive control shows the monomeric DRβ chain, as well as the heavier DRαβ heterodimer (Figure 5.9A, lane 1), neither of which were found in the mock transfected HT1080 sample (Figure 5.9A, lane 3). DRβ was successfully transfected, as shown by the ~ 30kDa band representing the DRβ chain (Figure 5.9, lanes 2 and 4). However the absence of a higher molecular weight band suggests that the DRα chain was not expressed in the co-transfectant. As multiple plasmids were being transfected here, it is possible that the ratio of DNA to transfection reagent was suboptimal in this experiment. To establish if this was the case, all plasmids were transfected into HT1080 cells, but at varying concentrations (Figure 5.9A, lanes 6, 7, and 8). 0.5 µl DNA was required to be able to see expression of the DRβ chain. However, although the DRβ chain was expressed, no DRαβ heterodimer was evident. This suggests that the DRα chain was not successfully transfected and expressed.

This experiment was repeated, transfecting just the DRα and DRβ chain to reduce the amount of DNA being taken up by the cell. Cell lysates from the transfectants were analysed by SDS-PAGE and western blotting, as before. Immunoblotting with the anti-DRβ antibody confirmed

that DRβ and the DRαβ heterodimer was present in the control MelJuSo sample (Figure 5.9B, lane 1). In the HT1080 transfectants, the DRβ construct was successfully transfected, with a band representing the DRβ chain, as well as a higher molecular weight band, which is likely to be DRβ homodimers, as DRα is not present (Figure 5.9B, lane 3 and 5). There was no signal when cells were transfected with DRα alone, as expected because the membrane was probed with an anti DRβ antibody (Figure 5.9B, lane 4). When both chains were transfected (Figure 5.9B, lane 5), two bands were seen, the lower being DRβ, the higher being either a DRαβ heterodimer or a DRβ homodimer (as seen in Figure 5.9B lane 3). To clarify whether DRα was expressed, the same samples were probed with an anti DRα antibody (Figure 5.9C). This revealed that the DRα construct was not transfected, with the only signal being in the positive control MelJuSo sample (Figure 5.9C, lane 1). From these experiments, it was concluded that it would be too challenging to investigate the role of TLR3 in the assembly and stability of HLA-DR by reconstituting HLA-DR, DM and Ii in HT1080 cells by transfection.

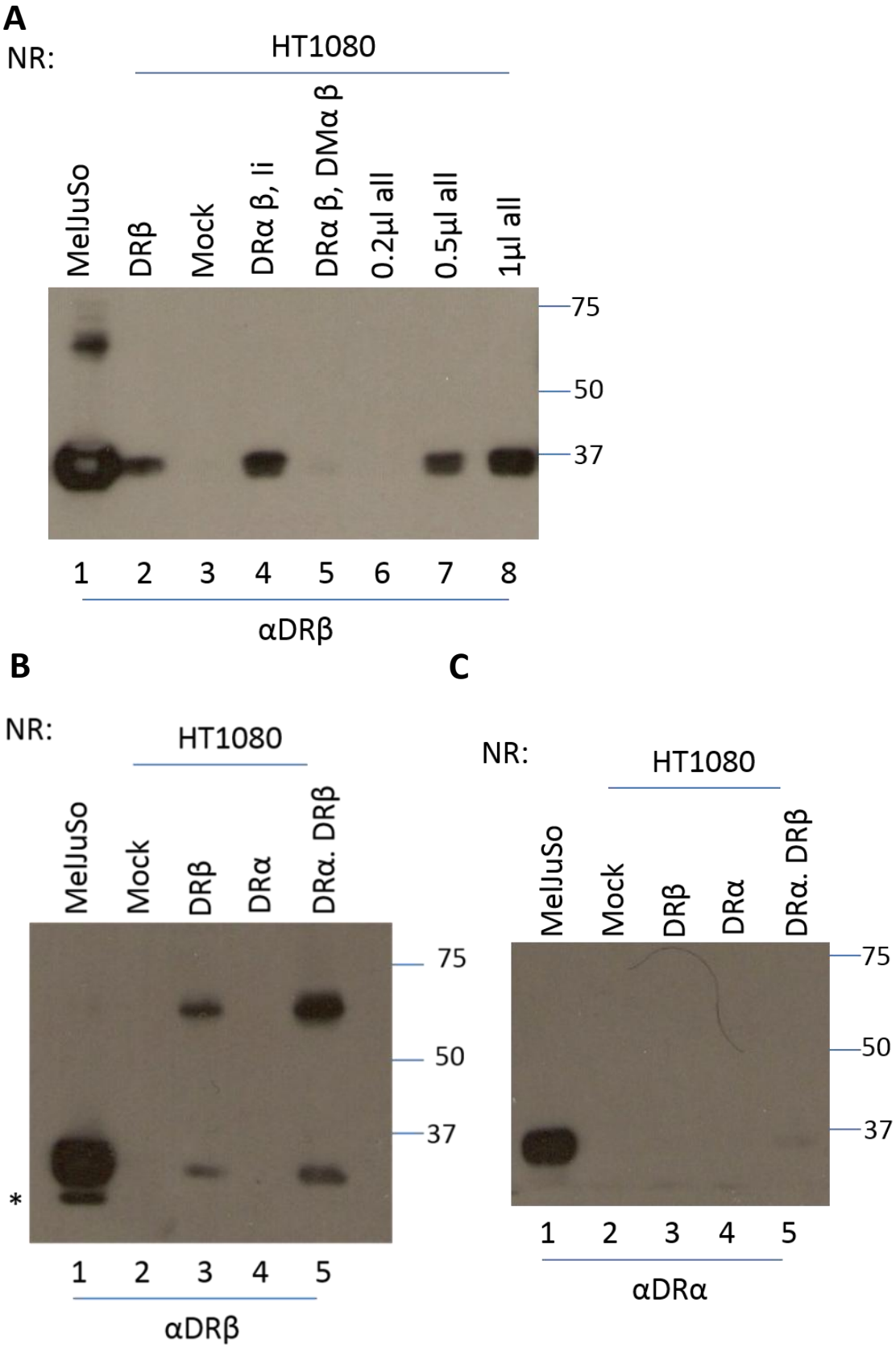

Figure 5.9. Transfection of the MHC class II system

HT1080 cells were transfected with combinations of DRα, DRβ, Ii, DMα and DMβ or mock transfected and lysed in MNT buffer. Along with MelJuSo lysates, the HT1080 lysates were then subjected to non-reducing (NR) SDS-PAGE and subsequent Western blotting with the antibodies αDRβ (**A** and **B**) or αDRα (**C**). Background bands are indicated (*).

5.2.4 Effect of homocysteine on MHC class II stability

The previous chapters have shown that homocysteine increases the amount of OX1 Ero1α and may thus influence its activity, with implications for the oxidative protein folding and quality control of "client" proteins in the ER. Here, MHC class II is used to explore how the homocysteine-induced change in Ero1, and other potential changes in the ER may affect ER "client" proteins. As the stability of MHC class II is known to be temperature sensitive, with DR losing its dimer at 60 ^{o}C, MelJuSo cells were treated with homocysteine to determine if this is another factor which causes changes in MHC class II stability (Figure 5.10). The cell lysates were analysed under boiling and non-boiling conditions; this means that they were subjected to boiling for 5 minutes following lysis. This acts as a control, confirming that the heavier band seen is the dimer.

Although MHC class II heterodimers do not have inter-molecular disulphide-bonds, their assembly is still dependent on the correct formation of intra-molecular disulphide bonds. However, the stability of MHC class II dimers did not appear to change upon homocysteine treatment (Figure 5.10A and B, lanes 1, 2, 3 and 4). This result suggests that changes to the homocysteine-induced Ero1 oxidation state do not impact the stability of the overall MHC class II pool. It remains to be seen whether the ER redox state or Ero1α activity are required for the early stages of MHC class II monomer folding.

Although there were no gross homocysteine-induced changed, the amount of MHC class II monomer (DR) increased slightly with homocysteine treatment under non-reducing conditions, with no, or very little monomer in untreated cells (Figure 5.10 A, lanes 1, 2, 3 and 4). Under

reducing conditions, the recovery of DR monomers was greater than that obtained under non-reducing conditions. Lysates were probed with an αactin antibody as a control (Figure 5.10 C).

Although the overall pool of stable DR heterodimers did not appear to be influenced by homocysteine, it remains possible that the peptide loading of DP and DQ allelic variants are influenced by homocysteine, and this may be worthy of further investigation in the future.

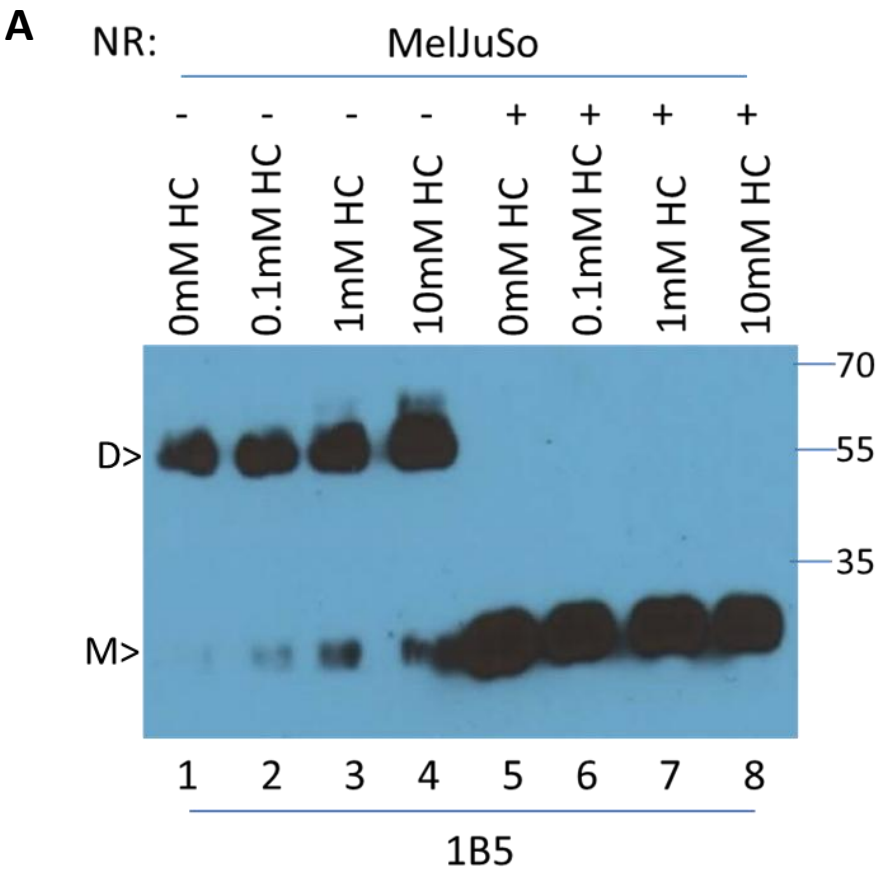
A
NR:
MelJuSo
- - - - + + + +
0mM HC
0.1mM HC
1mM HC
10mM HC
0mM HC
0.1mM HC
1mM HC
10mM HC
70
55
35
D>
M>
1 2 3 4 5 6 7 8
1B5

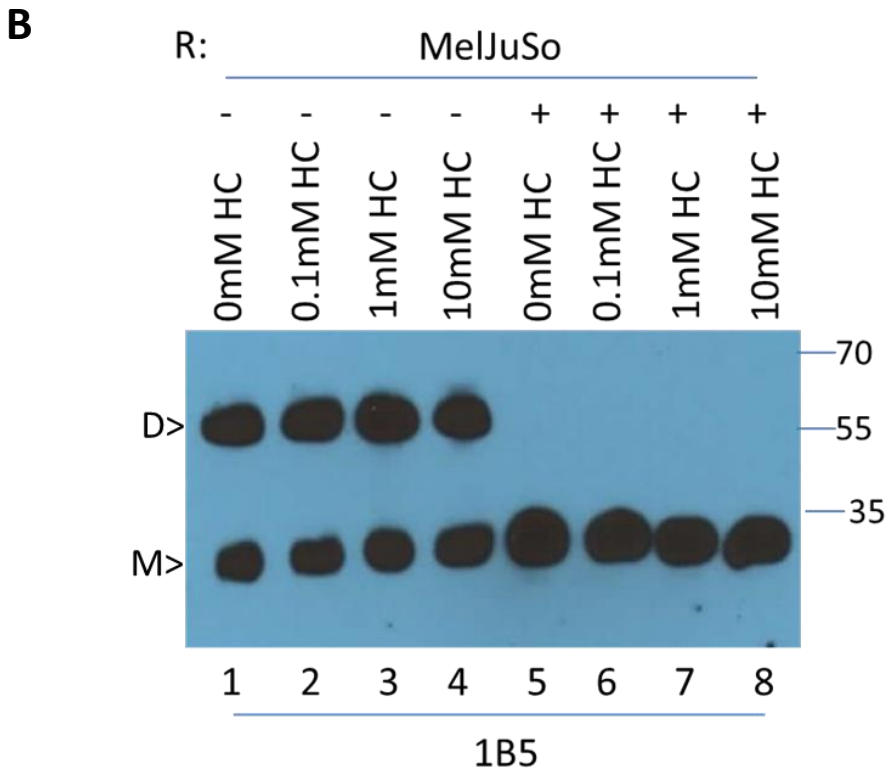
B
R:
MelJuSo
- - - - + + + +
0mM HC
0.1mM HC
1mM HC
10mM HC
0mM HC
0.1mM HC
1mM HC
10mM HC
70
55
35
D>
M>
1 2 3 4 5 6 7 8
1B5

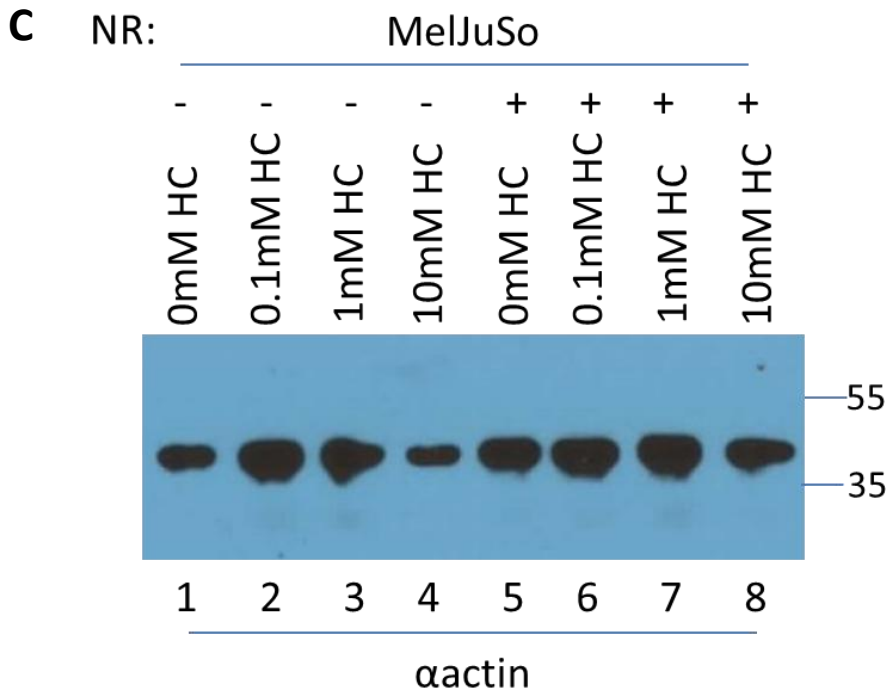

Figure 5.10. Homocysteine does not affect the stability of the HLA-DR pool in MelJuso cells

MelJuSo cells were treated with 0, 0.1, 1 or 10 mM HC for 1 hour then lysed in MNT buffer. Prior to analysis by non-reducing (NR) or reducing (R) SDS-PAGE and subsequent Western blotting, the lysates were boiled (+), or left at room temperature (-) for 5 minutes. The antibodies 1B5 (**A** and **B**) or αactin (**C**) were used on the western blot. DR monomers (M) and dimers (D) are labelled.

5.3 Discussion

The MHC class II molecules, HLA-DR, DP, and DQ have different requirements for assembly, with DP able to form SDS-stable dimers in the absence of Ii (van Lith, 2010). The work in this chapter further builds upon this observation. Here HLA-DR and DP are shown to have different stability thresholds not only, as previously shown, in the absence of Ii, but in its presence, with DP able to resist being denatured at a higher temperature than DR (Figure 5.2). DP and DR alleles on average show ~70% similarity to each other, so whether the differences in stability are due to structural differences between the molecules or a consequence of another factor stabilising the dimer remains open to question.

Despite the requirement for Ii for targeting MHC class II molecules to the endosomal-lysosomal compartments, without it some αβ complexes are folded and able to leave the ER. By comparing the localisation of the DP and DR molecules when the breakdown of Ii is inhibited, it would be possible to see how this occurs, and whether DP has an alternative pathway which may help account for its differential stability. The localisation of both DR and DP appeared similar, and further investigation into the lysosomal morphology also did not show any clear differences in the distribution of DR and DP (Figure 5.3 and 5.4). However these results do confirm the expected endosomal localisation of MHC class II molecules in general.

There are conflicting views regarding the expression of TLR3, with it being suggested that TLR3 is only found in DCs by some whilst others propose a much wider expression (Muzio et al., 2000; Zarember, 2002). This is investigated in this chapter by testing four different cell types (Figure 5.5), none of which are DCs. With 3 out of 4 cell lines weakly expressing TLR3,

expression of this molecule may be wider than originally proposed, and it is not solely expressed in antigen presenting cells. This allows for exploration of the TLR-MHC class II interaction by transfecting MHC class II into cells where it is not endogenously expressed. Given a cell line which endogenously expresses both TLR3 and MHC class II it would have interesting to stain for these to see the co-localisation. It would also have been interesting to co-stain for TLR3, HLA-DP/DR and Ii in DC subtypes obtained from tissues, to see if and where the MHC class II molecules exist independently of Ii.

The cell lines tested here only had low levels of TLR3 expression which most likely would not have been high enough to functionally analyse if the presence of MHC class II had an impact on the cells response to a foreign peptide. The expression of TLR3 failed to increase upon differentiation of immortalised THP1 monocytes to macrophages and ligand stimulation with LPS or Poly(I:C). Had the experiment proceeded, TLR3 could have been transfected into one of the cell lines tested here, or a higher expressing cell line could have been used for the experiment.

In order to test whether the presence of TLR has an effect on MHC class II, a MHC class II transfected cell line was to be used. Although the transfection of all components necessary for a stably bound MHC class II dimer has been achieved in the past (van Lith, 2010), this was challenging for some cell lines and it was not possible here. This may be due to too many plasmids being co-transfected. It would not have been effective to transfect individual alleles into a cell line which naturally expresses MHC class II. This is because the transfection of MHC class II molecules would result in the overexpression of MHC class II, and because tagging the MHC class II molecule can adversely affect its localisation. It may however have been possible to use fibroblasts with knocked out MHC class II expression, providing these cells expressed

functional levels of DM and Ii. Another potential solution would have been to use a retroviral system to introduce the necessary genes into a cell line which does not express MHC class II.

MHC class II has been shown to interact with a number of other molecules which can mediate its signalling at the cell membrane and intracellularly. An example of this is tetraspanins which associate with MHC class II at different cellular locations (Engering and Pieters, 2001). As MHC class II lacks any signalling motifs in its cytoplasmic tail it has been suggested that interactions with these molecules are used to initiate signalling (Hassan and Mourad, 2011). Little is known about how and where MHC class II molecules interact with other molecules to control signalling. It would therefore be interesting to investigate whether any of these signalling molecules preferentially interacted with different MHC class II isotypes or had stabilising or localising effects on MHC class II (Al-Daccak et al., 2004).

An increasing amount of cross-talk between TLR and MHC class II is becoming apparent, with the TLR trafficking chaperone UNC93B1 shown to interfere with the MHC class II presentation pathway, and more recently, Ii shown to interact with, and negatively regulate TLR7 signalling (Manoury, 2015). How such a relationship affects its binding to MHC class II may be of note, but more importantly the increasing number of nodes between the pathways may have implications for MHC class II stability and trafficking.

HLA-DP has been shown to present some ER protein-derived peptides on the cell surface; whether these peptides are loaded in the ER or are obtained at the cell surface, or during recycling is yet to be determined, and again may have implications for DP stability (Diaz et al., 2005).

The stability of the MHC class II dimer is indirectly reliant on disulphide bonds, as shown by the presence of dimers under both reducing and non-reducing conditions when samples are non-boiled (Figure 5.10 A and B). However, intramolecular molecular disulphides are present. Under non-reducing, non-boiling conditions no, or very little monomer was seen in untreated cells (Figure 5.10 A lane 1), whereas it was clearly present in reducing conditions (Figure 5.10B, lane 1). The increase in MHC class II monomer seen with homocysteine treatment under non-boiling, non-reducing conditions, suggests that disulphide bonds might be being broken. This may be because homocysteine is acting as a reducing agent, or it may be due to the change in OX1 of Ero1α. This could be further investigated with the use of an MHC class II antibody to detect if the change in MHC class II monomer concentration is due to a conformational change. The use of a constitutively active or dominant negative Ero1α mutants may also help determine where MHC class II folding and stability can be influenced by changes in Ero1 activity.

6. Final Discussion

6. Final Discussion

Previous studies have shown a link between homocysteine and Ero1, with treatment of mammalian cells with homocysteine leading to an increase in the Ero1 OX1 form (Battle et al., 2013). These experiments were carried out using the oesophageal cell line, OE33, which has high levels of Ero1α expression and are derived from a cellular location in which the cells will have been exposed to, and may respond to, fluctuating dietary factors by changing the poise of the oxidative folding machinery. This thesis has further characterised the relationship between homocysteine and Ero1 proteins, finding that the effect of homocysteine is not restricted to Ero1α in the OE33 cell line. Millimolar concentrations of homocysteine were found to have the same effect of increasing the amount of "OX1-like" Ero1β when cell lines are transfected with Ero1β (Figures 4.3 and 4.5), but not in pancreatic cells.

Ero1α with mutated cysteine residues, namely those which form structural or functional disulphide bonds, were also used to explore where in the Ero1α redox cycle homocysteine was having its reducing effect, and if OX1 still increased when regulatory disulphides were removed. Despite the mutants existing in different OX1:OX2 ratios when untreated all, except the constituently active C104A/C131A, are pushed into a lower mobility state following homocysteine treatment. As some of the other mutants tested (C391A, C394A/C397A and C391A/C394A/C397A) may lack certain structures or may lack active site cysteines, these results show that the effect of homocysteine is not reliant on the complete 3D structure of Ero1α, nor on the complete transfer of electrons. As the increase in OX1 is not impaired by the loss of these cysteine residues, it is likely that homocysteine is not having a direct reducing effect on them. The effect is likely to be indirect, as supported by experiments in which incubation of purified Ero1α protein with mM concentrations of homocysteine showed no

change in Ero1α activity (unpublished work, personal communication, Bulleid laboratory). Thus homocysteine is likely to work through an intermediate, or indirect, pathway.

Although GSH is a poor substrate for Ero1α, an equilibrium is maintained between the redox states of Ero1α and GSH, with GSH maintaining the redox state of PDI to ensure efficient isomerization of non-native disulphide bonds (Chakravarthi and Bulleid, 2004; Molteni et al., 2004). Homocysteine could act through GSH by altering its levels, thus causing a redox imbalance with Ero1α. It would be interesting to measure any change in GSSG:GSH ratio upon homocysteine treatment to determine if it is buffering the effects of the active Ero1α, or if Ero1α is responding to changes in the redox environment.

This study also provides evidence that homocysteine stimulates a modification of Ero1. When cells are treated with homocysteine, the monoclonal antibody 2G4 is unable to detect Ero1α (Figure 3.3-3.5). This cannot be due to the changes in disulphide bonds stimulated by homocysteine treatment, as whilst the 2G4 detects Ero1α when fully reduced, it does not when Ero1α has been treated with 10 mM homocysteine. Therefore a modification to the antibody epitope is likely to be preventing the binding of 2G4. The modification to Ero1α by homocysteine was observed in the HT1080, HeLa and OE33 cell lines, however not in the liver tissue (Figure 3.3, 3.14 and 4.6). It is difficult to be certain what the modification could be as the 2G4 antibody epitope, whose signal is lost upon homocysteine treatment, has not been mapped. Given this information, or by using truncation mutants to map the epitope, it would be possible to identify where the modification is happening, which may give clues as to the type of modification and whether it is a direct effect of homocysteine, whether it is through another molecule (e.g glutathionylation or nitrosylation) or whether is it caused by changes in the ER, for example changes in the redox equilibrium. With this information it may also be possible to determine if the same modification occurs in Ero1β. If so, it may be possible to

understand the structural basis of the homocysteine modified form and whether it is the same as the active OX1 form. It is possible that the modification affects Ero1 function. This could be tested by site-directed mutagenesis of the modified residue, comparing the changes in oxidative folding capacity upon ER redox and ER stress induction in Ero1 transfectants and in the activity of purified Ero1α mutant proteins *in vitro.*

Induction of Ero1α OX1 by homocysteine was observed in multiple cell lines. In some of these experiments, Ero1α was strongly expressed by transfection, which has the potential to increase the production of ROS (Harding et al., 2003). This can be counteracted by activation of the UPR resulting in increased glutathione synthesis and thus higher antioxidant capacity (Appenzeller-Herzog et al., 2008), however the expression levels of Ero1α and Ero1β in some tissues are as high, or higher, than those in the transfectants. To check whether the transfections result in UPR, RT-PCR could be utilised to see if XBP1 is activated, or whether stress chaperones like BiP are induced.

The OX1:OX2 ratio differs between cell lines, as does their folding capacity and ability to respond to cellular stress; for example, Ero1α exists almost entirely in the OX2 form in the HT1080 cell line, whereas in the THP-1 cell line, although there is still a higher proportion of OX2, a significant amount of OX1 exists (Benham et al., 2013). However, these differences between cell lines do not appear to affect the ability of homocysteine to increase the amount of Ero1α OX1. To understand how Eros behaved in a system more representative of the *in vivo* environment, tissue derived cells were used (Figures 4.6 and 4.7). Ero1α OX1-like induction by homocysteine was seen in liver cells, however the same was not seen in Ero1β from pancreatic tissue cells. This may suggest that certain cells have a different redox poise, regulatory environment or different levels of Ero1 control to protect them from homocysteine. As Ero1β is not induced by hypoxia, this may indicate that it is not as vulnerable as Ero1α to changes in

the redox environment of the ER. To test if Ero1β would be more vulnerable to homocysteine when there are larger changes in the redox environment, the pancreas cells could be exposed to hypoxic conditions in a hypoxia chamber, or treated with peroxide, prior to homocysteine treatment.

As the pancreas has a high level of Ero1β expression and a high secretory output, greater levels of homocysteine may be needed to influence Ero1β and the redox conditions. The high expression may also indicate that although Ero1β is physiologically required in cells with high secretory output, it may not solely function as a UPR responsive gene. Why do some cells possess high levels of inactive Ero1β (e.g. pancreas) and Ero1α (e.g. liver) when, under stress, cells respond by increasing transcription of these genes rather than activating the protein pool? Perhaps a high threshold of protein concentration is needed for it to be pushed into the active version, but it has also been suggested that inactive Ero1α may possess another function as a chaperone complex or client protein complex (Dias-Gunasekara, 2005).

The proposed looser regulation of Ero1β (Wang et al., 2011) may also explain to the lack of change in Ero1β in tissue derived pancreas cells. With looser regulation, and thus being more active, Ero1β would be expected to produce more ROS than Ero1α. The main off setters of ROS production are GPx8 and PrxIV, however there is some evidence that GPx8 is functionally coupled to Ero1α and knock down of PrxIV does not cause the same elevation of the UPR as with GPx8 knockdown suggesting functional separation (Ramming et al., 2014). Little is known about the differences in how H_2O_2 produced by Ero1α and Ero1β are offset, and whether Ero1β is coupled in the same way. If H_2O_2 production is also increased by homocysteine treatment, there may be differences in the ability of Ero1α and Ero1β to deal with it, perhaps through differences in the interactions with the GPx/PrdxIV detoxification machinery.

Ero1β expression has not been detected in any immortalised cell lines. Ero1β is constitutively expressed in pancreatic cells, however the pancreas is composed of a number of specialised cell types with specialist secretory functions and of these, Ero1β expression has been shown in islet cells. Ero1β expression is not found in the pancreatic cell line PANC1. This could be because the cell line is epithelial thus its main function is not secretion, or because *in vivo* factors required for the induction of Ero1β expression are absent in cell culture. Nevertheless, transfection of Ero1β into pancreas-derived cell such as PANC1 and the insulin secreting rat INS-1 line may help determine whether the lack of homocysteine effect in pancreatic tissue is due to pancreas-specific factors, or the metabolic environment.

High levels of homocysteine have been reported to induce oxidative stress and increase generation of ROS, with increased levels of ATF6, XBP-1 and PERK (Yang, 2014). This study also shows that this stress is mediated, at least in part, by Ero1α, with the UPR response attenuated with over expression of Ero1α and increased when Ero1α is knocked out. When these results are compared with the homocysteine induced increase in Ero1α OX1 seen in this thesis, it seems that the increase in OX1 may be a response to the increase oxidative stress. However these experiments would need to be tied together and could be done by a pulse-chase metabolic labelling experiment to see if homocysteine treatment results in changes in UPR-induced protein translation.

It would also be interesting to see how other chemical inducers of ER oxidative stress change the Ero1 OX1:OX2 balance. If they do not induce the same increase in OX1, yet homocysteine treatment results increased OX1 and a UPR, then it is possible that homocysteine is not

increasing OX1 via a stress response, but the increase in OX1 results in a stress response. This would be similar to the UPR induced by the constitutively active Ero1α mutant (Hansen, 2012).

The UPR described as a result of homocysteine would be expected to increase Ero1 expression. It is difficult to say if such a change is seen in this study; a more suitable method for quantifying expression, such as quantitative RT-PCR, would be required to determine this. Whether the increased Ero1 expression would impact the Ero1 OX1:OX2 ratio is unknown.

The OX1:OX2 ratio of Ero1 present in the ER is generally determined by the redox equilibrium of the ER, whereas stress, for example UPR and hypoxia, causes changes in transcription. Thus it would seem that homocysteine increases OX1 by causing changes in the redox equilibrium. Alternatively, homocysteine could directly push the ER redox balance towards a more reducing state. PDI could potentially directly oxidise homocysteine into its oxidised form, homocystine, pushing Ero1 into its OX1 form. This may also provide an explanation as to why homocysteine does not affect Ero1 in all cells, as seen with Ero1β in pancreatic cells. As Ero1β interacts with different PDI family members, for example in the pancreas Ero1 interacts with PDIp (Fu et al., 2009), certain partners of Ero1β may not be as sensitive to homocysteine. If homocysteine were oxidised by PDI, and different PDI family members differed in their sensitivity to homocysteine, there could be knock on effects on Ero1β.

Patients with hyperhomocysteinemia and homocystinuria have defects in their homocysteine metabolism pathways which leads to a build-up of plasma homocysteine, and results in millimolar concentrations of circulating homocysteine (Faraci and Lentz, 2004). The detrimental effects of homocysteine can be reduced by increasing the amount of vitamin B in the diet (Elanchezhian et al., 2012), however further characterisation of how metabolic defects

of homocysteine metabolism influence the regulation of disulphide bond formation in diseases with a redox imbalance is required. Such studies may provide further information about targets for drug development and biomarkers for diseases with an oxidative folding component.

Having looked at the Ero1 PDI partnership, a client protein was looked at in chapter 5. Following the investigation of the effect of homocysteine on Ero1, here homocysteine was shown not to have a direct effect on MHC class II molecules (Figure 5.10). Despite this, further experiments are required to determine whether homocysteine has any subtle effects. A pulse chase analysis of MHC class II with and without homocysteine would establish whether homocysteine has an impact of MHC class II assembly.

MHC class II was further investigated, finding that the DP dimer is able to resist being denatured at higher temperatures than DR, despite appearing to have the same localisation (Figure 5.2-5.4). This builds upon previous studies showing that the MHC haplotypes DR, DP and DQ have different requirements to form stable dimers (van Lith, 2010).

It was not possible to determine whether the TLR pathway influences the hetero-dimerisation or stability of a specific MHC class II isotype (Figure 5.4-5.9, Chapter 5). The interaction between MHC class II and TLR3 via CD40 has been shown in mice (Liu et al., 2011) but is relatively uncharacterised and many other questions remain unanswered, such as whether CD40 binds to MHC class II directly in humans, as well as how CD40 is trafficked to the endosomes; this could be dependent on its binding to MHC class II. A stable interaction between MHC class II and CD40 has also been found in other cells or subcellular compartments, for example in tonsillar B cells where they associate after stimulation of either molecule, which

could provide another system in which the interaction could also be investigated (Leveille et al., 1999).

Homocysteine does not seem to affect MHC class II stability (Figure 5.10), however further knowledge as to how homocysteine affects the clients of the oxidative folding machinery, as well as the impact of an increased Ero1 OX1 level, is required to predict how other proteins, including PDI substrates, respond to homocysteine. Oxidative folding is important for the folding of MHC class II molecules, with the β chain containing two long range disulphides and the α chain containing one. Although it is known that MHC class II molecules interact with the ER resident chaperones calnexin, ERp72 and GRP94 during early folding and assembly (Anderson 1994, Arunachalam 1995, Schaiff 1992), less is known about the formation of the disulphides. In HLA-DM, the individual chains direct the oxidation of the partner chain, with DMα preventing misoxidation of DMβ whose own disulphides are required for correct oxidation of DMα (Van Lith, 2006). With these intrinsic properties determining oxidative folding, rather than the ER oxidation machinery, and with high sequence homology between the MHC class II family members, this may have implications for the folding of the classical MHC class II molecules, with the potential of oxidative folding redundancy here too. The DM folding mechanism, and the presence of an extra disulphide that allows DM to form a stable heterodimer able to leave the ER without a bound peptide, which is required by the classical molecules (van Lith and Benham, 2006), may make it more susceptible to changes in the oxidative folding environment. DPβ contains an extra cysteine residue, and a disulphide linked DPαβ has been shown to exist. Although the extra disulphide bond does not account for its stability (van Lith, 2010), it may have implications for its folding mechanism; whether DP alleles perform more like DM, with its extra disulphide, or whether the free cysteine allows for an interaction with oxidoreductases remains to be established.

Ero1α has been shown to be important in the folding of MHC class I, with Ero1α binding non-covalently to calnexin, which has an association with the MHC class I heavy chain. PDI has been suggested to mediate the formation of disulphides in the MHC class I heavy chain (Cho et al., 2011; Kukita et al., 2015). When Ero1α is overexpressed, the amount of oxidized MHC class I heavy chain increases (Kukita et al., 2015). This has implications for cancers where Ero1α expression is increased during hypoxia, and studies show that low MHC class I is associated with poor prognosis of osteosarcoma (Tsukahara et al., 2006).

Although little is known about how disulphide bonds are formed, and which oxidoreductases are involved in the early stages of the MHC class II pathway, more is known about the later stages. Gamma-interferon-inducible lysosomal thiol reductase (GILT), the only thiol reductase known to exist in the lysosome and able to function at low pH, is related to the thioredoxin family of oxidoreductases (Arunachalam et al., 2000). GILT reduces disulphide containing antigens, allowing their presentation by MHC class II (Maric et al., 2001). GILT also regulates the function of cathepsin S, one of the proteases that cleaves Ii and large polypeptides for MHC class II presentation. GILT has been shown to both assist the degradation of cathepsin S and maintain its proteolytic activity. These roles seem to oppose each other, so more needs to be known regarding these how these processes function, and how the outcome is determined, before it is possible to say how they affect antigen presentation (Balce et al., 2014; Phipps-Yonas et al., 2013). GILT levels are another factor believed to relate to cancer prognosis, with low levels associated with poor survival in patients with diffuse large B-cell lymphoma (DLBCL). Antigen processing is vital for producing tumour-specific epitopes, which can be presented by MHC class II, thus a decreased GILT expression diminishes presentation of tumour antigens and the resulting T cell mediated anti-tumour response. The loss of GILT expression in patients with DLBCL may represent a form of immune evasion (Phipps-Yonas et al., 2013). The known functions of GILT are becoming more diverse. One recent development is GILTs involvement in

the regulation of the cellular redox state. In the absence of GILT the proportion of oxidised GSH increases resulting in oxidative stress (Chiang and Maric, 2011).

DP could be interacting with one of a number of molecules, and as DP is found at the cell surface with ER protein derived peptides, it is clear that DP is able to bind peptides in the ER, with the possibility that these are stabilising DP. With a peptide binding motif which is different to that of ER loaded MHC class I molecules, MHC class I and DP will not compete for the same peptides, but it is unclear whether these DP binding ER peptides are competing with Ii (Diaz et al., 2005).

Whilst there is still much to be discovered about the oxidative folding of MHC class II molecules, there is potential for differences in folding pathways to exist between the isotypes, as well as interactions between these molecules and oxidoreductases. The interaction between MHC class II and CD40 recently described in the literature also presents another potential stabilising relationship, which has been studied here and provides a groundwork for further investigation.

6. References

Aebi, M. (2013). N-linked protein glycosylation in the ER. Biochim Biophys Acta *1833*, 2430-2437.

Akalin, A., Alatas, O., and Colak, O. (2008). Relation of plasma homocysteine levels to atherosclerotic vascular disease and inflammation markers in type 2 diabetic patients. Eur J Endocrinol *158*, 47-52.

Al-Daccak, R., Mooney, N., and Charron, D. (2004). MHC class II signaling in antigen-presenting cells. Curr Opin Immunol *16*, 108-113.

Alder, N.N., Shen, Y., Brodsky, J.L., Hendershot, L.M., and Johnson, A.E. (2005). The molecular mechanisms underlying BiP-mediated gating of the Sec61 translocon of the endoplasmic reticulum. J Cell Biol *168*, 389-399.

Alexandrov, N. (1993). Structural argument for N-terminal initiation of protein folding. Protein Sci *2*, 1989-1991.

Anderson, M.S., and Miller, J. (1992). Invarient chain can function as a chaperone protein for class II major histocompatibility complex molecules. Proc Natl Acad Sci USA *89*, 2282-2286.

Anelli, T., Alessio, M., Bachi, A., Bergamelli, L., Bertoli, G., Camerini, S., Mezghrani, A., Ruffato, E., Simmen, T., and Sitia, R. (2003). Thiol-mediated protein retention in the endoplasmic reticulum: the role of ERp44. EMBO J *22*, 5015-5022.

Anelli, T., Alessio, M., Mezghrani, A., Simmen, T., Talamo, F., Bachi, A., and Sitia, R. (2002). ERp44, a novel endoplasmic reticulum folding assistant of the thioredoxin family. EMBO J *21*, 835-844.

Anelli, T., and van Anken, E. (2013). Missing links in antibody assembly control. Int J Cell Biol *2013*, 606703.

Anfinsen, C.B. (1973). Principles that govern the folding of protein chains. Science *181*, 223-230.

Appenzeller-Herzog, C., Riermer, J., Christensen, B., Sorenson, E.S., and Ellgaard, L. (2008). A novel disulphide switch mechanism in Ero1α balances ER oxidation in human cells. EMBO J *27*, 2877-2987.

Appenzeller-Herzog, C., Riermer, J., Zito, E., Chin, K., Ron, D., Spiess, M., and Ellgaard, L. (2010). Disulphide production by Ero1α–PDI relay is rapid and effectively regulated. EMBO J *29*, 3318-3329.

Apweiler, R., Hermjakob, H., and Sharon, N. (1999). On the frequency of protein glycosylation, as deduced from analysis of the SWISS-PROT database. Biochim Biophys Acta *1473*, 4-8.

Araki, K., and Nagata, K. (2011). Functional in vitro analysis of the ERO1 protein and protein-disulfide isomerase pathway. J Biol Chem *286*, 32705-32712.

Arunachalam, B., Phan, U.T., Geuze, H.J., and Cresswell, P. (2000). Enzymatic reduction of disulfide bonds in lysosomes: characterization of a gamma-interferon-inducible lysosomal thiol reductase (GILT). Proc Natl Acad Sci USA *97*, 745-750.

Awazawa, M., Futami, T., Sakada, M., Kaneko, K., Ohsugi, M., Nakaya, K., Terai, A., Suzuki, R., Koike, M., Uchiyama, Y.*, et al.* (2014). Deregulation of pancreas-specific oxidoreductin ERO1β in the pathogenesis of diabetes mellitus. Mol Cell Biol *34*, 1290-1299.

Baker, K.M., Chakravarthi, S., Langton, K.P., Sheppard, A.M., Lu, H., and Bulleid, N.J. (2008). Low reduction potential of Ero1α regulatory disulphides ensures tight control of substrate oxidation. EMBO J *27*, 2988-2997.

Balce, D.R., Allan, E.R., McKenna, N., and Yates, R.M. (2014). gamma-Interferon-inducible lysosomal thiol reductase (GILT) maintains phagosomal proteolysis in alternatively activated macrophages. J Biol Chem *289*, 31891-31904.

Ballar, P., Pabuccuoglu, A., and Kose, F.A. (2011). Different p97/VCP complexes function in retrotranslocation step of mammalian ER-associated degradation (ERAD). Int J Biochem Cell Biol *43*, 613-621.

Banhegyi, G., Braun, L., Csala, M., Puskas, F., Somogyi, A., Kardon, T., and Mandl, J. (1998). Ascorbate and environmental stress. Ann Ny Acad Sci *851*, 292-303.

Banhegyi, G., Lusini, L., Puskas, F., Rossi, R., Fulceri, R., Braun, L., Mile, V., di Simplicio, P., Mandl, J., and Benedetti, A. (1999). Preferential transport of glutathione versus glutathione disulfide in rat liver microsomal vesicles. J Biol Chem *274*, 12213-12216.

Barton, G.M., and Medzhitov, R. (2003). Toll-like receptor signaling pathways. Science *300*, 1524-1525.

Battle, D.M., Gunasekara, S.D., Watson, G.R., Ahmed, E.M., Saysell, C.G., Altaf, N., Sanusi, A.L., Munipalle, P.C., Scoones, D., Walker, J.*, et al.* (2013). Expression of the endoplasmic reticulum oxidoreductase Ero1α in gastro-intestinal cancer reveals a link between homocysteine and oxidative protein folding. Antioxid Redox Signal *19*, 24-35.

Benham, A.M. (2012). The Protein Disulfide Isomerase Family: Key Players in Health and Disease. Antioxid Redox Signal *16*, 781-789.

Benham, A.M., Cabibbo, A., Fassio, A., Bulleid, N., Sitia, R., and Braakman, I. (2000). The CXXCXXC motif determins the folding structure and stability of human Ero1-Lα. EMBO J *19*, 4493-4502.

Benham, A.M., van Lith, M., Sitia, R., and Braakman, I. (2013). Ero1-PDI interactions, the response to redox flux and the implications for disulfide bond formation in the mammalian endoplasmic reticulum. Philos Trans R Soc Lond B Biol Sci *368*, 20110403.

Berg, J.M., Tymoczko, J.L., and Stryer, L. (2002). Section 33.2 The Immunoglobulin fold consists of a beta-sandwich framework with hypervariable loops. Biochemistry 5th edition, New York, W H Freeman.

Berger, A.C., and Roche, P.A. (2009). MHC class II transport at a glance. J Cell Sci *122*, 1-4.

Bernardi, K.M., Williams, J.M., Inoue, T., Schultz, A., and Tsai, B. (2013). A deubiquitinase negatively regulates retro-translocation of nonubiquitinated substrates. Mol Cell Biol *24*, 3545-3556.

Bernasconi, R., Galli, C., Calanca, V., Nakajima, T., and Molinari, M. (2010). Stringent requirement for HRD1, SEL1L, and OS-9/XTP3-B for disposal of ERAD-LS substrates. J Cell Biol *188*, 223-235.

Bernasconi, R., and Molinari, M. (2011). ERAD and ERAD tuning: disposal of cargo and of ERAD regulators from the mammalian ER. Curr Opin Cell Biol *23*, 176-183.

Bertoli, G., Simmen, T., Anelli, T., Molteni, S.N., Fesce, R., and Sitia, R. (2004). Two conserved cysteine triads in human Ero1alpha cooperate for efficient disulfide bond formation in the endoplasmic reticulum. J Biol Chem *279*, 30047-30052.

Bertolotti, A., Wang, X., Novoa, I., Jungreis, R., Schlessinger, K., Cho, J.H., West, A.B., and Ron, D. (2001). Increased sensitivity to dextrin sodium sulfate colitis in IREβ-deficient mice. J Clin Invest *107*, 585-593.

Blaschke, K., Ebata, K.T., Karimi, M.M., Zepeda-Martinez, J.A., Goyal, P., Mahapatra, S., Tam, A., Laird, D.J., Hirst, M., Rao, A.*, et al.* (2013). Vitamin C induces Tet-dependent DNA demethylation and a blastocyst-like state in ES cells. Nature *500*, 222-226.

Blobel, G., and Dobberstein, B. (1975). Transfer of proteins across membranes. I. Presence of proteolytically processed and unprocessed nascent immunoglobulin light chains on membrane-bound ribosomes of murine myeloma. J Cell Biol *67*, 835-851.

Bottomley, M.J., Batten, M.R., Lumb, R.A., and Bulleid, N.J. (2001). Quality control in the endoplasmic reticulum: PDI mediates the ER retention of unassembled procollagen C-propeptides. Curr biol *11*, 1114-1118.

Boushey, C.J., Beresford, S.A.A., Omenn, G.S., and Motulsky, A.G. (1995). A Quantitative Assessment of Plasma Homocysteine as a Risk Factor for Vascular-Disease - Probable Benefits of Increasing Folic-Acid Intakes. JAMA *274*, 1049-1057.

Braakman, I., Hebert, D. N. (2013). Protein folding in ther Endoplasmic Reticulum. Cold Spring Harb Perspect Biol *5*.

Braakman, I., Hoover-Litty, H., Wagner, K.R., and Helenius, A. (1991). Folding of influenza hemagglutinin in the endoplasmic reticulum. J Cell Biol *114*, 401-411.

Brange, J., and Langkjoer, L. (1993). Insulin structure and stability. Pharm Biotechnol *5*, 315-350.

Brock, C., Boudier, L., Maurel, D., Jaroslav, B., Pin, JP. (2005). Assembly-dependent surface targeting of the heterodimeric GABAb receptor is controlled by COPI but not 14-3-3. Mol Cell Biol *16*, 5572-5578.

Brundage, L., Hendrick, J. P., Schiebel, E., Driessen, A. J., Wickner, W. (1990). The purified E. coli integral membran protein SecY/E is sufficient for reconstitution of SecA-dependent precursor protein tranlocation. Cell *62*, 649-657.

Burgess, J.K., Hotchkiss, K. A., Suter, C., Dudman, N. P., Szollosi, J., Chesterman, C. N., Chong, B. H., Hogg, B. H. (2000). Physical proximity and functional association of glycoprotein 1bα and protein-disulfide isomerase on the platelet plasma membrane. J Biol Chem *275*, 9758-9766.

Busch, R., Rinderknecht, C.H., Roh, S., Lee, A.W., Harding, J.J., Burster, T., Hornell, T.M.C., and Mellins, E.D. (2005). Achieving stability through editing and chaperoning: regulation of MHC class II peptide binding and expression. Immunol Rev *207*, 242-260.

Cabibbo, A., Pagani, M., Fabbri, M., Rocchi, M., Farmery, M. R., Bulleid, N. J., Sitia, R. (2000). ERO1 - L, a human protein that favors disulfide bond formation in the endoplasmic reticulum. J Biol Chem *275*, 4827-4833.

Cai, H., Wang, C.C., and Tsou, C.L. (1994). Chaperone-Like Activity of Protein Disulfide-Isomerase in the Refolding of a Protein with No Disulfide Bonds. J Biol Chem *269*, 24550-24552.

Campbell, I.D., Bork, P. (1993). Epidermal growth factor-like modules. Curr Opin Struct Biol *3*, 385-392.

Cao, S.S., Kaufman, R. J. (2012). Unfolded protein response. Curr Biol *22*, R622-R626.

Chakravarthi, S., and Bulleid, N.J. (2004). Glutathione is required to regulate the formation of native disulfide bonds within proteins entering the secretory pathway. J Biol Chem *279*, 39872-39879.

Chakravarthi, S., Jessop, C.E., and Bulleid, N.J. (2006). The role of glutathione in disulphide bond formation and endoplasmic-reticulum-generated oxidative stress. EMBO reports *7*, 271-275.

Chambers, J.E., Tavender, T.J., Oka, O.B., Warwood, S., Knight, D., and Bulleid, N.J. (2010). The reduction potential of the active site disulfides of human protein disulfide isomerase limits oxidation of the enzyme by Ero1α. J Biol Chem *285*, 29200-29207.

Chen, W., and Helenius, A. (2000). Role of ribosome and translocon complex during folding of influenza hemagglutinin in the endoplasmic reticulum of living cells. Mol Cell Biol *11*, 765-772.

Chiang, H.S., and Maric, M. (2011). Lysosomal thiol reductase negatively regulates autophagy by altering glutathione synthesis and oxidation. Free Radic Biol Med *51*, 688-699.

Cho, J., Cho, S., Lee, S.O., Oh, C., Kang, K., Ryoo, J., Lee, S., Kang, S., and Ahn, K. (2011). Redox-regulated peptide transfer from the transporter associated with antigen processing to major histocompatibility complex class I molecules by protein disulfide isomerase. Antioxid Redox Signal *15*, 621-633.

Christianson, J.C., Olzmann, J.A., Shaler, T.A., Sowa, M.E., Bennett, E.J., Richter, C.M., Tyler, R.E., Greenblatt, E.J., Harper, J.W., and Kopito, R.R. (2012). Defining human ERAD networks through an integrative mapping strategy. Nature Cell Biol *14*, 93-U176.

Cormier, J.H., Tamura, T., Sunryd, J.C., and Hebert, D.N. (2009). EDEM1 recognition and delivery of misfolded proteins to the SEL1L-containing ERAD complex. Mol Cell *34*, 627-633.

Cox, J.S., Shamu, C. E., Walter, P. (1993). Transcriptional induction of genes encoding endoplasmic reticulum reisdent proteins requires a trasnmembrane protein kinase. Cell *73*, 1197-1206.

Creddle, J.J., Finer-Moore, J. S., Papa, F. R., Stroud, R. M., Walter, P. (2005). On the mechanism of sensing unfolded protein in the endoplasmic reticulum. Proc Natl Acad Sci USA *102*, 18773-18784.

Cresswell, P., and Roche, P.A. (2014). Invariant chain-MHC class II complexes: always odd and never invariant. Immunol Cell Biol *92*, 471-472.

Csala, M., Braun, L., Mile, V., Kardon, T., Szarka, A., Kupcsulik, P., Mandl, J., and Banhegyi, G. (1999). Ascorbate-mediated electron transfer in protein thiol oxidation in the endoplasmic reticulum. FEBS letters *460*, 539-543.

Cui, L., Aleksandrov, L., Chang, X.B., Hou, Y.X., He, L., Hegedus, T., Gentzsch, M., Aleksandrov, A., Balch, W.E., and Riordan, J.R. (2007). Domain interdependence in the biosynthetic assembly of CFTR. J Mol Biol *365*, 981-994.

Danilczyk, U.G., and Williams, D.B. (2001). The lectin chaperone calnexin utilizes polypeptide-based interactions to associate with many of its substrates in vivo. J Biol Chem *276*, 25532-25540.

Denisov, A.Y., Maattanen, P., Dabrowski, C., Kozlov, G., Thomas, D.Y., and Gehring, K. (2009). Solution structure of the bb' domains of human protein disulfide isomerase. FEBS J *276*, 1440-1449.

Derouiche, F., Bole-Feysot, C., Naimi, D., and Coeffier, M. (2014). Hyperhomocysteinemia-induced oxidative stress differentially alters proteasome composition and activities in heart and aorta. Biochem Biophys Res commun *452*, 740-745.

Desilva, M.G., Notkins, A. L., Lan, M. S. (1997). Molecular characterization of a pancrease-specific protein disulfide isomerase, PDIp. DNA Cell Biol *16*, 269-274.

Dias-Gunaseka, s., Gubbens, J., van Lith, M., Dunne, C., Williams, J. A., Kataky, R., Scoones, D., Lapthorn, A., Bulleid, N. J., Benham, A. M. (2005). Tissue-specific expression and dimerization of the endoplasmic reticulum oxidoreductase Ero1beta. J Biol Chem *280*, 33066-33075.

Dias-Gunasekara, s., Gubbens, J., van Lith, M., Dunne, C., Williams, G., Kataky, R., Scoones, D., Lapthorn, A., Bulleid, N. J., Benham, A. M. (2005). Tissue-specific expression and dimerization of the endoplasmic reticulum oxidoreductase Ero1b. J Biol Chem *280*, 33066-33075.

Dias-Gunasekara, s., van Lith, M., Williams, G. J. A., Kataky, R., Benham, A. M. (2006). Mutations in the FAD binding domain cause stress-induced misoxidation of the endoplasmic reticulum oxidoreductase Ero1b. J Biol Chem *281*, 25018-25025.

Diaz, G., Canas, B., Vazquez, J., Nombela, C., and Arroyo, J. (2005). Characterization of natural peptide ligands from HLA-DP2: new insights into HLA-DP peptide-binding motifs. Immunogenetics *56*, 754-759.

Dick, T.P., Bangia, N., Peaper, D.R., and Cresswell, P. (2002). Disulfide bond isomerization and the assembly of MHC class I-peptide complexes. Immunity *16*, 87-98.

Diedrichs, M., and Schendel, D.J. (1989). Differential surface expression of class II isotypes on activated CD4 and CD8 cells correlates with levels of locus-specific mRNA. J Immunol *142*, 3275-3280.

Dierks, T., Volkmer, J., Schlenstedt, G., Jung, C., Sandholzer, U., Zachmann, K. (1996). A microsomal STP-binding protein involved in efficient protein transport into the mammalian endoplasmic reticulum. EMBO J *15*, 6931-6942.

Dong, G., Wearsch, P.A., Peaper, D.R., Cresswell, P., and Reinisch, K.M. (2009). Insights into MHC Class I Peptide Loading from the Structure of the Tapasin-ERp57 Thiol Oxidoreductase Heterodimer. Immunity *30*, 21-32.

Eklund, H., Gleason, F.K., and Holmgren, A. (1991). Structural and Functional Relations among Thioredoxins of Different Species. Proteins *11*, 13-28.

Elanchezhian, R., Palsamy, P., Masdon, C.J., Lynch, D.W., and Shinohara, T. (2012). Age-related cataracts: Homocysteine coupled endoplasmic reticulum stress and suppression of Nrf2-dependent antioxidant protection. Chem Biol Interact *200*, 1-10.

Ellis, R.J., and van der Vies, S.M. (1991). Molecular chaperones. Annu Rev Biochem *60*, 321-347.

Engering, A., and Pieters, J. (2001). Association of distinct tetraspanins with MHC class II molecules at different subcellular locations in human immature dendritic cells. Int Immunol *13*, 127-134.

Faraci, F.M., and Lentz, S.R. (2004). Hyperhomocysteinemia, oxidative stress, and cerebral vascular dysfunction. Stroke *35*, 345-347.

Fernando, M.M., Stevens, C.R., Walsh, E.C., De Jager, P.L., Goyette, P., Plenge, R.M., Vyse, T.J., and Rioux, J.D. (2008). Defining the role of the MHC in autoimmunity: a review and pooled analysis. PLoS genetics *4*, e1000024.

Finley, D., Ulrich, H.D., Sommer, T., and Kaiser, P. (2012). The ubiquitin-proteasome system of Saccharomyces cerevisiae. Genetics *192*, 319-360.

Flynn, G.C., Pohl, J., Flocco, M.T., and Rothman, J.E. (1991). Peptide-binding specificity of the molecular chaperone BiP. Nature *353*, 726-730.

Foresti, O., Ruggiano, A., Hannibal-Bach, H. K., Ejsing, C. S., Carvalho, P. (2013). Sterol homeostais requires degradation of squalene monooxygenase by the ubiquiting ligase Doa10/Teb4. eLife *2*, 300953.

Frand, A.R., and Kaiser, C.A. (1998). The ERO1 gene of yeast is required for oxidation of protein dithiols in the endoplasmic reticulum. Mol Cell *1*, 161-170.

Frickel, E.M., Frei, P., Bouvier, M., Stafford, W.F., Helenius, A., Glockshuber, R., and Ellgaard, L. (2004). ERp57 is a multifunctional thiol-disulfide oxidoreductase. J Biol Chem *279*, 18277-18287.

Frydman, J., Nimmesgern, E., Ohtsuka, K., and Hartl, F.U. (1994). Folding of nascent polypeptide chains in a high molecular mass assembly with molecular chaperones. Nature *370*, 111-117.

Fu, X.M., Dai, X.C., Ding, J., and Zhu, B.T. (2009). Pancreas-specific protein disulfide isomerase has a cell type-specific expression in various mouse tissues and is absent in human pancreatic adenocarcinoma cells: implications for its functions. J Mol Hist *40*, 189-199.

Galli, C., Bernasconi, R., Solda, T., Calanca, V., and Molinari, M. (2011). Malectin participates in a backup glycoprotein quality control pathway in the mammalian ER. PloS one *6*, e16304.

Geierhass, C.D., Paci, E., Vendruscolo, M., Clarke, J. (2004). Comparison of the transition states for folding of two Ig-like proteins from different superfamilies. J Mol Biol *343*, 1111-1123.

Germain, R.N., and Margulies, D.H. (1993). The biochemistry and cell biology of antigen processing and presentation. Ann Review Immunol *11*, 403-450.

Gess, B., Hofbauer, K.H., Wenger, R.H., Lohaus, C., Meyer, H.E., and Kurtz, A. (2003). The cellular oxygen tension regulates expression of the endoplasmic oxidoreductase ERO1-Lalpha. Eur J Biochem *270*, 2228-2235.

Gidalevitz, T., Stevens, F., and Argon, Y. (2013). Orchestration of secretory protein folding by ER chaperones. Biochim Biophys Acta *1833*, 2410-2424.

Gilchrist, A., Au, C.E., Hiding, J., Bell, A.W., Fernandez-Rodriguez, J., Lesimple, S., Nagaya, H., Roy, L., Gosline, S.J., Hallett, M.*, et al.* (2006). Quantitative proteomics analysis of the secretory pathway. Cell *127*, 1265-1281.

Goldberger, R.G., Epstein, C. J., Anfinsen, C. B. (1963). Acceleration of a reactivation of reduced bovine pancreas ribonuclease by a microsomal system from rat liver. J Biol Chem *238*, 628-635.

Greenblatt, E.J., Olzmann, J. A., Kopito, R. R. (2011). Derlin-1 is a rhomboid pseudoprotease required for the dislocation of mutant α-1 antitrypsin from the endoplasmic reticulum. Nature Struct Biol *18*, 1147-1152.

Grinna, L.S., and Robbins, P.W. (1980). Substrate Specificities of Rat-Liver Microsomal Glucosidases Which Process Glycoproteins. J Biol Chem *255*, 2255-2258.

Gross, E., Kastner, D.B., Kaiser, C.A., and Fass, D. (2004). Structure of Ero1p, source of disulfide bonds for oxidative protein folding in the cell. Cell *117*, 601-610.

Haas, I.G., and Wabl, M. (1983). Immunoglobulin heavy chain binding protein. Nature *306*, 387-389.

Hamman, B.D., Chen, J.C., Johnson, E.E., and Johnson, A.E. (1997). The aqueous pore through the translocon has a diameter of 40-60 angstrom during cotranslational protein translocation at the ER membrane. Cell *89*, 535-544.

Hamman, B.D., Hendershot, L. M. Johnson, A. E. (1998). BiP maintains the permeability barrier of the ER membrane by dealing the luminal end of the translocon por before and early in translocation. Cell *92*, 721-732.

Hammond, C., Braakman, I., Helenius, A. (1994). Role of N-linked oligiosaccharide recognition, glucose trimming, and calnexin in glycoprotein folding and quality control. Proc Natl Acad Sci USA *91*, 913-917.

Hansen, H.G., Schmidt, J. D., Soltoft, C. L., Ramming, T., Geertz-Hansen, H. M., Christensen, B., Sorensen, E. S., Junker, A. S., Appenzeller-Herzog, C., Ellgaard, L. (2012). Hyperactivity of the Ero1α oxidase elicits endoplasmic reticulum stress but no broad antioxidant response. J Biol Chem *287*, 39513-39523.

Hansen, H.G., Soltoft, C. L., Schmidt, J. D., Birk, J., Appenzeller-Herzog, C., Ellgaard, L. (2014). Biochemical evidence that regulation of Ero1β activity in human cells does not involve the isoform-specific cysteine 262. Biosci Rep *34*, e00103.

Hansen, R.E., and Winther, J.R. (2009). An introduction to methods for analyzing thiols and disulfides: Reactions, reagents, and practical considerations. Anal Biochem *394*, 147-158.

Hanson, S.R., Culyba, E.K., Hsu, T.L., Wong, C.H., Kelly, J.W., and Powers, E.T. (2009). The core trisaccharide of an N-linked glycoprotein intrinsically accelerates folding and enhances stability. Proc Natl Acad Sci USA *106*, 3131-3136.

Harding, H.P., Zhang, Y., Zeng, H., Novoa, I., Lu, P.D., Calfon, M., Sadri, N., Yun, C., Popko, B., Paules, R.*, et al.* (2003). An integrated stress response regulates amino acid metabolism and resistance to oxidative stress. Mol Cell *11*, 619-633.

Harty, C., Strahl, S., and Romisch, K. (2001). O-mannosylation protects mutant alpha-factor precursor from endoplasmic reticulum-associated degradation. Mol Cell Biol *12*, 1093-1101.

Haselbeck, A., Tanner, W. (1983). O-glycosylation in Saccharomyces cerevisiae is initiated at the endoplasmic reticlum. FEBS letters *158*, 335-338.

Hassan, G.S., and Mourad, W. (2011). An unexpected role for MHC class II. Nature Immunol *12*, 375-376.

Hebert, D.N., and Molinari, M. (2007). In and out of the ER: protein folding, quality control, degradation, and related human diseases. Physiol Rev *87*, 1377-1408.

Hebert, D.N., Zhang, J. X., Chen, W., Foellmer, B., Helenius, A. (1997). The number and location of glycans on influenza hemmagglutinin determine folding and association with calnexin and celreticulun. J Cell Biol *139*, 613-623.

Helenius, A., and Aebi, M. (2004). Roles of N-linked glycans in the endoplasmic reticulum. Ann Rev Biochem *73*, 1019-1049.

Hendershot, L.M. (2004). The ER chaperone BiP is a master regulator of ER function. Mt Sinai J Med *71*, 289-297.

Higo, T., Hattori, M., Nakamura, T., Natsume, T., Michikawa, T., Mikoshiba, K. (2005). Subtype-specific and ER lumenal environment-dependent regulation of inositol 1,4,5-triphosphate receptor type 1 by ERp44. Cell *120*, 85-98.

Hillson, D.A., Lambert, N., and Freedman, R.B. (1984). Formation and isomerization of disulfide bonds in proteins: protein disulfide-isomerase. Methods Enzymol *107*, 281-294.

Hitbold, E.M., Roche, P. A. (2002). Trafficking of MHC class II molecules in the late secretory pathway. Curr Opin Immunol *14*, 30-35.

Hoffstrom, B.G., Kaplan, A., Letso, R., Schmid, R.S., Turmel, G.J., Lo, D.C., and Stockwell, B.R. (2010). Inhibitors of protein disulfide isomerase suppress apoptosis induced by misfolded proteins. Nature Chem Biol *6*, 900-906.

Hollien, J., Lin, J.H., Li, H., Stevens, N., Walter, P., and Weissman, J.S. (2009). Regulated Ire1-dependent decay of messenger RNAs in mammalian cells. J Cell Biol *186*, 323-331.

Hosokawa, N., Tremblay, L.O., Sleno, B., Kamiya, Y., Wada, I., Nagata, K., Kato, K., and Herscovics, A. (2010). EDEM1 accelerates the trimming of alpha1,2-linked mannose on the C branch of N-glycans. Glycobiology *20*, 567-575.

Houck, S.A., Ren, H.Y., Madden, V.J., Bonner, J.N., Conlin, M.P., Janovick, J.A., Conn, P.M., and Cyr, D.M. (2014). Quality control autophagy degrades soluble ERAD-resistant conformers of the misfolded membrane protein GnRHR. Mol Cell *54*, 166-179.

Hsing, L.C., and Rudensky, A.Y. (2005). The lysosomal cysteine proteases in MHC class II antigen presentation. Immunol Rev *207*, 229-241.

Hulpke, S., and Tampe, R. (2013). The MHC I loading complex: a multitasking machinery in adaptive immunity. Trends Biochem Sci *38*, 412-420.

Hwang, C., Sinskey, A.J., and Lodish, H.F. (1992). Oxidized redox state of glutathione in the endoplasmic reticulum. Science *257*, 1496-1502.

Ihara, Y., Cohen-Doyle, M.F., Saito, Y., and Williams, D.B. (1999). Calnexin discriminates between protein conformational states and functions as a molecular chaperone in vitro. Mol Cell *4*, 331-341.

Inaba, K., Masui, S., Lida, H., Vavassori, S., Sitia, R., Suzuki, M. (2010). Crystal structures of human Ero1α reveal the mechanisms of regulated and targeted oxidation of PDI. EMBO J *29*, 3330-3343.

Ishida, Y., and Nagata, K. (2011). Hsp47 as a collagen-specific molecular chaperone. Methods Enzymol *499*, 167-182.

Jansens, A., van Duijn, E., and Braakman, I. (2002). Coordinated nonvectorial folding in a newly synthesized multidomain protein. Science *298*, 2401-2403.

Jastaniah, W.A., Alessandri, A.J., Reid, G.S.D., and Schultz, K.R. (2006). HLA-DM expression is elevated in ETV6-AML1 translocation-positive pediatric acute lymphoblastic leukemia. Leuk Res *30*, 487-489.

Johnsen, I.B., Nguyen, T.T., Ringdal, M., Tryggestad, A.M., Bakke, O., Lien, E., Espevik, T., and Anthonsen, M.W. (2006). Toll-like receptor 3 associates with c-Src tyrosine kinase on endosomes to initiate antiviral signaling. EMBO J *25*, 3335-3346.

Jorgensen, C.S., Heegaard, N.H., Holm, A., Hojrup, P., and Houen, G. (2000). Polypeptide binding properties of the chaperone calreticulin. Eur J Biochem *267*, 2945-2954.

Kabani, M., Kelley, S.S., Morrow, M.W., Montgomery, D.L., Sivendran, R., Rose, M.D., Gierasch, L.M., and Brodsky, J.L. (2003). Dependence of endoplasmic reticulum-associated degradation on the peptide binding domain and concentration of BiP. Mol Cell Biol *14*, 3437-3448.

Kamatani, Y., Wattanapokayakit, S., Ochi, H., Kawaguchi, T., Takahashi, A., Hosono, N., Kubo, M., Tsunoda, T., Kamatani, N., Kumada, H*., et al.* (2009). A genome-wide association study identifies variants in the HLA-DP locus associated with chronic hepatitis B in Asians. Nature genetics *41*, 591-595.

Kapoor, M., Srinivas, H., Kandiah, E., Gemma, E., Ellgaard, L., Oscarson, S., Helenius, A., and Surolia, A. (2003). Interactions of substrate with calreticulin, an endoplasmic reticulum chaperone. J Biol Chem *278*, 6194-6200.

Karamyshev, A.L., Patrick, A.E., Karamysheva, Z.N., Griesemer, D.S., Hudson, H., Tjon-Kon-Sang, S., Nilsson, I., Otto, H., Liu, Q., Rospert, S*., et al.* (2014). Inefficient SRP interaction with a nascent chain triggers a mRNA quality control pathway. Cell *156*, 146-157.

Kawaguchi, T., Miyazawa, K., Moriya, S., Ohtomo, T., Che, X.F., Naito, M., Itoh, M., and Tomada, A. (2011). Combined treatment with bortezomib plus bafilomycin A1 enhances the cytocidal effect and induces endoplasmic reticulum stress in U266 myeloma cells: Crosstalk among proteasome, autophagy-lysosome and ER stress. Int J Oncol *38*, 643-654.

Kemmink, J., Dijkstra, K., Mariani, M., Scheek, R.M., Penka, E., Nilges, M., and Darby, N.J. (1999). The structure in solution of the b domain of protein disulfide isomerase. J Biomol NMR *13*, 357-368.

Khaminets, A., Heinrich, T., Mari, M., Grumati, P., Huebner, A.K., Akutsu, M., Liebmann, L., Stolz, A., Nietzsche, S., Koch, N*., et al.* (2015). Regulation of endoplasmic reticulum turnover by selective autophagy. Nature *522*, 354-358.

Kim, S., Sideris, D.P., Sevier, C.S., and Kaiser, C.A. (2012). Balanced Ero1 activation and inactivation establishes ER redox homeostasis. J Cell Biol *196*, 713-725.

Kimata, Y., Ishiwata-Kimata, Y., Ito, T., Hirata, A., Suzuki, T., Oikawa, D., Takeuchi, M., and Kohno, K. (2007). Two regulatory steps of ER-stress sensor Ire1 involving its cluster formation and interaction with unfolded proteins. J Cell Biol *179*, 75-86.

Koch, N., McLellan, A. D., Neumann, J. (2007). A revised model for invarient chain-mediated assembly of MHC class II peptide receptors. Trends Biochem Sci *32*, 532-537.

Koch, N., Zacharias, M., Konig, A., Temme, S., Neumann, J., Springer, S. (2011). Stoichiometry of HLA class II-invarient chain oligomers. PloS one *6*, e17257.

Kojer, K., and Riemer, J. (2014). Balancing oxidative protein folding: the influences of reducing pathways on disulfide bond formation. Biochim Biophy acta *1844*, 1383-1390.

Kopito, R.R. (2000). Aggresomes, inclusion bodies and protein aggregation. Trends Cell Biol *10*, 524-530.

Kozlov, G., Maattanen, P., Thomas, D.Y., and Gehring, K. (2010). A structural overview of the PDI family of proteins. FEBS J *277*, 3924-3936.

Kukita, K., Tamura, Y., Tanaka, T., Kajiwara, T., Kutomi, G., Saito, K., Okuya, K., Takaya, A., Kanaseki, T., Tsukahara, T*., et al.* (2015). Cancer-Associated Oxidase ERO1-alpha Regulates the Expression of MHC Class I Molecule via Oxidative Folding. J Immunol *194*, 4988-4996.

Kundra, R., and Kornfeld, S. (1999). Asparagine-linked oligosaccharides protect Lamp-1 and Lamp-2 from intracellular proteolysis. J Biol Chem *274*, 31039-31046.

Lamb, C.A., Cresswell, P. (1992). Assembly and transport properties of the invarient chain trimers and HLA-DR-invariant chain complexes. J Immunol *148*, 3478-3482.

Land, A., Zonneveld, D., Braakmann, I. (2003). Folding of HIV-1 envelope glycoprotein involves extensive isomerization of disulfide bonds and conformation-dependent leader peptide clevage. FASEB J *17*, 1058-1067.

Landmann, S., Muhlethaler-Mottet, A., Bernasconi, L., Suter, T., Waldburger, J.M., Masternak, K., Arrighi, J.F., Hauser, C., Fontana, A., and Reith, W. (2001). Maturation of dendritic cells is accompanied by rapid transcriptional silencing of class II transactivator (CIITA) expression. J Exp Med *194*, 379-391.

Larriba, G., Elorza, M.V., Villanueva, J.R., and Sentandreu, R. (1976). Participation of dolichol phosphomannose in the glycosylation of yeast wall mannoproteins at the polysomal level. REBS Lett *71*, 316-320.

Lee, A.H., Iwakoshi, N.N., and Glimcher, L.H. (2003). XBP-1 regulates a subset of endoplasmic reticulum resident chaperone genes in the unfolded protein response. Mol Cell Biol *23*, 7448-7459.

Lee, J., Ozcan, U. (2014). Unfolded protein response signaling and metabloic diseases. J Biol Chem *289*, 1203-1211.

Lee, K.P., Dey, M., Neculai, D., Cao, C., Dever, T.E., and Sicheri, F. (2008). Structure of the dual enzyme Ire1 reveals the basis for catalysis and regulation in nonconventional RNA splicing. Cell *132*, 89-100.

Lee, Y.K., Brewer, J.W., Hellman, R., and Hendershot, L.M. (1999). BiP and immunoglobulin light chain cooperate to control the folding of heavy chain and ensure the fidelity of immunoglobulin assembly. Mol Cell Biol *10*, 2209-2219.

Leveille, C., Chandad, F., Al-Daccak, R., and Mourad, W. (1999). CD40 associates with the MHC class II molecules on human B cells. Eur J Immunol *29*, 3516-3526.

Levine, C.G., Mitra, D., Sharma, A., Smith, C.L., and Hegde, R.S. (2005). The efficiency of protein compartmentalization into the secretory pathway. Mol Cell Biol *16*, 279-291.

Levinthal, C. (1968). Are there pathways for protein folding? J Chim Phys *65*, 44-45.

Li, J., Soroka, J., and Buchner, J. (2012). The Hsp90 chaperone machinery: conformational dynamics and regulation by co-chaperones. Biochim Biophys acta *1823*, 624-635.

Li, Y., and Camacho, P. (2004). Ca2+-dependent redox modulation of SERCA 2b by ERp57. J Cell Biol *164*, 35-46.

Li, Y., Lu, W., Schwartz, A.L., and Bu, G. (2002). Receptor-associated protein facilitates proper folding and maturation of the low-density lipoprotein receptor and its class 2 mutants. Biochemistry *41*, 4921-4928.

Li, Z.H., and Srivastava, P.K. (1993). Tumor Rejection Antigen Gp96/Grp94 Is an Atpase - Implications for Protein-Folding and Antigen Presentation. EMBO J *12*, 3143-3151.

Liu, X., Zhan, Z., Li, D., Xu, L., Ma, F., Zhang, P., Yao, H., and Cao, X. (2011). Intracellular MHC class II molecules promote TLR-triggered innate immune responses by maintaining activation of the kinase Btk. Nature Immunol *12*, 416-424.

Loibl, M., Wunderle, L., Hutzler, J., Schulz, B.L., Aebi, M., and Strahl, S. (2014). Protein O-Mannosyltransferases Associate with the Translocon to Modify Translocating Polypeptide Chains. J Biol Chem *289*, 8599-8611.

Lorenz, O.R., Freiburger, L., Rutz, D.A., Krause, M., Zierer, B.K., Alvira, S., Cuellar, J., Valpuesta, J.M., Madl, T., Sattler, M.*, et al.* (2014). Modulation of the Hsp90 chaperone cycle by a stringent client protein. Mol Cell *53*, 941-953.

Lowe, J.B., and Marth, J.D. (2003). A genetic approach to Mammalian glycan function. Annual Rev Biochem *72*, 643-691.

Lukacs, G.L., Mohamed, A., Kartner, N., Chang, X.B., Riordan, J.R., and Grinstein, S. (1994). Conformational maturation of CFTR but not its mutant counterpart (delta F508) occurs in the endoplasmic reticulum and requires ATP. EMBO J *13*, 6076-6086.

Lukacs, G.L., and Verkman, A.S. (2012). CFTR: folding, misfolding and correcting the Delta F508 conformational defect. Trends Mol Med *18*, 81-91.

Lyles, M.M., and Gilbert, H.F. (1991). Catalysis of the oxidative folding of ribonuclease A by protein disulfide isomerase: dependence of the rate on the composition of the redox buffer. Biochemistry *30*, 613-619.

Ma, K., Vattem, K.M., and Wek, R.C. (2002). Dimerization and release of molecular chaperone inhibition facilitate activation of eukaryotic initiation factor-2 kinase in response to endoplasmic reticulum stress. J Biol Chem *277*, 18728-18735.

Madden, D.R. (1995). The three-dimensional structure of peptide-MHC complexes. Ann Rev Immunol *13*, 587-622.

Malhotra, J.D., Miao, H., Zhang, K., Wolfson, A., Pennathur, S., Pipe, S.W., and Kaufman, R.J. (2008). Antioxidants reduce endoplasmic reticulum stress and improve protein secretion. Proc Natl Acad Sci USA *105*, 18525-18530.

Mancini, R., Aebi, M., Helenius, A. (2003). Multiple endoplasmic reticulum-associated pathways degrade mutant yeast carboxypeptidase Y in mammaliun cells. J Biol Chem *278*, 46895-46905.

Manoury, B., Maschalidi, S., Achour, K., Lennon-Dumenil, AM., Tohme, M. (2015). The MHC class II-associated invariant chain regulates TLR7 trafficking and signaling in B cells. J Immunol *194*, Supplement 113.111.

Marciniak, S.J., Yun, C. Y., Oyadomari, S., Novoa, I., Zhang, Y., Jungreis, R., Nagata, K., Harding, H. P., Ron, D. (2004). CHOP induced cell death by promoting protein synthesis and oxidation in the stressed endoplasmic reticulum. Genes Dev *18*, 3066-3077.

Marcinowski, M., Rosam, M., Seitz, C., Elferich, J., Behnke, J., Bello, C., Feige, M.J., Becker, C.F., Antes, I., and Buchner, J. (2013). Conformational selection in substrate recognition by Hsp70 chaperones. J Mol Biol *425*, 466-474.

Maric, M., Arunachalam, B., Phan, U.T., Dong, C., Garrett, W.S., Cannon, K.S., Alfonso, C., Karlsson, L., Flavell, R.A., and Cresswell, P. (2001). Defective antigen processing in GILT-free mice. Science *294*, 1361-1365.

Marquette, K.A., Pittman, D.D., and Kaufman, R.J. (1995). A 110-amino Acid Region within the A1-domain of Coagulation Factor VIII Inhibits Secretion from Mammalian Cells. J Biol Chem *270*, 10297-10303.

Marsh, S.G.E., Parham, P., Barber, L. D. (2000). Three-Dimensional Structures of HLA Class II Molecules. The HLA facts book, Academic Press, San Diego 57-60.

Mast, S.W., Diekman, K., Karaveg, K., Davis, A., Sifers, R.N., and Moremen, K.W. (2005). Human EDEM2, a novel homolog of family 47 glycosidases, is involved in ER-associated degradation of glycoproteins. Glycobiology *15*, 421-436.

Masui, S., Vavassori, S., Fagioli, C., Sitia, R., Inaba, K. (2011). Molecular bases of cyclic and specific disulfide interchange between human ERO1alpha protein and protein-disulfide isomerase (PDI). J Biol Chem *286*, 16261-16271.

McCarty, J.S., Buchberger, A., Reinstein, J., and Bukau, B. (1995). The role of ATP in the functional cycle of the DnaK chaperone system. J Mol Biol *249*, 126-137.

McCully, K.S. (1969). Vascular pathology of homocysteinemia: implications for the pathogenesis of arteriosclerosis. Am J Path *56*, 111-128.

Medzhitov, R., Preston-Hurlburt, P., and Janeway, C.A., Jr. (1997). A human homologue of the Drosophila Toll protein signals activation of adaptive immunity. Nature *388*, 394-397.

Melnick, J., Dul, J.L., and Argon, Y. (1994). Sequential interaction of the chaperones BiP and GRP94 with immunoglobulin chains in the endoplasmic reticulum. Nature *370*, 373-375.

Meunier, L., Usherwood, Y.K., Chung, K.T., and Hendershot, L.M. (2002). A subset of chaperones and folding enzymes form multiprotein complexes in endoplasmic reticulum to bind nascent proteins. Mol Cell Biol *13*, 4456-4469.

Mezghrani, A., Fassio, A., Benham, A., Simmen, T., Braakman, I., and Sitia, R. (2001). Manipulation of oxidative protein folding and PDI redox state in mammalian cells. EMBO J *20*, 6288-6296.

Minor, E.A., Court, B.L., Young, J.I., and Wang, G. (2013). Ascorbate induces ten-eleven translocation (Tet) methylcytosine dioxygenase-mediated generation of 5-hydroxymethylcytosine. J Biol Chem *288*, 13669-13674.

Miyazaki, J., Appella, E., Zhao, H., Forman, J., and Ozato, K. (1986). Expression and function of a nonglycosylated major histocompatibility class I antigen. J Exp Med *163*, 856-871.

Molinari, M., Calanca, V., Galli, C., Lucca, P., and Paganetti, P. (2003). Role of EDEM in the release of misfolded glycoproteins from the calnexin cycle. Science *299*, 1397-1400.

Molteni, S.N., Fassio, A., Ciriolo, M.R., Filomeni, G., Pasqualetto, E., Fagioli, C., and Sitia, R. (2004). Glutathione limits Ero1-dependent oxidation in the endoplasmic reticulum. J Biol Chem *279*, 32667-32673.

Muzio, M., Polentarutti, N., Bosisio, D., Prahladan, M.K.P., and Mantovani, A. (2000). Toll-like receptors: a growing family of immune receptors that are differentially expressed and regulated by different leukocytes. J Leuk Bio *67*, 450-456.

Nagata, K. (1996). Hsp47: A collagen-specific molecular chaperone. Trends Biochem Sci *21*, 23-26.

Nguyen, V.D., Saaranen, M.J., Karala, A.R., Lappi, A.K., Wang, L., Raykhel, I.B., Alanen, H.I., Salo, K.E.H., Wang, C.C., and Ruddock, L.W. (2011). Two Endoplasmic Reticulum PDI Peroxidases Increase the Efficiency of the Use of Peroxide during Disulfide Bond Formation. J Mol Biol *406*, 503-515.

Nilsson, I., and Vonheijne, G. (1993). Determination of the Distance between the Oligosaccharyltransferase Active-Site and the Endoplasmic-Reticulum Membrane. J Biol Chem *268*, 5798-5801.

Nishikawa, S.I., Fewell, S.W., Kato, Y., Brodsky, J.L., and Endo, T. (2001). Molecular chaperones in the yeast endoplasmic reticulum maintain the solubility of proteins for retrotranslocation and degradation. J Cell Biol *153*, 1061-1070.

Oda, Y., Okada, T., Yoshida, H., Kaufman, R.J., Nagata, K., and Mori, K. (2006). Derlin-2 and Derlin-3 are regulated by the mammalian unfolded protein response and are required for ER-associated degradation. J Cell Biol *172*, 383-393.

Oikawa, D., Tokuda, M., Hosoda, A., and Iwawaki, T. (2010). Identification of a consensus element recognized and cleaved by IRE1 alpha. Nucleic Acids Res *38*, 6265-6273.

Oka, O.B.V., Pringle, M.A., Schopp, I.M., Braakman, I., and Bulleid, N.J. (2013). ERdj5 Is the ER Reductase that Catalyzes the Removal of Non-Native Disulfides and Correct Folding of the LDL Receptor. Mol Cell *50*, 793-804.

Okuda-Shimizu, Y., Hendershot, L. M. (2007). Characterization of an ERAD pathway for non-glycosylated BiP substrates, which require Herp. Mol Cell *28*, 544-554.

Okumura, M., Kadokura, H., and Inaba, K. (2015). Structures and functions of protein disulfide isomerase family members involved in proteostasis in the endoplasmic reticulum. Free radic Biol Med *83*, 314-322.

Onda, Y., Kumamaru, T., and Kawagoe, Y. (2009). ER membrane-localized oxidoreductase Ero1 is required for disulfide bond formation in the rice endosperm. Proc Natl Acad Sci USA *106*, 14156-14161.

Oslowski, C.M., Hara, T., O'Sullivan-Murphy, B., Kanekura, K., Lu, S.M., Hara, M., Ishigaki, S., Zhu, L.H.J., Hayashi, E., Hui, S.T.*, et al.* (2012). Thioredoxin-Interacting Protein Mediates ER Stress-Induced beta Cell Death through Initiation of the Inflammasome. Cell Metab *16*, 265-273.

Otero, J.H., Lizak, B., and Hendershot, L.M. (2010). Life and death of a BiP substrate. Semin Cell Dev Biol *21*, 472-478.

Otsu, M., Bertoli, G., Fagioli, C., Guerini-Rocco, E., Nerini-Molteni, S., Ruffato, E., and Sitia, R. (2006). Dynamic retention of Ero1alpha and Ero1beta in the endoplasmic reticulum by interactions with PDI and ERp44. Antioxid Redox Signal *8*, 274-282.

Pagani, M., Fabbri, M., Benedetti, C., Fassio, A., Pilati, S., Bulleid, N.J., Cabibbo, A., and Sitia, R. (2000). Endoplasmic reticulum oxidoreductin 1-lbeta (ERO1-Lbeta), a human gene induced in the course of the unfolded protein response. J Biol Chem *275*, 23685-23692.

Patil, N.S., Pashine, A., Belmares, M.P., Liu, W., Kaneshiro, B., Rabinowitz, J., McConnell, H., and Mellins, E.D. (2001). Rheumatoid arthritis (RA)-associated HLA-DR alleles form less stable complexes with class II-associated invariant chain peptide than non-RA-associated HLA-DR alleles. J Immunol *167*, 7157-7168.

Pearse, B.R., Gabriel, L., Wang, N., and Hebert, D.N. (2008). A cell-based reglucosylation assay demonstrates the role of GT1 in the quality control of a maturing glycoprotein. J Cell Biol *181*, 309-320.

Phipps-Yonas, H., Semik, V., and Hastings, K.T. (2013). GILT expression in B cells diminishes cathepsin S steady-state protein expression and activity. Eur J Immunol *43*, 65-74.

Pieters J., B., O., Dobberstein, B. (1993). The MHC class II-associated invariant chain contains two endosomal targeting signals within its cytoplasmic tail. J Cell Sci *106*, 831-846.

Pihlajaniemi, T., Helaakoski, T., Tasanen, K., Myllyla, R., Huhtala, M.L., Koivu, J., and Kivirikko, K.I. (1987). Molecular-Cloning of the Beta-Subunit of Human Prolyl 4-Hydroxylase - This Subunit and Protein Disulfide Isomerase Are Products of the Same Gene. EMBO J *6*, 643-649.

Pittman, D.D., Tomkinson, K.N., and Kaufman, R.J. (1994). Post-translational requirements for functional factor V and factor VIII secretion in mammalian cells. J Biol Chem *269*, 17329-17337.

Pollard, M.G., Travers, K.J., and Weissman, J.S. (1998). Ero1p: a novel and ubiquitous protein with an essential role in oxidative protein folding in the endoplasmic reticulum. Mol Cell *1*, 171-182.

Primm, T.P., Walker, K.W., and Gilbert, H.F. (1996). Facilitated protein aggregation. Effects of calcium on the chaperone and anti-chaperone activity of protein disulfide-isomerase. J Biol Chem *271*, 33664-33669.

Qin, S.Y., Hu, D., Matsumoto, K., Takeda, K., Matsumoto, N., Yamaguchi, Y., and Yamamoto, K. (2012). Malectin forms a complex with ribophorin I for enhanced association with misfolded glycoproteins. J Biol Chem *287*, 38080-38089.

Quan, H., Fan, G., and Wang, C.C. (1995). Independence of the chaperone activity of protein disulfide isomerase from its thioredoxin-like active site. J Biol Chem *270*, 17078-17080.

Raddrizzani, L., Sturniolo, T., Guenot, J., Bono, E., Gallazzi, F., Nagy, Z.A., Sinigaglia, F., and Hammer, J. (1997). Different modes of peptide interaction enable HLA-DQ and HLA-DR molecules to bind diverse peptide repertoires. J Immunol *159*, 703-711.

Ramming, T., Hansen, H.G., Nagata, K., Ellgaard, L., and Appenzeller-Herzog, C. (2014). GPx8 peroxidase prevents leakage of H2O2 from the endoplasmic reticulum. Free radic Biol Med *70*, 106-116.

Ramming, T., Okumura, M., Kanemura, S., Baday, S., Birk, J., Moes, S., Spiess, M., Jeno, P., Berneche, S., Inaba, K.*, et al.* (2015). A PDI-catalyzed thiol-disulfide switch regulates the production of hydrogen peroxide by human Ero1. Free rad Biol Med *83*, 361-372.

Rane, N.S., Chakrabarti, O., Feigenbaum, L., and Hegde, R.S. (2010). Signal sequence insufficiency contributes to neurodegeneration caused by transmembrane prion protein. J Cell Biol *188*, 515-526.

Reithinger, J.H., Yim, C., Kim, S., Lee, H., and Kim, H. (2014). Structural and functional profiling of the lateral gate of the Sec61 translocon. J Biol Chem *289*, 15845-15855.

Richeldi, L., Sorrentino, R., and Saltini, C. (1993). HLA-DPB1 glutamate 69: a genetic marker of beryllium disease. Science *262*, 242-244.

Ritter, C., and Helenius, A. (2000). Recognition of local glycoprotein misfolding by the ER folding sensor UDP-glucose:glycoprotein glucosyltransferase. Nature struct Biol *7*, 278-280.

Ritter, M., Mennerich, D., Weith, A., and Seither, P. (2005). Characterization of Toll-like receptors in primary lung epithelial cells: strong impact of the TLR3 ligand poly(I:C) on the regulation of Toll-like receptors, adaptor proteins and inflammatory response. J Inflam *2*, 16.

Rock, F.L., Hardiman, G., Timans, J.C., Kastelein, R.A., and Bazan, J.F. (1998). A family of human receptors structurally related to Drosophila Toll. Proc Natl Acad Sci USA *95*, 588-593.

Rubenstein, E.M., Kreft, S. G., Greenblatt, W., Swanson, R., Hochstrasser, M. (2012). Aberrant substrate engagement of the ER translocon trigger degreadation of hte Hrd1 ubiquitin ligase. Cell Biol *197*, 761-773.

Rudiger, S., Buchberger, A., and Bukau, B. (1997). Interaction of Hsp70 chaperones with substrates. Nature Struct Biol *4*, 342-349.

Ruggiano, A., Foresti, O., and Carvalho, P. (2014). Quality control: ER-associated degradation: protein quality control and beyond. J Cell Biol *204*, 869-879.

Rutkevich, L.A., and Williams, D.B. (2012). Vitamin K epoxide reductase contributes to protein disulfide formation and redox homeostasis within the endoplasmic reticulum. Mol Cell Biol *23*, 2017-2027.

Saito, Y., Ihara, Y., Leach, M. R., Cohen-Doyle, M. F., Williams, D. B (1999). Calreticulin functions in vitro as a molecular chaperone for both glycosylated and non-glycosylated proteins. EMBO J *18*, 6718-6729.

Sanders, C.R., and Myers, J.K. (2004). Disease-related misassembly of membrane proteins. Ann Rev Biophys Biomol Struct *33*, 25-51.

Schulman, S., Wang, B., Li, W., Rapoport, T. A. (2010). Vitamin K epitope reductase prefers ER membrane-anchored thioredoxin-like redox partners. Proc Natl Acad Sci USA *107*, 15027-15032.

Schwarz, F., and Aebi, M. (2011). Mechanisms and principles of N-linked protein glycosylation. Curr Opin Struct Biol *21*, 576-582.

Selhub, J. (1999). Homocysteine metabolism. Ann Rev Nutr *19*, 217-246.

Seshadri, S., Beiser, A., Selhub, J., Jacques, P.F., Rosenberg, I.H., D'Agostino, R.B., Wilson, P.W.F., and Wolf, P.A. (2002). Plasma homocysteine as a risk factor for dementia and Alzheimer's disease. N Engl J Med *346*, 476-483.

Sevier, C.S., Qu, H., Heldman, N., GRoss, E., Fass, D., Kaiser, C. A. (2007). Modulatino of cellular disulfide-bond formation and the ER redox environment by feedback of Ero1. Cell *129*, 333-344.

Shaffer, K.L., Sharma, A., Snapp, E.L., and Hegde, R.S. (2005). Regulation of protein compartmentalization expands the diversity of protein function. Dev Cell *9*, 545-554.

Shaw, A.S., Rottier, P.J., and Rose, J.K. (1988). Evidence for the loop model of signal-sequence insertion into the endoplasmic reticulum. Proc Natl Acad Sci USA *85*, 7592-7596.

Sheperd, C., Oka, O. B. V., Bulleid, N. J. (2014). Inactivation of mammalian Ero1α is catalysed by specific protein disulfide-isomerases. J Biochem *461*, 107-113.

Sidney, J., Steen, A., Moore, C., Ngo, S., Chung, J., Peters, B., and Sette, A. (2010). Five HLA-DP molecules frequently expressed in the worldwide human population share a common HLA supertypic binding specificity. J Immunol *184*, 2492-2503.

Silveira, L.J., McCanlies, E.C., Fingerlin, T.E., Van Dyke, M.V., Mroz, M.M., Strand, M., Fontenot, A.P., Bowerman, N., Dabelea, D.M., Schuler, C.R*., et al.* (2012). Chronic beryllium disease, HLA-DPB1, and the DP peptide binding groove. J Immunol *189*, 4014-4023.

Singh, A.K., Bhattacharyya-Pakrasi, M., and Pakrasi, H.B. (2008). Identification of an atypical membrane protein involved in the formation of protein disulfide bonds in oxygenic photosynthetic organisms. J Biol Chem *283*, 15762-15770.

Slominska-Wojewodzka, M., Sandvig, K. (2015). The role of lectin-carbohydrate interactions in the regulation of ER-associated protein degredation. Molecules *20*, 9816-9846.

Snapp, E.L., Sharma, A., Lippincott-Schwartz, J., and Hegde, R.S. (2006). Monitoring chaperone engagement of substrates in the endoplasmic reticulum of live cells. Proc Natl Acad Sci USA *103*, 6536-6541.

Song, B.L., Sever, N., and DeBose-Boyd, R.A. (2005). Gp78, a membrane-anchored ubiquitin ligase, associates with Insig-1 and couples sterol-regulated ubiquitination to degradation of HMG CoA reductase. Mol Cell *19*, 829-840.

Soriano, F.G., Virag, L., and Szabo, C. (2001). Diabetic endothelial dysfunction: role of reactive oxygen and nitrogen species production and poly(ADP-ribose) polymerase activation. J Mole Med *79*, 437-448.

Stockton, J.D., Merkert, M.C., and Kellaris, K.V. (2003). A complex of chaperones and disulfide isomerases occludes the cytosolic face of the translocation protein Sec61p and affects translocation of the prion protein. Biochemistry *42*, 12821-12834.

Strubin, M., Berte, C., and Mach, B. (1986). Alternative splicing and alternative initiation of translation explain the four forms of the Ia antigen-associated invariant chain. EMBO J *5*, 3483-3488.

Summers, D.W., Douglas, P.M., Ramos, C.H., and Cyr, D.M. (2009). Polypeptide transfer from Hsp40 to Hsp70 molecular chaperones. Trends Biochem Sci *34*, 230-233.

Sun, R.Q., Wang, H., Zeng, X.Y., Chan, S.M., Li, S.P., Jo, E., Leung, S.L., Molero, J.C., and Ye, J.M. (2015). IRE1 impairs insulin signaling transduction of fructose-fed mice via JNK independent of excess lipid. Biochim Biophys acta *1852*, 156-165.

Swaroop, M., Moussalli, M., Pipe, S.W., and Kaufman, R.J. (1997). Mutagenesis of a potential immunoglobulin-binding protein-binding site enhances secretion of coagulation factor VIII. J Biol Chem *272*, 24121-24124.

Szabo, A., Langer, T., Schroder, H., Flanagan, J., Bukau, B., and Hartl, F.U. (1994). The ATP hydrolysis-dependent reaction cycle of the Escherichia coli Hsp70 system DnaK, DnaJ, and GrpE. Proc Natl Acad Sci USA *91*, 10345-10349.

Szarka, A., and Lorincz, T. (2014). The role of ascorbate in protein folding. Protoplasma *251*, 489-497.

Tagliavacca, L., Wang, Q., and Kaufman, R.J. (2000). ATP-dependent dissociation of non-disulfide-linked aggregates of coagulation factor VIII is a rate-limiting step for secretion. Biochemistry *39*, 1973-1981.

Tannous, A., Pisoni, G.B., Hebert, D.N., and Molinari, M. (2015). N-linked sugar-regulated protein folding and quality control in the ER. Semin Cell Dev Biol *41*, 79-89.

Thomas, R., Thio, C.L., Apps, R., Qi, Y., Gao, X., Marti, D., Stein, J.L., Soderberg, K.A., Moody, M.A., Goedert, J.J.*, et al.* (2012). A novel variant marking HLA-DP expression levels predicts recovery from hepatitis B virus infection. J Virol *86*, 6979-6985.

Tirasophon, W., Welihinda, A.A., and Kaufman, R.J. (1998). A stress response pathway from the endoplasmic reticulum to the nucleus requires a novel bifunctional protein kinase/endoribonuclease (Ire1p) in mammalian cells. Genes Dev *12*, 1812-1824.

Tokuhiro, K., Ikawa, M., Benham, A. M., Okabe, M. (2012). Protein disulfide isomerase homolog PDILT is required for quality control of sperm membrane protein ADAM3 and male fertility. Proc Natl Acad Sci USA *109*, 3850-3855.

Tsukahara, T., Kawaguchi, S., Torigoe, T., Asanuma, H., Nakazawa, E., Shimozawa, K., Nabeta, Y., Kimura, S., Kaya, M., Nagoya, S.*, et al.* (2006). Prognostic significance of HLA class I expression in osteosarcoma defined by anti-pan HLA class I monoclonal antibody, EMR8-5. Cancer science *97*, 1374-1380.

Tsunoda, S., Avezov, E., Zyryanova, A., Konno, T., Mendes-Silva, L., Pinho Melo, E., Harding, H.P., and Ron, D. (2014). Intact protein folding in the glutathione-depleted endoplasmic reticulum implicates alternative protein thiol reductants. eLife *3*, e03421.

Tu, B.P., Weissman, J. S. (2002). The FAD- and O2-dependent reaction cycle of Ero1-mediated oxidative protein folding in the endoplasmic reticulum. Mol Cell *10*, 983-994.

Tyedmers, J., Lerner, M., Wiedmann, M., Volkmer, J., and Zimmermann, R. (2003). Polypeptide-binding proteins mediate completion of co-translational protein translocation into the mammalian endoplasmic reticulum. EMBO reports *4*, 505-510.

Uehara, T., Nakamura, T., Yao, D., Shi, Z.Q., Gu, Z., Ma, Y., Masliah, E., Nomura, Y., and Lipton, S.A. (2006). S-nitrosylated protein-disulphide isomerase links protein misfolding to neurodegeneration. Nature *441*, 513-517.

Urano, R., Wang, X., Bertolotti, A., Zhang, Y., Chung, P., Harding, H. P., Rob, D. (2000). Coupling of stress in the ER to activatino of JNK protein kinases by transmembrane protein kinase IRE1. Science *287*, 664-666.

Ushioda, R., Hoseki, J., Araki, K., Jansen, G., Thomas, D. Y., Nagata, K. (2008). ERdj5 is required as a disulfide reductase for degeneration of misfolded proteins in the ER. Science *321*, 569-572.

Van den Berg, B., Clemons, W.M., Jr., Collinson, I., Modis, Y., Hartmann, E., Harrison, S.C., and Rapoport, T.A. (2004). X-ray structure of a protein-conducting channel. Nature *427*, 36-44.

Van Lith, M., Benham, A. M. (2006). The DMalpha and DMbeta chain co-operate in the oxidation and folding of HLA-DM. J Immunol *177*, 5430-5439.

Van Lith, M., Karala, A.R., Bown, D., Gatehouse, J.A., Ruddock, L.W., Saunders, P.T.K., and Benham, A.M. (2007). A Developmentally Regulated Chaperone Complex for the Endoplasmic Reticulum of Male Haploid Germ Cells. Mol Cell Biol *18*, 2795-2804.

van Lith, M., McEwan-Smith, R. M., Benham, A. M. (2010). HL-DP, HLA-DQ, and HLA-DR have different requirements for invariant chain and HLA-DM. J Biol Chem *275*, 40800-40808.

Vashist, S., Kim, W., Belden, W.J., Spear, E.D., Barlowe, C., and Ng, D.T. (2001). Distinct retrieval and retention mechanisms are required for the quality control of endoplasmic reticulum protein folding. J Cell Biol *155*, 355-368.

Veal, E.A., Day, A. M., Morgan, B. A. (2007). Hydrogen peroxide sending and signaling. Mol Cell *26*, 1-14.

Von Heijne, G. (1985). Signal sequences: The limits of variation. J Mol Biol *184*, 99-105.

Walter, F., Schmid, J., Dussmann, H., Concannon, C.G., and Prehn, J.H. (2015). Imaging of single cell responses to ER stress indicates that the relative dynamics of IRE1/XBP1 and PERK/ATF4 signalling rather than a switch between signalling branches determine cell survival. Cell Death Differ *22*, 1502-1516.

Walter, P., and Ron, D. (2011). The unfolded protein response: from stress pathway to homeostatic regulation. Science *334*, 1081-1086.

Wang, C., Yu, J., Huo, L., Wang, L., Feng, W., and Wang, C.C. (2012). Human Protein-disulfide Isomerase Is a Redox-regulated Chaperone Activated by Oxidation of Domain a '. J Biol Chem *287*, 1139-1149.

Wang, L., Li, S.J., Sidhu, A., Zhu, L., Liang, Y., Freedman, R.B., and Wang, C.C. (2009). Reconstitution of human Ero1-Lalpha/protein-disulfide isomerase oxidative folding pathway in vitro. Position-dependent differences in role between the a and a' domains of protein-disulfide isomerase. J Biol Chem *284*, 199-206.

Wang, L., Zhang, L., Niu, Y., Sitia, R., Wang, C. C. (2014). Glutathione peroxidase 7 utilizes hydrogen peroxide generated by Ero1α to promote oxidative protein folding. Antioxid Redox Signal *20*, 545-556.

Wang, L., Zhu, L., and Wang, C.C. (2011). The endoplasmic reticulum sulfhydryl oxidase Ero1beta drives efficient oxidative protein folding with loose regulation. Biochem J *434*, 113-121.

Wetterau, J.R., Combs, K.A., Spinner, S.N., and Joiner, B.J. (1990). Protein Disulfide Isomerase Is a Component of the Microsomal Triglyceride Transfer Protein Complex. J Biol Chem *265*, 9800-9807.

Wiertz, E.J., Tortorella, D., Bogyo, M., Yu, J., Mothes, W., Jones, T.R., Rapoport, T.A., and Ploegh, H.L. (1996). Sec61-mediated transfer of a membrane protein from the endoplasmic reticulum to the proteasome for destruction. Nature *384*, 432-438.

Wild, K., Rosendal, K.R., and Sinning, I. (2004). A structural step into the SRP cycle. Mol Microbiol *53*, 357-363.

Wolynes, P.G., Onuchic, J.N., and Thirumalai, D. (1995). Navigating the folding routes. Science *267*, 1619-1620.

Wouters, M.A., Rigoutsos, I., Chu, C.K., Feng, L.L., Sparrow, D.B., and Dunwoodie, S.L. (2005). Evolution of distinct EGF domains with specific functions. Protein Sci *14*, 1091-1103.

Xu, Y., Cai, M., Yang, Y., Huang, L., Ye, Y. (2012). SGTA recognizes a noncanonical ubiquitin-like domain in the Bag6-Ubl4A-Trc35 complex to promote endoplasmic reticulum-associated degreadation. Cell reports *2*, 1633-1644.

Yang, X., Xu, H., Hao, Y., Zhoa, L., Cai, X., Tian, J., Zhang, M., Han, X., Ma, S., Cao, J., Jiang, Y. (2014). Endoplasmic reticulum oxidoreductin 1α mediates hepatic endoplasmic reticulum stress in homocysteine-induced atherosclerosis. Biochim Biophys acta *46*, 906-910.

Yoshida, H., Matsui, T., Yamamoto, A., Okada, T., and Mori, K. (2001). XBP1 mRNA is induced by ATF6 and spliced by IRE1 in response to ER stress to produce a highly active transcription factor. Cell *107*, 881-891.

Yoshida, H., Oku, M., Suzuki, M., and Mori, K. (2006). pXBP1(U) encoded in XBP1 pre-mRNA negatively regulates unfolded protein response activator pXBP1(S) in mammalian ER stress response. J Cell Biol *172*, 565-575.

Zarember, K.A., Godowski, P. J. (2002). Tissue expression of human Toll-like receptors and differential regulation of Toll-like receptor mRNAs in leukocytes in response to microbes, their products, and cytokines. J Immunol *168*, 554-561.

Zha, X., Yue, Y., Dong, N., Xiong, S. (2015). Endoplasmic reticulum stress aggrevates viral myocarditis by raising inflammation through the IRE1-associated NF-kK pathway. Can J Cardiol *31*, 1032-1040.

Zhang, H., and Burrows, F. (2004). Targeting multiple signal transduction pathways through inhibition of Hsp90. J Mol Med *82*, 488-499.

Zhang, L., Niu, Y., Zhu, L., Fang, J., Wang, X., Wang, L., Wang, CC. (2014). Different interaction modes for protein disulfide isomerase (PDI) as an efficient regulator and a specific substrate of endoplasmic reticulum oxidoreductin-1α (Ero1α). J Biol Chem *289*, 31188-31199.

Zhang, Z.R., Bonifacino, R. S., Hegde, R. S. (2013). Deubiquitinases sharpen substrate discrimination during membrane protein degratation from the ER. Cell *154*, 609-622.

Zinszner, H., Kuroda, M., Wang, X.Z., Batchvarova, N., Lightfoot, R.T., Remotti, H., Stevens, J.L., and Ron, D. (1998). CHOP is implicated in programmed cell death in response to impaired function of the endoplasmic reticulum. Genes Dev *12*, 982-995.

Zito, E., Chin, K.T., Blais, J., Harding, H.P., and Ron, D. (2010). ERO1-beta, a pancreas-specific disulfide oxidase, promotes insulin biogenesis and glucose homeostasis. J Cell Biol *188*, 821-832.

Zito, E., Hansen, H.G., Yeo, G.S., Fujii, J., and Ron, D. (2012). Endoplasmic reticulum thiol oxidase deficiency leads to ascorbic acid depletion and noncanonical scurvy in mice. Mol Cell *48*, 39-51.